Mechanical and Biological Aspects of Impaction Bone Grafting in Revision Hip Surgery and the use of a New Synthetic Bone Graft.

Douglas G Dunlop

Doctor of Medicine Thesis

The University of Edinburgh

February 2001 AD

Declaration

I hereby declare that this thesis is composed entirely of my own work, as a member of a research group. Contributions from other members of the research group are acknowledged in the appropriate sections where this has occurred. I have not submitted this thesis in candidature for any other degree, diploma or professional qualification

.....
Douglas G Dunlop MB BCh FRCS FRCSEd(Tr&Orth)

"A man's reach should exceed his grasp, or what is heaven for?"

Robert Browning
1812-1889

Acknowledgements

I would like to thank the trustees of the RI Stirling Fund for their financial support of my fellowship year. I would like to thank Mr Colin Howie for all his help and encouragement as my supervisor, including his visit to Adelaide, and Professor Bill Gillespie who inspired the project. Special thanks should also be extended to my Australian colleagues who made my family and I so welcome and who helped set up the project by e-mail before I arrived. They include Professor Don Howie and Oksana Holubowycz, John Field, Professor Trevor Hearn, John Costi, Dan Barker, Marg McGee, Phillipa Sharpe and Angelo Carbone.

I would like to acknowledge the help of the staff at the following:

Princess Margaret Rose Orthopaedic Hospital (PMROH)
University of Adelaide Orthopaedic Department, Royal Adelaide Hospital (RAH)
Department of Bioengineering, Repatriation General Hospital, Adelaide
Royal (Dick) School of Veterinary Studies, Summerhall (UnivEd)
Department of Veterinary Clinical Studies, Roslin (UnivEd)
The Marshall Building, Animal Research Facility, Roslin
Animal Research Facilities at RAH & Gillies Plains, Adelaide
Bone Pathology & Histology Laborotories, RAH
Quintiles Inc. (Research facility, Herriot Watt)
Institute of Biology (Animals Scientific Procedures Act)
The Civil Engineering Department (UnivEd)
The Mechanical Engineering Department (UnivEd)
The Geotechnical Centrifuge Centre (Cambridge University)
Civil Engineers of the M74 motorway upgrade
Prosthetic machinists (PMROH)
Howmedica and Giltech Ltd (Sponsors)
Scottish Council for Postgraduate Medical and Dental Education
Medical Personnel, Lister Postgraduate Institute
Mike Devlin, Medical illustration (PMROH)

Special acknowledgement resides with my wife Helen
and our daughter Megan
for their unending support and understanding for the duration of this project
and to my parents
who instilled in me, patience and determination.

Abstract

Aims

This thesis aims to examine the biological and mechanical factors which influence the strength of impacted morsellised bone graft. The use of synthetic materials as bone graft enhancers was also analysed (Controlled Release Glass – Corglaes®, Giltech Ltd, Ayr, Scotland and Tricalcium Phosphate Hydroxyapatite – TCP/HA, Stryker Howmedica Osteonics, Berkshire, UK).

Methods

Phase I - the mechanical strength of different fresh frozen human bone graft preparations were analysed in the laboratory, looking specifically at the effect of particle size, washing the graft and using synthetic additives.

Phase II - mixtures of bone graft and bone graft/Corglaes®, which had been identified as being mechanically stronger than standard bone graft, were analysed for their biological response in an in-vivo ovine defect model, compared to controls. Bone densitometry and histological analysis was performed.

Phase III - a mixture of bone graft and Corglaes® was compared to the current 'gold standard' of allograft bone alone, in a simulated revision in-vivo ovine femoral hip replacement model. Outcome measures of subsidence, micromotion on cyclical loading and histomorphometry were performed.

Results

Phase 1 - Fresh frozen human bone-graft behaves in a similar fashion to theoretical predictions based on Engineering principles. These principles follow Soil Mechanics theory and are commonly used by engineers when designing stable foundations for roads or buildings. In general, when the spread of different particle sizes is uniform over a given range, the material is stronger (more resistant to shear) than if the particles are all the same size. This allowed determination of which bone mills produce the strongest graft. These results were dependent on the degree of fluid release on graft milling, with more fluid release when the average particle size is

reduced. Shear strength was improved for all mills after washing the morsellised graft or by the addition of synthetic additives (Corglaes® and TCP/HA).

Phase 2 - The defect model allowed analysis of remodelling of the impacted pellets, highlighting rapid dissolution of the Corglaes®, without a significant inflammatory response. The model may be closer to a fracture model when the histological results of phase III are considered.

Phase 3 - No statistically significant difference in subsidence over the implantation period (12 weeks) or micromotion of the retrieved implant / femur composites could be elicited between the two groups. Histological analysis revealed the distal impacted graft to be in an isolated environment, both from biological ingress and solution exchange. Bone graft and Corglaes® that was remodelled or resorbed after time in the Phase II defect experiments, was little changed with time in the distal femur. The proximal femur histologically behaved in a similar fashion to the defect experiments. This suggests that a defect model alone is not ideal to analyse materials for impaction grafting.

Conclusions

- Graft strength is variable depending on the bone mill that produces it - washing bone graft improves the strength from all bone mills tested.
- Tight compaction with smaller particles does not inhibit neovascularisation.
- Novel biomaterials by themselves were inferior mechanically and biologically.
- 50/50 mixes of allograft and Corglaes® are stronger mechanically and do not appear to have an adverse effect on biological incorporation.
- In this sheep hemiarthroplasty model, subsidence, micromotion and histomorphometry results better replicate the equivalent reported human results than previous models, especially unloaded defect models in lower vertebrates.

Table of Contents

Table of Figures

Table of Graphs

Table of Tables

Publications, Awards, Presentations & Posters

Publications

An ovine model to evaluate the biologic properties of impacted morselized bone graft substitutes
DJ Griffon, DG Dunlop, JN Pratt, CR Howie, TJ Gilchrist, N Smith.
J Biomed Meter Res 2001 Sep 5;56(3):444-51

Incorporation of idealised, impacted Bonesave® in metaphyseal defects
DJ Griffon, JN Pratt, DG Dunlop, N Smith, CR Howie.
Journal of Bone and Joint Surgery JBJS [Br] 2001**; 83-B**: Supp II;187-188

Ovine hip hemiarthroplasty: reducing dislocation
DG Dunlop, JR Field
Vet Comp Orthop Traumatol. 2000:**13**;115-8

An ovine model for total hip replacement: operative procedure and complications
JR Field, A Carbone, H Aberman, P Sharpe, N Smith, DG Dunlop, DW Howie
Vet Comp Orthop Traumatol. In press. 2001:1

Design and Evaluation of a Method for Measuring Three-Dimensional Micromotion of Impaction Grafted Cemented Femoral Stem Prostheses
DG Dunlop, JJ Costi, DS Barker, CR Howie, JR Field, TC Hearn
Journal of Bone and Joint Surgery JBJS [Br] 2000; **82-B**: Supp III;261-262

An ovine model to evaluate impacted pellets of new synthetic bone graft substitutes
DG Dunlop, D Griffon, CR Howie, SPG Madabhushi, AS Usmani and WJ Gillespie
Journal of Bone and Joint Surgery JBJS [Br] 2000; **82-B**: Supp I;65-66

Factors influencing bone graft strength – to wash or not to wash?
DG Dunlop, N Brewster, SPG Madabhushi, AS Usmani, CR Howie
Journal of Bone and Joint Surgery JBJS [Br] 2000; **82-B**: Supp I;78

Awards

North American Travelling Fellowship
National Zimmer Award
DG Dunlop
January 2001

Young Investigator of the Year Award
The Design and Evaluation of a System for Measuring Three-Dimensional Micromotion in a Sheep Hip Replacement Model
JJ Costi, DG Dunlop, DS Barker, CR Howie, JR Field, TC Hearn
ANZORS, Brisbane, Australia, 15 October 1999

Presentations

Mechanical considerations in impaction bone grafting
Dunlop DG
5th Congress of the European Federation of National Associations of Orthopaedics & Traumatology (**EFORT**) Rhodes, 3-7 June 2001

Incorporation of idealised, impacted BoneSave® in metaphyseal defects
Griffon DJ, Pratt JNJ, Dunlop DG, Smith N, Howie CR.
5th Congress of the European Federation of National Associations of Orthopaedics & Traumatology (**EFORT**) Rhodes, 3-7 June 2001

Biomechanical properties of bone graft
Dunlop DG
ABC Fellows visit from N. America, Royal Infirmary of Edinburgh, 7 May 2001

Development of a novel method for measuring three-dimensional micromotion in an ovine hip replacement model
Costi JJ, Dunlop DG, Barker DS, Howie CR, Field JR, Hearn TC
Asia Pacific Orthopaedic Association (**APOA**) 13th Triennial Congress, Adelaide, South Australia, 1-6 April 2001.

Biomechanical properties of bone graft
Dunlop DG
Faculty member. Advanced Exeter Hip Symposium, Amsterdam, November 2000

An ovine model to evaluate impacted pellets of new synthetic bone graft substitutes
Griffon DJ, Dunlop DG, Howie CR, Pratt J, Gillespie WJ
European College of Veterinary Surgeons (**ECVS**) Annual Scientific Meeting, Bern, Switzerland, July 7-9 2000.

Incorporation of idealised, impacted, morselised, allograft and hydroxyapatite - tricalcium phosphate in metaphyseal bone defects
Pratt JNJ, Griffon DJ, Dunlop DG, Howie CR, Tomlinson L.
European College of Veterinary Surgeons (**ECVS**) Annual Scientific Meeting, Bern, Switzerland, July 7-9 2000.

An ovine model to evaluate impacted pellets of new synthetic bone graft substitutes
DG Dunlop, D Griffon, CR Howie, SPG Madabhushi, AS Usmani and WJ Gillespie
British Orthopaedic Association (**BOA**) Annual Congress, Glasgow, 15-17 September 1999

Factors influencing bone graft strength – to wash or not to wash?
DG Dunlop, CR Howie, SPG Madabhushi, AS Usmani
British Orthopaedic Association (**BOA**) Annual Congress, Glasgow, 15-17 September 1999

Design and Evaluation of a Device for Measuring 3D Micromotions of Impaction Grafted Cemented Femoral stem Prostheses
DG Dunlop, JR Field, J Costi, CR Howie, DW Howie, TR Hearn
Scottish Orthopaedic Association Annual Meeting, Stirling, 4 June 1999

Posters

An ovine model to evaluate the biological properties of impacted morsellised bone graft substitutes
Griffon DJ, Dunlop DG, Howie CR, Pratt JNJ, Gilchrist TJ, Smith N.
5th Congress of the European Federation of National Associations of Orthopaedics & Traumatology (**EFORT**) Rhodes, 3-7 June 2001

Design and evaluation of a method for measuring three-dimensional micromotion in a hip replacement model
J. J. Costi, D. G. Dunlop, D. S. Barker, C. R. Howie, J. R. Field, D. W. Howie and T. C. Hearn. 12th Conference of the European Society of Biomechanics (**ESB**), 27 - 30 August 2000, Trinity College Dublin, Ireland.

A New method for measuring 3D micromotion of femoral stem prostheses
DG Dunlop, JJ Costi, DS Barker, CR Howie, DW Howie, JR Field, TC Hearn.
12th Conference of the European Society of Biomechanics (**ESB**), 27 - 30 August 2000, Trinity College Dublin, Ireland.

Design and Evaluation of a Method for Measuring Three-Dimensional Micromotion of Impaction Grafted Cemented Femoral Stems
DG Dunlop, JJ Costi, DS Barker, CR Howie, JR Field, TC Hearn.
British Orthopaedic Research Society (**BORS**) Leicester, 17-18 April 2000.

The Design and Evaluation of a System for Measuring Three-Dimensional Micromotion in a Sheep Hip Replacement Model
JJ Costi, DG Dunlop, DS Barker, CR Howie, JR Field, TC Hearn
American Orthopaedic Research Society (**AORS**) Annual Meeting, March 12-15, 2000, Orlando, USA.

Mechanical Aspects of impaction grafting in THR – the effect of particle size distribution, additives and washing
DG Dunlop, CR Howie, Pankaj, SPG Madabhushi, AS Usmani
4th Congress of the European Federation of National Associations of Orthopaedics & Traumatology (**EFORT**) Brussels, 3-8 June 1999.

A New Approach for Ovine Hip Replacement
DG Dunlop, JR Field
Poster / Abstract. Orthopaedic Animal Models – Cambridge Healthcare Institute, Virginia USA, June 1999.

An Ovine Model for Total Hip Replacement: Operative Procedure and Complications
JR Field, A Carbone, H Aberman, P Sharpe, N Smith, DG Dunlop, DW Howie
Poster / Abstract. Orthopaedic Animal Models – Cambridge Healthcare Institute, Virginia USA, June 1999.

Design and Evaluation of a Device to Measure Instantaneous Three-Dimensional Micromotions of a Femoral Stem Prosthesis
DG Dunlop, JR Field, J Costi, D Barker, CR Howie, T Hearn
Poster / Abstract. Orthopaedic Animal Models – Cambridge Healthcare Institute, Virginia USA, June 1999.

Major Null-hypothesis

"Changing the composition of impacted bone graft has no effect on its mechanical or biological behaviour when compared with standard impacted bone graft."

The study has been divided into three sub-sections:

Phase I

Biomechanical Aspects of Impaction Grafting –
Shear Testing and In Vitro Modelling

Phase II

Biological Aspects of Impaction Grafting –
An Ovine Defect Model

Phase III

Clinical Aspects of Impaction Grafting –
An Ovine Hemiarthroplasty Model

Background

Chapter 1

1.1. Introduction

The use of bone graft from donor individuals of the same species (allograft)[1]and from different species (Xenograft)[1-2]occurred centuries before orthopaedic surgeons first performed operations where individuals received bone graft from themselves (autograft). Autograft is commonly used in current orthopaedic practice due to its predictable outcome to augment surgical fusion and replace lost bone. Bone grafts, when used in revision hip and knee surgery, are usually required in large quantities to replace extensive bone loss. Autograft is the graft of choice, but is usually precluded due to donor site morbidity in harvesting large quantities from an osteoporotic pelvis. Bone banks have attempted to bridge this shortfall of bone graft by providing allograft femoral heads, from different patients undergoing primary hip replacement surgery. Consent from these donors is often freely given, as today's donors may well be tomorrow's recipients. However, demand is increasing and the use of Xenograft and synthetic materials instead of allograft is coming under closer investigation. Study of suitable replacement materials forms the basis for this thesis.

Total hip arthroplasty (THA) is currently one of the most successful operations performed by any surgeon, with great improvement in Quality Adjusted Life Years (QALY's) for the patient. Total knee arthroplasty is fast approaching similar levels of success. From the Swedish hip register the success rate of cemented THA's at ten

years post operatively lies around 95% [3-8], with 75% of those requiring revision being due to aseptic loosening. The ten year success rate of subsequent revision hip surgery is significantly lower than for primary THA[9-10] at between 80-87%, depending on the end point chosen. The utilisation of allograft bone is increasing as the number of revisions of failed joint arthroplasty rises and techniques for bone replacement gain wider acceptance [11; 12].

Results of revision THA performed with impaction grafting has been centre dependent, with femoral subsidence measured as; mild, moderate or massive. This variability is multifactorial and may be a result of technique as well as graft type used. The publication of good results from an increasing number of centres, together with marketing forces will increase the demand for allograft bone. Indeed, major tissue banks are showing an increasing demand for all forms of allograft tissue[13; 14]. Future demand will inevitably increase as the number of primary joint arthroplasties perfomed per annum rise and this will be further exacerbated as operations are offered to younger patients and the population as a whole, live longer. Current estimates place the total number of hip replacements performed in the UK as 50,000 (worldwide over 800,000) per annum, with revision rates around 15% in major centres.

There is therefore a large and increasing demand for stores of bone graft. As supply may not always be able to meet demand, research into alternatives to bone graft, such as this project, have been prompted. According to a survey of emerging technologies in orthopaedics, synthetic substitutes are on the verge of expanding their current share of the market from 10%, to a potential 35% in 2003 [15].

1.2. Aims of Femoral Revision

The aim of this thesis is to increase our understanding of the biomechanical properties of fresh bone allograft and to determine potential ways of increasing its strength, either alone or with the addition of synthetic materials.

Having identified a biomechanically suitable graft we tested the material in-vivo in a simulated revision hip animal model, based on the aims of femoral revision[16] surgery;

1. Achieve implant stability
2. Relieve pain and restore mobility
3. Restore bone stock
4. Load the proximal femur
5. Achieve long term durability
6. Make future revision easier

1.3. Technique of Impaction Grafting

Professor Tom Slooff [20] and his colleagues in Nijmegen first used the technique in the acetabulum, in the late 1970's. The technique was introduced in the UK (and in the femur) by Professor Robin Ling, Graham Gie and colleagues in Exeter in May 1987 [19]. Since that time the technique has changed little in principle, but more effective dedicated instruments have been developed [17-23].

After the previous failed primary femoral implant and cement have been removed, the femoral canal is thoroughly cleaned and any lining membrane removed. The canal is then occluded distally with a cement restrictor. A guide rod attaches to the cement restrictor, over which the cannulated impactors run. Milled femoral head allograft is then added and tamped distally with blunt nosed impactors, then as the proximal femur is filled, an impactor which is similar but larger than the final stem is used (Section 1.7). When this impactor is solidly impacted to the required position, a trial reduction of the hip joint can be performed. Once this is satisfactory, the impactor is removed and the 'neomedulla' is pressurised with cement, followed by final placement of the stem as for a primary hip replacement.

1.4. Subsidence

With the Exeter and other collarless polished taper stem designs[24] an initial subsidence is expected, often of 1mm or less followed by a much reduced annual creep reported of around 0.3mm. This is thought to provide a 'taper slip' fit with proximal femoral loading, and is one reason for placing an air filled centraliser on the tip, to prevent end bearing of the implant. This same mode of action is thought to also function with impaction grafted femora. Different stem geometry leads to different modes of subsidence and at different interfaces[25-27]. The Charnley Elite has reduced axial subsidence but marked postero-medial rotary subsidence, occurring at both interfaces of the cement.

Recent reports of impaction grafting have demonstrated highly variable results between centres. The Exeter group has the longest experience and has performed over 500 femoral impactions. The first 68 cases will have been followed up beyond 10 years with a minimum of 7 ½ years. Only 1 patient in this initial group so far has failed as a result of aseptic stem loosening. Other centres however have had a different experience. In Bristol, a group of 79 hip replacements followed up for just over one year, in whom impaction grafting of the femur had been performed, 9 (11%) showed evidence of massive subsidence[28]. This was defined as subsidence of over 10mm and in all cases occurred in the first 3 months post-operatively. Six hips required subsequent re-revision. Interestingly one hip was reported to have subsided to a position of stability. A series in Australia found similar subsidence values of 9mm (range 2-37mm) compared to cemented revisions at 24 months[29]. One problem with impaction grafting is that the decision of when the graft is suitably compacted is very subjective and this may explain the variation in results. This has provoked recent interest, with some centres attempting to quantify an endpoint of compaction (unreported work, J Richardson – Oswestry, UK), though this is still in its infancy. The endpoint of satisfactory compaction in this thesis was determined as that stage when 10 blows with the mallet failed to cause further stem movement, as measured on the calibrated cannulated phantom.

Torsional stability is thought to be less dependent to stem anteversion but related to stem x-sectional geometry.

From this information we can see that if subsidence occurs it is usually in the immediate post-operative phase, can be very large and if ongoing, is often detrimental.

1.5. Mechanisms of Failure of Total Hip Replacement

Comparative study of outcomes of different THA's, such as the Swedish hip register or experience with the matt Exeter stems and more recently the 3M Capitol hip prosthesis, have allowed orthopaedic surgeons to identify design errors and implant incompatibilities in primary hip arthroplasty[6;30]. However, precise design characteristics that predetermine a successful outcome in hip arthroplasty have yet to be defined [31-33]. Analysis is further complicated as THA is a multi-step procedure, with confounding variables ever present (e.g. Boneloc cement [30]). This is particularly the case for revision surgery where techniques are still evolving and long term outcomes for large numbers are not available. The utilisation of bone replacement at the time of revision surgery is dependent on many factors, such as surgeon choice and extent of bone loss. Retrieval studies have shown that the bone resorption [34-36] is likely to be the result of mechanical events[37-41] from either accumulated-damage failure (micro-cracks, debonding and micromotion) or particulate-reaction failure scenarios (giant cell reaction, fibrosis, osteolysis) or more likely, a combination of the two.

Histological analysis of retrieved impacted graft has been reported as individual case reports, but the sequence of events is as yet, only just coming to light[42; 43]. Impaction grafting is a unique technique where the surgeon's technique has an effect on the physical properties of the graft.

1.6. Bone Graft

Autograft provides the best bone for re-incorporation in impaction grafting, but donor site morbidity and lack of volume usually prevents harvesting autograft from an individual at the same time as performing their revision hip surgery. Femoral heads removed at the time of primary hip surgery and subsequently deep-frozen are a

ready, sterile supply of allograft, which is the next most preferable graft type. Immunogenic incompatability between donor and recipient is attenuated by the act of freezing. The marrow elements within the cancellous bone are thought to be responsible for the majority of this immunogenicity[44] and in the past have been recognised as only a minor problem[45-48]. There has been recent interest in the detrimental effect of this immunogenic response[44; 49-52], with a number of authors already reporting improved incorporation and biomechanical performance with histocompatability-matched grafts[53]. This thesis touches on an alternative potential means of reducing this immunogenic load, by washing the graft. Unsurprisingly Hyligers[54] has found bone graft cells to be viable (in vitro) at 6 months, with the relevance of this and the host response to them as yet unclear.

Increased demand and the move for centres to perform their own revision operations has prompted many smaller centres to set up facilities to perform their own bone banking of allograft femoral heads at the time of primary hip arthroplasty. Alternatively, large amounts of bone could be harvested in a clean manner from cadaveric donors and then sterilised. Current sterilisation techniques still produce bone of an inferior quality with regard to incorporation compared to fresh frozen allograft[55; 56]. Only demineralised bone shows increased osteoinductive potential. Concerns have been expressed over the ability to adequately destroy pathogens, such as viruses when they may be present. HIV infected bone is not sterilised[57] by the current dose of 25 kGy. The irradiation dose required to inactivate a potential viral load and achieve a sterility assurance level of 10^{-6} probability of virus surviving is 89 kGy. The use of 89 kGy irradiation would almost certainly denature the entire integrity of the bone. Interestingly, some centres with the highest reported subsidence rate, have been using irradiated bone (25kGy)[29].

This thesis tests the mechanical shear strength of impacted graft according to engineering principles for testing aggregates, as previously reported[58]. The relationship between density (% porosity) and material properties, so characteristic of trabecular bone cannot be applied, as the graft no longer has structural continuity[53]. As a more valid representation, fresh frozen human allograft bone with clinically utilised bone mills was used for Phase I.

1.7. Cement Mantle

Kawate et al[59] examined 8 autopsy-retrieved femurs, looking at the thickness of the cement mantles around cemented femoral components. 5mm sections were made of these previously stable implants and examined by contact radiography. Although overall on the entire cross sections 9% of the aggregated cement mantles were classified as cement <1mm thick, 92 of the 101 cement cracks occurred in areas of the mantles that were less than 1mm thick. The impactors now used are larger than before, in an attempt to increase the thickness of the cement mantle. As the amount of cement is less than in primary hip replacement, any malposition of the stem within this cement will also reduce the uniformity of the mantle[60]. Studies have also shown that stem design, surgical factors and the amount of distal graft, influence the early stability of impaction grafted implants[61]. In Phase III of this project, identical stems, impactors and surgical technique have been used to allow comparison between the two groups. Standard optimum cement preparation techniques were utilised[62; 63].

1.8. Stem Design

Previous work in an ovine model by Brumby et al[64] involved a custom made stem tapered in the medio-lateral plane (6.5 degrees) only. For our ovine study it was felt important to reproduce a stem in current clinical use. A 4-degree, double tapered, polished stem modelled as a miniature, modular Exeter femoral prosthesis was chosen. The stem was similar to the human prosthesis in all dimensions except length. There is abundant literature on different stem materials and designs [62; 65-72], although little on the effect of different taper angles [61]. The stem used in our study has several advantages over the previous stem used for ovine study at this centre[64]. It will provide a more testing scenario for the graft as it is more likely to subside more rapidly than the 6.5 degree stem – indeed from theoretical mathematical modelling (Appendix) - ~1.5 times reduction in push-in force for each degree reduction in angulation. The narrower stem also allows more space to accommodate the impacted graft and the cement mantle.

1.9. Synthetic Materials

Bone graft alone, either morsellised or whole, has had some success in replacing lost bone stock[20; 73-80], however, limited supply and increasing concerns regarding transmission of pathogens has prompted interest in synthetic materials. There has been an increasing interest in bone substitute materials[15], which may be osteoconductive[81; 82] (providing a scaffold over which bone may grow) or osteoinductive[83] (active stimulation of osteoblast activity +/- a scaffold), although their current use and future role have yet to be defined, together with cost-benefit analysis. Developments in tissue engineering and recent interest in gene therapy[84] are providing further avenues of study.

Inert materials with high mechanical strength have been tested clinically[85-90]. Pro-Osteon, a naturally occurring material has been investigated as a bone void filler in several studies[91]. Apatite-wollastonite (A-W) glass ceramic has been used in combination with milled allograft and fibrin glue[86] with some success in revision THA's. Direct bonding between bone and A-W glass ceramic granules was seen histologically. There is no replacement over time of the lost bone stock, should a subsequent revision be necessary. Interest in bioactive materials has evolved to address this problem. Osteogenic Protein-1 (BMP-7) (Stryker Biotech) is a growth factor in the TGF-β superfamily and has been shown to stimulate bone producing cells in vitro and in vivo[92-95]. It may also enhance bone incorporation around implants, whereas Hydroxyapatite (HA) may be an alternative to bone allograft.

Controlled Release Glass - Corglaes®

The primary synthetic material under examination in this thesis is Controlled Release Glass - Corglaes® (Giltech Ltd. Ayr, Scotland), a soluble, non-silicated glass. There has been extensive previous clinical experience with this compound[96-99] though not as a bone graft enhancer. The properties and manufacture of Corglaes® are outlined in the Appendix.

A quantity of Tricalcium Phosphate/Hydroxyapatite – TCP/HA (Stryker Howmedica Osteonics, Berkshire, England)) was tested in Phase I only and is undergoing further

analysis by other authors using similar models to Phase II and III, based on refinements suggested by this thesis.

1.10. Previous Edinburgh University Research Laboratory Results

Impaction grafting of contained bone defects can be analysed according to Soil Mechanics Theory [100; 101], where the graft behaves as an aggregate, resisting shearing forces depending on its particle size distribution (grading), applied axial load (normal stress) and degree of compaction. In-vitro experiments were performed [58] using bone graft from femoral heads that had been morsellised and then preserved by washing in alcohol and acetone. These experiments showed the mechanical properties of this graft improved with increasing normal stress and also with increasing shear strains (strain hardening). Resistance to shear (the usual mode of failure) could be further increased by raising the compactive energy applied and / or by the addition of Corglaes® to improve the grading of the subsequent mixture. Milling bone while still frozen did not alter the resultant particle size distribution compared to thawed bone. Osteoporotic bone had a similar particle size distribution compared to normal bone, but there was quantitatively less.

1.11. Summary

The role of physical agents to act as bulking agents to help with the current demand for graft, or to improve the shear strength by improving particle size distribution, are currently under development and form the basis for this thesis. The addition of promoters such as chemical, biological or cellular, remains an exciting future prospect.

Improvements in surgical conceptualisation of the exacting impaction technique may reduce regional variability. Furthermore, a greater understanding of the properties of morsellised bone graft may allow centralised production of higher quality pre-milled and pre-washed sterile fresh frozen graft at regional centres, rather than in-house production of variable quality femoral heads.

Phase I

Biomechanical Aspects of Impaction Grafting – Shear Testing and In-Vitro Modelling

2.1. Introduction

For centuries engineers have been laying foundations and building roads with variable degrees of success as far as subsidence is concerned. The most durable structures have been built on solid bedrock[104]. Properties of non-solid (particulate) materials used for foundations have now been defined by Soil Mechanical Engineers, using experimental and mathematical models of sand, gravel and boulder mixtures. These engineers are able to predictably produce foundations and embankments with minimal subsidence. Using this knowledge of the behaviour of particles under load, this thesis analyses the properties of particulate bone graft[102;103].

Particle Size Distribution – 'Grading'

Soil Mechanics states that the mechanical properties of any collection of particles (aggregate) are dependent primarily upon the particle size distribution or 'grading',

as well as the individual properties of each particle. The particle size distribution of all test materials in this project was therefore determined using sieve analysis. Two different bone mills were chosen that were known to produce milled bone graft of different particle size distributions. Reconstituted mixtures of bone graft from these mills that theoretically, had improved particle size distributions were also tested.

Production of a 'well-graded' sample theoretically produces the aggregate most resistant to shear. This grading has been determined for spherical particles by Fuller[100-101] and is best understood by considering the problem of making a pyramid of marbles. Fuller has mathematically determined a graphical curve of particle distribution that represents the sequence of marble sizes to fit the 'gaps' (Figure 1.) which if carried to infinitely small sizes of marbles will allow an infinitely steep pyramid to be constructed (aggregate approaches properties of a solid, cf. fractals).

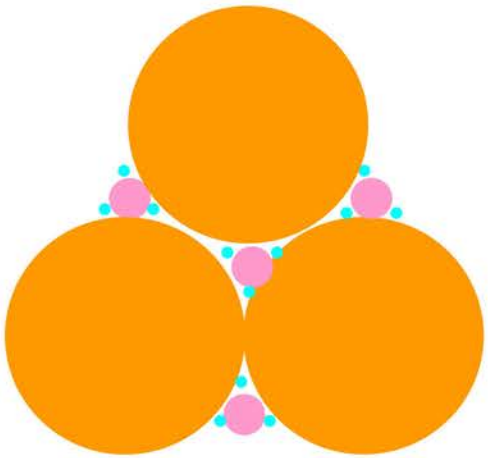

Figure 1. Relative particle sizes that allow ideal compaction

When considering irregularly shaped particles, it is normal practice to use a linear log of the range of available sizes, to determine an ideal mixture. The Linear Log particle size distribution has certain advantage in experimental use, for two main reasons:

1. Fuller is based upon packing of "spheres", which are quite different from sharp or angular particles such as those found in milled bone.

2. In theory, Fuller requires almost 30% of its particle sizes to be below the minimum currently produced by bone mills (the bone mills tested produce less than 0.1% of the graft as particles less than 300microns in size). This means that by using Fuller's curve, there may even be loss of strength.

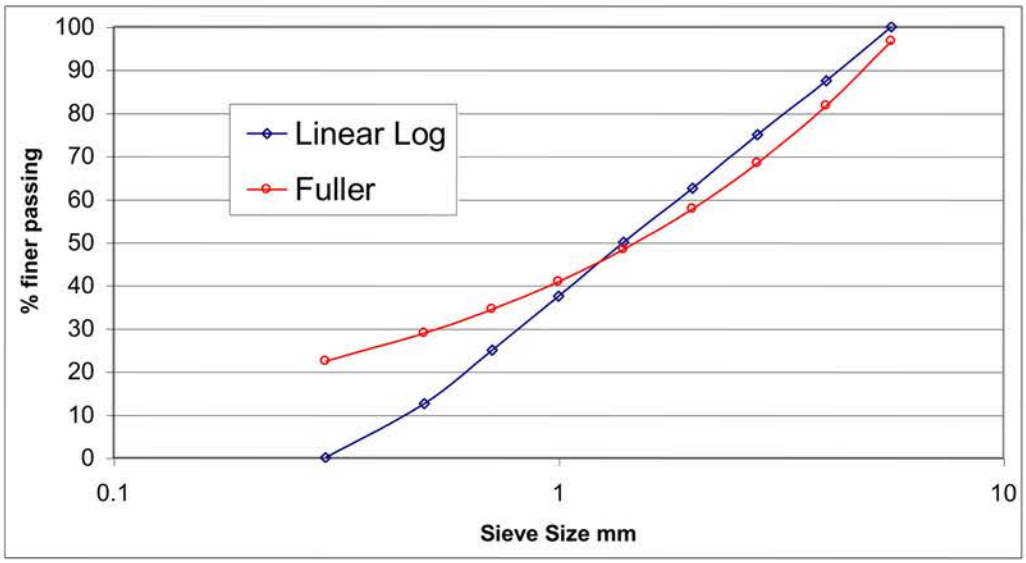

Graph 1. Particle size distribution lines for mixtures exhibiting either Fuller or Linear Log grading characteristics.

The linear log line was therefore used in this thesis. The sieve sizes chosen were based on a logarithmic scale. Therefore, if the same amount of material was used from each sieve, then an aggregate that had a linear log particle distribution could easily be created. The mechanical testing of a pure bone linear log could therefore not be performed on fresh milled graft as it necessitates sieving. Fresh, washed graft was used to produce the best approximation to the linear log line, based on the mathematical calculation of the ideal proportions from the two mills either side of the line. This technique, rather than adding different amounts of sieved graft to produce a linear log line, was used as it is nearer to what may happen in the clinical setting. In the future it may be possible to design a mill with variable grater sizes on a single drum which will allow production of fresh, well graded graft.

Mechanical Shear Testing

Shear strength is one of the most important properties of aggregates. It is a measure of their ability to sustain stresses without failure. The shear strength (τ'_f) of a granular aggregate like that of the bone graft depends upon the angle of internal friction (ϕ') and interlocking (c') of the particles. The frictional resistance varies in proportion with the effective normal stress (σ').

The relationship between these parameters can be expressed by the Mohr Coulomb failure law: $\tau'_f = c' + \sigma' \tan\phi'$.

The angle of internal friction (ϕ') or angle of shearing resistance is determined mainly by the particle size distribution (grading) of a sample and to a certain extent on the particle shape. Steeper pyramids of aggregates can be made with improved grading, as the particle size distribution is brought closer to a theoretical ('ideal') distribution, which contains particles of all sizes.

The Mohr Coulomb equation for bone graft is experimentally developed through shear tests on allograft samples. The shear strength is read from the shear strain Vs shear stress curves plotted for different normal stresses. From the Mohr Coulomb failure law it can be seen that ϕ' can be deduced from the slope of the line (cf. y = mx + c).

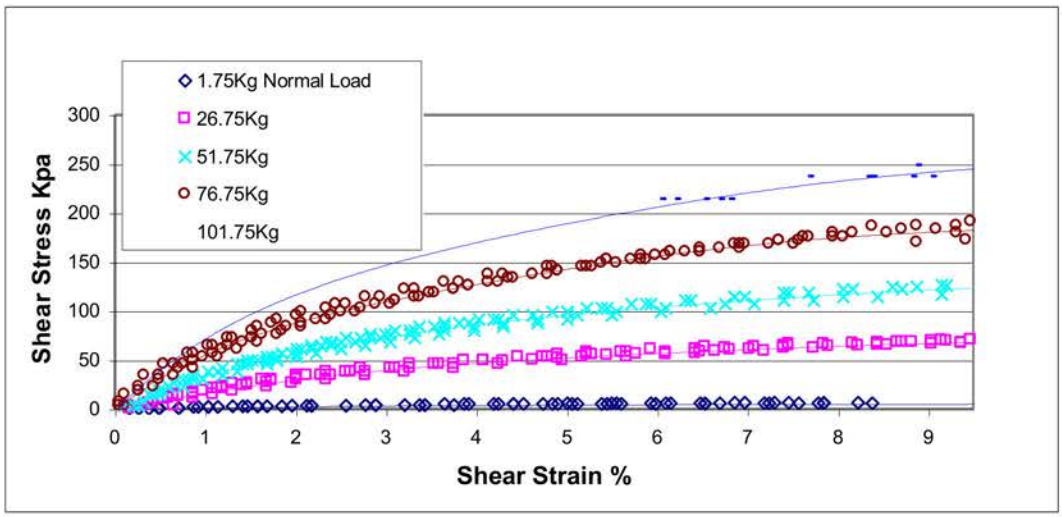

Graph 2. Stress versus Strain curves with increasing axial stress, for a typical test mixture (Aesculap 6mm Fresh Frozen Bone FFB).

In this study shear stress at 9.5% shear strain is taken as shear strength (Graph 2.) because the stress-strain behaviour of the bone graft was such that in most cases there was no further increase in shear stress by increasing the shear strain further.

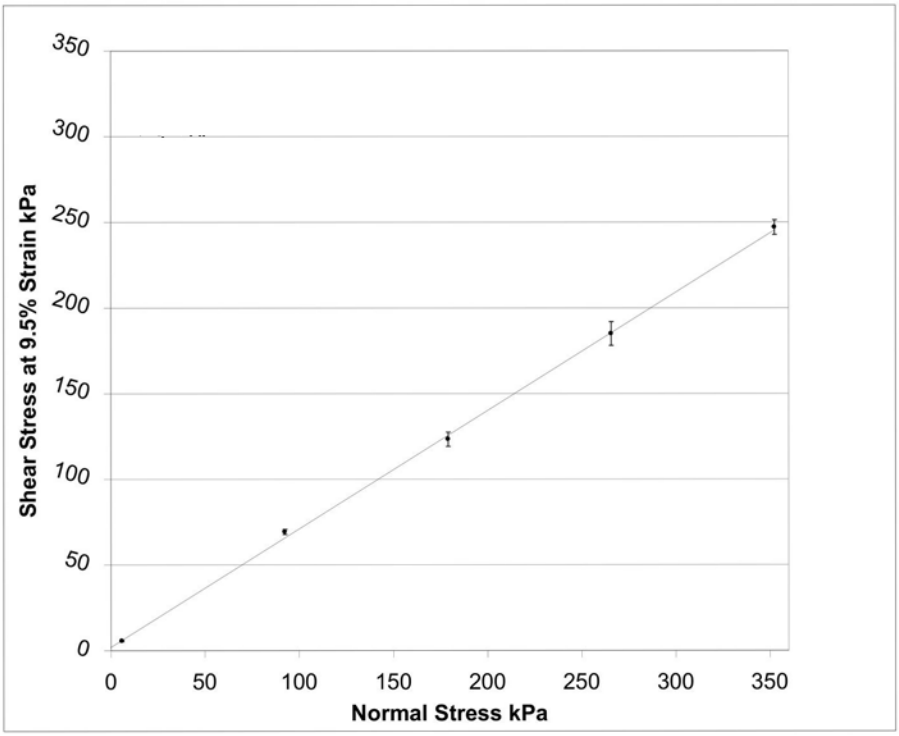

Graph 3. Mohr Coulomb failure envelope derived from graph 2, (kPa = kilo Pascals).

The best fit straight line variation between normal stress, σ', and shear strength, τ'_f, represent the Mohr Coulomb failure envelope (Graph 3.). The slope of the line, lies around 35 degrees for sandy soils, compared to 55 degrees for gravel. The intersection of this line with the shear stress axis represents the interlocking of the particles (c').

Shear strength of a granular aggregate can be measured by a number of different techniques, ranging from basic to highly sophisticated. The ideal method is 3

dimensional (tri-axial) testing[105], as the aggregate is allowed to shear in its weakest plane. Well-compacted graft is isotropic (properties equal in all directions) and thus a 2D-testing regime can be applicable. One disadvantage of the 3D method is the large amount of graft required for each test and complexities of impacting samples in an elastic membrane. The commonest method used by engineers is a direct shear test, in which samples are sheared across a predetermined 2 dimensional failure plane between two rings in a test cell. This was the technique adopted in this study.

Summary

According to Soil Mechanics theory, to produce an aggregate most resistant to shear stress, it should have the following characteristics;

1. Well graded particle size distribution
2. Low state of Hydration
3. Sequential layered impaction of well mixed material
4. Impacted with a large amount of Joules/Volume
5. Rigid containment

With these guidelines in mind, the mechanical properties of different mixtures of bone graft were determined, according to the null hypotheses below.

2.2. Null Hypotheses

The five secondary null hypotheses below were addressed in this chapter;

1. *"There is no difference between the mechanical properties of fresh graft from different bone mills"*

2. *"Well graded bone graft is not mechanically stronger than standard bone graft"*

3. *"Well graded (with synthetic material) bone graft is not mechanically stronger than standard bone graft"*

4. *"Well graded synthetic material used as a bulking agent in a 50/50 mix with bone graft is not mechanically stronger than standard bone graft"*

5. *"Bone graft that has been washed of fat and marrow is not mechanically stronger than standard bone graft"*

2.3. Aims

Previous work at our centre[58] has focused on the mechanical properties of preserved bone aggregates rather than of fresh bone graft used clinically. The aim of this project was therefore to consider the primary null hypothesis through analysis of the five secondary null hypotheses (Section 2.2), using thawed fresh frozen human allograft bone:

- Secondary null hypothesis No. 1; In the clinical scenario it is important to know if there are significant differences between different bone mills.

- Secondary null hypothesis No. 2; It is important to determine if attempting to improve the grading of the graft mixture by mixing predetermined mill products together will improve its mechanical properties.

- Secondary null hypothesis No. 3; Adding 'missing' particle sizes in the form of a synthetic material, with the specific aim of acting primarily to improve initial strength.

- Secondary null hypothesis No. 4; Improving the grading by bulking up the total volume of graft with the addition of a given amount of well graded synthetic material, with the specific aim of acting primarily as a bulking agent.

- Secondary null hypothesis No. 5; The clinical practice of washing bone graft to remove the fat and marrow to reduce fluid damping during impaction is used in a small number of centres. The rationale for this practice has never been proven, so a model to do this was devised.

2.4. Study Design

Drawbacks in our previous studies have rested mainly on the small number of tests performed and the use of bone that has been preserved in some way[58; 105; 106]. The

tests in this study were performed using a large stock of fresh frozen human femoral heads, obtained with consent from the hospital Bone Bank.

The particle size distribution curves for each mill were determined by sieving graft produced from five femoral heads that passed through each mill. Each different mechanical test required a further ten femoral heads, which were also prepared and milled in the same way. This involved, thawing in warm saline, removal of soft tissue and cystic areas, removal of all cortical bone remnants such as the femoral calcar and division into large chunks before milling (Figure 2.).

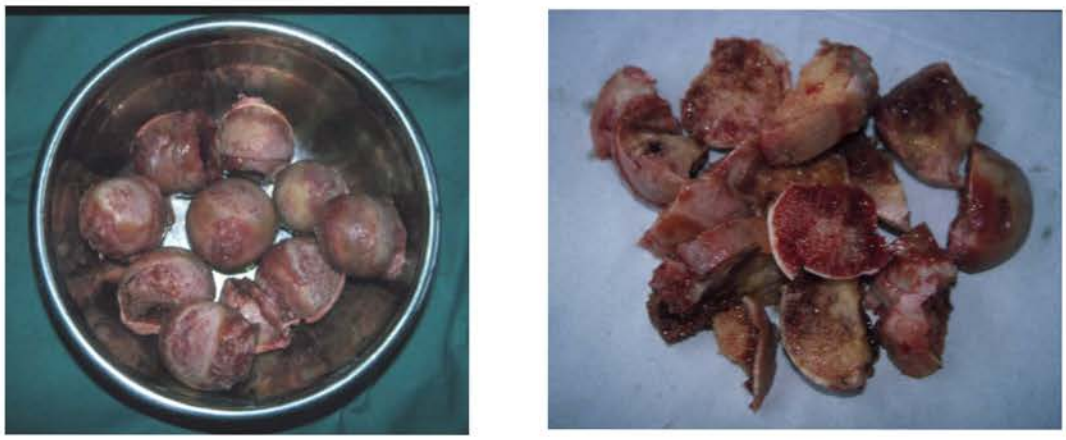

Figure 2. a) grouped femoral heads prior to b) division into cancellous chunks for milling.

Twenty-five separate mechanical tests were performed for each sample. The initial mixture was divided into five equal samples, which were each tested separately at the five different axial loads. The results are presented as a 'family of curves' - five individual lines at each of the five loads. All samples were kept at room temperature, in moisture retaining containers during the tests.

The test groups, based on the null hypotheses (Section 2.2), were as follows:

1. *"There is no difference between the mechanical properties of fresh graft from different bone mills"*

Aesculap 6mm mill

versus

Straumann mill

2. *"Well graded bone graft is not mechanically stronger than standard bone graft"*

Well graded bone graft mix*

versus

Aesculap 6mm or Straumann mill (1. Above)

* Grading of fresh graft can only be improved by combining predetermined amounts of different mill products. Mathematical determination of optimum grading predicted 66% and 33% from the 3mm and 6mm Aesculap mills respectively. An additional reconstituted linear log mix was also tested, but it should be remembered that this sample was washed in the production process – see 5. below.

3. *"Well graded (with synthetic material) bone graft is not mechanically stronger than standard bone graft"*

Well graded graft by adding synthetic material of missing particle sizes (Straumann mill plus Corglaes®)

versus

Aesculap 6mm or Straumann mill (1. Above)

4. *"Well graded synthetic material used as a bulking agent in a 50/50 mix with bone graft is not mechanically stronger than standard bone graft"*

Bulked graft with synthetic material (50/50 mixture by volume, at one standard compactive effort of graft (6mm Aesculap mill) plus idealised Corglaes® or TCP/HA (two separate groups)

versus

Aesculap 6mm or Straumann mill (1. Above)

5. *" Bone graft that has been washed of fat and marrow is not mechanically stronger than standard bone graft"*

Washed milled graft (6mm Aesculap mill or Straumann mill or Linear Log (comprised of sieve separated then reconstituted particles) (three separate groups, all washed over a 300micron sieve – see 3.2.2.)).

versus

Aesculap 6mm or Straumann mill (1. Above)

Figure 3. a) Aesculap mill 6mm and 3mm graters with resultant milled graft b) Straumann mill.

2.5. Stratification and Randomisation

The femoral heads were taken at random from the store where they were kept in unmarked, sealed, blinded containers. They had previously been provided for use with permission in humans, but were excluded from clinical use, due to potential contamination, either due to a positive bacteriology swab or unavailability of the donor at six months for seroconversion testing. These factors were not felt to prejudice the mechanical properties of the donor bone, or represent an unacceptable biohazard during testing.

The femoral heads were milled and the graft was thoroughly mixed in a single container to reduce the variation between different femoral heads. The data was taken down by hand for the shear testing and was inputted to a spreadsheet on completion of all the tests. This ensured that results were not available before the tests were completed, which may have influenced the experimenter.

2.6. Ethical Approval

Institutional ethics approval was obtained prior to the study, based on the study design, Infection Control and Health and Safety Guidelines. All tests were performed with adherence to Health & Safety Guidelines using Universal Precautions.

Chapter 3 Sieve Analysis

3.1. Introduction

Bone graft produced from a bone mill may be analysed to find the particle size distribution by passing it through a series of sieves. Previous studies have analysed samples of dehydrated or de-fatted bone as these samples can be sieved using 'dry' apparatus. Treating the bone prior to sieving may alter the actual particle sizes and distribution, either by mechanical or chemical effects. There are no reports of particle size distribution using 'wet' sieving apparatus. We have therefore performed both 'wet' and 'dry' sieving of graft samples to observe any difference. These earlier studies on dried graft aggregates[58] also used uniformity coefficient - a grading parameter sometimes used by engineers for guidance. However, the grading of aggregates is best determined by direct observation of its particle size distribution curve[101]. The particle size and distribution characteristics have been produced for the different bone mills, both wet and dry. On the graph the Linear Log distribution has been drawn for reference (Graph 6).

3.2. Materials and Methods

The particle size distribution curves for each mill were determined by sieving graft produced from five femoral heads passed through each mill (See section 2.4.).

3.2.1. Sieving

An Endocots™ Sieve shaker was used according to British Standards[107] for all analyses (Figure 4). The following range of sieve sizes was used; 8.0mm, 5.6mm,

4.0mm, 2.8mm, 2.0mm, 1.4mm, 1.0mm, 0.71mm, 0.5mm, 0.3mm and sump collector. 99.99% of the bone graft was trapped and separated between 5.6mm and 0.3mm. This range allowed determination of 8 fractionations for each sample.

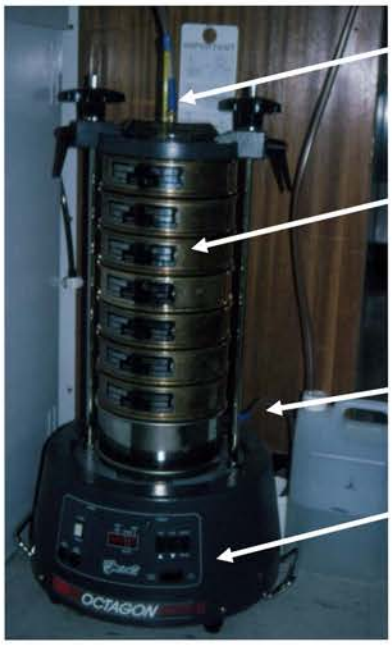

Figure 4. Wet Sieving apparatus

The wet spray head adapter, sealer rings and collection tub was used for the wet analyses. A spray head of water at 35-40°C, flowing at 10L/min was used to wash the bone across the sieves. Each sample was vibrated at 50Hz with intermittent vertical oscillation (Level 9, 2 seconds off, 5 seconds on) for 90 minutes. The first most apparent finding with this regime was that there was a significant problem with sieving wet graft. During the wet sieving process it was noted that 'clumping' of graft on the upper side of each sieve occurred. This was thought to be due to a combination of the natural hydrophilic nature of the graft and also the effect of small gelatinous strands of soft tissue, that were still present within the milled bone, preventing the normal passage of smaller particles to their correct sieve level. Increasing the fluid flow rate, oscillation power or time did not reduce this phenomenon. The wet bone from each sieve tray was weighted before and after being placed on a damp towel in an incubator at 40°C and 40% humidity overnight. The incubator was utilised to remove the fluid used to wash the graft through the sieving tower, as this would necessarily have been included in the first measurement.

It was found that the relative proportions of graft, when determined by weight, was not affected by the state of hydration. What was noted however was that the graft was no longer 'clumping' after the period in the incubator, and the particles themselves were still 'moist' and as flexible as when they were first milled. For this reason the samples were then re-sieved moist without washing and noted to pass rapidly to their correct sieve level. Each sample was vibrated at 50Hz with intermittent vertical oscillation (Level 6, 5 seconds off, 2seconds on) for 60 minutes. After this time, each sieve tray was weighed and sieving continued for a further 5 minutes until there was a less than 1% change in weight of any of the trays. The new particle size distribution was then determined.

3.2.2. Washing Technique

A technique for washing bone graft was devised so that it could be easily performed in a sterile fashion in an operating theatre. This was felt necessary so that if a benefit of washing was shown, then an identical technique could be used clinically. A British Standard sieve tower was made, consisting of a large sieve (2mm) over the 300 micron sieve, which was placed over a drainage tin with suction attached (Figure 5). The milled bone for each of the test mixtures was placed onto the top sieve and washed through. The top sieve helped to hold large particles stationary during washing and prevent blocking the lower 300 micron (0.3mm) sieve. All particles larger than 300 microns were trapped in the two sieves. Washing was performed with warmed 0.9% saline 'pulse lavaged' over the graft until the graft appeared clear of macroscopically obvious fat and marrow tissue, which passed through the sieve into the suction vessel. The contents of the two sieves were then combined.

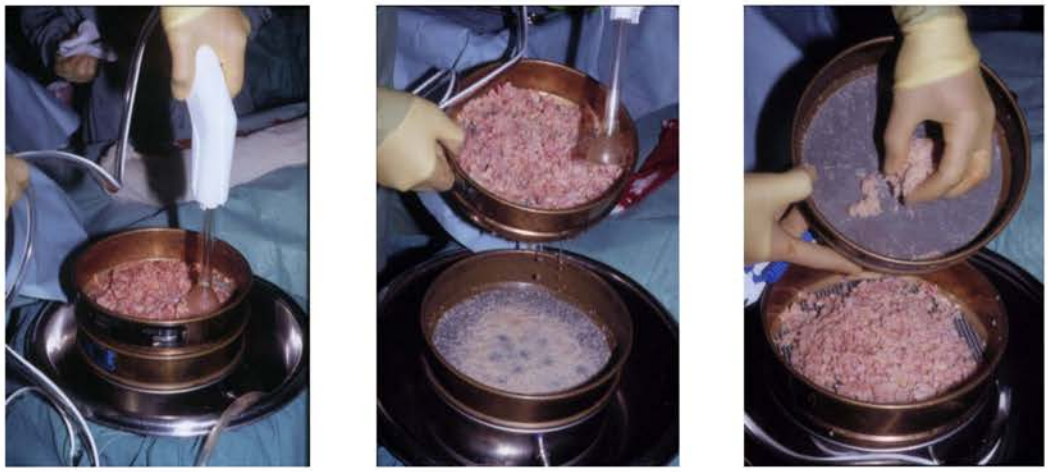

Figure 5. a) Washing apparatus sieving tower b) Washed graft trapped in upper 2mm and lower 300 micron sieves c) graft combined.

3.3. Validation

Wet Sieving

The weight of the sieve trays could not be used to determine when sieving was complete, as they were wet. A longer period of sieving was therefore used during wet sieving. Samples left to wet sieve through the tower for 480minutes were found to have a similar matching curve compared to themselves when sieved again on the above regime, indicating adequate sieving with our technique. This technique and dry sieving below, may not be applicable to mills that produce a lot of long rods.

Dry sieving

A sample of five femoral heads that had been milled and prepared 'moist' was analysed on five separate occasions by sieving, using the above technique. The results are presented graphically and demonstrate the repeatability of the procedure (Graph 4).

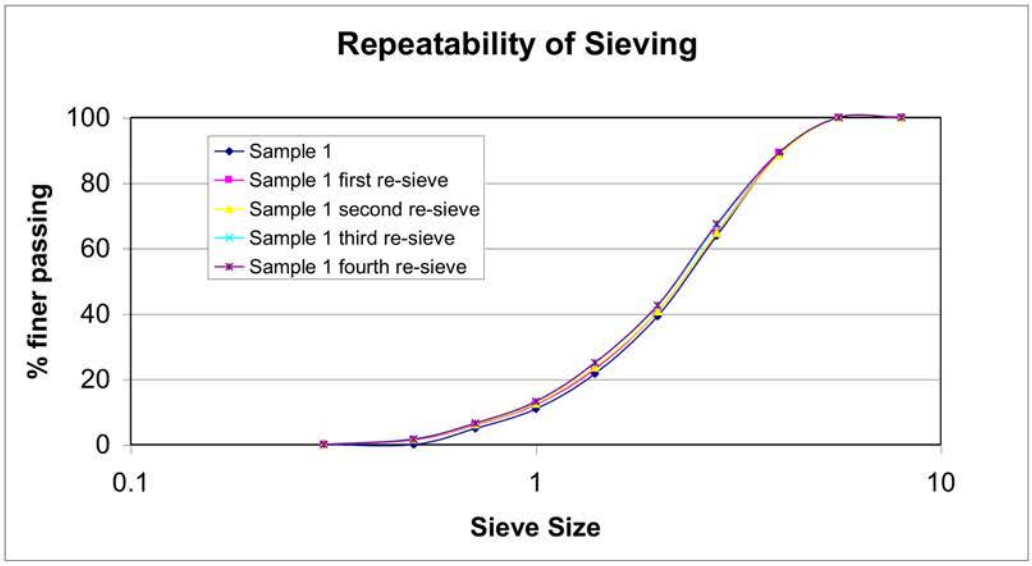

Graph 4. Repeatability of sieving.

3.4. Results

The grading curves for the different test samples are shown in Graph 5.

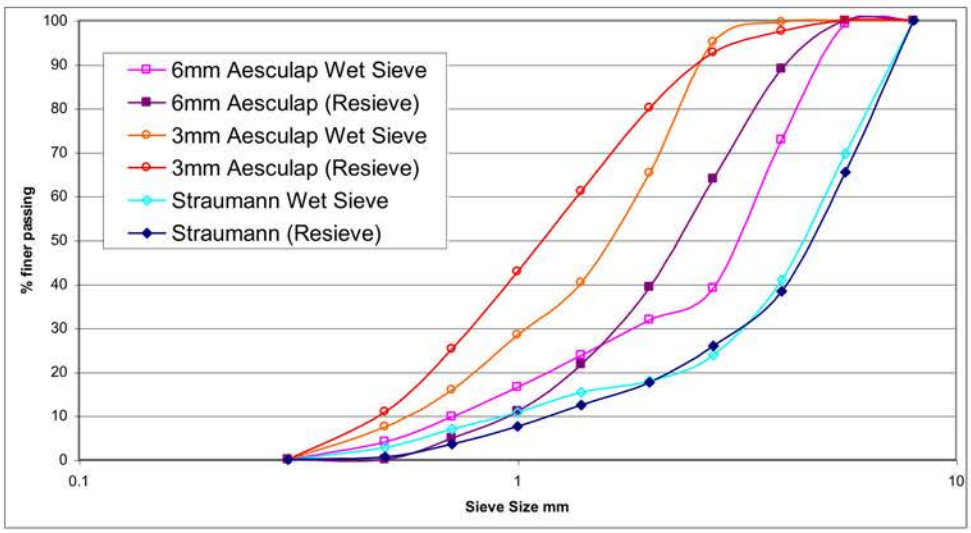

Graph 5. Particle size distributions for all test mixtures.

From Graph 5 we can see that there is a marked difference in particle size distribution for the two Aesculap mills (3 & 6mm) between washed and re-sieved bone graft. There is a much less obvious difference between the two Straumann mill mixtures. This difference was noted in the laboratory during the sieving process to be due to clumping of the relatively smaller particles produced by these mills – the Straumann mill produced a larger proportion of larger particles which were less likely to clump. This clumping is artefactual, as can be seen on re-sieving (Graph 6). For this reason the wet sieving results have been rejected.

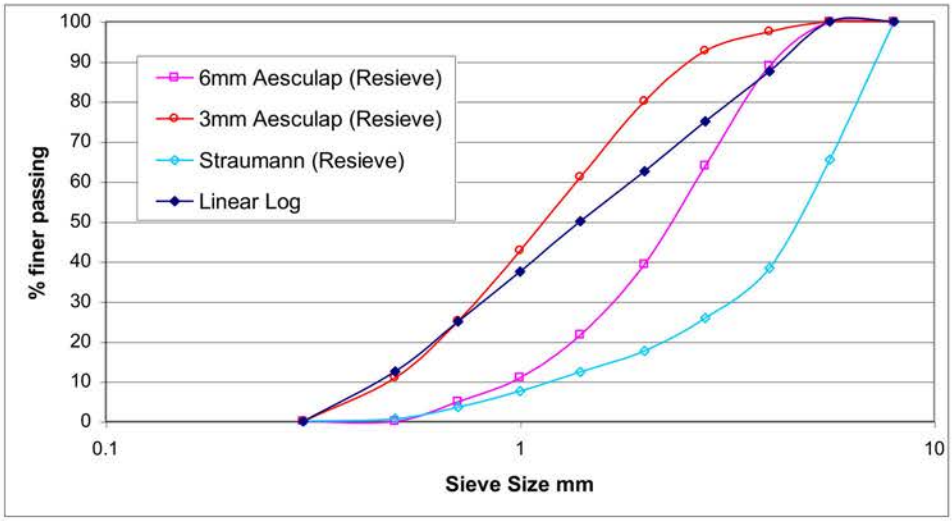

Graph 6. Final particle size distribution for each test mixture.

As noted earlier, for particles of irregular shape, a well-graded mix is a straight line on a logarithmic grading chart (Graph 1. Linear Log line). From this point of view, it can be seen that both of the Aesculap mixtures are reasonably well graded in the particle size range 1-5.6 mm, with slightly better conformity for the 3mm mill. The theoretical well graded mixture of 66% and 33% of the 3mm and 6mm Aesculap mills respectively (see 2.4.2.), was determined mathematically from Graph 6 and confirms this analysis, lying closer to the linear log line.

The best way to characterise grading is through the shape of the distribution curve. Both of the Aesculap samples are better graded than the Straumann -they are closer to the Linear Log line and the Straumann line constantly stays on one side of the

Linear Log line. The curve for the Straumann mixture is flat in the small particle size range and rises steeply in the large particle size range. This indicates an absence of small particles and poor grading.

The particle size distribution (grading) for the 3 mills improves from the Straumann to the 6mm Aesculap and to the 3mm Aesculap respectively. We can also predict that the theoretical well-graded mixture of 66% 3mm and 33% 6mm Aesculap mills respectively, should be the best-graded mixture. Therefore we can conclude the relationship of the test mixtures is as shown in Figure 6.

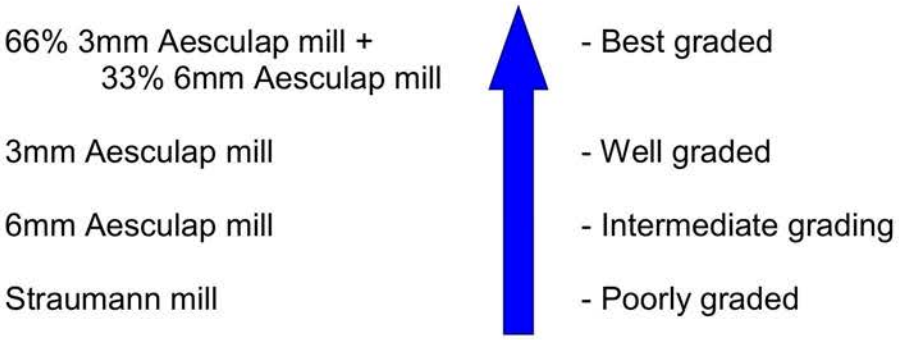

Figure 6. Mixture particle size distribution (grading). The arrow indicates predicted increasing shear strength

These ratings are important because according to Soil Mechanics theory, the level of grading should be proportional to the shear strength, as depicted by the arrow. This will be examined in the next chapter.

Chapter 4 Shear Testing

4.1. Introduction

Basic engineering principles of Young's Modulus or beam testing applied to solid materials cannot be applied to the particulate nature of our test aggregates[100-101]. Shear testing allows properties such as the angle of internal friction, cohesion and Mohr Coulomb failure envelopes to determine the various properties of aggregates.
Previous work at our centre on impaction grafting of preserved bone utilised two currently available devices normally used for testing civil engineering aggregates such as sand or clay. These were the Proctors impactor and the Jenike shear tester and their use has previously been described[58]. Certain modifications were made to allow fluid drainage during compaction of wet materials. The energy applied to each test pellet was equivalent to the energy to perform 'one standard femoral impaction', calculated from a simulation performed on a force plate. Five test samples from each of the test groups were mechanically tested. The samples from each test group were tested separately at five different normal loads. All samples were kept at room temperature, in moisture retaining containers during the tests.

4.2. Materials and Methods

The test groups that were analysed are outlined in section 2.4.

4.2.1. Proctors Impactor Design

The impacted pellet produced by the impactor, to be tested in the shear tester, should ideally have a diameter at least twenty times the average particle size. Too large a

diameter would waste test material, which was limited in its supply. As our particle range was from 300microns to 5.6mm, an impactor diameter of 60mm was considered optimal (~30 times greater than the mean particle size seen in Graph 6).

The Proctor's impactor that was used by Brewster et al[58] was modified, with the help of the Mechanical Engineering Department at the University of Edinburgh.

Figure 7. Proctors impactor a) before and b) after modification

The design was modified to allow for the compaction of wet material such as fresh human graft. To allow moisture, but not particles to escape (as liquids are relatively incompressible), minute holes were LASER drilled into the piston head. Fluid was also able to escape between the impactor rings. The plunger was originally designed to rise and fall with each blow, which had a considerable damping effect, especially when wet. This was modified to allow an equivalent mass to fall, acting on the plunger without damping. The energy applied to each test pellet was equivalent to one 'standard femoral impaction'. This has previously been calculated by measuring the energy applied to a force plate by the distal end of a femur, undergoing a 'routine' impaction grafting[58] and is equivalent to a 1.98kg weight, falling 6.5cms, 72 times. A different combination of number of heights and weights could have been used, but it was felt that this best represented the clinical scenario. This is accepted as

a limitation of the study, but was standardised throughout the tests to limit this potential variable.

4.2.2. Sequence of Impaction:

Each material to be tested was introduced into the top of the impactor in three equal portions, to ensure even compaction.

The first third was placed evenly in the chamber, the piston lowered onto the sample and the weight dropped 24 times from the given height. The piston was then rotated (to prevent test material sticking to its underside) and removed.

The middle third of the test sample was then laid on top of the first and impacted 24 times as before.

The remaining third was then added and impacted in a similar fashion, so that the finished pellet received 72 blows.

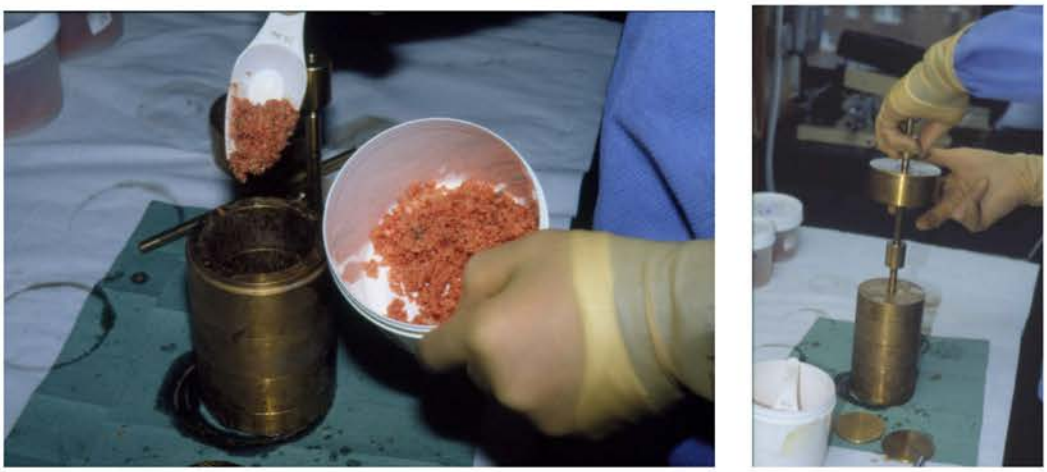

Figure 8. a) Test material introduced into impactor and b) compacted

The impaction rate was approximately 1.5Hz, similar to the clinical scenario and slow enough to allow fluid to escape. This was maintained throughout the study period.

4.2.3. Cam Shear Tester Design

The strength of all test materials in this project were determined using the Cam (Cambridge) shear tester, which was developed in collaboration with the Schofield Geotechnical Centrifuge Centre at Cambridge University.

The internal diameter of the test cell of the Cam shear tester was exactly the same as the Proctors impactor (60mm) – and thus would accept the pellets produced from the impactor exactly, based upon the ideal of at least twenty times the diameter of the average test particle. The metal parts in the vicinity of the test material were fabricated in aluminium, brass and stainless steel to allow testing of 'wet' material without corrosion. The test cell itself was not sealed and allowed for some escape of fluid on application of the axial load, similar to the clinical situation. A circular test cell was used to reduce 'edge effect', which can be a problem with square test cells.

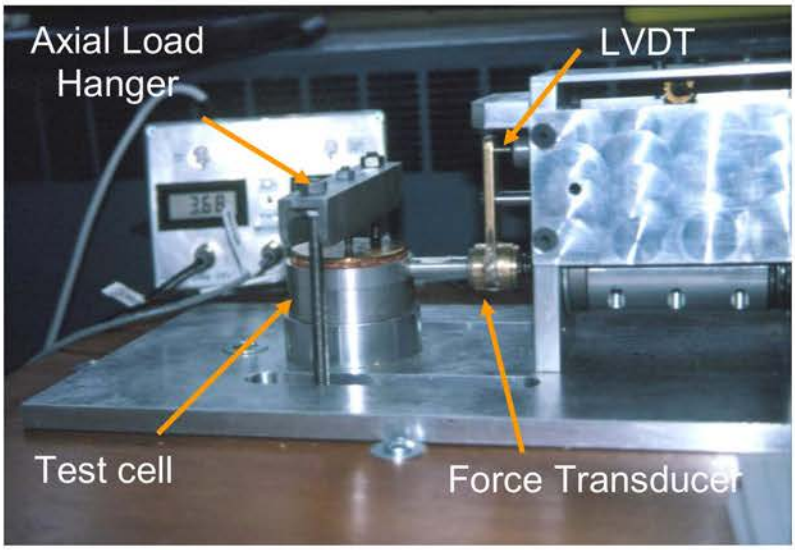

Figure 9. Cam Shear Tester.

In a square box, the corners suffer intense shear stresses and as a result they would accumulate shear strains and fail first. This reduces the contact area to an unknown amount and hence we cannot be sure of the shear stress (we measure horizontal force and divide by area to give shear stress). In a Jenkine type circular shear tester this problem is avoided. It is the stress concentration that matters, as once you have about 10% strain you have mobilised all the strength in the material so there is no question of any more increase in the shear stress. (10% of 60 mm diameter is 6mm and peak strength is reached for dilatant material at about 2 to 3 % strain).

The lower shearing ring was fixed to the base plate, the upper ring was mobile. A push rod attached to the upper ring received the shearing force during testing. This rod would cause the upper ring to move a constant distance in a constant time (constant strain rate) relative to the lower ring, and hence apply a shear stress to the cell contents. A load cell (force transducer) at the tip of the push rod recorded the load applied. The distance travelled was recorded with a linearly variable differential transformer (LVDT) in mm (see validation below).

To generate a family of stress / strain graphs, five separate normal (axial) stresses were applied and tested independently for each sample. The normal stresses were; 10kPa (the weight of the hanger alone), 95kPa, 180kPa, 265kPa and 350kPa (about one-hundredth crushing strength of concrete). These stresses were chosen to produce a family of curves within the lower range of normal human physiological stresses experienced by impacted graft in a typical revision hip replacement.

To obtain normal stress, the load in kg is multiplied by 9.81 to give the force (F) in Newtons (N). This is then divided by the area of the test cell in square mm ($\pi r2$ =2827.43 mm2). The resulting stress is in MPa (N/(mm2)). To obtain stress in kPa the resulting value is multiplied by 1000.

Figure 10. a) Compacted test sample b) transferred to shear tester.

4.2.4. Sequence of Testing:

1. The test sample was transferred to the shearing rings after compaction.

2. The normal load plate was placed over the test material to distribute the normal load evenly and contain the test sample within the test cell. The hanger was then engaged. The test sample was left to equilibrate for five minutes in the test cell.
3. Shearing of the test cell was commenced, recording the voltage from the LVDT and force transducer, which were converted to shear stress (kPa) and shear strain (%) respectively, from the calibration set-up (Section 4.3).
4. Once the test was complete, the sample was removed, broken up and re-mixed, together with any lost fluid collected with a brush.
5. All equipment was then thoroughly cleaned and dried before the next test.
6. The test sample was then re-impacted and tested in the above sequence, but with an additional 85kPa.
7. The sequence is repeated until a family of curves has been generated for the one sample up to 350kPa (100kg axial weight applied to the test cell).
8. The Mohr Coulomb Failure Envelope is plotted for each shear stress at 9.5% shear strain, against the normal stress. From this graph, the shear strength (τ_f), angle of internal friction (ϕ) and interlocking or cohesion (c) is determined.

Figure 11. a) Axial load applied via hanger b) further fat extrusion after 5 minutes equilibration prior to shearing c) shearing complete.

4.3. Validation

After initial installation of the Cam Shear Tester the LVDT and load cells were calibrated (Graph 7.). All the electrical equipment was turned on 10 minutes before

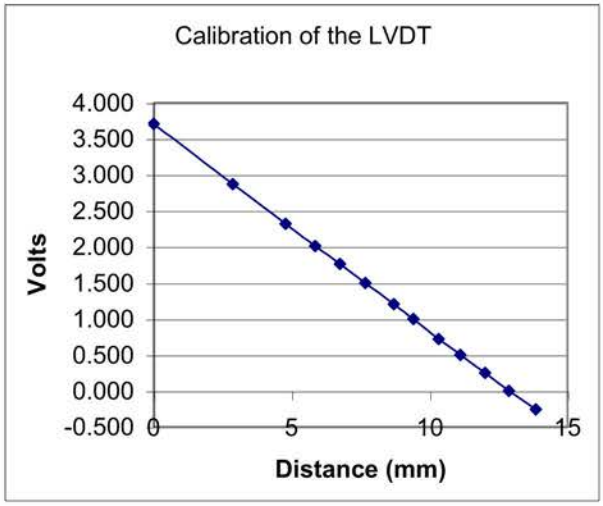

Graph 7. Load cell calibration

testing to allow for thermal equilibration of the sensitive voltmeters. Samples of sand with known shear strengths were then tested in the shear box and found to conform to standardised results.

The results for each human bone test sample at each normal load were inputted to an Excel spreadsheet as raw data voltage points. From the calibration graphs at the initial set-up, an equation to derive calibration constants for the LVDT (inverse of the slope of the Volts/mm line) and the load cell (inverse of the slope of the Volts/kg line after converting kg to kN) were derived. For each test point the shear stress (shear load kN / area of test cell) and shear strain (actual displacement expressed as % of test cell diameter) could then be derived. These were plotted graphically as a family of curves. The five individual samples and their family of five curves each were then plotted together. The degree of intra-sample error can be seen graphically at each normal load. As these samples were derived from the same source, the points were plotted together and a 'least squares' curve applied with the statistical software supplied with Excel. A manual graphical exercise was also performed, whereby the average stress at given strains for each of five curves at a given normal load was plotted. These curves were found to match the statistically derived curves closely.

A single Mohr Coulomb line (Section 4.2.4(8)) is therefore derived from several thousand points of data from twenty-five separate tests (five samples tested at five increasing normal loads).

Throughout the entire testing procedure all samples were kept moist in air-tight containers to prevent drying, as Currey et al[108] have shown that the modulus of elasticity of fresh bovine bone was changed significantly if the bone was allowed to become dehydrated.

4.4. Results

Graphical representation of the trends was the most appropriate means of representation. Mohr Coulomb failure envelopes with 95% confidence intervals is the normal means of comparison for soil mechanical engineers, with reliance on graph shape and absolute values rather than further statistical analysis.

The stress versus strain curves for each test sample is shown in Graphs 8 -16 below.

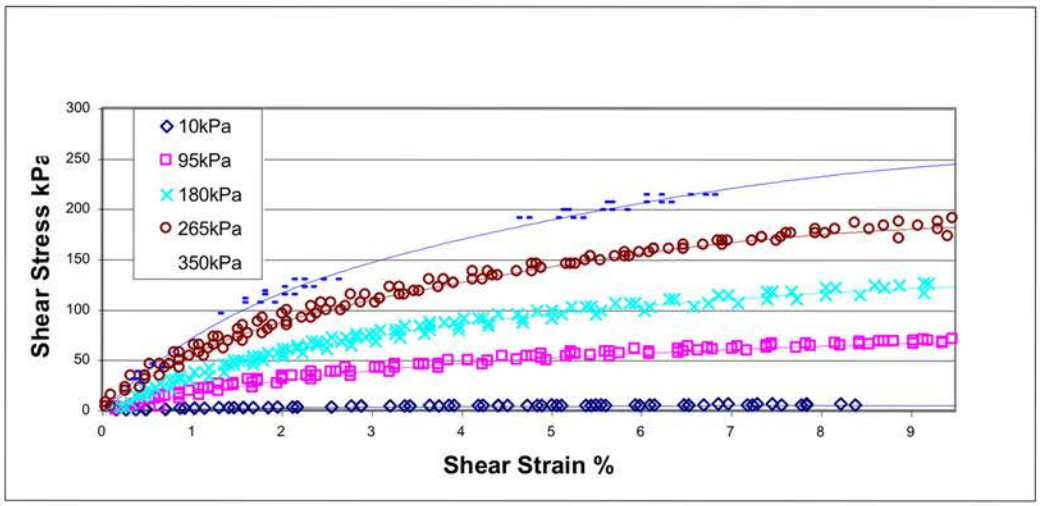

Graph 8. Aesculap 6mm FFB (fresh frozen bone)

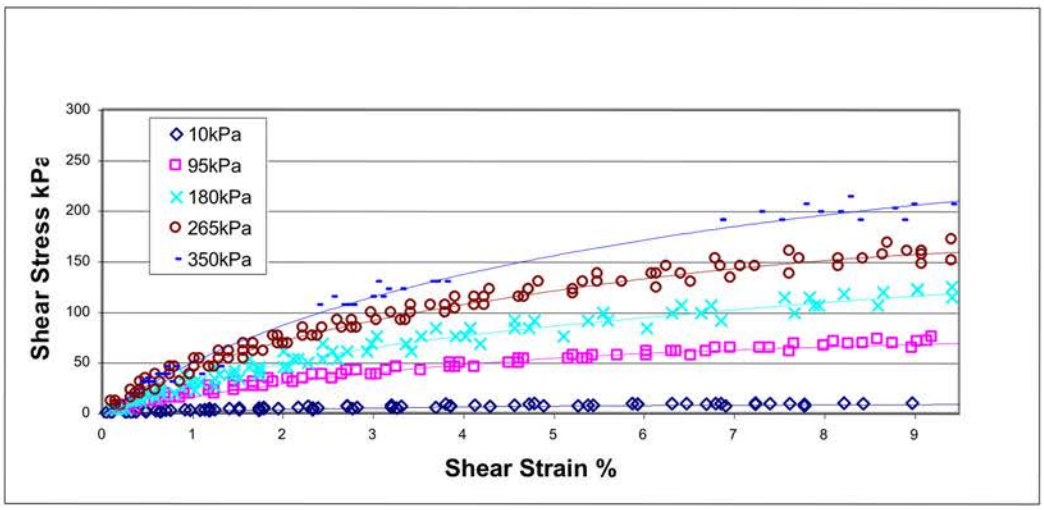

Graph 9. Straumann FFB

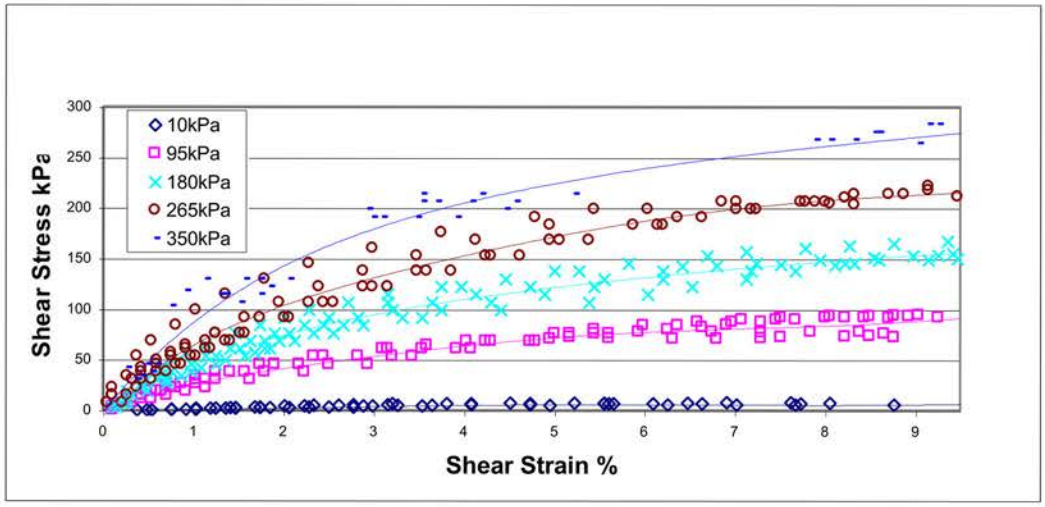

Graph 10. Straumann FFB Idealised to Linear Log with Corglaes®

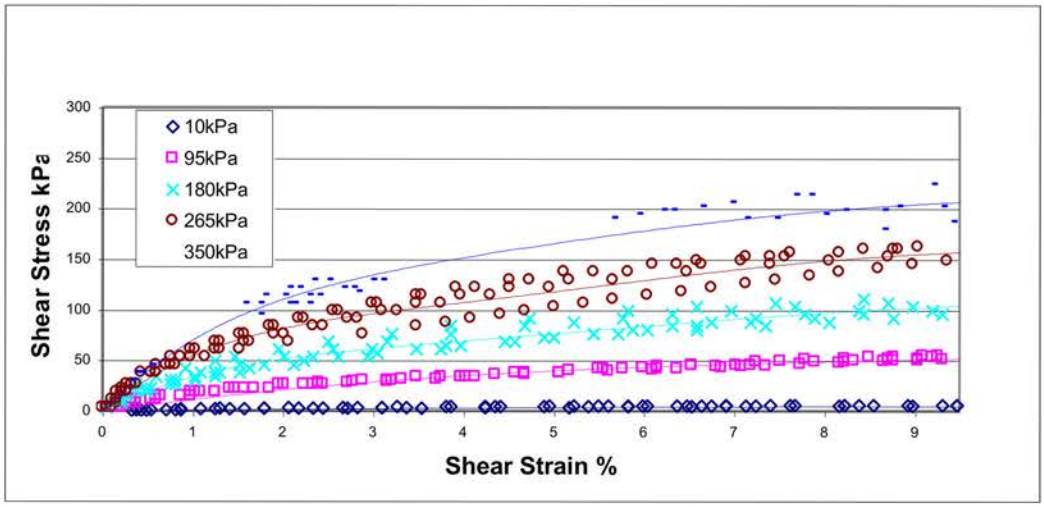

Graph 11. Aesculap Theoretical Idealisation FFB

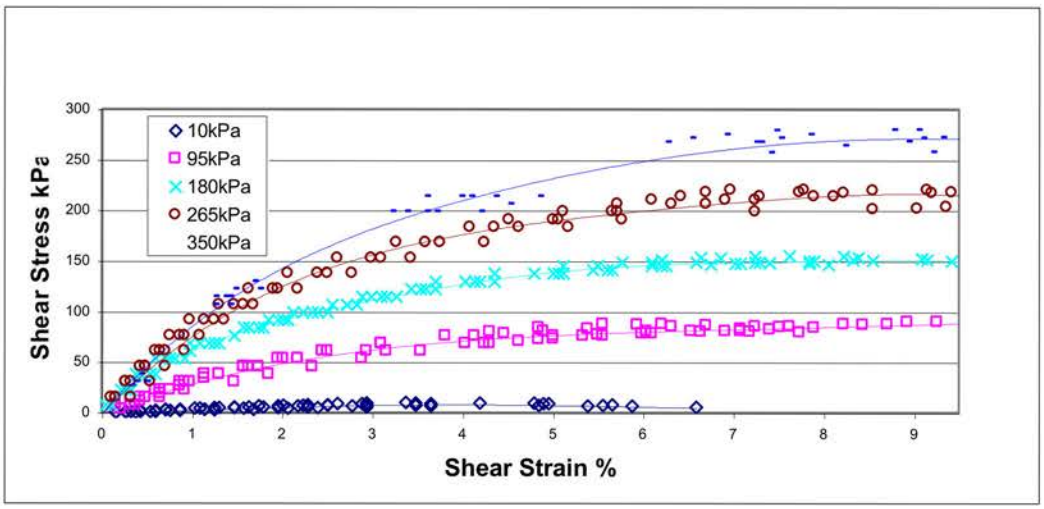

Graph 12. Aesculap 6mm FFB / TCP HA - 50/50

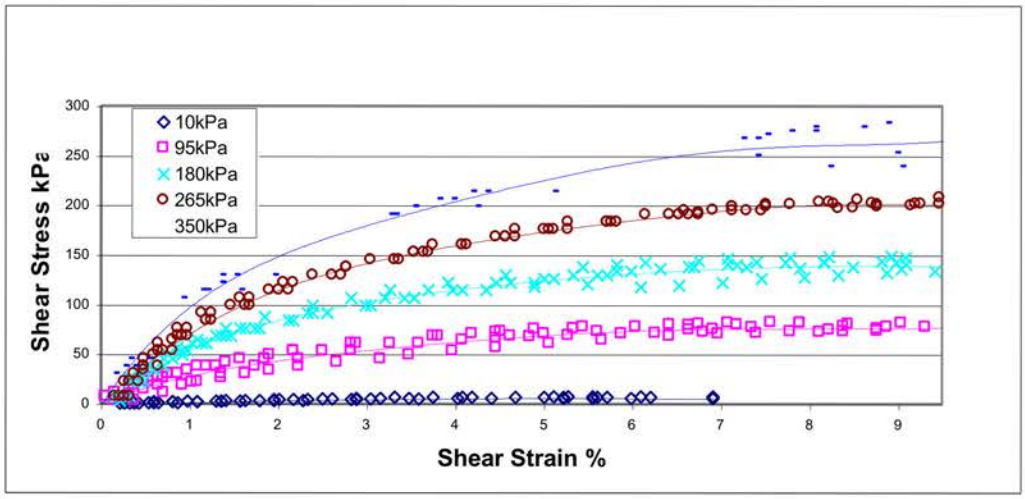

Graph 13. Aesculap 6mm FFB / Corglaes® - 50/50

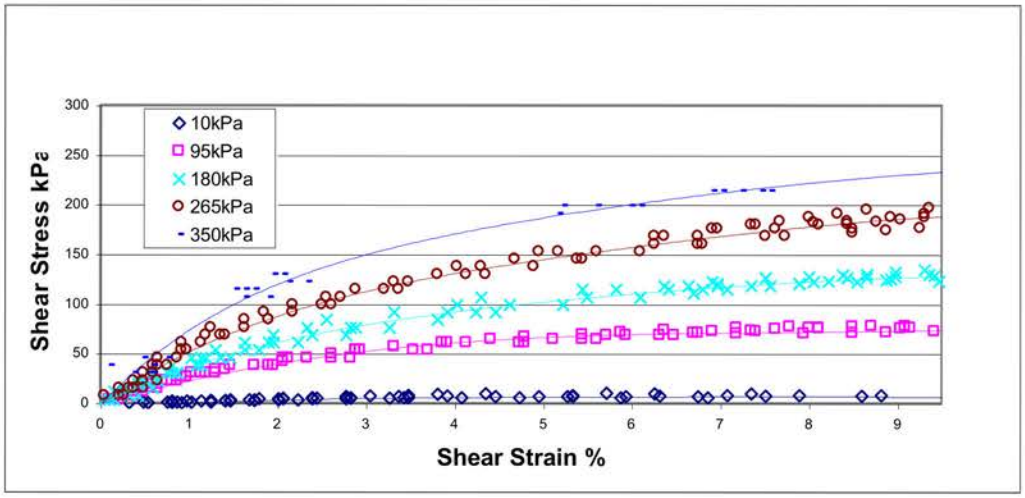

Graph 14. Straumann Washed

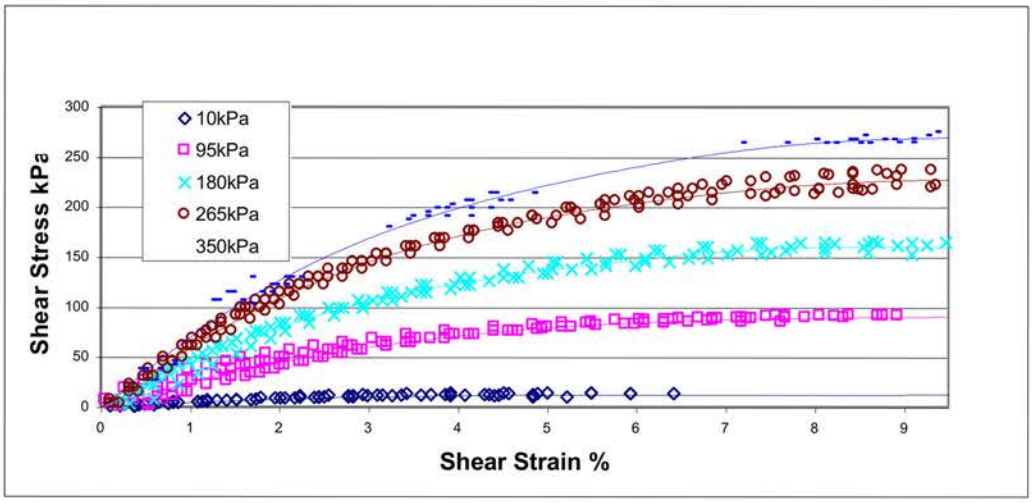

Graph 15. Aesculap 6mm Washed

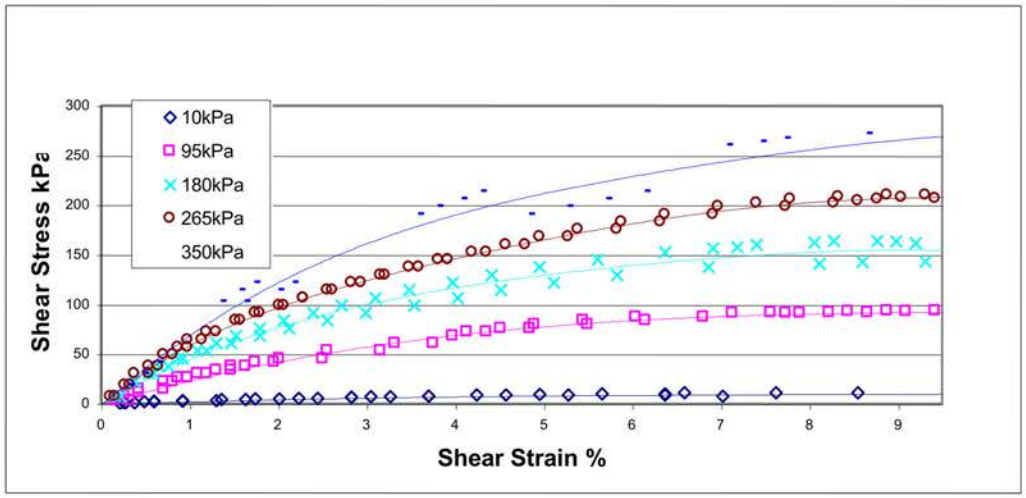

Graph 16. Aesculap Washed - Linear Log (2 test samples only)

From these stress versus strain graphs, the shear strength envelopes (Mohr Coulomb Failure Envelopes) for each mix at 9.5% shear strain are derived and are shown in Graphs 17 - 25.

Regression Analysis:

Individual results with regression analysis and addition of trend lines showing gradients, intercepts and R^2 values.

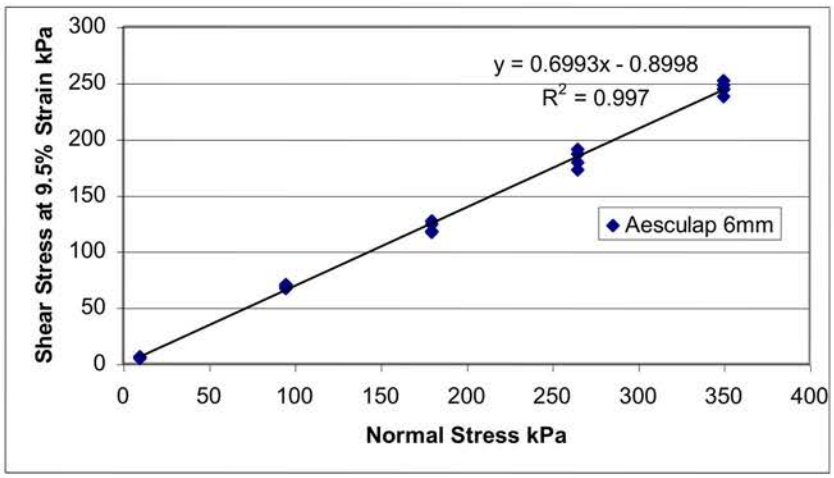

Graph 17. Aesculap 6mm FFB

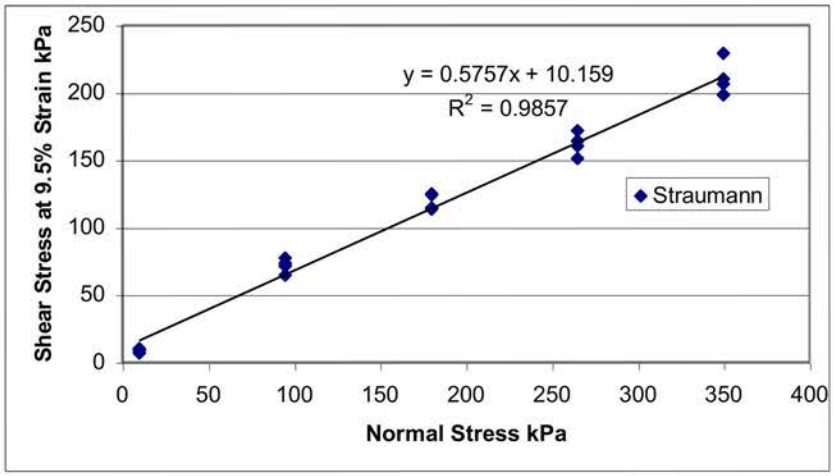

Graph 18. Straumann FFB

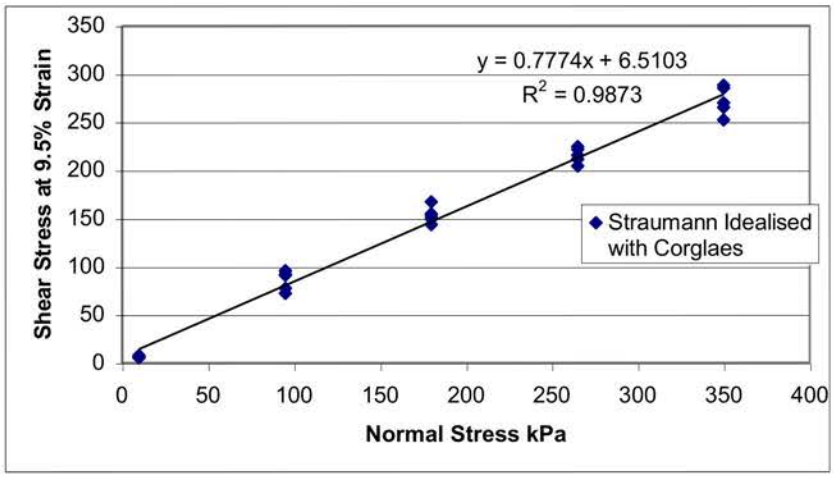

Graph 19. Straumann FFB Idealised to Linear Log with Corglaes®

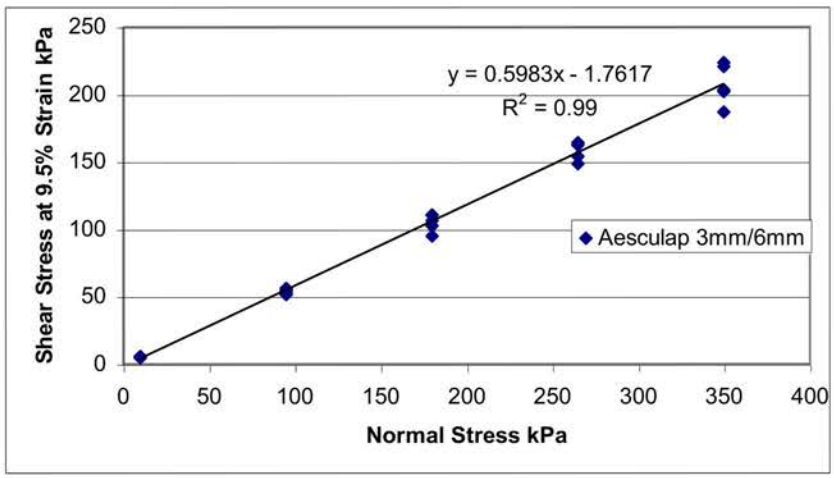

Graph 20. Aesculap Theoretical Idealisation FFB

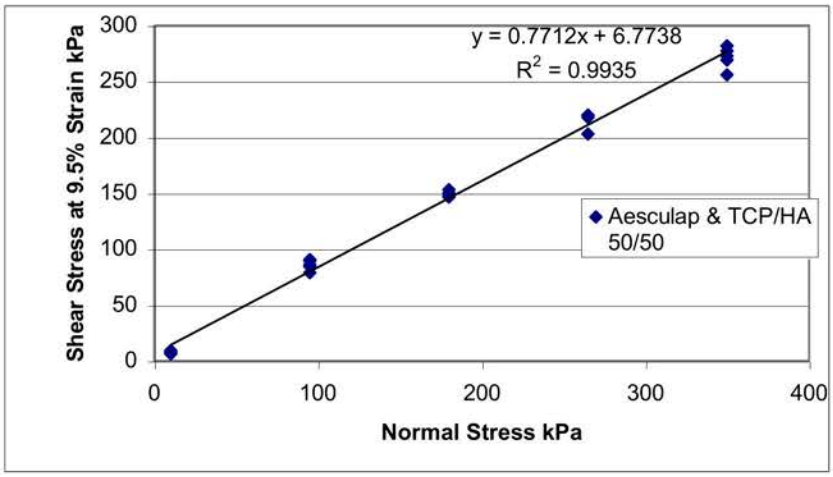

Graph 21. Aesculap 6mm FFB / TCP HA – 50/50

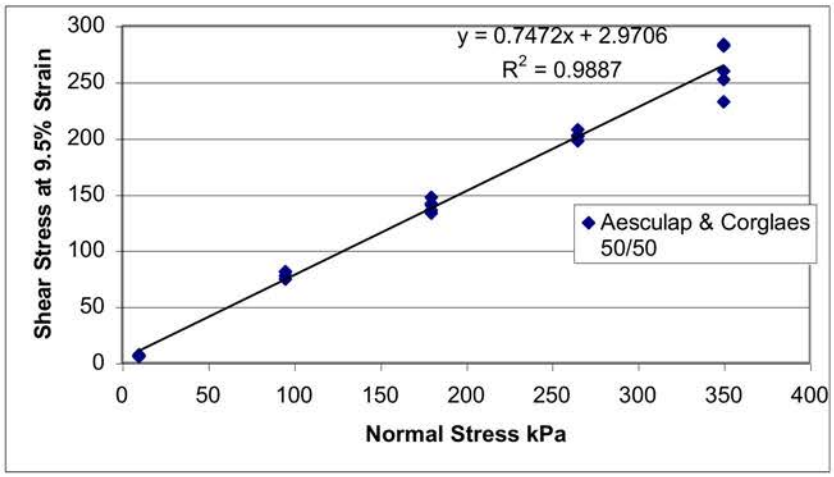

Graph 22. Aesculap 6mm FFB / Corglaes® - 50/50

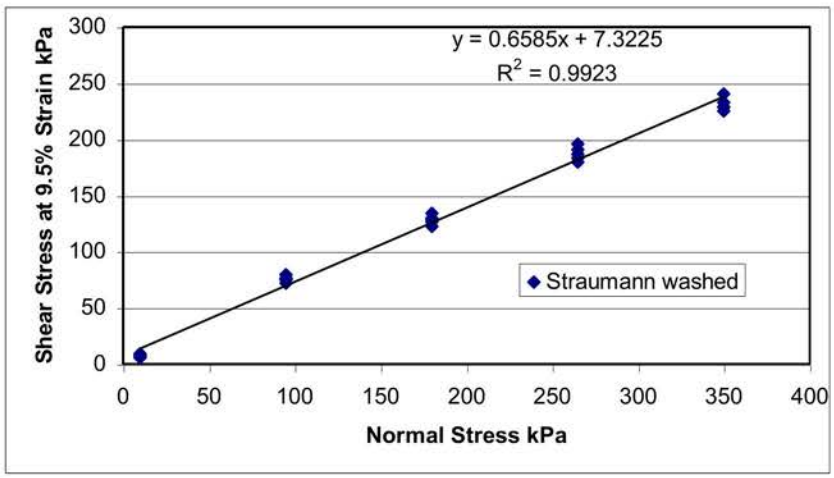

Graph 23. Straumann Washed

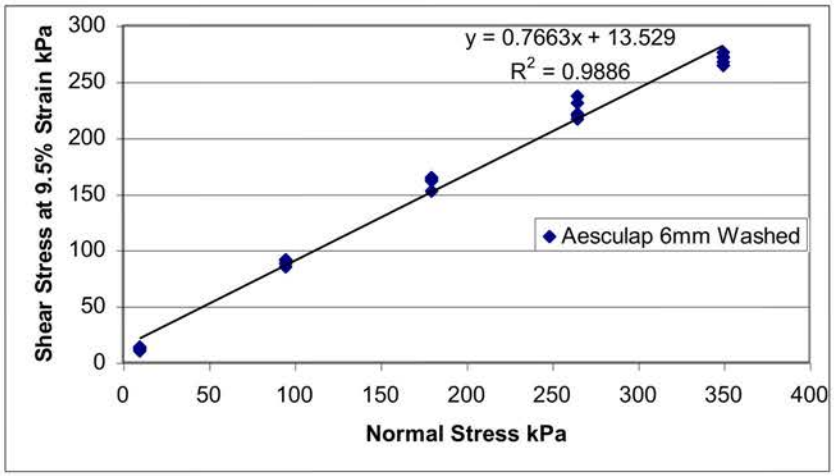

Graph 24. Aesculap Washed

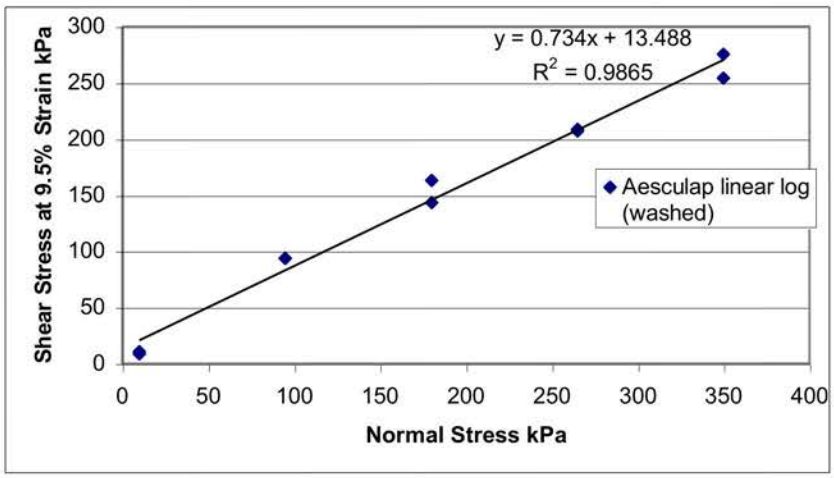

Graph 25. Aesculap Washed – Linear Log

It can be seen from these graphs that the experimental results satisfy the Mohr Coulomb failure law quite closely. A comparison of interlocking and friction angles is given in Table 1.

Interlocking (c') is read directly from the y axis intersection. The angle of internal friction (ϕ') = inv. tan of slope of the envelope (hence Atan dy/dx). The angle of internal friction and interlocking basically define the strength of the bone graft. Typically for sandy soils this could be 35 deg with 5-10 kPa interlocking. The shear strength (τ'_f) is calculated from the Mohr Coulomb failure law: $\tau'_f = c' + \sigma' \tan\phi'$.

	Interlocking (kPa)	Angle of Internal Friction Atan dy/dx	Shear Strength (kPa) at σ = 350 kPa
Aesculap 3mm/6mm	-1.8	30.9	**208**
Straumann	10.2	29.9	**211**
Straumann washed	7.3	33.4	**238**
Aesculap 6mm	-0.9	35.0	**244**
Aesculap & Corglaes 50/50	3.0	36.8	**264**
Aesculap linear log (washed)	13.5	36.3	**270**
Aesculap & TCP/HA 50/50	6.8	37.6	**277**
Straumann Idealised with Corglaes	6.5	37.8	**278**
Aesculap 6mm washed	13.5	37.5	**282**

Table 1. Shear testing results

The Mohr Coulomb graphs have been categorised into five groups according to the null hypotheses to allow easy comparison between samples. To allow greater graphical clarity, only the average values with 95% confidence intervals are indicated (error bars +/- 2 standard errors).

A grouped linear regression analysis was performed on the data; comparing Mix A washed with mix A unwashed etc. looking to see if the slopes were significantly different. All mixes were significantly different from each other apart from Mix B and C washed and Mix A washed and Mix B unwashed. For example, the effect of washing: Mix A washed versus Mix A unwashed $P<0.0001$, Mix B washed versus Mix B unwashed $P=0.0009$, Mix C washed versus Mix C unwashed $P<0.0001$.

Dealing with each null hypothesis (Section 2.2) in turn:

1. *"There is no difference between the mechanical properties of fresh graft from different bone mills"*

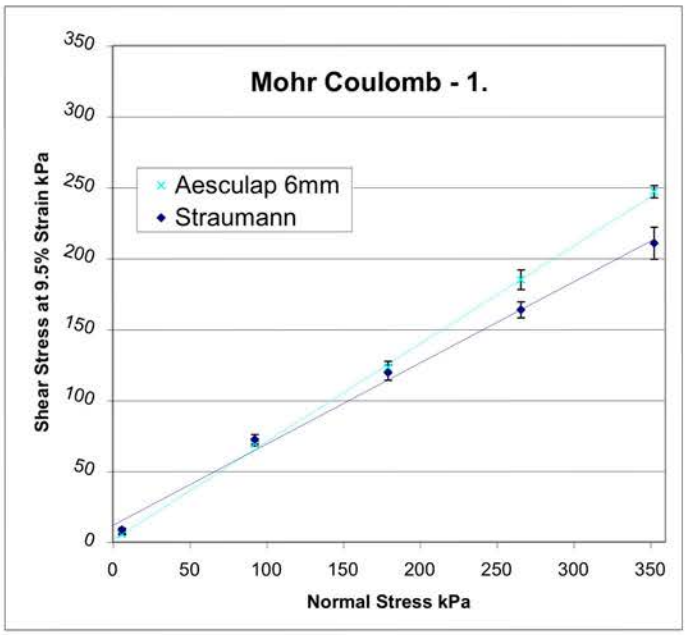

Graph 26. Aesculap 6mm mill – versus – Straumann mill (slope $\propto$ to shear strength)

There are large differences between the mechanical properties of fresh human bone graft derived from a 6mm Aesculap bone mill compared to the Straumann mill (Graphs 17, 18 and Table 1). These two mills were chosen due their widely different particle size distributions (Section 3.4, Figure 6). It was hypothesised that the poor grading of particles produced by the Straumann mill would produce an aggregate less resistant to shear. This is indeed demonstrated in the shear tests. The Staumann mill graft has a weaker shear strength of 211kPa compared to the Aesculap at 244kPa, athough there is a greater degree of interlocking between the larger fragments.

2. "Well graded bone graft is not mechanically stronger than standard bone graft"

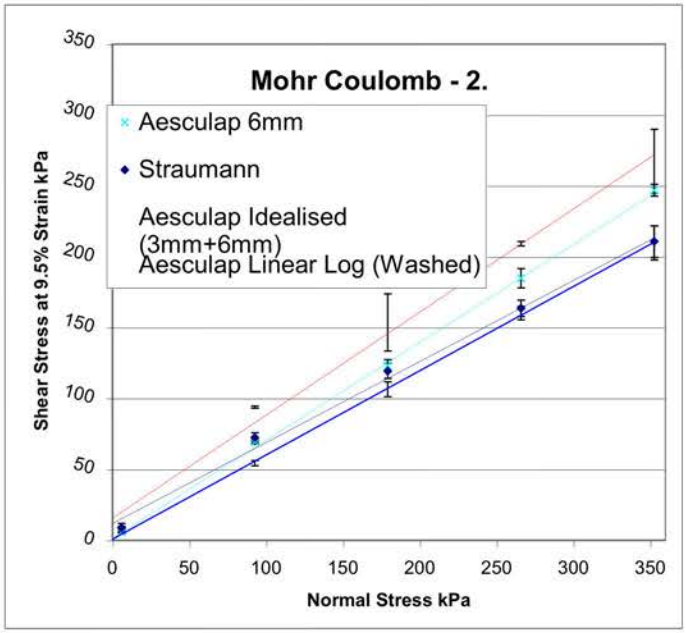

Graph 27. Well graded bone graft mix – versus – Aesculap 6mm or Straumann mills (slope $\propto$ to shear strength)

The theoretical 'idealised' fresh mixture (Aesculap 3mm + 6mm) is less resistant to shear (Shear strength 208kPa) than graft from the standard parent mill (Shear strength 244kPa) (Graphs 17, 20 and Table 1). This may be due to the reduction in interlocking due to graft from the 3mm mill producing smaller, rounded particles, or possibly due to increased fat and marrow release acting as an inter-particle lubricant (Section 5.1.2.).

The second theoretically improved (necessarily washed, sieved and reconstituted) mixture, based on the Linear Log line is stronger than fresh graft from the parent mill (Graph 17, 25 and Table 1). This may however be a consequence of the washing process as seen in the dramatic improvement in interlocking (13.5kPa)(see No.5 below). The experiment cannot be performed without washing.

3. *"Well graded (with synthetic material) bone graft is not mechanically stronger than standard bone graft"*

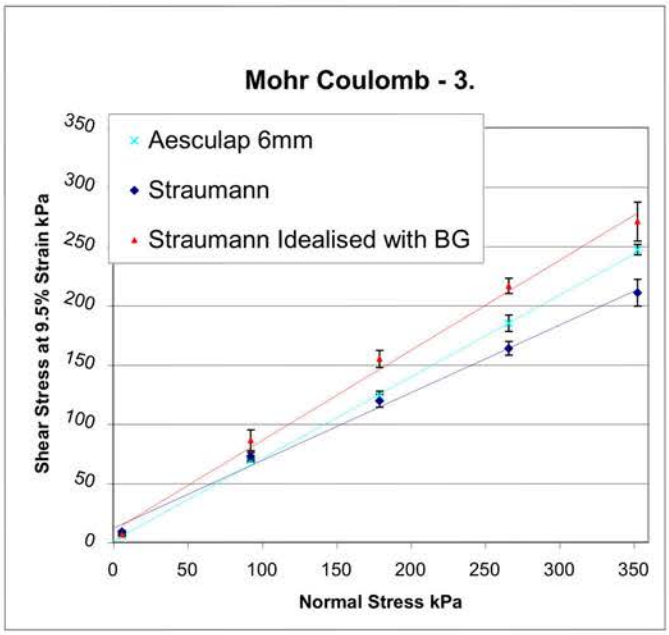

Graph 28. Well graded graft by adding synthetic material of missing particle sizes (Straumann mill plus Corglaes®) – versus – Aesculap 6mm or Straumann mills (slope ∝ to shear strength)

There was a significant improvement in the ability of bone graft to resist shear after the addition of the missing particle sizes by the synthetic material (Graphs 18, 19 and Table 1.). This was seen in the Straumann mill on the addition of Corglaes® (increase of 211kPa to 278kPa). It could be expected that such an improvement would be more marked on idealisation of the Straumann mill compared with the Aesculap mill (Graph 29), as the latter already has a relatively good grading . The interlocking of the Straumann and the Aesculap mills are reduced slightly with the addition of synthetic materials.

4. *"Well graded synthetic material used as a bulking agent in a 50/50 mix with bone graft is not mechanically stronger than standard bone graft"*

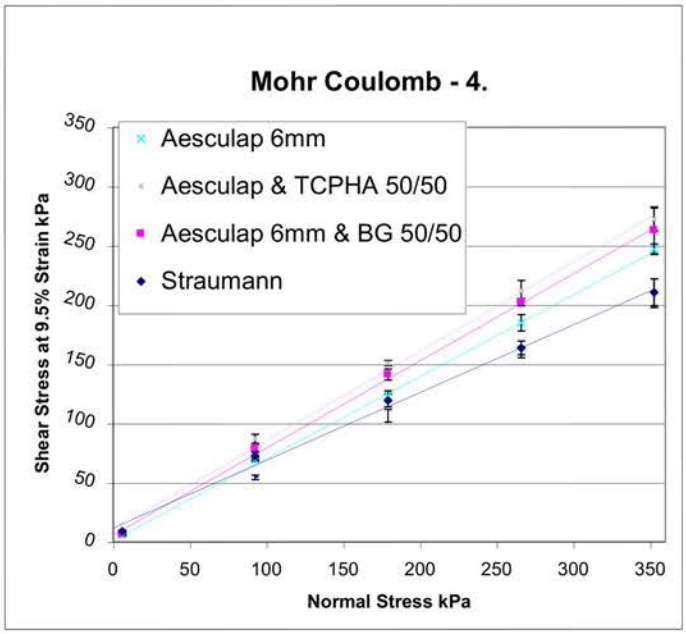

Graph 29. Bulked graft with synthetic material (50/50 mixture by volume, at one standard compactive effort of graft (6mm Aesculap mill) plus idealised Corglaes® or TCP/HA (two separate groups) – versus – Aesculap 6mm or Straumann mills (slope ∝ to shear strength)

All milled bone graft when combined with either Corglaes® or TCP/HA became more resistant to shear (Graphs 28, 29 and Table 1). This effect was seen in bone from both bone mills, and was particularly noticeable in the Straumann mill. This is possibly due to the greater overall improvement in the mixture grading when Straumann millings are combined with a well graded additive, compared to the Aesculap mill, whose initial grading is already good (Figure 6).

There is an increase in the shear strength between a 50/50 mixture of TCP/HA, compared with Corglaes® using the Aesculap mill. Improved interlocking, possibly due to the porous nature of the TCP/HA, that reduces the interparticle lubricant effect, may be the cause. This effect may not be shown with the Straumann mill, which releases less fluid and already has good interlock.

5. *"Bone graft that has been washed of fat and marrow is not mechanically stronger than standard bone graft"*

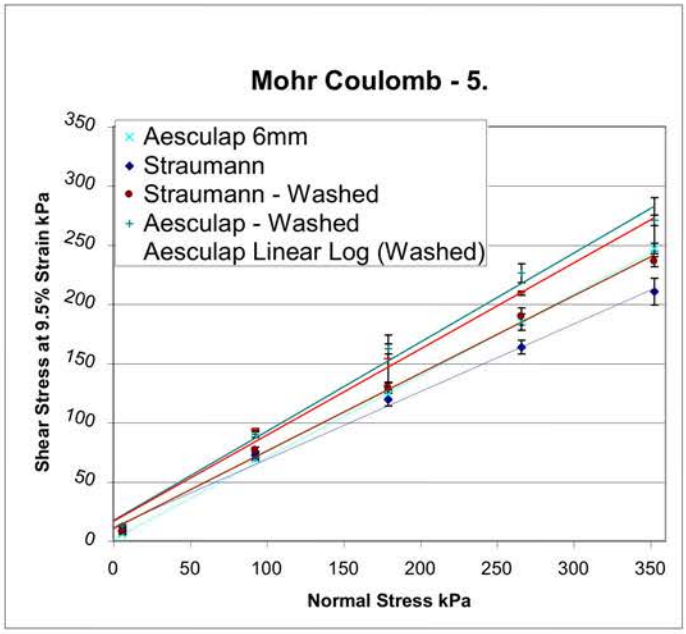

Graph 30. Washed, milled graft - three separate groups, all washed over a 300micron sieve (6mm Aesculap mill, Straumann mill & Linear Log (comprised of sieve separated then reconstituted particles) – versus – Aesculap 6mm or Straumann mills (slope $\propto$ to shear strength)

Washing the graft results in an increase of the corresponding shear strength for all mixes (Graphs 23-25, 30 and Table 1.). Thus at high normal loads a washed graft mix has a higher shear strength in comparison to the corresponding fresh graft mix. Shear strengths at a normal load of 350 kPa are listed in Table 1. and show a consistent increase in shear strength due to washing.

For the Straumann this increase takes place due to an increase in the friction angle (not much change in interlocking). For Aesculap both interlocking and friction angle increase, supporting the hypothesis that fat and marrow act as inter-particle lubricants.

Chapter 5 Phase I Summary

5.1. Discussion

5.1.1. Sieve Analysis

Different mills have previously been shown to produce different particle size distributions when a small amount of preserved bone was analysed[58]. Our tests confirmed this finding, using the more clinically relevant fresh human bone graft. The actual shear strength of the mills closely matched the predicted shear strength in Figure 6. The comparative distribution curves are similar in shape for both the 3mm and 6mm Aesculap mills, but poor for the Straumann mill. The 3mm mill is closest to the ideal linear log line. Further research looking at new mills that produce a linear log distribution is suggested.

Most of the data in the Engineering literature is for 'dry' sieving, with occasional use of wet sieving, usually for discrete particles. Fresh bone graft however does not behave as discrete particles when wet and tends to clump, often due to a combination of hydrophilic attraction and occasional fibrous strands between particles. Thus small particles may be held up from passing to their correct level due to this process. The technique described for partially drying the wet graft in a moist environment, re-mixing and re-sieving was therefore used. The results of this for each sample can be seen, confirming that the re-sieved material has a higher proportion of smaller particles. This later result was taken to represent the true mill output (Section 3.4. Graph 6).

Sieving was shown to be a highly reproducible method of determining particle size distribution, without significant errors of particle break up potentially caused by the sieving process (Graph 4).

5.1.2. Shear Testing

Although more than five test samples would have been a theoretical advantage, it was not possible to divide the original sample into more than five groups and still have enough for each test. Repeat tests were not performed because re-mixing and repeated testing of the material would have introduced error, due to irreplaceable fat extrusion on compaction. Twenty-five separate tests were performed on each sample, with regression analysis of the point data (Graphs 17-25) and the standard errors of the means (Graphs 26-30) represented graphically, showing significant differences between sample comparisons (Table 1.) (Section 4.4.).

Preserved segmental bone has previously been shown to have different mechanical characteristics to fresh bone[109-113]. Previous work at this centre has been performed on formalinised bone dried after washing in acetone and alcohol. The mechanical characteristics of fresh milled human allograft from donated femoral heads have only recently been reported[102; 103].

It is well known that granular materials can exhibit dilative or contractile behaviour on shearing depending upon their initial density. The addition of small amounts of fluid to the aggregate may be advantageous, causing an increase in the shear strength (analogous to making sandcastles). Soil mechanics theory recognises this as a feature of suction created in the pore fluid as the aggregate exhibits volumetric dilatation on shearing. However, if too much fluid is present and not allowed to drain, the mechanical strength of the mixture is reduced (analogous to quicksand). Again, this is explained based on the positive pore fluid pressures generated as the aggregate exhibits volumetric contraction.

Interestingly, the unwashed, well graded mixture (66% 3mm/ 33% 6mm Aesculap) was not stronger than the Straumann mill and was actually weaker than the 6mm Aesculap alone, with poor interlocking. This reflects the clinical impression that smaller mill graters produce wetter graft (‘slurry’). We hypothesise that this is due to the increased fluid released from the interstices of the graft acting as an inter-particle lubricant.

We found that the washed, well graded mixture (Aesculap Linear Log) and washed 6mm Aesculap alone were both significantly more resistant to shear than the washed Straumann graft. It is interesting to note that the washed theoretically improved (Aesculap Linear Log) graft was not more resistant to shear than the washed standard Aesculap 6mm mill. This was thought to be due to the 6mm Aesculap mill producing graft close to the ideal grading already, compared to the Straumann mill. The critical size for release of maximum fluid appears to be when the majority of particles are around 1mm in size (or smaller) and this is corroborated by microscopic examination of bone (Figure 12.). The well-graded mixture produced from the Aesculap mills (which was originally like slurry due to the predominance of smaller particles) was much stronger after washing. Fluid load may explain why it becomes stronger than the Straumann, which has a predominance of large particles, but not superior to the 6mm Aesculap graft after washing – i.e. it may actually be disadvantageous to produce smaller particles if the graft is not going to be washed.

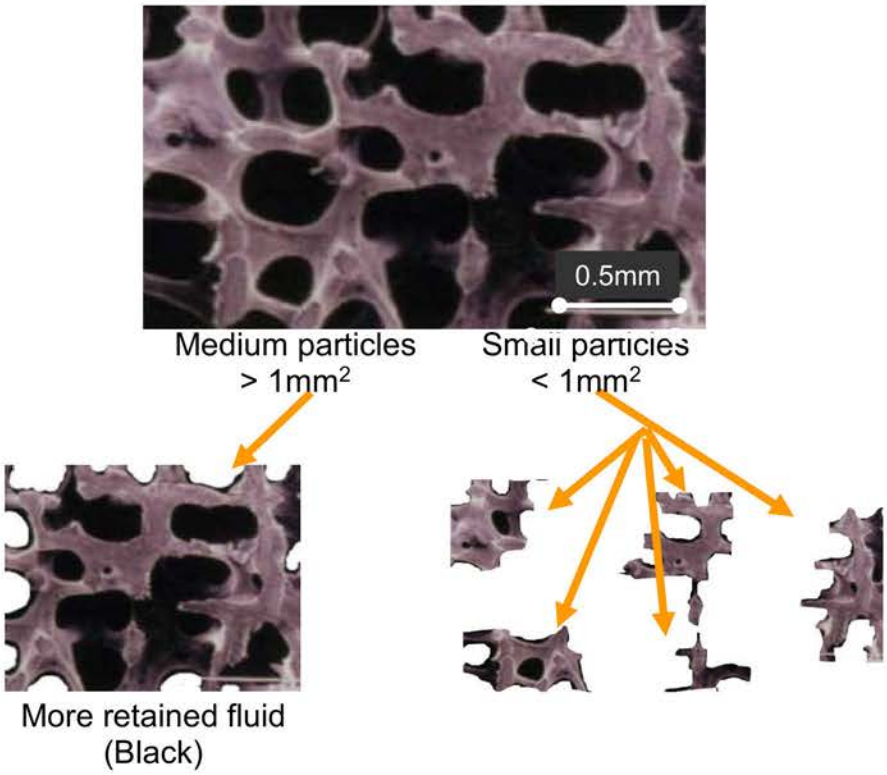

Figure 12. Micrograph of cancellous bone showing fluid release is dependent on particle size production

As cancellous bone is fragmented into smaller particles, there comes a time when the particles are no longer porous. From Figure 12, this can be seen to happen for particles smaller than ~1 mm. The particles tend to be rounded solid bone spicules, compared to their more angular longer porous originators. It is well established in soil mechanics that angular particles interlock more thoroughly and have better contact with each other giving rise to increased friction angle than the rounded particles. Hence aggregates composed of angular particles give rise to increased shear strength compared to aggregates with rounded particles[114]. Thus while the Aesculap 3mm/6mm mixture represents a better particle size distribution in the range 0.3-5.6 mm, particles in the range 0.3-1 mm have a lower angularity which apparently results in the lowest shear strength.

Future test scenarios should examine the mechanical characteristics of the much larger particles or 'croutons' used in Njimegen. From these experiments it could be hypothesised that these particles may produce their clinical success in resisting shear by releasing little fluid on production and having excellent interlocking, despite their poor grading. A direct comparison with this data would be most illuminating.

5.2. Conclusions & Clinical Relevance

It appears that sieving is a reliable method of determining particle size distribution from a mill. The particle size distribution of fresh graft from any mill provides a clue as to how that milled graft will perform when subjected to shear testing. Washed graft however, has exactly the same particle size distribution as its pre-washed state, but uniformly has an increased resistance to shear, no matter which mill it is from. Previous experiments where graft was washed through a swab (this practice is performed routinely by some surgeons in the operating theatre, prior to compaction of graft) showed many of the smaller particles are lost in the wash, affecting the particle size distribution. These lost particles are particularly important to maintain the grading of the graft. We have devised a washing system applicable to the intra-operative preparation of bone graft for impaction grafting. In the clinical scenario we also found it a useful way to examine the graft to remove 'rubbish' such as cystic material or pieces of articular cartilage, which might cause focal defects in the impacted mantle.

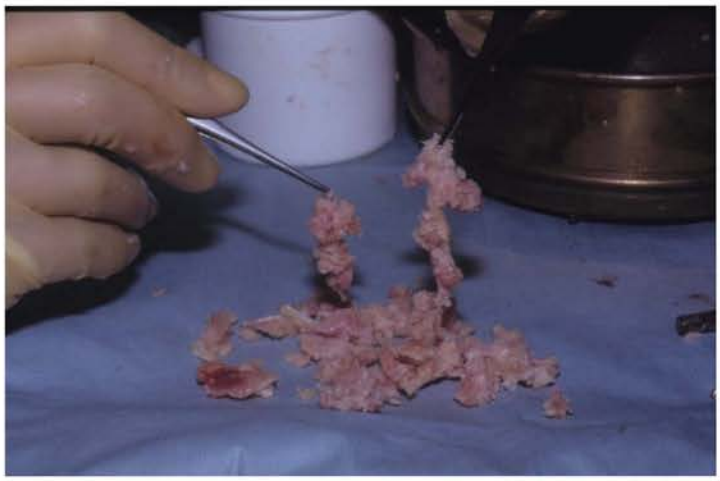

Figure 13. Removal of deleterious material in a human operative case.

The testing method is clearly important when comparing samples. Different techniques have found significant differences[115] or no difference[105] in altering the particle size. The role of fluid and porosity in these models is not clear. We believe

we have devised a compaction and shear testing technique, which most nearly simulates clinical surgical practice. Laboratory studies often test non-human graft (due to the expense and regulations limiting supply of human bone), but the validity of comparing this animal tissue to human allograft is questionable. We have found marked differences at our laboratory using ovine graft, which produces different particle size distributions from the same mills (ovine bone is more brittle) and has fat of a different viscosity. We therefore feel it is important to produce mechanical tests for fresh human allograft that is used clinically.

The degree of saturation of an aggregate with pore fluid determines its mechanical behaviour. Fluid should be allowed to escape during impaction as fluids are incompressible and will absorb any energy applied in increasing the fluid pressure, rather than increasing the density of the aggregate. The viscosity of the fluid is important, as a more viscous fluid, such as fat, will drain through the porosity of a material less readily than a less viscous fluid, such as 0.9% saline.

We have shown that washed graft enhances graft strength by improving the characteristics of aggregate mechanical strength. This is due to an increase in the friction angle. This is thought to be due to the removal of the fat and marrow tissues, allowing tighter graft compaction. The fact that the washed particles appear to give more strength than fat covered particles makes absolute sense. The particles when washed and dried have little lubrication at the contacts with other particles so the frictional resistance will be higher. However, with lubrication in the form of fat and marrow at the contacts, the frictional resistance will be reduced. The results therefore appear to be logical, though not proven.

During surgery, the decision as to when the graft is suitably compacted is subjective. Optimum compaction of a whole variety of aggregates is well understood by civil engineers. Based on soil mechanics of friable particulate aggregates, to produce a compacted aggregate most resistant to shear stress (which is the mode of failure), it should have the following characteristics:

- Be rigidly contained

- Have a well graded particle size distribution
- Containment should be porous to allow fluid escape and thereby minimise any pore fluid generation
- Sequential layered compaction of well mixed material
- Large compaction energies should be used
- Vibration during compaction should be utilised.

Previous work at this centre has shown that bone graft that has had its grading improved by the addition of synthetic particles of the correct size can improve shear strength[102]. This is because the mechanical properties of any collection of particles, is more dependent upon the particle size distribution and their shape than on the individual properties of the particle material, unless there is a significant release of lubricant fluid. Currently the porosity and the behaviour of fresh graft to the addition of synthetic materials are being investigated at our centres.

Clinical Relevance

It was noted that production of a well-graded graft by adding graft from a small (3mm grater) mill produced graft that was almost liquid in consistency. This was due to the bone chips being so small that they were no longer complex cancellous chunks but simple spicules – and there was thus a greater release of fat and marrow from the interstices (Figure 12). This may explain why some clinicians recommend the 'dryer' larger chunks or croutons, rather than the 'slurry' produced by these mills[18]. A recent report[116] suggested improved strength with larger bone chunks, which has not been our experience. We believe this may be due to the fact that un-washed smaller particles are more difficult to impact properly due to the excessive fat release which may not be allowed to drain away and may damp the compactive effort. The interparticle lubrication effect may also be significant. We specifically designed our test system to adequately drain the graft during the compaction process, which may explain our improved results.

We have shown that removing excessive and lubricating fluid from the interstices of graft for impaction grafting improves the overall graft strength. This is advantageous

and based on sound engineering principles[100; 101]. There will potentially be more inter-particle spaces empty of dead foreign tissue available for faster invasion by host angioneogenesis. The removal of fat and marrow tissue from allograft, which is foreign to the host, may have the additional benefit of reducing the immunogenic load experienced by the host, damping the initial inflammatory phase of graft incorporation[44-46; 49; 117]. Whether the potential reduction in the level of growth factors present in the washed graft matrix is important, is currently a matter for investigation. Previous work has questioned the activity of donor graft growth factors[118-120]. Ultimately the graft may be incorporated primarily by an increased expression of host growth factors, analogous to fracture healing[49].

The synthetic additives used here, Corglaes® and TCP/HA, uniformly improved graft strength when used as either bulking or idealising agents, which is extremely encouraging. These agents may ultimately be used as carriers for growth promoters, which may negate any negative effects of washing. The addition of growth factors to scaffolds, including bone graft has been a subject of recent interest[51; 121-124], with clinical trials in progress. Currently the practice of pre-washing the graft before impaction is being undertaken at our centre and will be reported in due course.

The results in the context of the null hypothesis were examined:

1. *"There is no difference between the mechanical properties of fresh graft from different bone mills"*

This hypothesis is **false**.

2. *"Well graded bone graft is not mechanically stronger than standard bone graft"*

This is **unproven**, as it appears to depend on the method of idealisation. The role of increasing fluid release when smaller particles are generated is important and can be removed by washing (see 5. below).

3. *"Well graded (with synthetic material) bone graft is not mechanically stronger than standard bone graft"*

This hypothesis is **false**.

4. *"Well graded synthetic material used as a bulking agent in a 50/50 mix with bone graft is not mechanically stronger than standard bone graft"*

This hypothesis is **false**.

5. *" Bone graft that has been washed of fat and marrow is not mechanically stronger than standard bone graft"*

This hypothesis is **false**.

It appears therefore that, changing the composition of impacted bone graft does have an effect on the mechanical behaviour when compared to standard impacted bone graft.

Phase II

Biological Aspects of Impaction Grafting – An Ovine Defect Model

6.1. Introduction

Soil mechanics and civil engineering principles may well determine the optimisation of aggregate behaviour, but the application of these principles must be shown not to have a deleterious affect on the biological response of the individual to the modified mixture, or vice versa. This effect may be mechanical as well as biochemical. The cellular response to the local concentrations of dissolving bioactive material also needs to be examined. We have therefore developed an animal model[50; 125; 126].

Previous work[127-129] using unloaded cylindrical titanium implants coated with hydroxyapatite in the femoral condyles of Labrador dogs have been reported. The 'Push out' strength at 3 weeks and histological appearances were reported. The use

of impacted graft[130] in a cancellous 'cell' covered with bone cement for our study was chosen as it was thought to more nearly reflect the local factors that could be experienced by unloaded graft, though loading has recently been described[131; 132]. Phase III of this thesis allows the extra dimension of loading to be analysed.

6.2. Null Hypotheses

The two secondary null hypotheses below were addressed in this chapter;

1. *"Bone graft idealised with synthetic material is not re-incorporated in a biologically similar fashion to bone graft alone"*

2. *"Bone graft with synthetic material used as a bulking agent in a 50/50 mixture by volume is not re-incorporated in a biologically similar fashion as bone graft alone"*

6.3. Aims

The purpose of the study was to evaluate the in-vivo biological response to different impacted bone graft mixtures, by comparison of the biological re-incorporation of six different graft materials impacted into boney defects, as seen by histological, radiographic and mineral density determination.

6.4. Study Design

12 Greyface sheep underwent surgical procedures to implant pellets of graft mixtures in six defect sites in their hind limbs. The allocation of pellet to defect site was randomised according to a Latin square randomisation design.

The six pellets were;

1. 100% autograft (+ve control)
2. blank defect (-ve control)
3. 100% allograft (current standard)

4. allograft whose particle size distribution had been improved by the addition of synthetic material
5. 50% allograft / 50% synthetic material by volume
6. 100% synthetic material

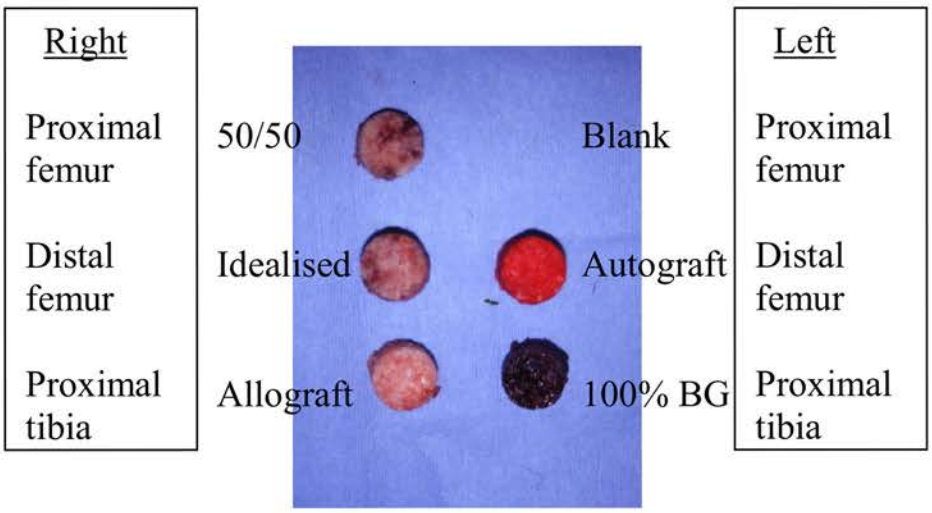

Figure 14. Pellet layout in a typical randomisation.

The defect sites were drilled in areas of cancellous bone in the proximal femur, distal femur and proximal tibia, in both hind limbs. A specialised miniature impactor was designed to produce pellets ($15mm^3$) at a known standard compactive effort (equating to the energy used in a standard human impaction grafting (Section 4.2.2)). The pellets were then inserted into the defects and sealed with bone cement. The animals were given double pulse fluorochrome bone labels and allowed to mobilise over a fourteen week period. After which time the animals were euthanised and the limbs formalin fixed. Each defect site was then assessed histologically and radiologically with Computerised Tomography Scanning.

6.4.1. Calculation of Sample Size

The sample size required to test the hypothesis is based on an estimate of expected histological appearances. This outcome measure is not continuous but qualitative and therefore prone to subjective errors.

As the histological interpretation had never been performed with the various morsellised test mixtures in an in-vivo model, it was decided the design should be a pilot study, to delineate the clinically important differences. For ethical reasons it was decided to optimise the results by placing each of the six pellets into the same animal, instead of placing only one of the six different test pellets into each animal. This greatly reduced the number of animals used. Ethical approval for twelve animals, each with the six defects, was obtained, as a pilot study, to demonstrate trends between the pellets. Six animal were allocated to an 'early' euthanasia at 7 weeks and six animals were allocated to 'late' euthanasia at 14 weeks, to demonstrate trends in healing rates. From these results, future studies will be able to determine study numbers necessary to detect significant differences.

Review of the relevant literature was unable to suggest a complication rate, so a revised sample to account for dropouts could not be calculated. Instead, replacements for withdrawn animals in the post-operative week were used, with an ethical approval limit of 25% replacement for complications.

Initially twelve sheep underwent surgical procedures, with three replacement animals undergoing identical procedures, after withdrawals in the early post-operative period (An additional animal was replaced subsequent to an anaesthetic complication).

6.4.2. Study Animals

Sheep were purchased from a single breeder, to ensure a uniform environmental and genetic background. The animals were kept together in 15x20m barn and allowed to familiarise themselves with their surroundings and human contact. Half of the barn was converted to individual pens for the post-operative recovery period. The sheep were kept together as a group during the study period to allow maintenance of social interaction for animal well-being. The animals were recovered in their pens post-operatively, thus minimising transport.

6.4.3. Study Groups

Twenty sheep were allocated to the study. This comprised the 12 sheep for the defect group, two donor sheep that were harvested of cancellous bone prior to the first hemiarthroplasty, and six extra sheep from which replacements could be used if necessary.

6.4.4. Inclusion and Exclusion Criteria

All animals were assessed for physical fitness prior to inclusion in the study by a veterinary surgeon. Full mouth mature Grey Face ewes, greater than 60 Kg, were included in the study.

6.4.5. Stratification and Randomisation

Randomisation was performed using blank sealed envelopes containing an enclosure with the template for the six defects and each graft material for each defect drawn and labelled upon it. The allocation of graft type to defect position was randomised according to a Latin Square design. These were then each sealed in a blank envelope and shuffled independently. The envelopes were held in theatre and one was picked at random and opened for each sheep on the morning of surgery. Thus each animal had all six graft materials, but there were six subgroups of animals depending on graft position. With 12 animals there were two sheep in each sub group (i.e. who had the same graft material in the same defect site) – the first of each matching pair was allocated to the early euthanasia group, the second to the late euthanasia group.

6.4.6. Study Logistics

To improve uniformity of the model, identical operative procedures were performed in animals of the same sex and age from the same flock. The stock of allograft, from which the aggregate mixtures were made, was produced from pooled metaphyseal bone, which had previously been harvested from two donor animals under sterile conditions. Each of the test mixtures was then subdivided into individual samples for

each test animal, prior to commencement of the project and stored in identical conditions at –70°C. Microbiological culture assessment for all samples was negative prior to implantation.

Each animal was assigned a study number and an individual identification number. The details of graft type were kept separately. No details of graft type were kept with the usual post-operative individual case notes. At the time of Computerised Tomography (CT) scanning and histological evaluation, their individual number identified the animals only. Only once all results had been obtained and analysed were the graft types unblinded. There were no clues to graft type in the appearance of the limbs during CT analysis, however the histological sections showed evidence of graft type. An independent histologist, unaware of the differences between graft types therefore assessed the histomorphological differences.

6.4.7. Drop-out from the Study and use of Replacement Sheep

A Veterinarian and the surgeon assessed the sheep every day in the immediate post-operative period and weekly thereafter. Staff at the field hospital reviewed the animals daily. It was decided that any of the following complications would cause withdrawal of the animal from the study: failure to complete the operation, femoral or tibial fracture, sepsis, lameness different from normal rehabilitation, undue suffering or death due to unrelated causes (post-mortem to be performed).

Once the initial cohort of twelve animals had been entered into the study, an independent Veterinarian reviewed the complications resulting in withdrawal from the study. Replacement sheep were allocated to receive identical defect positions as those withdrawn, within the sample size allowance.

6.4.8. Control of Bias and Study Blinding

All defects were prepared in the same manner and only after this was done, was the surgeon un-blinded to allow the test pellets to be inserted into their allocated defect. The preparation and insertion of each impacted pellet was identical using the same

mechanical apparatus, reducing surgical bias. All animals each received all of the available test mixtures. The randomisation pattern for each animal was then hidden from view until after the analysis of the CT scans and histological reports were produced. An independent laboratory scientist was responsible for administering all the bone labels, arranging the euthanasia of the early and late groups and surgical removal / fixative preparation of the limbs, without identifying individual sheep to the project leader.

6.5. Ethical Approval

Institutional ethics approval was obtained prior to the study based on the study design and sample size calculations above. All procedures were performed under the ethical guidelines of the institution.

Chapter 7 Sheep Defect Model

7.1. Introduction

By applying soil mechanics principles in Phase I, we have shown that the addition of synthetic materials improves mechanical strength of graft in the laboratory, using small and very small particles. In- vivo however, it is conceivable that the inter-particle spaces may be filled at a cellular level and inhibit neo-vascularisation. Hence the need for an animal model which allows multiple test mixtures to be compared.

Other authors[127; 129] have developed similar defect models, but none have developed models that standardise the compactive effort to simulate the graft as it would actually be used in humans. Lamerigts et al have developed a repeated sampling bone chamber made of Titanium, which showed small amounts of bone ingrowth[133]. Their model is probably better suited for the study of bone inductive substances and was considered unsuitable compared to our model, which uses impacted graft directly inserted into a cancellous bed.

Three sites were chosen for the surgical defects: the proximal tibia, and the proximal and distal femur. These sites were chosen as they allowed 6 relatively accessible defects per sheep, in areas of metaphyseal bone at the end of weightbearing long bones. These areas were considered to simulate the local environment as far as blood flow, cell type and boney architecture were concerned in clinical impaction grafting, although the grafts themselves were not subjected to direct load. This latter feature is studied in phase III.

In order to test the biological incorporation of an impacted pellet, it was necessary to first standardise the manufacture of the impacted pellet. The 60mm pellets produced by the modified Proctors impactor above were too large to test in a sheep femoral defect. A smaller pellet that was impacted with the same energy per volume of test material, as the larger impactor was required. After trial laboratory testing, using sheep femora and various drill sizes, the largest defect that could be produced safely was found to have a diameter of 15mm. Grey Face sheep were chosen because their mesomorphic stature produces a stout skeleton. The defect produced was on average, 2mm narrower than the diameter of the metaphysis, in effect reducing the circumference of the bone by ~25% at its maximum. 15mm was considered to be similar to the upper limit of an impaction graft mantle thickness and therefore clinically relevant.

7.2. Materials and Methods

7.2.1. Test Material Production

Two sheep were euthanised before the main project as a source of allograft. The proximal humerii, proximal femora and distal femora were removed under sterile conditions, cleaned of soft tissue and cut from their diaphyses to produce 500g of cancellous graft. These were then divided into two equal groups and passed through the small (3mm diameter) and large (6mm diameter) Aesculap bone mill used in Phase I.

One third of the graft from the large mill was mixed (Figure 15.) with all the graft from the small mill to produce a more uniform particle size distribution. This ‘idealised' mixture was then divided in two, producing three groups of equal amount: With the addition of Corglaes®, four final groups were then produced:

1. Large mill graft idealised with Corglaes®
2. Idealised graft with idealised Corglaes® in a 50/50 mixture
3. Idealised graft alone
4. Idealised Corglaes® alone

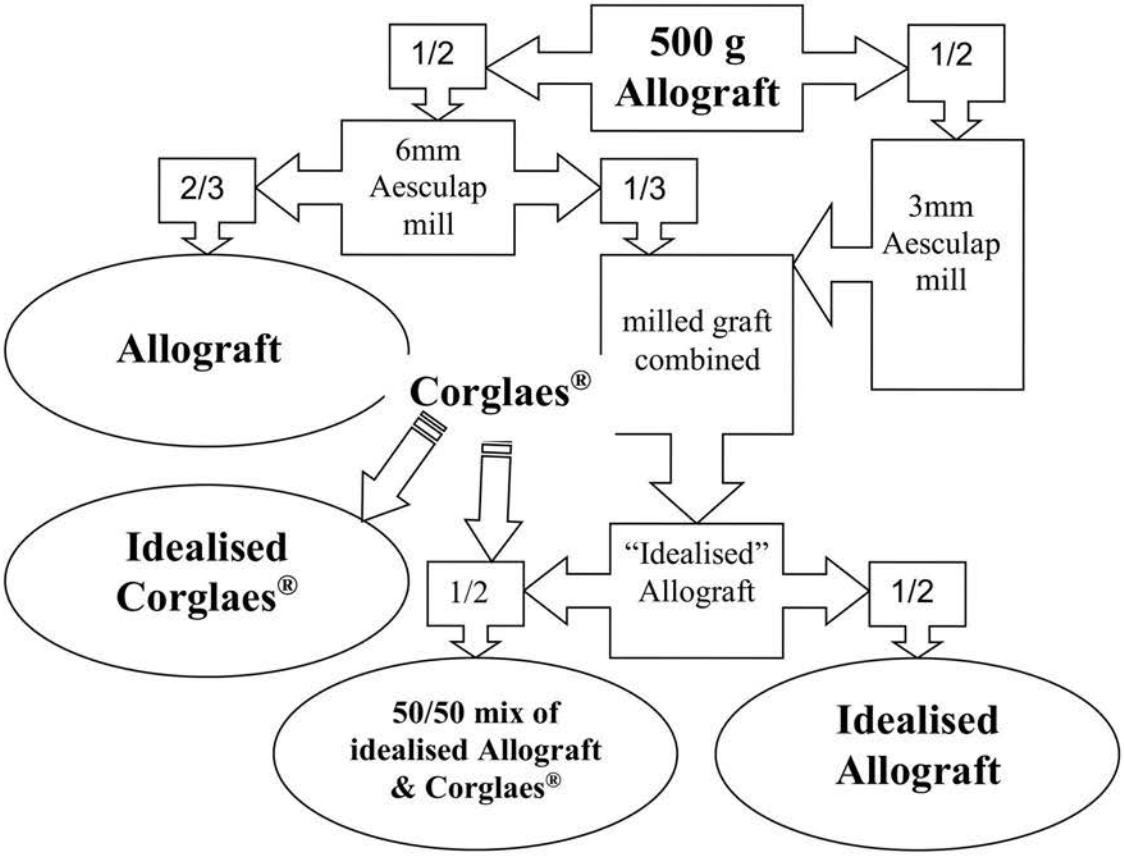

Figure 15. Test material production

Group 1 was produced by previously determining the particle size distribution of sheep bone produced from the large mill, then adding the correct amount by volume of Corglaes® of each particle size to produce a linear log particle size distribution.

Figure 16. Graft idealised with the addition of synthetic material.

Group 2 was produced by the addition of Corglaes® with a linear log particle size distribution in a 50/50 ratio by volume.

Figure 17. Graft and idealised synthetic material in a 50/50 ratio by volume.

The volume of Corglaes® compared to sheep bone was determined in the knowledge of mass and density at one standard impaction. Samples from the above four groups were then sent to microbiology for culture to ensure sterility before use. The groups were then divided into sixteen equal portions and individualised for each sheep in the subsequent study and stored at –20°C.

7.2.2. Pre-operative Set-up:

Each sheep underwent identical pre-operative, anaesthetic and post-operative management. Intravenous Thiopentone was used for induction of anaesthesia and maintained with Halothane from a vapouriser with the addition of oxygen and CO_2 extraction (circle circuit). The randomisation envelope was then picked and opened to determine on which side to commence. The side with the autograft was performed second to ensure adequate defect shavings from the other five holes to make an autograft pellet (four drill holes were usually adequate). The haunches were then clipped and the skin prepped first with aqueous Betadine. The surgery was performed one side at a time in the 10 degree head down, lateral position. Fresh drapes and alcoholic Betadine skin prep was used for each side. A side constituted the ipsilateral

femur and the contralateral tibia. Monopolar diathermy was utilised (oral earth bar). Intravenous Streptopen was given at induction. IM morphine was given at induction.

7.2.3. Operative Technique:

Proximal Femur:

A curvilinear incision was made following the line of the femur, slightly posterior proximally and anterior distally, from the greater trochanter to the knee joint. This was deepened to the fascia lata distally and the tensor fascia lata proximally. The fascia was split in the direction of its fibres, including the tensor in a similar manner to the skin incision. The site for the proximal femoral defect was exposed first. From templating of the pre-operative x-rays a point was identified some 2.5cms distal to the tip of the greater trochanter. Here, the muscular aponeurosis of the vastus lateralis was split in the direction of its fibres 1cm anterior (cephalad) to its posterior (caudal) insertion along the linea aspera. This muscle plane was deepened to the peri-osteum of the lateral aspect of the greater trochanter. A peri-osteal elevator was then used to strip the muscle attachment to allow placement of the template (Figure 18), used to align the pellet chamber. The peri-osteum was left in-situ. The distance distal to the tip of the greater trochanter at the most lateral point, with the leg in neutral rotation was marked with a cross. A 3mm pilot hole was drilled in the direction of the femoral neck with a drill stop at 15mm. When this was confirmed to lie in cancellous bone, centrally at the base of the neck it

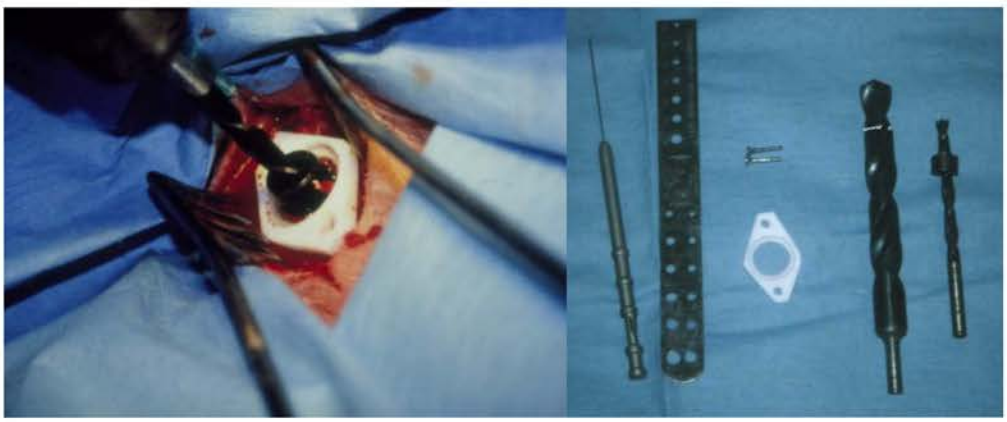

Figure 18. a) Pilot hole drilled with drill stop engaged b) Left to right: depth gauge, ruler, teflon template & screws, 15mm drill bit and pilot drill bit

was removed and the 15mm drill was then passed in a similar manner, with a drill stop set to 15mm.

Great care was taken to advance slowly in the same plane to produce a smooth cortical edge to the hole. The hole was examined and accepted if found to provide cancellous containment all around. Bone shavings from the hole were collected for the autograft pellet. The Teflon guide was then aligned over the hole and held in position with two AO Small Fragment screws drilled and tapped appropriately. The hole was then ready to receive its pellet, the technique is similar for all holes and has been described above.

Distal Femur:

After the proximal femoral defect was closed the distal femoral defect was created. The distal femoral flare was identified at the level of the patella and the extensor apparatus divided in the direction of its fibres onto but not through the knee joint capsule. A fairly consistent blood vessel (supero-lateral geniculate artery) was used as a marker, passing proximal to the intended area. The soft tissue (but not periosteum) was scraped away for an area large enough to accept the Teflon guide, with the 15mm hole centred over the widest point of the metaphyseal flare. Too proximal a drill hole in the region where the cortical bone commences was associated with post surgery femoral fractures. The 15mm hole was then drilled in a similar fashion to the proximal defect, with the alignment of the drills checked to pass into the centre of the cancellous bone. The Teflon plate was attached in a similar fashion and the pellet inserted as described above.

Proximal Tibia:

The third defect was performed on the inner aspect of the contralateral tibia with the sheep still in the lateral position. A marker needle is placed at the level of the knee joint line. A 6cm longitudinal incision is made down to periosteum on the inner aspect of the proximal tibia, one fingerbreadth distal to the joint line and posterior to the tibial tuberosity. A self-retainer holds the skin edges apart. The Teflon guide was placed over this flat region, such that the proximal Teflon fixation screw was just below the joint line, with the guide in the centre of the medial cortex in the long axis

of the tibia. The 15mm hole is carefully drilled with the check sleeve set to 15mm on the drill-bit as before, aiming to be centred in the cancellous bone of the tibial metaphysis. The Teflon plate was attached in a similar fashion and the pellet inserted as described above.

Once all three defects were complete and the wounds closed, the sheep was turned onto the opposite lateral side and an identical procedure as above, carried out on the ipsilateral femur and contralateral tibia.

7.2.4. Proctors Impactor Design Modification

A miniature impaction chamber, which produced a 15mm pellet, was manufactured (Figure 19). This was constructed in brass with holes in the piston to allow fluid to escape during impaction, similar to the larger impactor above. The chamber fitted inside the original impactor (Figure 7) allowing a scaled down weight to be dropped from the same height, the same number of times as before. The combined impactors were further modified to allow disassembly to fit inside a surgical theatre steam steriliser.

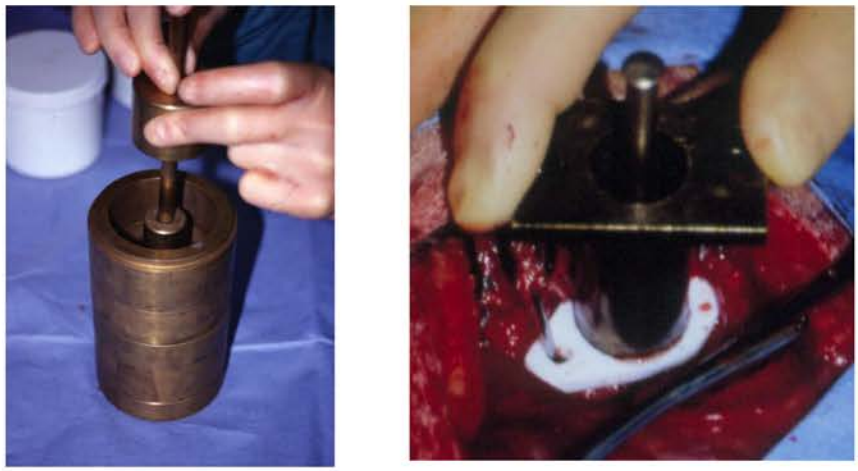

Figure 19. a) sample impacted b) docked onto Teflon guide.

7.2.5. Sequence of Impaction:

1. The surgical defect was created in the bone (see Defect Production above) and the Teflon guide screwed into position.
2. Each graft material for each defect position was split into three equal portions, to ensure even compaction.
3. On a sterile draped hard surface, the first third was placed evenly in the small impactor, the small piston lowered onto the sample and the small impactor was then placed inside the larger Proctors impactor. The small weight was dropped 24 times from the given height. The larger Proctors impactor piston and upper rings were removed and the piston of the small chamber was then rotated (to prevent test material sticking to its underside) and removed.
4. The middle third of the test sample was then laid on top of the first and impacted 24 times as before.
5. The remaining third was then added and impacted in a similar fashion, so that the finished pellet received 72 blows.
6. The small impactor with its piston was then taken over to the operative field and 'docked' onto the Teflon guide. The guide is durable, sterilizable and flexible to take in the contours of the underlying bone, preventing any slippage as the pellet is introduced.
7. The piston was then tapped in for 16mm to introduce the pellet into the 15mm deep hole, allowing 1mm for the Teflon guide.

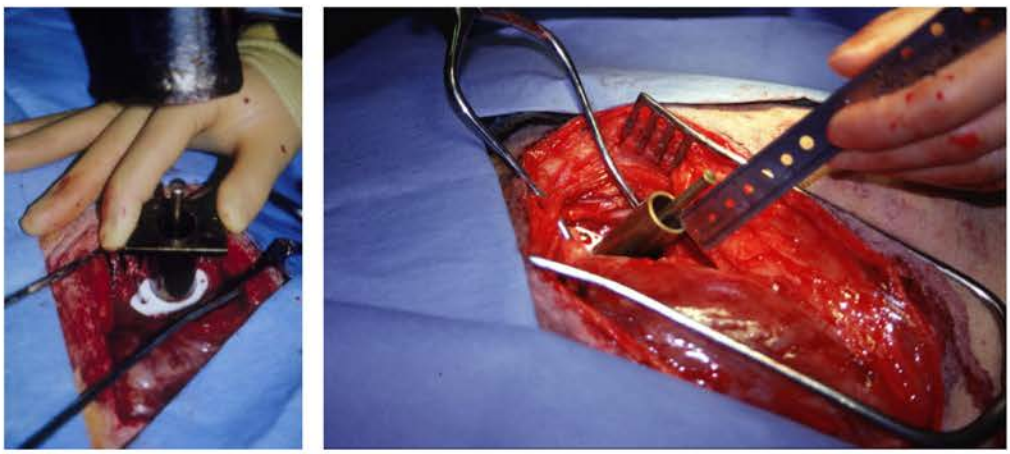

Figure 20. a) piston tapped to introduce pellet b) until correct depth obtained

8. After the pellet has been inserted, the Teflon guide is removed together with its screws. Any residual graft is brushed off flush with the cortex and the area washed of debris.
9. The area is dried with a swab and Polymethylmethacrylate bone cement (One 20 gram packet of Surgical Simplex P cement divided between 6 defects (Howmedica Inc., Rutherford, New Jersey, USA) was then mixed in a bowl and poured over the area as a sealant. A cross is imprinted in the cement to mark the position of the defect and allow easier localisation at histological sectioning.
10. Once the cement has polymerised, the soft tissues are closed over the cement plug with 2/0 Vicryl and the skin closed in the standard fashion.

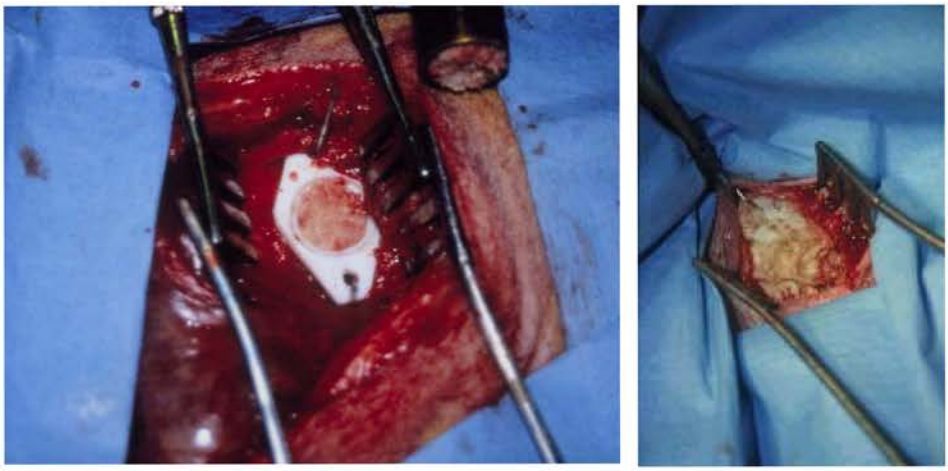

Figure 21. a) cylinder removed c) teflon guide removed and cemented over

The impaction rate was approximately 1.5Hz, similar to the clinical scenario and slow enough to allow fluid to escape. This was maintained throughout the study period.

7.2.6. Post-operative Recovery:

Antero-posterior and lateral x-rays of the femur and tibia were performed with the animals still anaesthetised, to check for pellet position and presence of fractures. Following this the animals were taken to their individual pen where they were placed

prone and extubated when able to protect their own airway. Intravenous Streptopen was continued for 4 days. IM morphine was continued 4hourly for the first 8 hours postoperatively, followed by oral analgesia.

The animals were allowed to mobilise within their pens when they felt able. Any animal not mobilising after 24hrs was examined and X-rayed as indicated. To prevent uncoordinated mobilisation which was identified as a problem, the sheep were recovered supported in a sling with their hind limbs just off the floor for the first 24hrs, or until the affects of anaesthesia had worn off.

Figure 22. Post-operative animal mobilising in a pen

7.3. Results

Four animals were withdrawn from the study and were replaced.

Study No.	Weight Kg	Early Euthanasia	Late Euthanasia	Blank	Auto	Allo	Idealised	50/50	100% BG	Post Op. Complication	Op. Complications
1	70		Yes	LDF	LT	RPF	RDF	RT	LPF		Screw sheared off RDF
2	67		Yes	RPF	RDF	RT	LPF	LDF	LT		
3	73		Yes	RDF	RT	LPF	LDF	LT	RPF		
	61	Yes		RT	LPF	LDF	LT	RPF	RDF	# L femur	LDF defect too prox/anterior
4	80		Yes								
	84	Yes		LT	RPF	RDF	RT	LPF	LDF	# R femur	Drill bit # LT
5	79	Yes		RPF	RDF	RT	LPF	LDF	LT		
6	65	Yes		RDF	RT	LPF	LDF	LT	RPF		Very narrow RF, narrow LPF
	75	Yes		RT	LPF	LDF	LT	RPF	RDF	# L femur	LDF femur too prox/anterior
7	74	Yes									
8	73	Yes		LT	RPF	RDF	RT	LPF	LDF	Wasted R thigh ?OA hip	
9	78	Yes		LDF	LT	RPF	RDF	RT	LPF		
	83	Yes		RT	LPF	LDF	LT	RPF	RDF	Aspirated day 0	
10	76		Yes	LT	RPF	RDF	RT	LPF	LDF		
11	73	Yes		RT	LPF	LDF	LT	RPF	RDF		LDF defect a little anterior
12	69		Yes	RT	LPF	LDF	LT	RPF	RDF		

Table 2. Outcome table (results in red are withdrawn animals, matching colours are early and late group animals with identical defect allocation) (L=Left, R=Right, T=Tibia, PF=proximal femur, DF=distal femur).

Three of the withdrawals were due to femoral fracture and two of these three, were felt to be due to surgical error (Table 2). Both of these latter two sustained a spiral fracture of the femoral diaphysis, emanating from the distal femoral drill hole, which at post mortem was found to be too proximal and anteriorly placed.

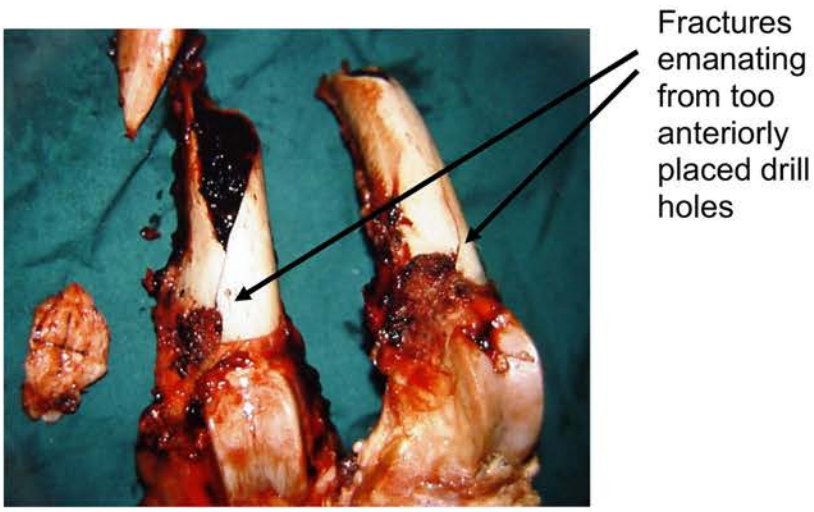

Figure 23. Post-mortem appearance of distal femurs below fractures

The position of the drill hole has since been more accurately delineated. The third femoral fracture occurred on the first post-operative night and was considered to be due to either awkward movement of the animal while still unsteady or as a result of some sudden exertion that occurred when the animals were startled. The drill holes were well positioned. In our later series of animals, as part of a different project, we now routinely rehabilitate the animals in a full support sling for the first 24hrs. The fourth withdrawal was due to an anaesthetic complication.

At the end of the trial period, six sheep had successfully entered the early euthanasia group and six into the late group.

Chapter 8 CT Scan Densitometry

8.1. Introduction

The use of CT scanning allows detailed examination in 3 dimensions, which was felt to be important, due to the variable angulations of the defects. High-density contact radiographs (Faxitron) were going to be used. These would allow the macroscopic radiological appearances of each defect to be determined in two dimensions only. CT scanning also allows quantification of bone density in precise areas.

8.2. Materials and Methods

Following euthanasia and limb fixation (Section 9.2.2) the specimens were taken to the CT Scan suite. Paired hind limbs of each sheep were placed alongside each other in a polystyrene box still sealed in their plastic sleeves. The Polystyrene box and the still attached soft tissues were found to give a good transitional edge for the CT images. The operative cement plug was used to localise the CT sections. Paired hind limbs were scanned together, an initial image taken of their entire length to allow identification of the 6 defects. Each defect was then orientated in a standard fashion within the focal ring and sequentially radiologically sectioned in 5mm sections. Focal average densitometry for each defect was determined as compared to a cortical control.

8.3. Results

Implantation sites were well identified on Computed Tomography, allowing assessment of;

a.) gross radiological appearance of soft tissues and bone

b.) bone lucency, trabeculation or fracture and

c.) average pellet density compared to a cortical control.

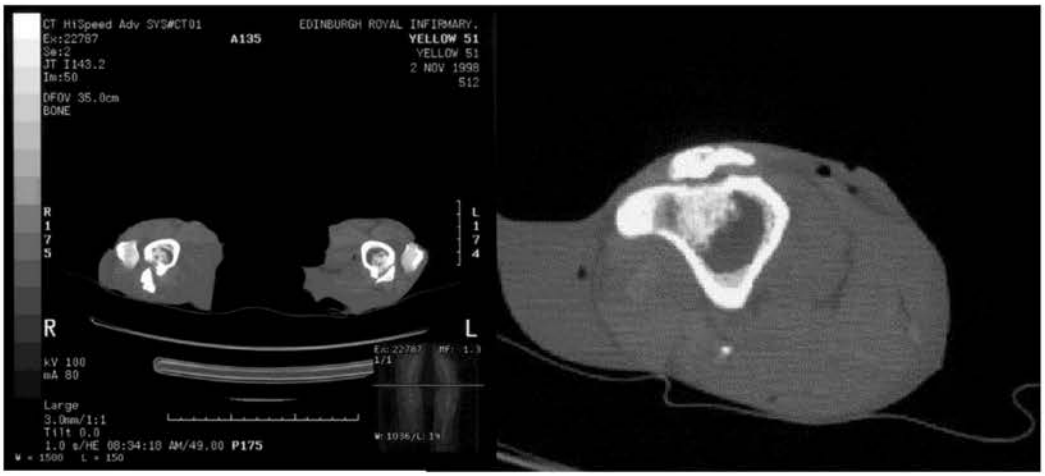

Figure 24. a) CT scan of both legs b) close up of defect with overlying cement plug

On gross radiological assessment there were no abnormalities detected in either the soft tissues or bone. There was no evidence of lucency, retrabeculation or fracture surrounding the pellets. On assessment of the pellets themselves, these are given as follows:

Early Group

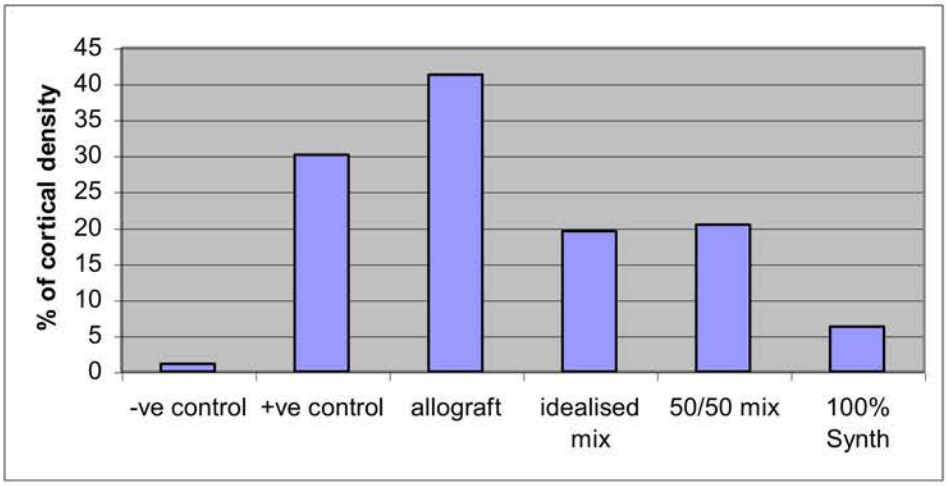

Graph 31. Early group. Pellet density as a percentage of cortical control.

Using Tukey's 'honesty significance difference' (test of difference among means, catering for standard deviations) there is evidence (all $p<0.05$) that:

- -ve control differs from +ve control and allograft
- +ve control differs from 100% synthetic material
- allograft differs from –ve control and any of the three synthetic mixtures.

Late Group

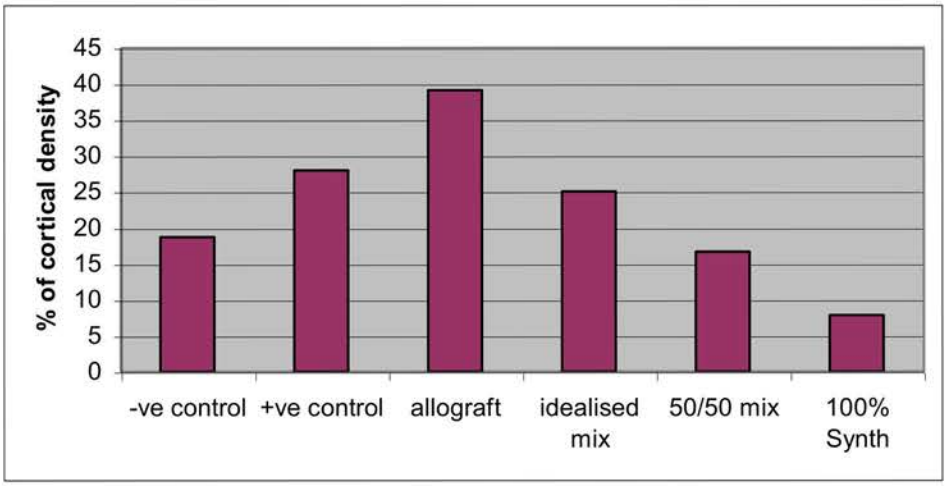

Graph 32. Late group. Pellet density as a percentage of cortical control.

Using Tukey's 'honesty significance difference' there is evidence (all $p<0.05$) that:

- +ve control differs from 100% synthetic material
- allograft differs from –ve control and the last two synthetic mixtures (50/50 mix and 100% synthetic)

Using one way analysis of variance (ANOVA) there is strong evidence of differences between treatment for both the early and late groups ($p<0.001$ for each case). There is no evidence of differences for position along the bone, or right versus left.

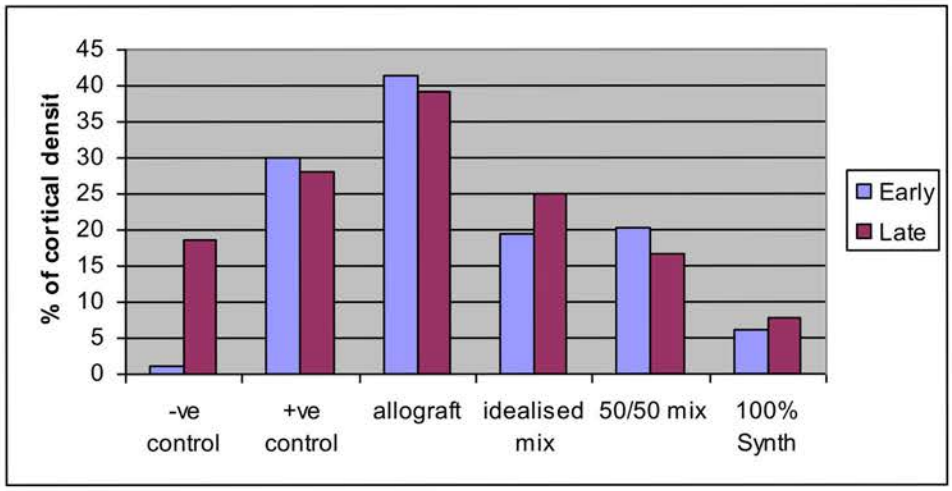

Graph 33. Early versus Late comparison.

The difference between progressing from the early to the late group is:

1.) loss of a difference between the –ve control from +ve control and allograft

2.) loss of a difference between allograft and the idealised synthetic mixture

Chapter 9 Histological Assessment

9.1. Introduction

The histological assessment was set up as a pilot study to delineate problems for future studies and as such, does not attempt to provide complete results for an exhaustive histological assessment. Under the guidance of Dr Donald Salter BSc MD FRCPath at the University of Edinburgh Pathology Department, the following protocol was devised. Preliminary tests using laboratory produced ovine defect models were analysed. After trial and error with a number of techniques to fix, embed, section and stain the received specimens, difficulties were found in:

- The ability to adequately hold the specimen, to prevent the Corglaes® particles from falling out during sectioning.
- Correctly identifying the defect for sectioning
- Preventing cracking of the specimen

The following protocol has attempted to correct these problems.

9.2. Materials and Methods

9.2.1. Fluorochrome Bone Labels

The Fluorochrome dosage regime was as follows:

- 30th and 42nd post-operative day: Oxytetracycline – 30mg/Kg administered as two separate single intravenous doses (double pulse).

- 56th post-operative day: Calcein Blue – 30mg/Kg administered as a single intravenous dose.

- 77th post-operative day: Alizarin Complexone – 30mg/Kg administered as a single intravenous dose.

- 84th post-operative day: Euthanasia.

The Fluorochrome bone labels fluoresce under UV light and the appearance of each band can be dated to the time of administration. The colour of fluorescence is as follows:

Oxytetracycline - Yellow
Calcein Blue - Blue
AlizarinComplexone - Red

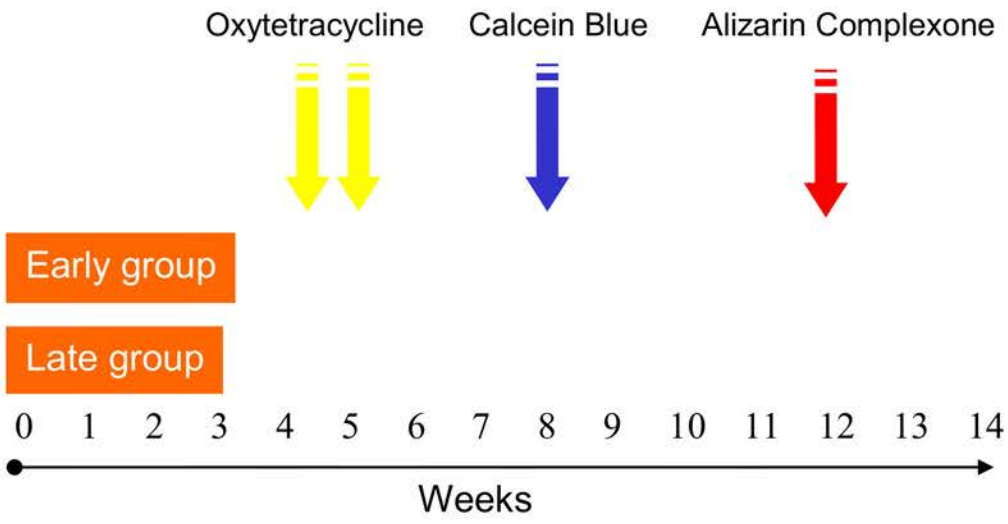

Figure 25. Time-line of fluorochrome administration.

9.2.2. Euthanasia, Fixation & CT Scanning

The specimens were fixed by the perfusion of 5 litres of 4% formaldehyde gravity fed through the common iliac artery of both hind limbs (aorta cross-clamped) immediately after death. The skin only was removed and the hind limbs disarticulated at the hip and sectioned across the mid-tibia. The limb was then

thermally sealed inside a plastic sleeve together with 2 litres of 4% formaldehyde. The limbs were then taken for CT scanning, after which they were delivered to the pathology department within 24hrs.

9.2.3. Embedment, Staining & Mounting

Bondaglass Resin Embedment

1. Specimens received in 4% formaldehyde put into 70% Alcohol for 4hours
2. 64op.Ethanol 4hours.
3. IMS 99. Ethanol 4hours X 2.
4. Absolute Ethanol 4hours X 2.
5. Chloroform overnight.
6. Absolute Ethanol 4hours X 4.
   (Gloves must be worn for stages 7 – 9)
7. Bondaglass Resin 2changes over 48hours.
8. Resin + Plasticiser 4changes over 48hours (vacuum at least one change).
9. Embed in Resin / plasticiser / catalyser / Inhibitor.
   Resin & Plasticiser
   Bondaglass 95cm^3
   Di-butyl phthalate 5cm^3
   Embedding Solution
   Resin & Plasticiser 100cm^3
   Butanox 50 1cm^3 (Gloves and face shield must be worn) 1% Hydroquinone in Abs. Ethanol 1cm^3
   Specimens are placed in embedding solution and placed on a roller-mixer for 6hours (specimens must be watched during this period). Embed the tissue in the same solution, and place the mould in cold water to dissipate the heat overnight.
10. Polymerise at 37 ^oC 24hours.
11. Complete at 60 ^oC 24hours.
12. Cut and sand the block to size.
13. Attach to wooden chuck with Cyanoacrylate adhesive.
14. Cut sections 6 - 10µm's on microtome.

Von Kossa Staining:

1. Rinse the section in distilled water
2. Transfer the sections to 2% Silver Nitrate solution and expose to strong light (60Watt bulb) for 30minutes.
3. Rinse in three changes of distilled water.
4. Transfer sections to 2% Sodium Thiosulphate for 5minutes.
5. Wash sections in water
6. Counterstain with 0.25% Safranin O
7. Wash in water.
8. Sections picked up on Melinex, blot dry.
9. Mount using Loctite UV 350.

Von Kossa staining has the following characteristics:

Mineralised bone	- Black
Osteoid	- Red

Mounting - Loctite UV 350

1. Free-floating stained sections are picked up and blotted with filter paper.
2. A drop of loctite UV 350 is placed on a clean dry slide and the section is picked using a pair of forceps and placed on top. Another drop of Loctite UV 350 is placed on the section and a clean coverslip is gently placed on top of this, any air bubbles are gently teased out.
3. This sandwich is then polymerised using long wavelength UV light (Goggles must be worn when using UV light)
4. The slides can then be cleaned up using Alcohol.

9.3. Results

As this section of the thesis is a pilot study (Section 9.1.) to evaluate the histological protocol, the results have been assessed in the form of a general overview. The current sample size is too small to allow statistical comparisons between groups that have a reasonable power. Future studies are underway, under different authorship, which will make an in depth, quantitative evaluation on individual sections.

Problems that have been observed include an inability to locate the defect for sectioning, due to migration of the cement cap (see Table 2). The model has now been modified with the use of a pair of Kirshner wires, instead of screws to hold the Teflon guide. These are retained and allow subsequent fixation for the cement cap with subsequent correct defect identification.

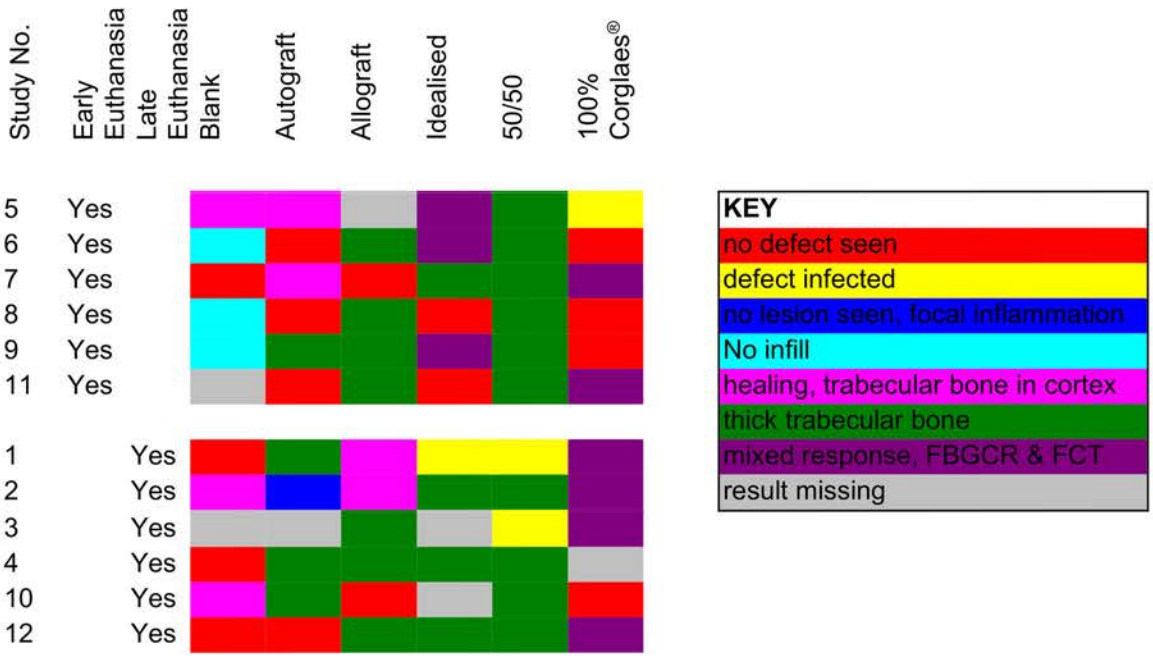

Table 3. Paraffin section results (FBGCR – foreign body giant cell response, FCT – fibroconnective tissue)

There now follows a representative slide for each of the defects.

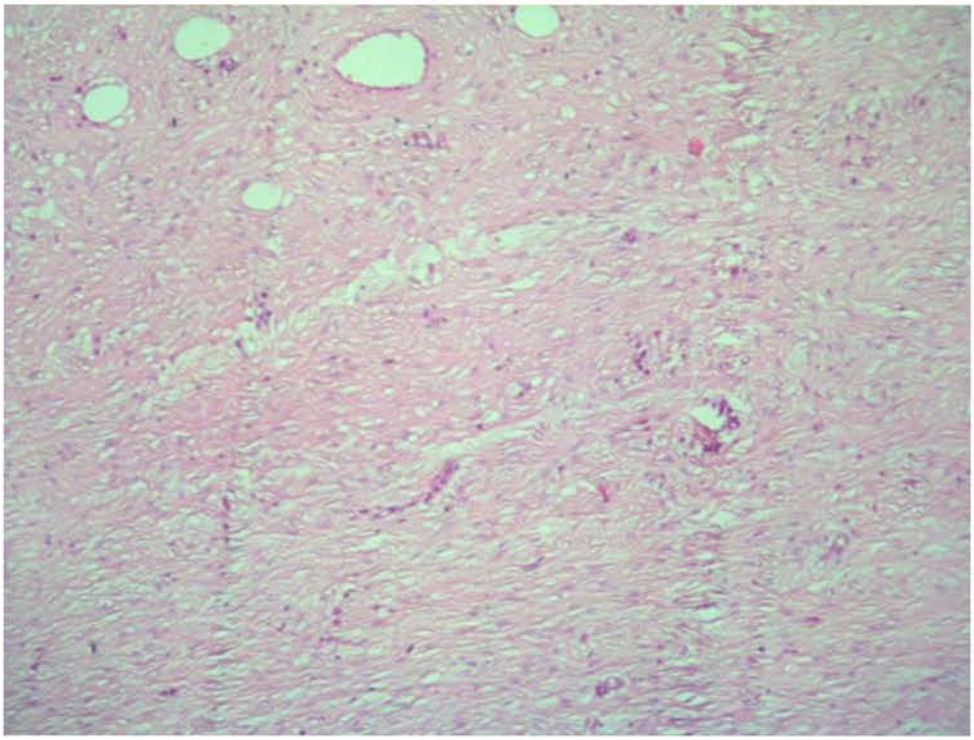

Figure 26. Paraffin section; Blank

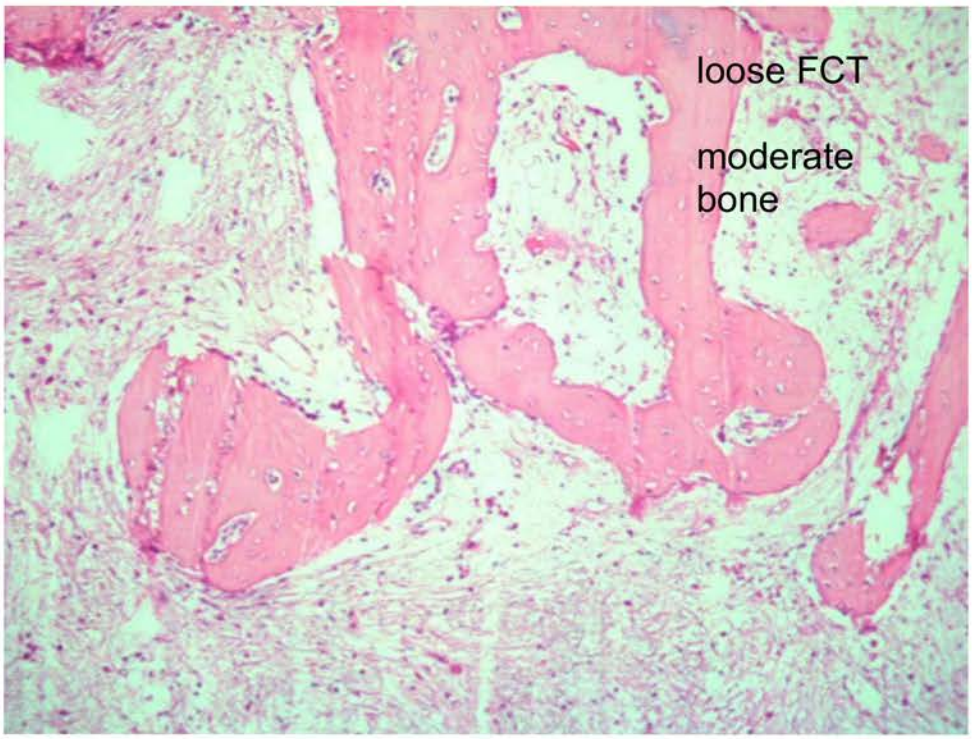

Figure 27. Paraffin section; Autograft

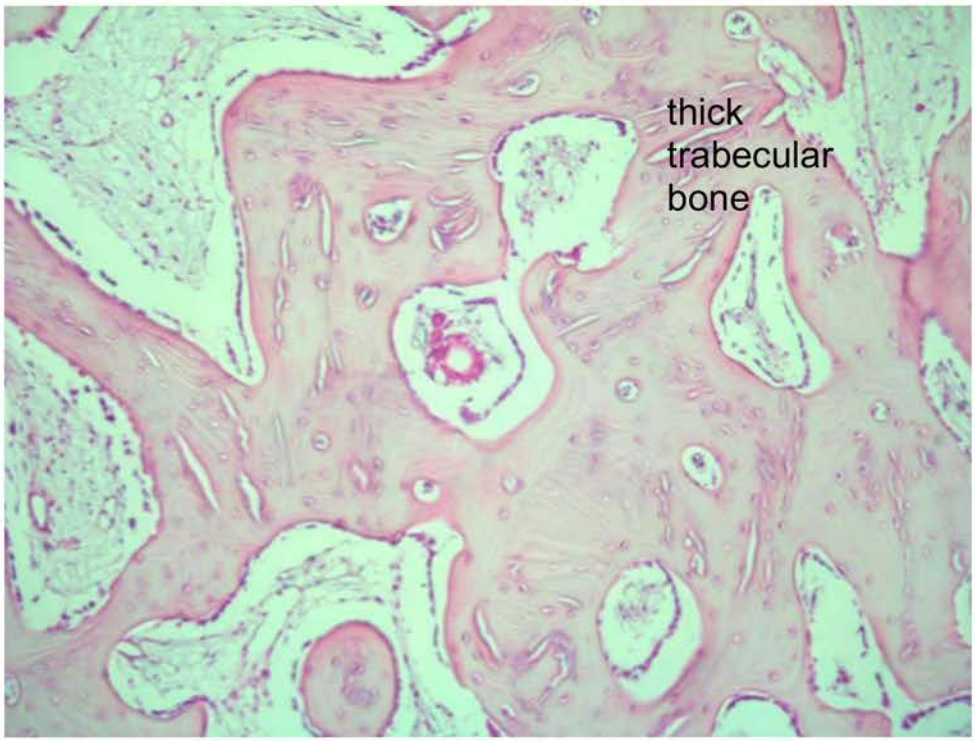

Figure 28. Paraffin section; Allograft.

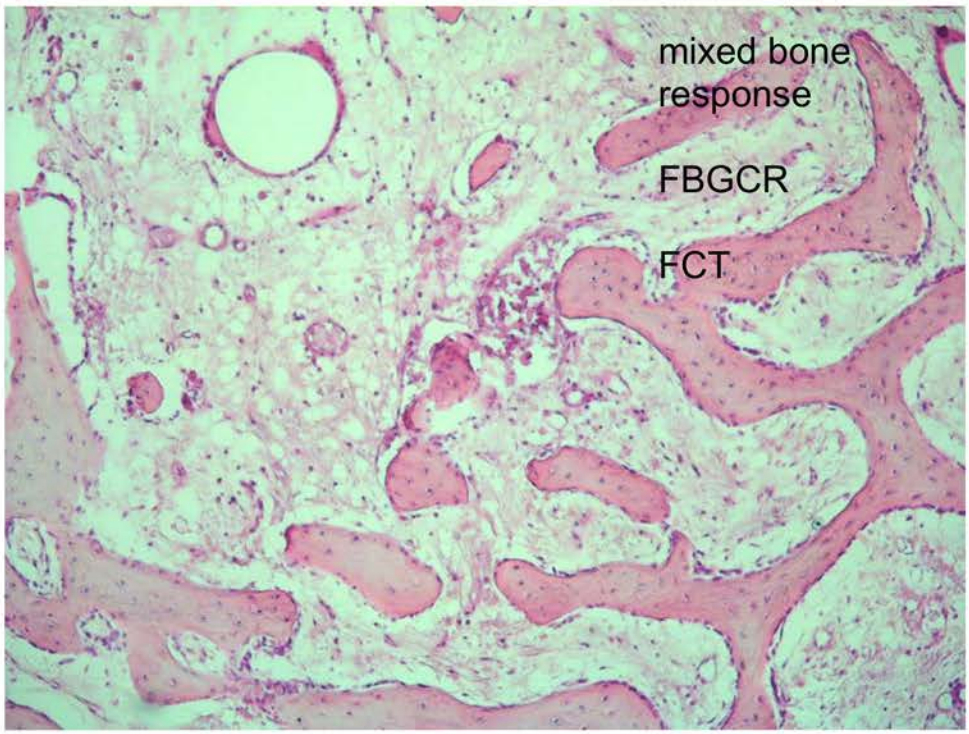

Figure 29. Paraffin section; Allograft idealised with Corglaes® .

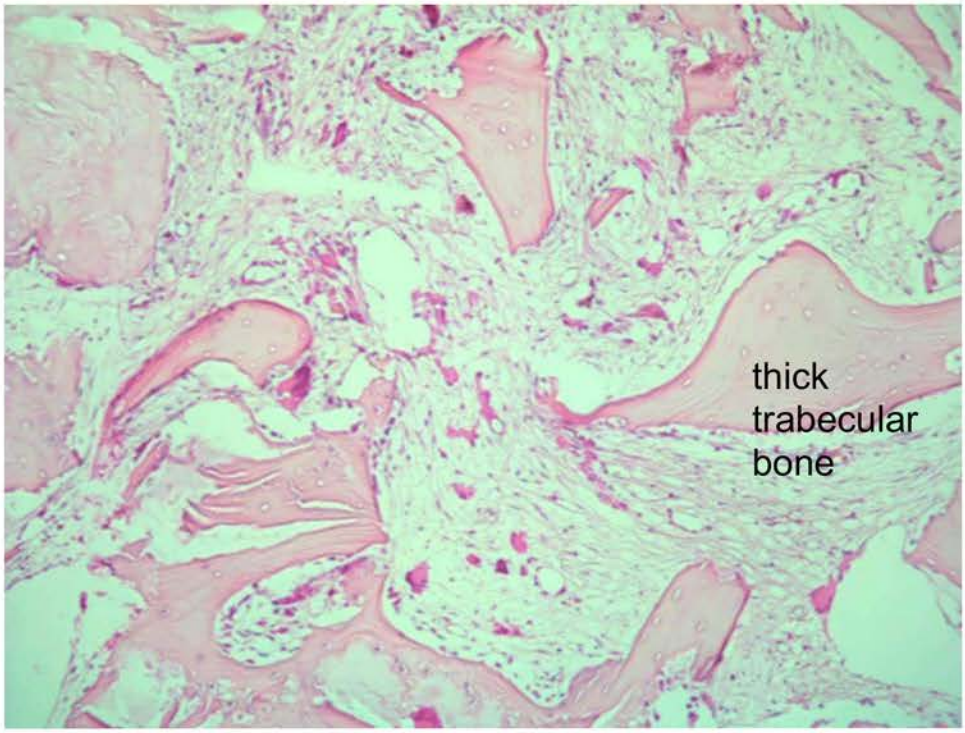

Figure 30. Paraffin section; Allograft / Corglaes® 50/50.

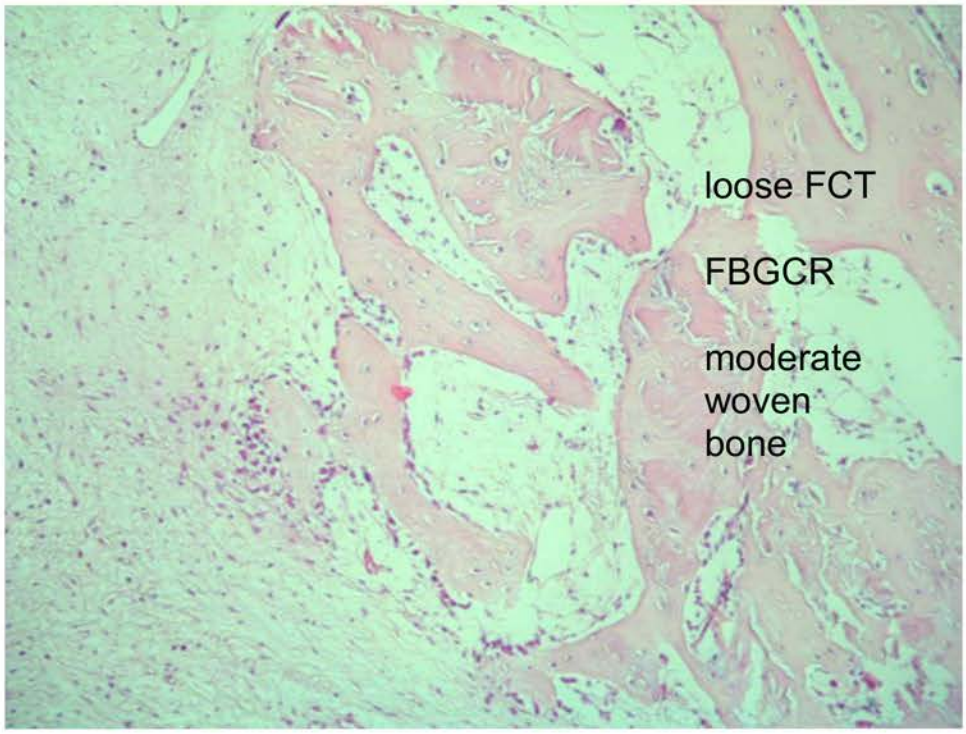

Figure 31. Paraffin section; 100% Corglaes® .

From these representative slides it can be seen that in no sample was there any evidence of any of the synthetic material. This is a particularly important finding because the half-life was a theoretical calculation based on in-vitro solubility combined with an in-vivo attenuation factor. This was determined to be in the order of 12 weeks, but is clearly less than 7 weeks. The attenuation factor, based on resorption of solid rods in a femoral head model is not transferable to this model, possibly due to an increase in vascularity of our model. This will need to be addressed in future when studying the relatively isolated environment of impacted graft in the distal femur (Appendix – Hemiarthroplasty Histology). This current model appears to behave more like the vascularity seen in a fracture model (Section 10.1.3) and may be useful as a representative environment for the proximally exposed graft in the femur, or of the acetabulum.

Fluorescent labelled pictures have successfully shown mineralisation fronts from which appositional bone growth rates were calculated to be ~1.8 – 2.0μm/day.

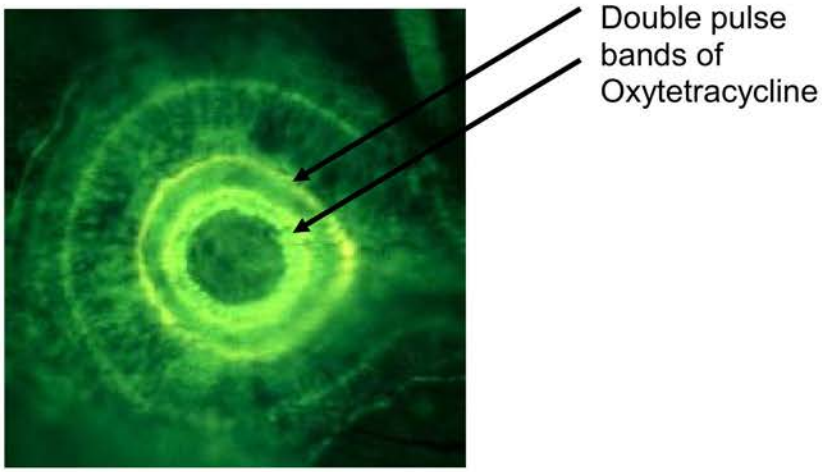

Figure 32. Fluorescent labelled photomicrograph

Chapter 10 Phase II Summary

10.1. Discussion

10.1.1. Animal model

We believe this pilot model allows the production of six defects per animal in an effective and humane manner. Modification of the protocol has reduced the incidence of fracture in subsequent series of animals performed at our centre. The addition of post-operative continuous analgesia, as used in Phase III would be an added advantage (Section 12.2.2).

The cement plugs were not found in a consistent position over the defect site and could therefore not be relied upon for positioning during histological sectioning. Subsequent studies have utilised a pair of Kirshner wires instead of screws to hold the teflon guide, these are left in situ and help to immobilise the cement plugs. Artefacts created by the Kirshner wires in these subsequent studies did not impede measurements of the density within each defect.

10.1.2. CT Scan Densitometry

The precise relationship between density measurement and evidence of remodelling is poorly defined. It would appear that CT densitometry is capable of detecting differences between pellets, but the effect of the additives needs to be controlled for in comparisons. We would now suggest control pellets should be prepared at the time of surgery and stored frozen until the CT scans. They could be defrosted and scanned alongside the limbs and represent the focal average density at Day 0, or day of surgery.

More useful is the comparison between the same pellets over different time periods. This allows an assessment of ongoing resorption or remodelling. Formal

interpretation will need to be made in combination with future histological findings. It should be noted that DEXA scanning of an impacted femur model at another centre has been confounded by the variable presence of radio-opaque cement[134]. A comparison between similar samples in the early and late group seems to be the most appropriate comparison to make (graph 33), because the synthetic additive density confounds variation between samples.

It is interesting to note the relatively poor autograft density compared to allograft, although this difference did not reach significance (Section 8.3). This was thought to be due to the use of cortico/cancellous shavings from drilling the other defects as the source. A better source of autograft should be used in future.

10.1.3. General Histological Observations

There was no evidence of any Corglaes® in any of the early or late specimens. The sections were confirmed to pass through the defects. This may be explained as either too rapid a dissolution rate of the Corglaes®, or processing and interpretation problems with the histology. The latter is thought to be unlikely, due to the absence of voids.

There was no evidence of inhibition of neovascularisation on the provisional slides. This is either attributable to the rapid dissolution rate of the Corglaes®, and/or possibly because the smallest particle sizes used in this project were larger than 300μm (red blood cell average diameter 7 microns and small capillaries around 50 microns).

The fluorescent label bone appositional rate results of 1.8 – 2.0μm/day is comparable to human results[135] which show an average rate of bone formation of 1.4 μm +/- 0.3 μm/day using a similar double pulse Oxytetracycline technique, but in iliac crest biopsy specimens. Values of 2-10μm/day have been reported in fracture models and 100-200μm/day is seen in distraction osteogenesis models.

10.2. Conclusion

The addition of small particles to optimise mechanical strength does not inhibit re-vascularisation. The ovine pellet model is a useful tool for evaluating new synthetic graft materials, particularly due to the reproduction of compaction, which has been shown to be an important variable[130]. It allows comparison of three test samples with a +ve control, a –ve control and standard treatment (allograft). This pilot study highlights avenues for future potential development. It should be compared with the histological results from Phase III, which suggests that the resorption rate of Corglaes® is much more rapid in this defect model than in the revision hip scenario. Indeed the defect model is similar in vascularity to a fracture model and as such is only similar to the most proximal environment of the femur in the revision model. Future models may consider the effect of loading the graft, as this has recently been reported to have a significant effect[131; 132]. Specific to our Corglaes®, it allowed early identification of possible premature synthetic material dissolution that might be expected in the proximal femur in Phase III.

Computerised Tomography scanning of the limbs allowed visualisation of any remodelling of the defects and allowed quantification of focal density - without side or defect position effects. Histological sectioning allowed cytological evaluation of the biological response to the impacted pellets, direct visualisation of bony architecture and determination of appositional bone growth rates.

The results in the context of the null hypothesis were examined:

1. *"Bone graft idealised with synthetic material is not re-incorporated in a biologically similar fashion to bone graft alone"*

This is **true** for CT assessment and **unproven** on histological examination (histological assessment is a pilot study with incomplete data (Table 3.)).

2. *"Bone graft with synthetic material used as a bulking agent in a 50/50 mixture by volume is not re-incorporated in a biologically similar fashion as bone graft alone"*

This is **true** for CT examination, but **unproven** for histological examination, (histological assessment is a pilot study with incomplete data, but there are similarities between allograft and the 50/50 mixture, seen and suggested from Table 3.)

Phase III

Clinical Aspects of Impaction Grafting in Revision Hip Replacement – An Ovine Hemiarthroplasty Model

11.1. Introduction

A model to simulate femoral impaction grafting was developed[136-139]. An ovine model has been used before for primary hip replacement [64,141] and has proved satisfactory. Other models include caprine and canine. Canine models have been shown to be problematic due to the animals failing to weight bear in the post-operative period. Caprine models common in Scandinavia were not locally available. One advantage of the ovine model is that, over-reaming of the ovine proximal femur produces a slippery tube which visually appears to emulate the proximal femur of

humans, which is presented to revision hip surgeons after removal of the failed implant, cement and lining membrane. The ovine model was therefore chosen due to this anatomical feature and also due to previous experience with these animals at the research centres.

11.2. Null Hypotheses

The two secondary null hypotheses below were addressed in this chapter;

1. "At 12 weeks after implantation, there is no difference in ***radiographic subsidence*** of the femoral prosthesis when cemented into in a 50/50 mix of sheep allograft / idealised Corglaes®, compared to sheep allograft alone."

2. "At 12 weeks after implantation, there is no difference in ***micromotion*** of the femoral prosthesis when cemented into in a 50/50 mix of sheep allograft / idealised Corglaes®, compared to sheep allograft alone."

A third, secondary null hypothesis is currently being addressed in Adelaide by other authors and as such does not form part of this thesis, but an abstract has been included for completeness (Appendix – Hemiarthroplasty Histology).

3. "At 12 weeks after implantation, there is no difference in ***biological re-incorporation*** of a 50/50 mix of sheep allograft / idealised Corglaes®, compared to sheep allograft alone."

11.3. Aims

- To produce a supply of sterile fresh frozen allograft bone of known particle distribution
- To produce a supply of sterile synthetic graft material of known particle size distribution

- To produce a 50/50 mixture by volume (at a standard compactive force) of allograft and Corglaes®
- To create, bench test and validate a laboratory Ovine femoral impaction grafting model
- To develop an in-vivo Ovine femoral impaction grafting model which can be performed in a standardised fashion
- To radiologically determine subsidence of the prosthesis within the proximal femur over a 3 month period
- To quantify the degree of micromotion of the prosthesis within the proximal femur at explantation

11.4. Study Design

11.4.1. Calculation of Sample Size

The sample size required to test the hypothesis is based on an estimate of expected subsidence within the first twelve weeks since implantation. There is a large variance of quoted subsidence for human impaction grafted total hip replacements with a range of average subsidence from 1-9mm within the first year[28], with individual subsidence ranges[29] up to 37mm. The new sheep model was hoped to equate to experiences in humans. Both graft groups were thought likely to subside, with the control group subsidence of 1mm +/- 1mm Standard Deviation. A clinically significant difference was estimated as 2.5mm

The Type I and Type II errors were assigned as $\alpha = 0.05$ and $\beta = 0.2$ (two tailed, 95% confidence with 80% power). The sample size was calculated using the above figures with the NHMRC (National Health & Medical Research Council) sample size calculation software (SAM). The number of animals determined for each group was 8. To be specific, with two groups of 8 sheep, there is 80% power to detect a difference between the means of 1.51 standard deviations at the 5% significance level, and 90% power to detect a difference of 1.75 SD's.

Review of the relevant literature of sheep hip arthroplasty[140] suggested a 10% complication rate might be expected. Local experience showed a complication rate of 40% for the cemented hemiarthroplasty model[141] and 20% for the cemented total hip replacement model[142]. The former figure represented the initial pilot study and the latter figure was felt to reflect early difficulties with the model. Our study involved a hemiarthroplasty rather than a total joint replacement, so a complication rate of 10% was allowed for. The revised sample (N') to account for dropouts was obtained by the following formula[141].

$$N' = N / (1 - R)^2$$

N' = revised sample rate
N = first estimate sample size
R = drop-out rate

$$N' = 8 / (1 - 0.1)^2 = 9.87$$

Therefore 10 animals were included in each group.

11.4.2. Study Animals

A flock of sheep was purchased from a single breeder, to ensure a uniform environmental and genetic background. The animals were kept together at the holding farm and allowed to familiarise themselves with their surroundings and human contact. They were brought into town in small groups for the two weeks around the time of surgery and kept 4 to a pen at the Royal Adelaide Hospital, where immediate pre and post-operative recovery was in pairs of individual pens to maintain social interaction of the animals.

11.4.3. Study Groups

Thirty sheep were allocated to the study. This comprised ten sheep for the allograft alone group, ten sheep for the allograft plus Corglaes® group, three donor sheep who were harvested of cancellous bone prior to the first hemiarthroplasty, and seven extra sheep to be used as replacements if necessary.

11.4.4. Inclusion and Exclusion Criteria

All animals were assessed for physical fitness prior to inclusion in the study by an independent veterinary surgeon. Full mouth mature Merino wethers (castrated adult males), greater than 50 kg, were included in the study.

11.4.5. Stratification and Randomisation

Randomisation was performed using blank sealed envelopes containing an enclosure with the phrase 'allograft alone' or 'allograft & Corglaes®' written on it. Ten of each enclosure were made, sealed and shuffled independently. The envelopes were held in theatre. An envelope was picked at random and opened for each sheep by an independent observer.

11.4.6. Study Logistics

Each animal was assigned a study number and an individual identification number. The independent observer kept all details of graft type. No details of graft type were kept with the usual post-operative individual case notes. At the time of surgery the surgeon was blinded up to the time of impaction. The observer defrosted the correct graft mixture out of view of the surgeon just prior to surgery. The surgeon was unblinded to the graft mixture only when the femoral canal had been finally prepared, ready for impaction. At the time of subsidence, micromotion and histological testing, their individual number identified the animals only. Only once all results had been obtained and analysed were the graft types unblinded. There were no clues to graft type in the appearance of the femurs during subsidence and micromotion analysis (performed by the author), however the histological sections

showed evidence of graft type. An independent histologist, unaware of any differences between graft types therefore assessed the histomorphological differences. A synopsis of the histological findings only is presented in Appendix – Hemiarthroplasty Histology.

11.4.7. Drop-out from the Study and use of Replacement Sheep

A Veterinarian and the surgeon assessed the sheep every day in the immediate post-operative period and weekly thereafter. Staff at the field hospital reviewed the animals daily. It was decided that any of the following complications would necessitate withdrawal of the animal from the study: failure to complete the operation, femoral fracture, dislocation, sepsis, walking score broadly different from normal rehabilitation, undue suffering or death due to unrelated causes. All withdrawals to be euthanised in the standard fashion (see below) and a post-mortem to be performed.

Once the initial cohort of twenty animals had been entered into the study, the independent observer calculated the actual number of sheep in each group after allowance for any withdrawals. The number of replacement sheep required to ensure ten sheep in each group on day 0 (and hopefully at least 8 in each group after 12 weeks), was calculated. Replacement sheep then underwent a hip hemiarthroplasty with allocated graft type as before. These were again blinded from the surgeon as before by the independent observer.

11.4.8. Control of Bias and Study Blinding

The same surgeon, the same anaesthetist, one assistant and one theatre orderly undertook the procedures. The randomisation was performed by an independent observer who only un-blinded the surgeon once the femur had been prepared and the graft had spent the morning defrosting from its –70°C storage. The independent observer only kept records of graft type, separate from all animal records and the project leader.

11.5. Ethical Approval

Institutional ethics approval was obtained prior to the study based on the study design and sample size calculations above. All procedures were performed under the ethical guidelines of the institution.

Chapter 12 Sheep Hip Hemiarthroplasty

12.1. Introduction

The ovine femoral diaphysis is devoid of cancellous bone and is extremely greasy. To simulate a revision situation the proximal femur is 'over-reamed' until there is just a thin cortical shell. This provides a good model of the similarly poor environment for surgery as found in hip revision cases seen in humans.

Autograft could have been used, such as in one of the drill holes in the defect model (Section 7.2.1). However, the volumes of bone required would have necessitated considerable donor site morbidity, so allograft was the next most appropriate source for our model[48; 143-148] and simulated the clinical use of allograft in the human revision hip scenario.

12.2. Materials and Methods - Operative Procedure

12.2.1. Test Material Production

Four sheep were euthanised (20ml Lethobarb via the jugular vein) before the main project as a source of allograft. The proximal humerii, proximal femora and distal

femora were removed under sterile conditions, cleaned of soft tissue and cut from their diaphyses to produce 1000g of cancellous graft. These were then divided into two unequal groups, 2/3 passed through the small (3mm diameter) and 1/3 through the large (6mm diameter) Aesculap bone mill used in Phase I & II (Section 2.4 & 7.2.1). The resultant graft was then combined to produce a more uniform particle size distribution. This 'idealised' mixture was then divided again into two unequal groups: 2/3 and 1/3 by weight respectively. With the addition of Corglaes® to the 1/3 idealised mixture, two final groups were then produced:

Test Materials

1. Idealised graft alone
2. Idealised graft with idealised Corglaes® in a 50/50 mixture

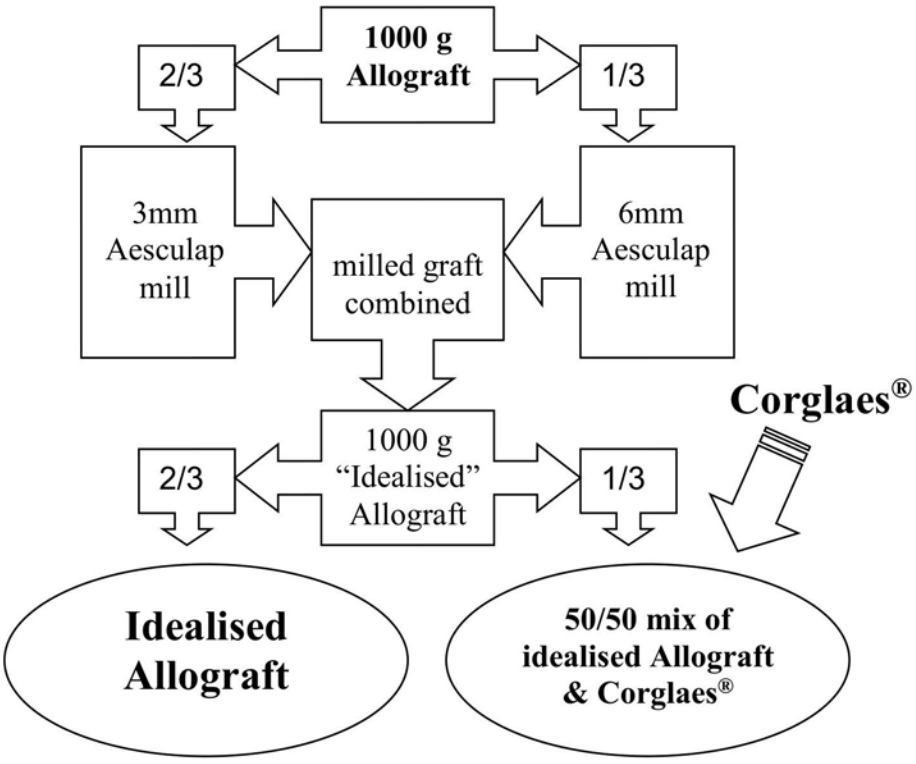

Figure 33. Schematic test material production

Group 2 was produced by the addition of Corglaes® with a linear log particle size distribution in a 50/50 ratio by volume (Figure 17). The volumes of Corglaes® compared to sheep bone were determined in the knowledge of mass and density at one standard impaction. Samples from the above two groups were then sent to microbiology for culture to ensure sterility before use. The groups were then divided into fifteen equal portions, labelled and stored[149] at –70ºC.

12.2.2. Anaesthesia and Antibiotics

The sheep were allocated individual pens and starved for 24 Hrs prior to surgery. Half an hour before anaesthetic induction, a premed of 0.1mg/kg body weight Xylazine was given intramuscularly for sedation and analgaesia. At induction the jugular vein was cannulated with a 10cm 18G catheter, attached to a 3 way tap and fixed in position (sutured and held with cyanoacrylate adhesive). 750mg-1g of Thiopentone was given intravenously to induce anaesthesia. The animal was then intubated with a cuffed tube, maintained on a circle circuit with Halothane 1-2.5% and 4L/min oxygen. Antibiotic cover was given according to the regime of Bruns et al[150]. 2g Cephalothin (1st generation Cephalosporin) was given at induction in 500ml 0.9% saline, with another 2g in 1000 ml 0.9% saline solution administered throughout the operative procedure. Following recovery from anaesthesia a further 2g in 500 ml of 0.9%l saline was administered intravenously and then at 4 hourly intervals for a further two doses. Non-steroidal anti-inflammatory cover during the first 24 hrs was provided by Flunixine Meglumine (50mg), which was administered intravenously at anaesthetic induction and prior to recovery from the procedure. Post-operative pain was alleviated by a continuous infusion of Xylazine (1mg/Hr) over the 48-72 hour post-operative period via a syringe driver (Graseby Medical, Watford, Hertfordshire, UK). These techniques were well tolerated by the sheep and in current studies appear to be providing good levels of analgesia and comfort.

12.2.3. Preparation

All preliminary skin preparation was performed in the anaesthetic induction suite with the animal positioned in right lateral recumbency. The left and right hind-legs were shorn, including the perineum, to a line 20cm cranial to the tuber coxae. Close wool trimmers were used in the immediate surgical site. The upper leg below the knee was wrapped in a crepe bandage and suspended away from the body. The leg was then scrubbed with aqueous betadine and washed sequentially with Povidone-iodine (10%) and alcohol (90%) and allowed to dry. Once the ethanol had evaporated, Povidine-iodine solution was applied. The animal was then moved to the surgical suite.

The leg was prepped with povidone-iodine and square draped around the body, with the leg enclosed in stockinet wrapped with a bandage. The final layer was a water-repellent hip drape (Johnson and Johnson, Adelaide, Australia). The surgeon and assistant wore standard disposable water-repellent gowns and double gloves.

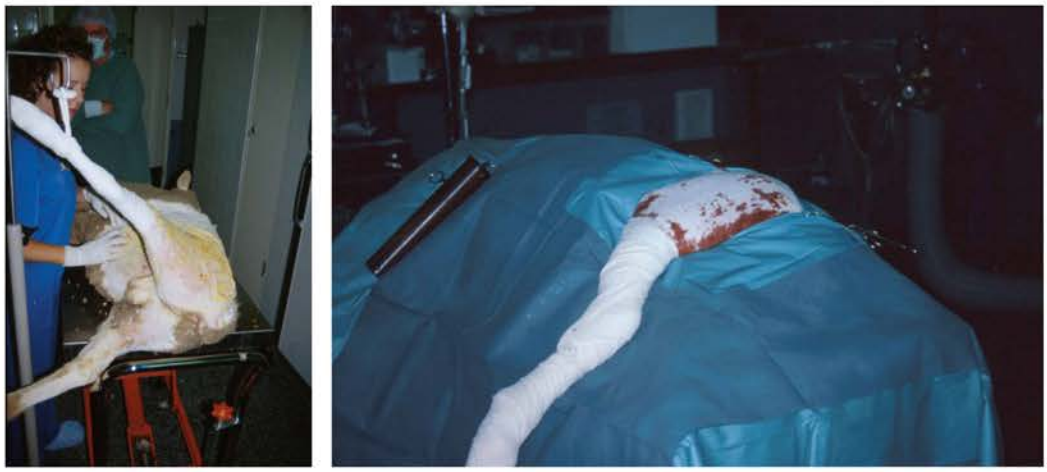

Figure 34. Operative site skin preparation.

12.2.4. Anatomical Exposure and Dissection

A curvi-linear incision was made, based over the greater trochanter. Commencing at the mid-point between the tuber coxae and the greater trochanter, the incision extended dorsally over the palpable greater trochanter, curving along the length of the femur for two-thirds of its length. Haemostasis was ensured with cautery and the skin edges sutured to the stockinet drape, to partition the skin from the surgical field. Swabs used up to this point were then discarded. The anterior border of the fascia

lata was then identified and dissected along the length of the wound to expose the underlying vastus lateralis and gluteal muscles. A pair of self retaining forceps held the wound open, while a plane was found between vastus lateralis and the middle gluteal muscle to reveal the flat shiny tendon of gluteus accessorius (deep gluteal). A consistent large vessel supplying the undersurface of the middle gluteal muscle was cauterised. The flat tendon was then incised across its width 3cms from its attachment to the femur. The incision was to only half of the tendon depth and the superficial fibres on the femoral side were teased towards the femur almost to their insertion, thus creating a tendinous flap.

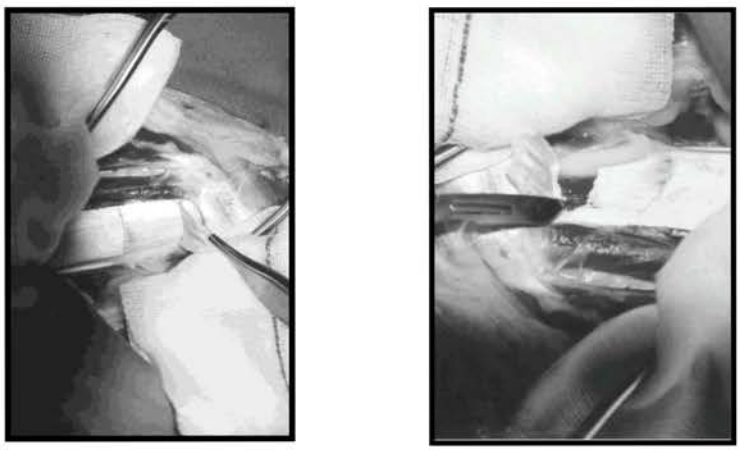

Figure 35. Double breasted exposure (Appendix – Ovine hip hemiarthroplasty)

The deeper half of the tendon was divided across its width at the insertion with the femur to allow a double-breasted closure. The deeper gluteals were divided 3mm from their femoral insertion to expose the capsule lying beneath. A 'T' shaped capsulotomy was performed, proximally based at the acetabular labrum, and the free corners marked with stay sutures. Haemostasis was again ensured at this stage. With traction on the leg, the joint was visualised and a pair of curved scissors used to section the ligamentum teres. Care was taken not to damage the acetabular cartilage. The femur was then dislocated and the neck exposed by subperiosteal reflection of vastus lateralis.

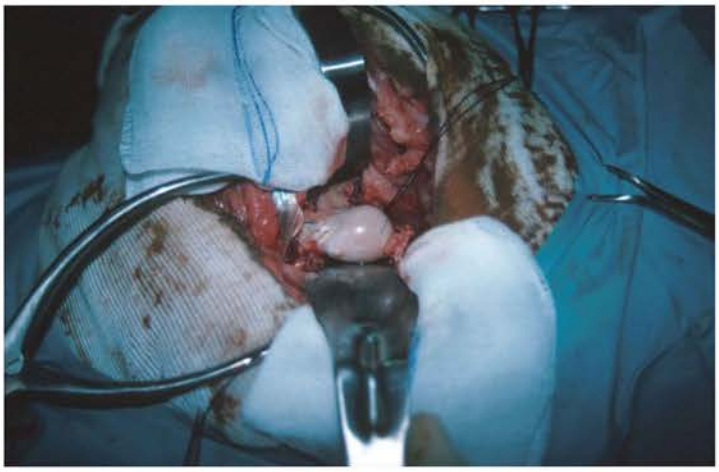

Figure 36. Surgical exposure, with flat retractor elevating the dislocated femoral head.

12.2.5. Femoral Preparation

Greater exposure than in a standard total hip replacement was carried out, using a perisoteal elevator to remove the soft-tissue remnants on the femoral neck ventral to the head to just beyond the level of the anterior tubercle laterally and the commencement of the lesser trochanter medially. A low femoral neck osteotomy, parallel to the base of the femoral head was performed using an oscillating saw (2.5 cm blade, battery operated saw - Stryker, Kalamazoo, Michigan, USA) with the leg held in external rotation. The head was then removed and its widest diameter measured. The acetabulum was inspected, any redundant ligamentum teres excised and a moist swab inserted for protection.

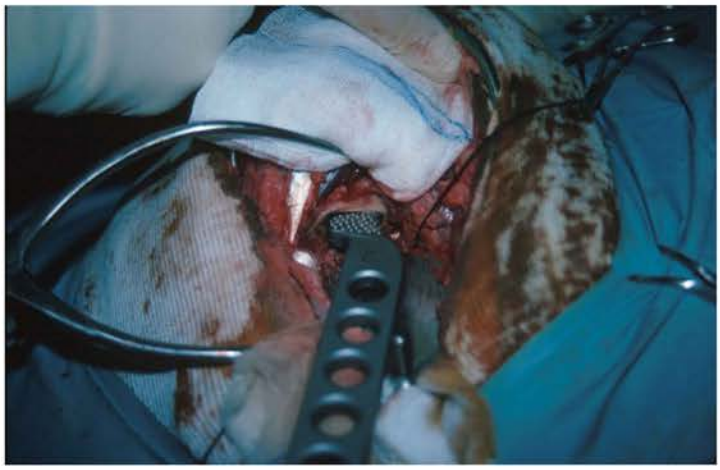

Figure 37. Femoral canal broached and reamed.

12.2.6. Canal Preparation

Howmedica Int. Inc. provided the surgical instruments for reaming and impaction grafting in the sheep. The femoral canal was reamed to remove all cancellous bone, leaving only a cortical sleeve. This was achieved by broaching the canal with the T-handled reamer and widening the canal with the size 1 & 2 rasps. Any remaining cancellous bone was removed with the curette. The sheep femoral medullary cavity contains mostly fat after the first 2cm when passing distally from the neck, and this fat was removed by brushing the canal (Johnson & Johnson, Adelaide, SA) followed by jet lavage to remove any remaining tissue. The canal was then inspected to ensure an empty slippery walled cortical tube, similar to the interior of a human revision hip replacement after removal of the cement mantle and fibrous membrane, had been produced.

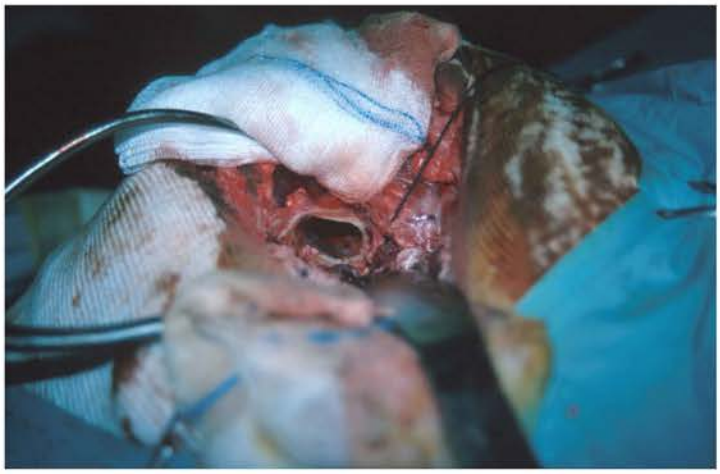

Figure 38. Femoral canal prior to impaction grafting.

12.2.7. Trans-luminal Wire

The lateral aspect of the femur at the caudal end of the wound was then exposed, 10cm distal to the cut edge of the medial femoral calcar. A 2mm K-wire was then drilled medially across the femur until just through the medial cortex (Section 13.2). The exact position and angulation of this wire was ninety degrees to the long axis and ninety degrees to the AP plane of the femur, across the diameter. The other end, protruding out the wound was protected with a cork.

12.2.8. Impaction Technique

The proximal femur was then exposed once more. The cement restrictor with its centralisation rod was passed down inside the femoral canal and felt to fully engage its slot over the K-wire just placed. Care was taken to hold the centralisation rod in neutral alignment while graft was impacted, to prevent subsequent implant mal-alignment. The graft was unblinded at this stage to the surgeon, having spent the morning defrosting from its –70°C storage. The tip of the barrel of a 2.5ml syringe was cut off and the barrel withdrawn. This was then pushed into the graft until full, to aid delivery of the graft and also to prevent inadvertent 'hand picking' of suitable clumps for impaction. The syringe was introduced fully into the femoral canal and the graft pressed in with the plunger.

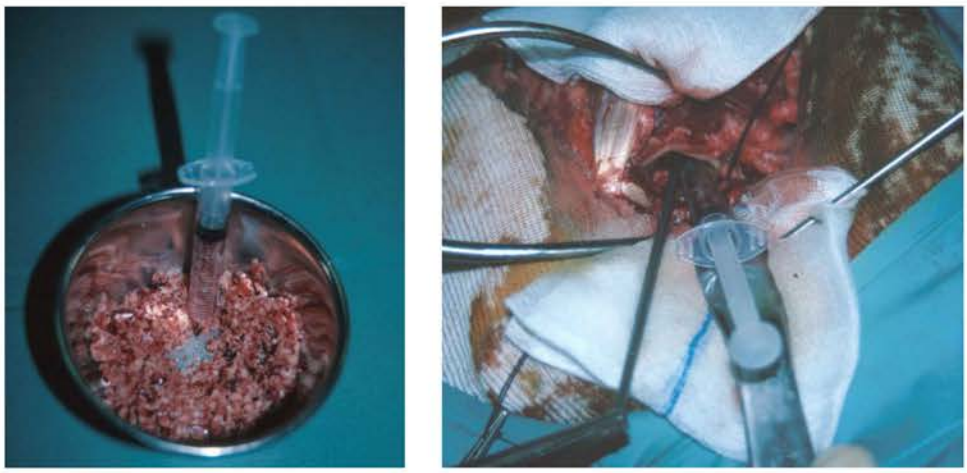

Figure 39. a) graft selected by 'sawn- off' syringe b) introduced around centraliser.

The graft was then tamped down hard with an intramedullary rod until the cement restrictor was firmly held. More graft was then introduced with the syringe and tamped down. As this process was repeated the femoral canal was slowly filled. When more than half full, the femoral stem phantom was used to impact the graft with blows from the hammer. Towards the end (after 6-8 syringes of graft), the phantom became increasingly difficult to impact further into the graft, with graft fluid being expelled around the mantle. Impaction at this stage was performed more

slowly, to allow the fluid to escape and to allow for any elastic deformation of the graft and femur. Correct phantom ante-version and axial alignment (to restore anatomical head position), with a circumferential graft mantle was aimed for. Close inspection of the cortical ring was maintained at this stage to detect any hairline fractures that might develop and to prevent graft / cement defects due to implant contact with the femur. The line on the centralisation rod aligned with the marker in the window of the phantom when correctly seated. Impaction was complete when the phantom reached this line, but could not be impacted further despite 10 further firm hammer blows. In cases of hairline cracks developing, the phantom was withdrawn slightly, a pair of cerclage wires were tensioned around the proximal femur and the phantom was re-impacted.

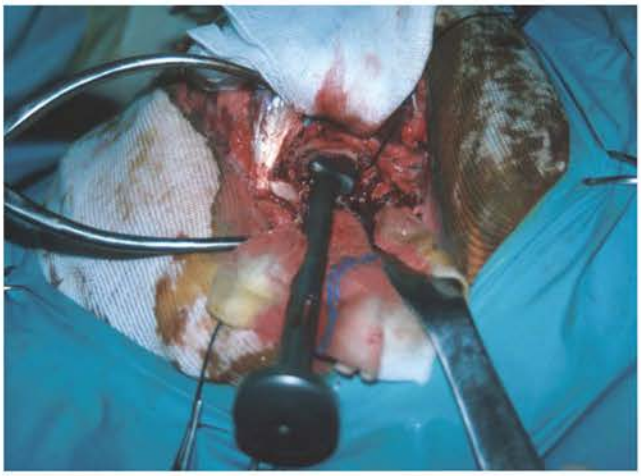

Figure 40. Phantom impactor driven to correct level.

12.2.9. Prosthesis Insertion

Polymethylmethacrylate bone cement (One 20 gram packet of Surgical Simplex P cement - Howmedica Inc., Rutherford, New Jersey, USA) was then mixed in a bowl and loaded into a cement gun fitted with a narrow revision nozzle. At 3 minutes the phantom was tapped out and the centraliser rod unscrewed from the cement restrictor, followed by retrograde injection and pressurisation (thumb occlusion) of the cement within the graft mantle. This was maintained until 5 minutes, at which point the final stem, fitted with a centraliser (lugs removed) was introduced. The implant was finally seated home in correct alignment after several axial blows with

the hammer to the insertion jig. All extraneous cement was trimmed from around the implant. Those implants without a bead on the shoulder had cement in apposition to the shoulder. Pressure was maintained on the implant until the cement had cured. The wound was then thoroughly lavaged and cleared of any remaining graft or cement and the acetabular swab removed. The taper of the modular stem was dried and the correct size head was then attached and a trial reduction performed. Occasionally, due to asymmetry of the natural femoral head (glans shape) the acetabulum would require a few turns with the correct sized reamer to allow good seating and suction captivation. The hip was then dislocated, the head secured on the taper with a blow from a covered blunt instrument and relocated. A final lavage of the wound was then performed.

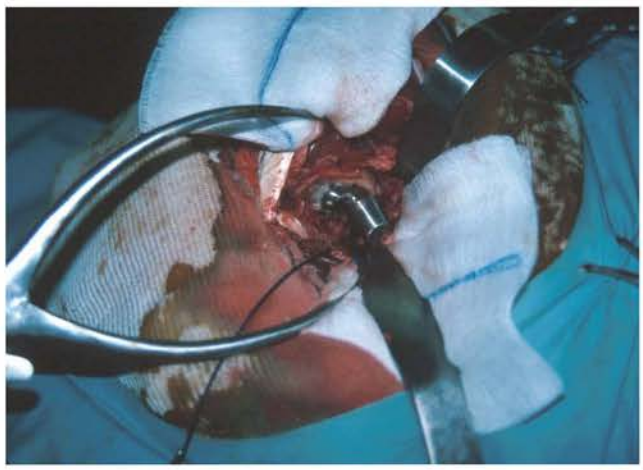

Figure 41. Femoral stem cemented in situ.

12.2.10. Anatomical Closure

The capsule was repaired with a continuous 1 PDS (Taper-cut needle - polydioxanone monofilament – Ethicon, EH11 4HE, Edinburgh) and the stay sutures removed. The deeper gluteal muscles were reattached to their tendinous cuff en-masse with continuous PDS. The Accessory Gluteal tendon was repaired to its original state by continuous PDS around the 4 sides of the double-breasted tenotomy, starting with the transverse deep layer. Joint stability was reassessed at this stage. The protruding K-wire in the distal femur was exposed again and the additional K-wires placed (Section 13.2). The original wire was then bent over and cut short, so as to lie flush with the long axis of the femur. Fascia lata was then repaired along its

length with 0 Vicryl. The deep fascia is opposed with 2/0 Vicryl, followed by a subcuticular 2/0 Vicryl suture layer. The skin edges were closed with metal staples, which remained in-situ for the duration of the experiment.

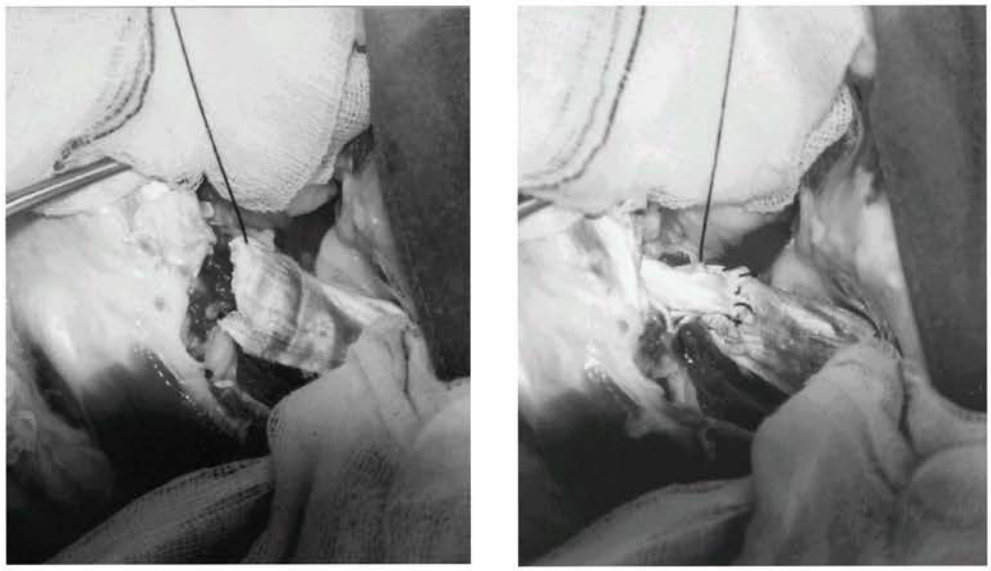

Figure 42. Double breasted wound closure (Appendix – Ovine hip hemiarthroplasty)

12.2.11. Post-operative Recovery

At the end of surgery, but while still anaesthetised, an antero-posterior and an extended ventro-dorsal X-ray were taken and when these were satisfactory the exposed wires were removed and the sheep allowed to recover. The sheep were suspended in a cotton/canvas sling during transfer from the operating room to the recovery pen (1m x 2m). The slings fully supported the sheep if they wished and were elevated posteriorly to allow only partial weight bearing on the hind limbs. The sheep remained in this sling for 24Hrs postoperatively, at which time the sling was then removed. The sheep were then transferred to a larger pen (3m x 3m), holding two individuals, to allow free ambulation and socialisation for 4-14 days prior to their transfer to a small grassed paddock (10 m x 20 m).

Figure 43. Post-operative recovery

12.2.12. Fluorochromes and Walking Scores

Every week the sheep were inspected in the field and herded into a pen through a race. Walking and running was observed and scored to ensure appropriate rehabilitation over time. An in-house scoring system was utilised, where lying = 1, standing abnormally = 2, stands normally = 3, walks normally = 4 and runs normally = 5 points (Table 5). At 28, 56 and 72 days the sheep were given an intra-muscular fluorochrome injection (Xylenol Orange, Calcein and Oxytetracycline respectively (Appendix)).

12.2.13. Euthanasia

On the 84th post-operative day the animals were euthanised (20ml Lethobarb via the jugular vein). At the time of euthanasia, both femurs were exposed and then carefully removed; a contact radiograph (Section 13.1) image was taken and the femur was then frozen to –70ºC in protective labelled sealed bags surrounded by vermiculite insulation to protect against 'freezer burn'.

12.3. Results

The major outcomes of subsidence, stability and biological response will be dealt with in chapters 13, 14 and 15 respectively.

Each animal was examined every week and the gait observed and scored. Any animal that fulfilled the drop-out criteria (Section 11.4.7) was withdrawn from the study. Of the twenty-six animals entered into the trial, eleven were withdrawn. There were five femoral fractures, two cases of deep infection, one dislocation, one failed anaesthetic, one post-operative aspiration and one death due to widespread Ovine Tuberculosis (Table 4).

Total number	26	
Surgical complication rate	8	(**31%**)
Total withdrawal rate	11	(42%)
Femoral fracture	5	(19%)
Infection	2	(8%)
Dislocation	1	(4%)
Anaesthetic complication	2	(8%)
Unrelated disease	1	(4%)

Table 4. Complications

Femoral Fracture:

Three femoral fractures were identified intra-operatively and were all treated by cerclage wiring. All three were longitudinal splits of the anteromedial cortex, which occurred during the final stages of impacting the proximal femur. One was the result of inadvertent abutment of the phantom impactor antero-medially during impaction, but no specific cause except the fact that ovine bone is more brittle than human bone could explain this. Once identified, unfortunately cerclage wiring could not prevent further propagation in the post-operative period, culminating in all 3 cases with a

mid-diapyseal spiral fracture (Figure 44). The two further cases of femoral fracture occurred at the time or shortly after unsupervised vehicular transportation to the field hospital and were thought to be a consequence of unprotected weight bearing during loading and unloading. Ideally transportation in the early postoperative period should be avoided.

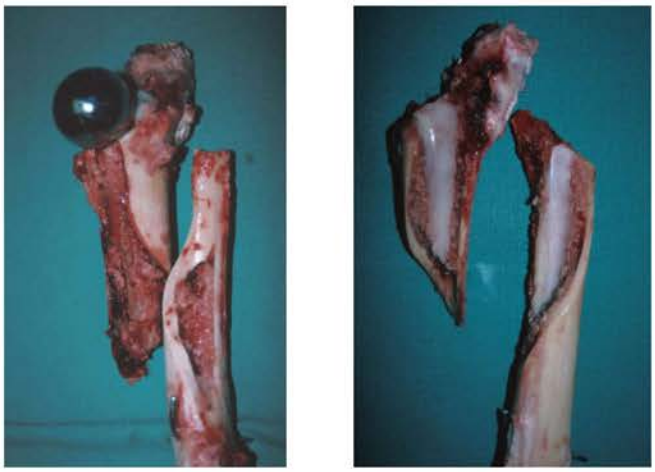

Figure 44. Post-mortem appearance of femoral fractures

Dislocation:

The dislocation rate was much improved compared to previous results from this centre. This may be due to the new surgical approach developed for this study, utilising a double-breasted repair of the anterior structures. This new approach (Appendix – Ovine hip hemiarthroplasty) was based on the principles of 'double-breasting' utilised in the Bankart procedure for shoulder stabilisation as modified by Zarins, McMahon and Rowe[151-153]. The single case of dislocation could have been avoided, as at the time of surgery it was noted that the femoral head was perhaps a little large, but no action was taken. At post-mortem the capsule repair was torn but the double-breasted repair was still intact.

At the end of the twelve-week period there were 8 animals in the allograft/synthetic graft group, but only 7 animals in the allograft alone group. The 'missing' animal in the allograft alone group was withdrawn one week before the endpoint, due to a deep infection, but was analysed as well to give useful information, as it may have represented a loose implant.

The results of the 15 animals remaining in the study are tabulated in Table 5.

Study No.	Weight Kg	Walking Score / Week												Walk score total
		1	2	3	4	5	6	7	8	9	10	11	12	
Allograft Group														
4	57.0	2	3	3	3	4	4	4	4	4	5	4	5	45
5	57.0	2	3	2	3	4	4	4	4	4	4	4	4	42
7	53.0	2	3	3	3	4	4	4	4	4	5	4	4	44
10	66.0	2	3	3	3	3	2	3	4	4	4	5	5	41
11	53.5	2	3	3	3	4	4	4	4	4	4	4	5	44
18	61.0	2	3	3	3	4	4	4	4	4	4	5	5	45
20	56.0	2	3	3	3	4	4	4	4	4	4	5	5	45
												Average		43.7
												SD		1.6
Allograft / Corglaes® Group														
3	57.0	2	3	3	3	4	4	4	4	4	4	4	5	44
6	52.0	2	3	3	3	4	4	4	4	4	4	4	4	43
8	52.0	2	3	3	3	4	4	4	4	4	5	5	5	46
13	52.5	2	3	3	3	4	4	4	4	3	3	4	4	41
15	53.5	2	3	3	3	4	4	4	4	4	5	4	5	45
17	60.0	2	3	3	3	4	4	4	4	4	4	5	5	45
23	55.0	2	3	3	3	4	4	4	4	4	4	5	5	45
26	58.5	2	3	3	3	3	4	4	4	4	4	4	4	42
												Average		43.9
												SD		1.7

Table 5. Weekly walking scores (where lying = 1, standing abnormally = 2, stands normally = 3, walks normally = 4 and runs normally = 5 points)

As can be seen from Table 5 there is no statistically significant difference between the walking scores of the two groups.

Chapter 13 Radiological Assessment of Stem Subsidence

13.1. Introduction

Instead of using roentgen stereophotogrammetric analysis (RSA) which has been described by others[154; 155] along with certain complications[156; 157], we developed a simpler system. We were able to reproduce the position of the femur in three-dimensions over an x-ray plate with reasonable precision on the two occasions that x-rays were taken, hence reducing the need for stereo X-rays. Fortunately, as subsidence tends to be relatively large in impaction models compared to primary cemented models, the tolerable error is increased.

Two radiographs were taken of each animal. The first radiograph was taken immediately post-operatively, while the animal was still anaesthetised to reduce movement artefact, and the second radiograph was a contact radiograph of the ex-planted femur (Faxitron contact radiography unit - Hewlett Packard, USA). A standard technique for each procedure was followed, after development of the most reliably accurate method from experimental trials. The x-rays were examined for evidence of radiolucent lines, subsidence, fracture or other significant abnormality [158]. Measurements from each x-ray were then taken, standardised for magnification variables and compared. From these comparisons a measure of the degree of subsidence of the femoral component down the femur could be calculated for the twelve-week period between the two x-rays.

13.2. Materials and Methods

The key to the radiological technique was the K-wire in the distal femur, which also acts to prevent distal migration of the cement restrictor. The exact position and angulation of this wire (ninety degrees to the long axis and ninety degrees to the AP

plane of the femur, across the diameter) was mirrored in two further removable wires used to align the femur during the post-operative x-ray.

Towards the end of the operation (Section 12.2.10), a second, full length 2mm K-wire was drilled across the diameter of the femur, 1cm distal and parallel to the first wire in both planes. The original wire was then bent over and cut short, so as to lie flush with the long axis of the femur. A third 2mm K-wire was then passed through tensor fascia lata and drilled across the diameter of the greater trochanter at the mid lateral point of the femur (proximal to the graft), parallel to the second long K-wire. These two wires indicate the mid-lateral points of the proximal and distal femur respectively and protrude out of the wound until after the post-op radiographs, at which point they are removed easily with a twist of a hand drill. All three wires can be seen in Figure 48, the two removable wires can be seen in Figure 45 below.

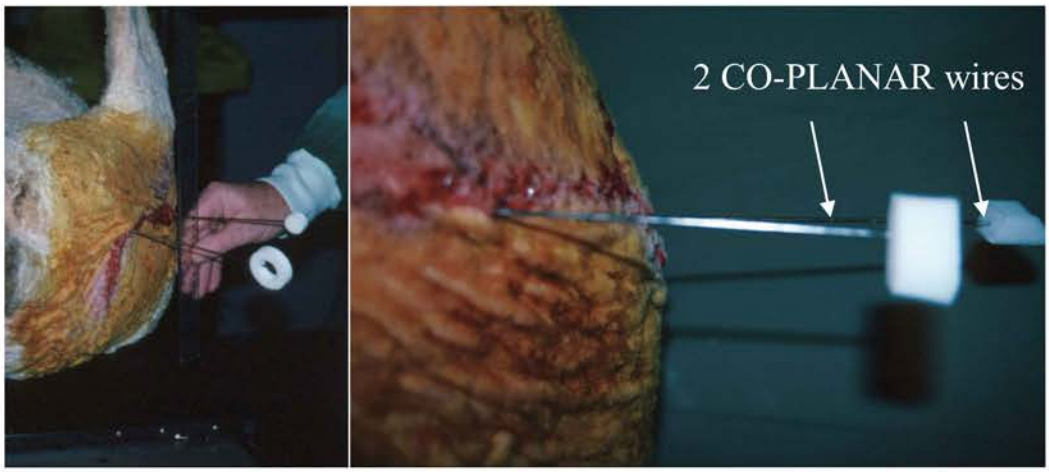

Figure 45. Post-operative AP X-ray set-up

After skin closure the sheep is turned over from the right lateral operative position to the supine position. A large format (CXR size) x-ray plate is positioned under the animal towards the side of the implant, centred over the hip joint. The x-ray tube was positioned above the animal, centred over the pelvis in the midline. An assistant draws the rear legs towards the chest and positions the femur so that both wires are parallel to the X-ray plate in both planes. This is checked with a flat rule as a 'spirit level' and checking the distance is the same for both wires to the plate. Rotation of the leg will also bring the wires to lie parallel when viewed from the side (Figure 45).

The x-ray source-plate distance was constant throughout at 110cms. The exposure was calculated from a standard tabulation based upon sheep weight. This film was then developed and checked for quality of detail and completeness to include the femur of interest.

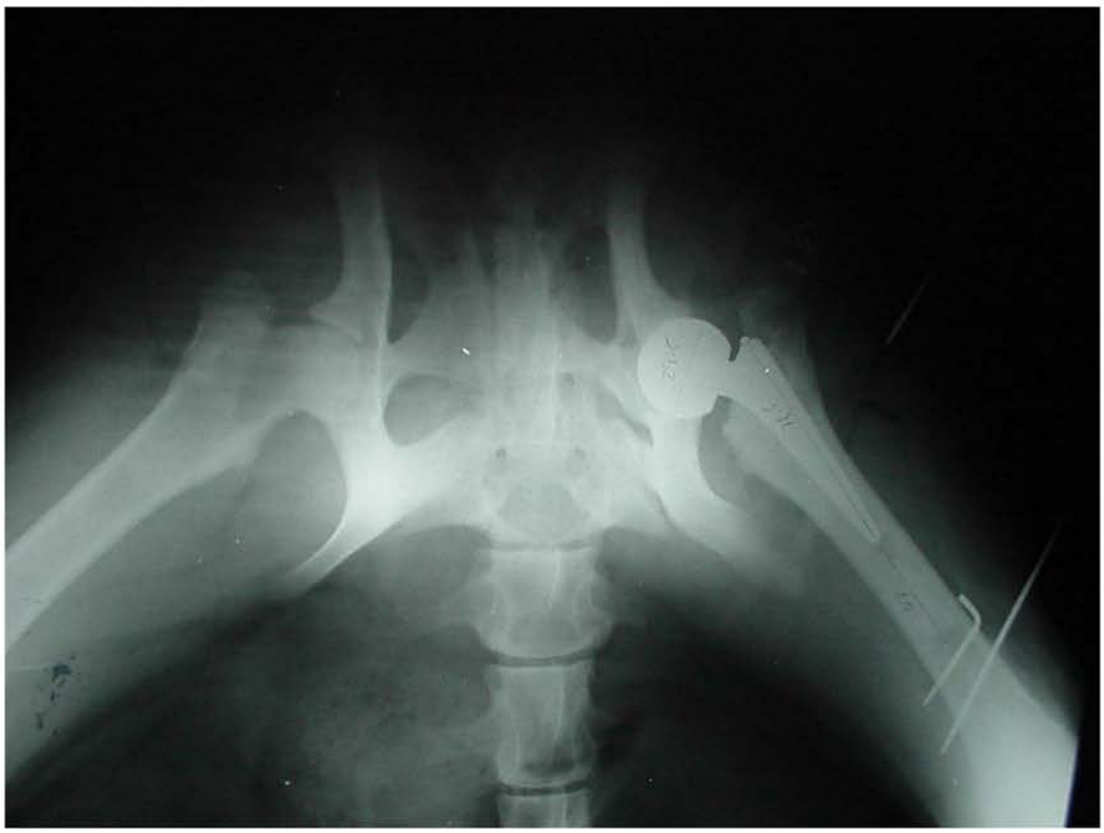

Figure 46. Post-operative AP X-ray (later re-taken, loose proximal wire)

After the AP film was taken, an 'extended vetro-dorsal' film, with the legs fully extended without notice to the wire position was then taken. This latter film gave a simulated lateral femur view to compare with the AP, allowing graft mantle and component alignment assessment.

The final x-rays were taken after euthanasia and harvest of the sheep femorae using a Faxitron x-ray machine. A 235mm x 175mm film was placed on the base plate with lead over one half, the revealed half centred over the centre grid. The AP was taken first by placing the fresh femur on absorbent paper over the film. Due to the length of the femur the femoral condyles were clear of the film. The original wire was easily identified and used to carefully position the femur (flexible supports used) such that

it was parallel to the plate in both planes, exactly as the post-operative film was positioned. The exposure was set for 59mV for 18 seconds. The film was then moved over and the lead adjusted to reveal the unexposed other half, centred over the beam. The femur was then placed to lie in a lateral position, together with identification number, and the film exposed similarly. This film was then developed and checked for quality of detail and completeness.

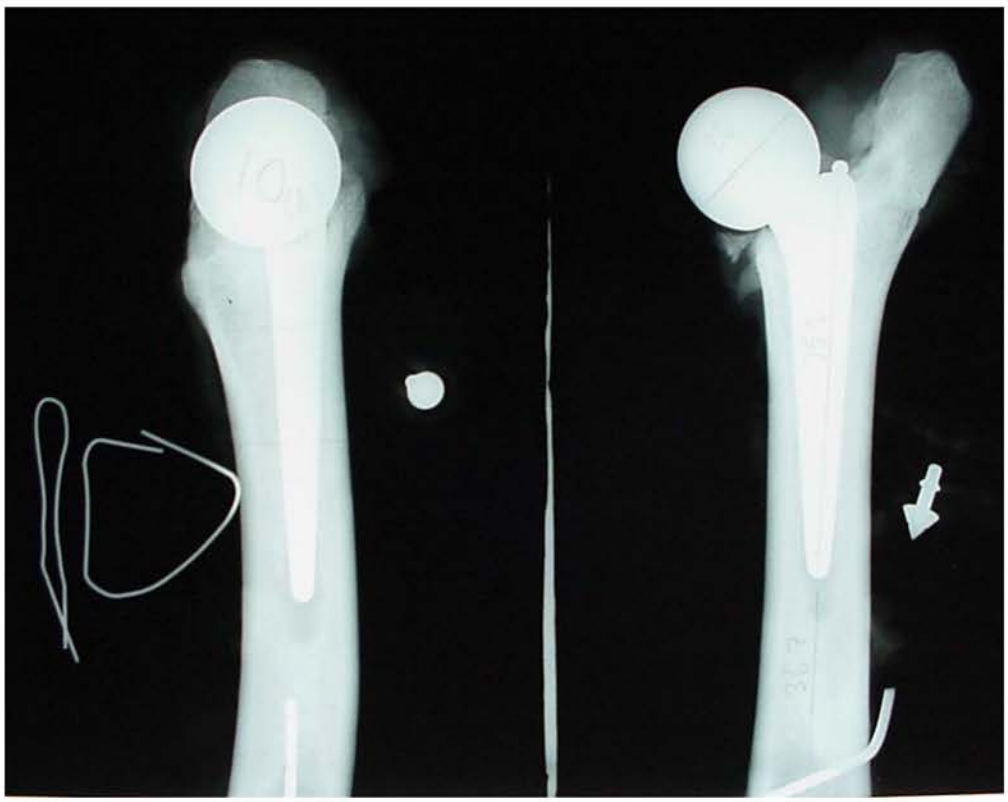

Figure 47. Post-mortem Faxitron image

13.2.1. Film analysis

The AP films were placed on a flat illumination box. A clear design architectural ruler (marked on the paper side to reduce parallax error) was used together with a 2B pencil to measure the radiographs. The measurements were felt to be discernible to ~ 0.2mm with the Faxitron films but less than this with the clinical films at ~0.3 - 0.4mm due to some haziness of the image.

All measurements were repeated on five separate occasions, tabulated and the average taken. The same technique for both the post-operative film and the final film was used to record the following x-ray details:

1. Implant head diameter measurement. A straight line was drawn on one side of the head to just intersect the edge. A second line, exactly parallel to this was drawn on the other side of the head. A third line at ninety degrees to these, at the widest point shown by the intersections, was then drawn. The first two parallel lines in the region of the head were then erased. The diameter of the head was then measured along this line, with reference to the edge of the head on the x-ray, rather than the original parallel lines.
2. Implant stem length measurement. A straight line was drawn down the longitudinal axis of the implant. This line was seen to pass through the centre of the tip distally and the centre of the shoulder proximally. This line was erased in the vicinity of either end. The length of the stem was then measured along this line, with reference to the edge of the stem on the x-ray. Those stems that had a bead attached to the shoulder were measured the same way, without reference to the bead.
3. Stem tip to wire centre measurement. A straight line was drawn down each outer cortex of the femur at the level of the K-wire. A line along the upper border of the wire was drawn to intersect these lines. The length of this latter wire was measured and the mid-point determined and marked. A line joining this mid-wire-point and the most distal point of the implant was drawn. Lines in the vicinity of the tip of the implant and the mid-point of the wire were then erased. The distance between the implant and the wire was then measured along this line, with reference to the tip of the stem and the proximal edge of the wire on the x-ray.
4. The AP and Lateral films were then viewed overall and notes made as to implant position and bone abnormalities.

13.3. Technique Validation

A fundamental difference between the method used here, and other methods, was the use of parallel marker wires to align the femur to the x-ray plate in all planes, in a reproducible manner, on the two separate occasions that the films were taken. The centre of the wire and the long axis of the implant all lie in alignment due to the

action of the guide rod during impaction. This rod is removed before cementation, but prior to this, it ensured the impacted neocavity and the wire centrepoint were aligned. All subsidence occurring along this longitudinal axis without undue deviation allowed accurate comparisons to be made. The use of the implant and a cortically transfixed distal wire as the only reference points for measurements was felt to reduce the errors due to bone remodelling if bone landmarks, such as the trochanters were used. This is a particular drawback in the femur compared to the acetabulum in RSA studies, due to femoral remodelling.

Experimental work showed that previous methods[141] using trigonometry were not accurate when the two x-rays were taken with the femur at slightly different angles. It was found that accurate positioning of the sheep femur in a live (anaesthetised) animal was not possible with an external jig alone. The post-operative positioning to obtain the midline pelvis AP, has previously been reported as providing the most accurately reproducible technique due to the ease of identifying the midline [141] (although the image plate is only placed on the side of interest).

As a check for correct positioning of the femur during this x-ray, the first twelve implants were fitted with a small bead welded to the centre of the shoulder. Small angles of out-of-plane flexion or extension would cause the shoulder of the implant to blunt the normally crisp bead neck. All twelve x-rays showed clear bead necks without blunting.

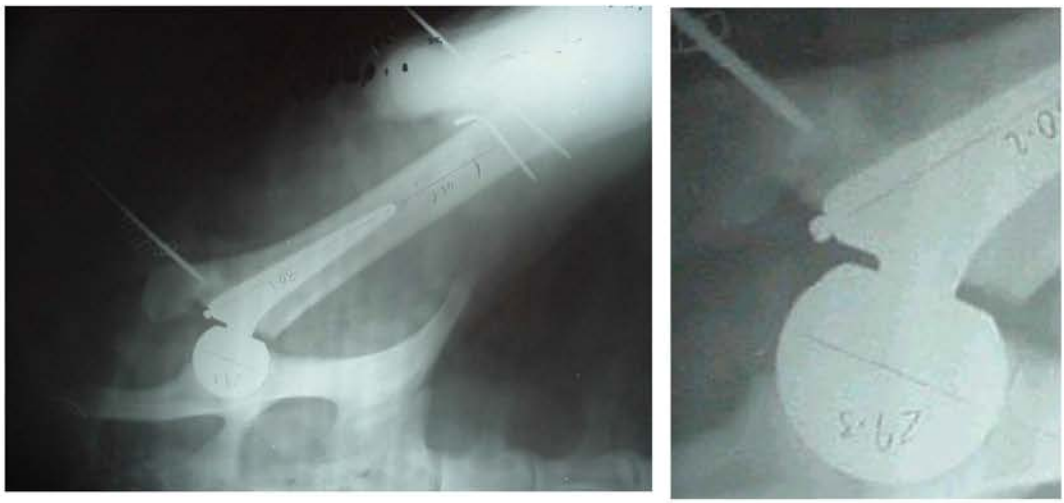

Figure 48. a) Typical post-operative X-ray showing clear bead neck b) implant bead close up

Repetition of the x-ray procedure was performed, with repositioning of the animal five separate times to determine the Replicate (Technique) error (Stem 71mm +/- 0.16mm; mean +/- 2SE's). The author then measured a random x-ray on separate occasions for a total of five times each. This allowed determination of the intra-observer error (Stem 74.7mm +/- 0.04mm; mean +/- 2SE's). Inter observer error (Table 6.) was determined between three different individuals looking at both the Faxitron (Stem 74.9mm +/- 0.18mm; mean +/- 2SE's) and Standard A/P post-op films (Stem 81.5mm +/- 0.26mm; mean +/- 2SE's). It is clear that these error margins are much smaller than the accuracy attainable from the measuring technique (Section 13.2.1.) with highly significant agreement, well beyond chance. The variation is equivalent to round off error at the last decimal place with no measurable variation between replicates.

	Observer **A**	Observer **B**
mean distance	74.7	74.9
t test	p<0.001	
	Observer **C**	Observer **B**
mean distance	74.7	74.9
t test	p<0.001	
	Observer **C**	Observer **A**
mean distance	74.7	74.7
t test	identical	

Table 6. Inter observer agreement

Comparison of the ratios of head/stem size between the Faxitron and Standard A/P films from the same animal allows a check for reliability of measurements. Ideally the ratios between the two films should be identical i.e. head1 / stem1 = head2 / stem2 or (head1 / stem1) / (head2 / stem2) = 1.0. An error of a single measurement

by 5% would produce a change in this latter ratio by +/- ~0.1. These ratios were calculated and show an average in the allograft group of 1.00 (SD 0.01) and in the allograft / Corglaes® group of 1.01 (SD 0.02) suggesting a high degree of comparative reliability obtained in these results.

13.4. Results

The results are tabulated and the average subsidence for the two test materials presented graphically.

Study No.	Stem Post Op	Head Post Op	Stem tip – wire Post Op	Stem Harvest	Head Harvest	Stem tip – wire Harvest	X-ray Subsidence (Head) mm	Actual Subsidence (Head)mm	X-ray Subsidence (Stem) mm	Actual Subsidence (Stem) mm	Head / Stem ratio	Shoulder X-ray subsidence mm	Actual Shoulder Subsidence mm
Allograft Group													
4	80.5	29.4	46.2	74.8	27.2	37.7	5.0	5.3	5.2	5.5	1.00	*	*
5	80.8	30.0	45.0	75.0	27.6	36.6	4.8	5.1	5.2	5.5	1.01	*	*
7	80.2	29.3	46.5	74.7	27.1	41.1	1.9	2.0	2.2	2.3	1.01	*	*
10	82.2	30.1	40.5	75.0	27.2	34.3	2.3	2.4	2.7	2.8	1.01	*	*
11	81.5	29.3	41.8	75.0	26.8	36.8	1.4	1.5	1.7	1.7	1.01	*	*
18	82.0	29.5	48.0	75.2	27.3	37.9	6.5	6.8	6.1	6.4	0.99	6.5	6.2
20	83.4	30.3	39.2	75.2	27.7	28.2	7.6	8.1	7.1	7.6	0.99	6.5	6.1
					Average		4.2	4.5	4.3	4.5	1.00		
					SD		2.4	2.6	2.1	2.3	0.01		
Allograft / Corglaes® Group													
3	81.2	29.6	38.5	75.0	27.2	31.7	3.7	3.8	3.9	4.0	1.01	*	*
6	76.5	29.5	47.0	74.7	27.2	42.0	1.3	1.4	3.9	4.1	1.06	*	*
8	81.4	29.9	34.5	75.1	27.4	29.4	2.2	2.3	2.4	2.6	1.01	*	*
13	82.7	29.9	44.9	74.7	27.0	38.1	2.4	2.5	2.5	2.6	1.00	*	*
15	84.0	30.0	42.0	74.5	27.0	33.2	4.6	4.8	4.1	4.2	0.99	3.6	3.5
17	84.0	30.2	51.0	75.2	27.3	40.0	6.1	6.4	5.7	5.9	0.99	4.6	4.4
23	81.6	29.7	40.5	74.4	26.8	34.3	2.2	2.3	2.6	2.7	1.01	2.2	2.1
26	81.8	30.0	50.2	74.1	27.2	42.6	2.9	3.0	2.9	3.0	1.00	2.4	2.3
					Average		3.2	3.3	3.5	3.6	1.01		
					SD		1.5	1.6	1.1	1.2	1.02		

Table 7. Radiological subsidence measurements (* denotes prostheses without shoulder beads)

X-Ray subsidence (stem)mm			
Plain Allograft		Allograft / Corglaes®	
	5.5		4.0
	5.5		2.6
	2.3		2.6
	2.8		4.2
	1.7		5.9
	6.4		2.7
	7.6		3.0
Total	31.8		25.0
Mean	4.5		3.6
SEM	2.3		1.2
Unpaired t-test	t=1	12DF	p=0.34

Table 8. Subsidence statistical analysis

No statistically significant difference in subsidence is detectable between the two groups (Table 8. Graph 26.). Based on these values, a sample size of 28 for each group would be required to detect a difference with any significant power, with 32 suggested to be on the safe side.

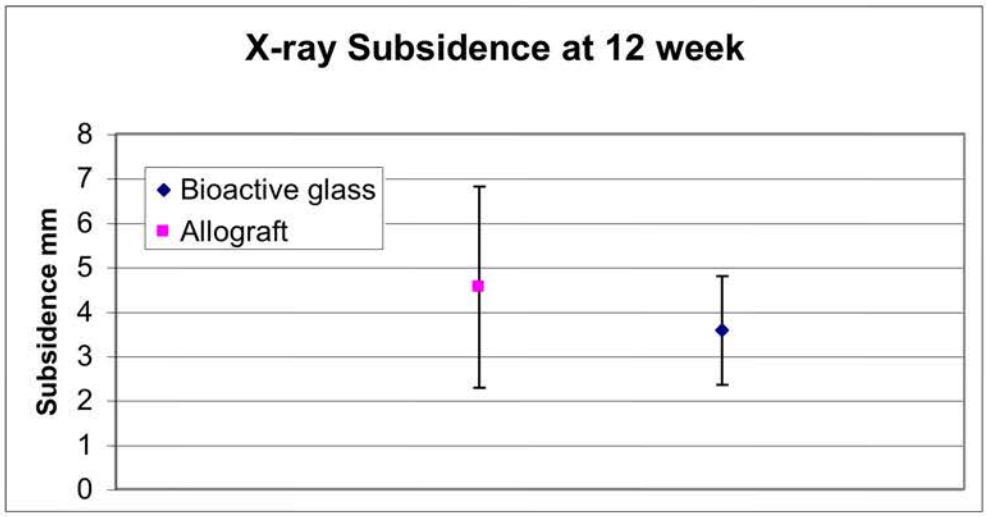

Graph 34. Graphical summary of subsidence

In one animal (No. 6) the proximal post-operative marker wire was noted to have come loose at the time of film analysis (but not when the film was taken). This

animal showed the worst head/stem ratio (Table 7) and for this reason was considered unreliable and excluded from the unpaired t-test group comparison.

Two animals (No. 17 & 20) were noted on the postoperative films to have perforated their plastic centralisers. This was despite removal of the 'wings' as in human revision surgery and reflected some difficulty with introduction of the stem. These implants were thus end-bearing from the first post-operative day. Interestingly both of these animals developed circumferential cement fractures at the stem tip, subsiding ~ 6mm to ~ 8mm respectively, much more than any other implants. Indeed, if these results are further excluded, the average subsidence (Head) for the groups changes;

Allograft group
3.8mm (SD 2.2) (was 4.5mm (SD 2.6))

Allograft / Corglaes® group
2.9mm (SD 1.1) (was 3.3mm (SD 1.6))

No other animals were noted to have cement fractures on radiography despite subsidence of ~ 4mm over 12 weeks. Further analysis of the cement mantles by X-sectional Faxitron imaging (Appendix – Hemiarthroplasty histology) has failed to show cement fractures. This suggests that the creep characteristics of cement in-vivo are vastly different to laboratory testing, where cement fractures would have occurred at this strain rate. Body temperature and fat saturation of the cement undoubtedly play a role.

The subsidence measured radiologically from the k-wire technique was also corroborated in these cases of massive subsidence due to the measurable cement space left above the shoulder of the implant (Figure 49.) and on histological sectioning.

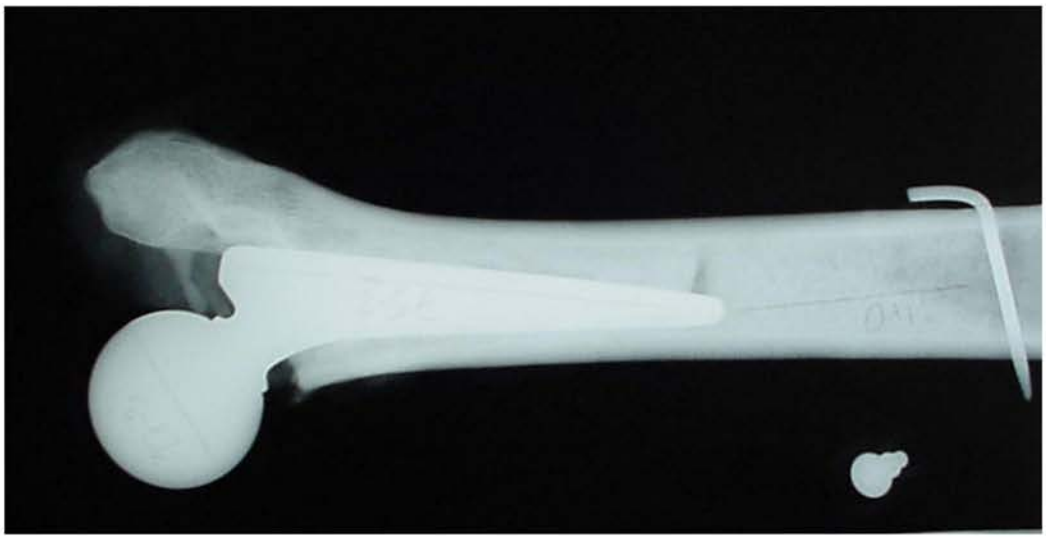

Figure 49. X-ray of cement tip fracture (also note implant/cement gap Zone 1 – shoulder)

Chapter 14 Assessment of Stem Micromotion

14.1. Introduction

The stability at the time of surgery and from thenceforward of the femoral stem is a major determinant of long-term success. Relatively small motions have been noted to prevent ingrowth for biological fixation[159; 160]. Given these small motions (around 1/20th of a millimetre), precisely measuring stability is not a simple task, especially when the femur itself deforms on loading, providing us the challenge of a moving

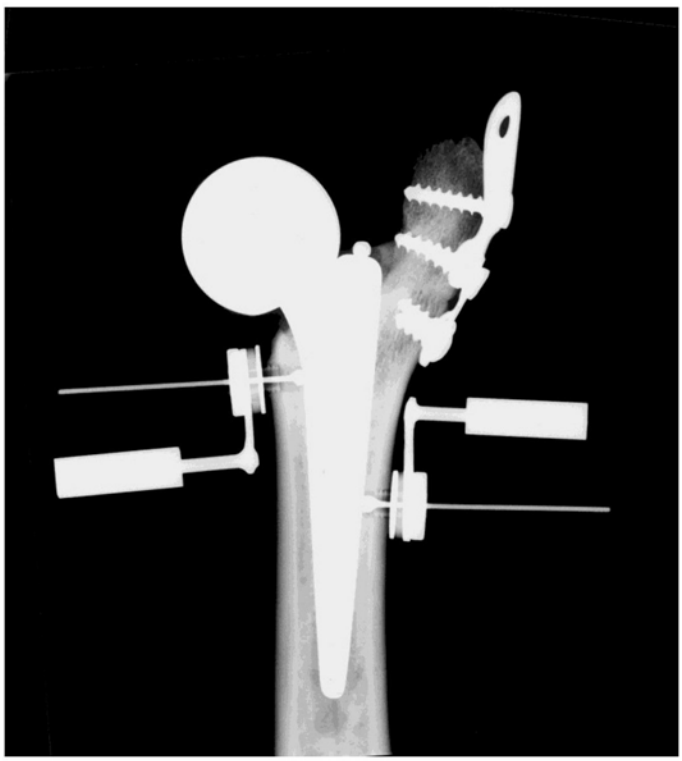

Figure 50. AP X-ray of target set-up (see also Figure 55).

target. Previous authors have often concentrated on either axial or rotational instability[64; 141; 161-164], usually due to the ease of doing so. As failure is usually a function of both of these components, we have measured the 3-dimensional movement of the implant relative to the femur.

14.2. Technique and Validation

Technique

A physiological model of the gait cycle of a sheep hind limb during normal walking was modelled. The simulated normal load during single legged stance on the hind limb of a quadruped was determined. 60% of the average total weight of a sheep is spread over the forelimbs due to the anteriorly placed head, with 40% (~24Kg) calculated to represent the average hind-limb load. This was defined as the maximum load (-240 Newtons) to pass through the femur during assessment of the model. Review of the relevant literature[165-168], photographs of sheep walking and skeletal reconstruction with cadaveric bones (Figure 51) was used to define the normal femur alignment during the midpoint of the weight-bearing (stance) phase.

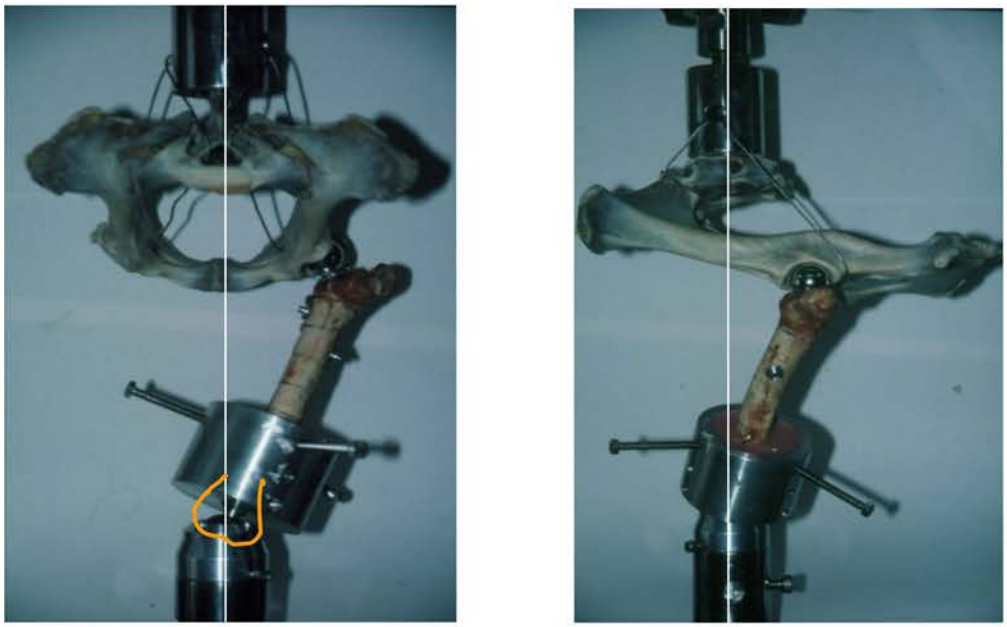

Figure 51. AP and lateral alignment mock-up (see Figure 52).

The load applied through the testing jig was modelled to be a composite from the acetabulum and the five major muscle groups around the hip joint, in a dynamic fashion to simulate the possible movements of the pelvis. Previous reports comment on the necessity to reproduce as many of the major muscle groups as feasibly possible to simulate the actual in-vivo situation. This model utilises the previously described abductor strap and iliotibial band together with a new design for simulating quadriceps and a hamstrings/adductor composite.

The femur was sectioned distally and potted in such a way that the centre of the knee joint coincided with the centre of the ball joint of the pot. This ensured that the load passed through the centre of the knee, irrespective of the femoral angulation. The ball joint was fixed during cycling. The simulated pelvic jig was free to move above the centre of the knee due to interposition of an X/Y table and ball & socket joint. The muscle straps were adjusted so that the load axis of the Instron passed through the midline of the pelvis and the centre of the knee joint in the antero-posterior projection. In the lateral view the load axis passed through the lumbrosacral joint and again through the centre of the knee joint. Load application over the lumbosacral joint reproduced the physiological femoral flexion seen in mid-stance. The choice of these positions was validated by reproduction of normal in-vivo ovine femoral strains for the given load (Section 14.3.2.).

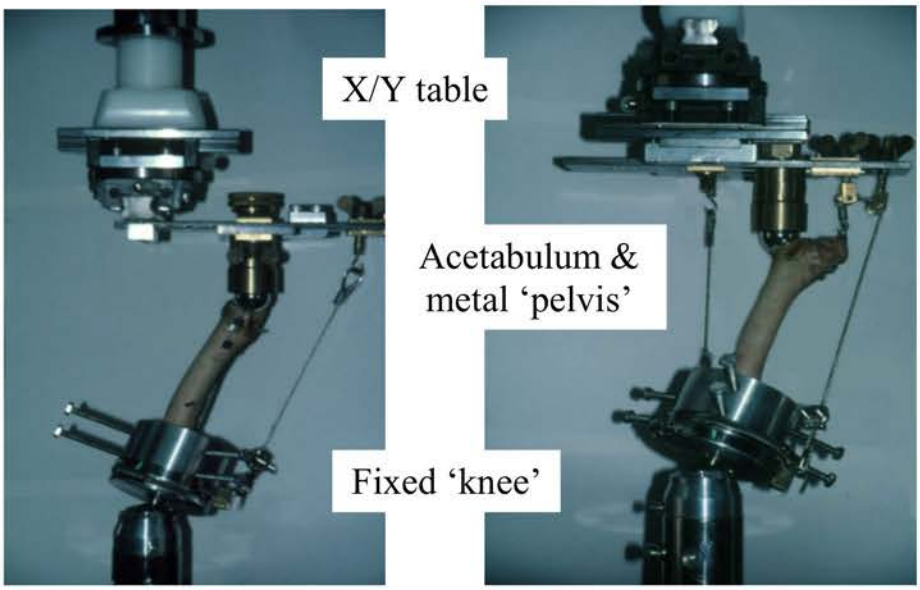

Figure 52. Testing jig alignment set-up

Previous experimenters using larger animal numbers (though ethically unsatisfactory) have often divided the animals into two groups at euthanasia. One group is mechanically tested, often to failure, using fresh specimens, while the other group is formalin fixed for histological assessment. The reason for this split is due to observations on the deleterious effects 'fixation' has on specimens[169; 170]. Finlay et al[171] reported on the dramatic anisotropic contractions that were seen when the cortical bone of a bovine femur was dehydrated. The contractions were 0.6% axially, 2% circumferentially and 3% radially and were statistically different from one another. These values translate to strains of 6,000, 20,000 and 30,000 microstrains respectively – i.e. considerably above the 3,000 microstrains that are reported in the literature for normal human activities of daily living. Embalming reduces these strains, but they still remain at levels of 0.5%, 1.2% and 2.1% respectively. Jasty et al[172] have used calcium chloride pellets for dehydration and Currey[108] showed that the modulus of elasticity of fresh bovine bone is changed insignificantly (1.8%) when the bone is subsequently dried and re-tested in its rehydrated state. However, the effects on histological appearance are not reported. Harman et al[173] has reported on the deleterious effect on cement by dehydration, but noted no change when cement specimens were treated either with Formalin or by freezing.

To allow both mechanical testing and subsequent histological assessment, (more ethically satisfactory) the femorae in our study were tested fresh, after storage at –70ºC and then placed in the series of fixative solutions.

Validation:

The classical model of Koch[174] (1917), who noted tension all down the lateral side of a dry femur has been largely superseded by more physiological models[175-181]. The traditional method has been to add an abductor strap to the greater trochanter, with the femur mounted vertically when viewed from the lateral view. More physiological strain patterns can be reproduced in the femur with the addition of more of the attached muscles, which has been shown in-vivo[182-186], in-vitro[187; 188] and by finite element analysis[166; 189-191]. Indeed the current concept is that the femur (and indeed, all long bones) is loaded in compression circumferentially. This concept obeys Wolff's Law[192-195], which states that 'bone in healthy subjects adapts to its

mechanical environment'. As a general rule, if a bone were cyclically loaded in tension then it would reabsorb and form tendon or ligament. This observation may only be relevant to the diaphyses as significant tension must occur in regions such as the trochanteric insertions. Our model reproduces the major muscle groups around the whole femur, which is mounted in its physiological position for one-legged mid-stance in the antero-posterior and lateral views. Single leg stance was chosen instead of two-legged stance to maximally stress the model[196]. The load on the hip from half the super-imposed bodyweight in two-legged stance increases to about 2 ½ body weights with one-legged weight bearing[197; 198].

The system was validated by a microstrain assessment of the proximal femur (Section 14.3.2.). The load and application position were seen to reproduce femoral microstrains within the in-vivo range previously reported by Lanyon et al[199-203] in the medial and lateral proximal femur.

The implant target cube (Figure 56.) moved with movement of the implant, but also with movement of the femur. Other authors have measured motion of the implant with reference to some 'fixed' area on the proximal femur. This technique is prone to error due to interfacial micromotion and femoral strains. A technique to overcome these problems has been reported[204] using a device similar in principle to our detection system. To measure, and subsequently subtract, the motion of the femur, the overlying drill hole to access the implant was used as the reference point. Due to the disproportion in offset of the implant target compared to the femoral target, there was potential for out of plane motion between the two. A control target was therefore utilised. This comprised a similar collar for fixation of the femoral target, to which the 'implant' target was bonded, instead of being bonded to the implant. Thus both targets in the control referenced the same point. Repeatability studies were performed and showed a high level of conformance. Instrument calibration showed an error of +/- 20 microns for the LASER / LVDT coupling.
Using orthogonal slotted bars for mounting the measuring devices reduced mal-alignment of any of the devices. It was calculated that mal-alignment of the targets of

10 degrees would produce an error of 7%, at no time was a mal-alignment as large as this seen.

14.3. Materials and Methods

14.3.1. Jig Fabrication:

1. The Artificial Pelvis

Two solid steel 6mm plates were fashioned to articulate in a cross pattern, held together with a locking bolt. The acetabulum was made from brass with a polyethylene liner to match the implant head sizes (26 & 28mm) and could be positioned anywhere in three planes relative to the load application point. An X/Y table (allows almost friction free translational movements in the horizontal plane) was attached to the plate perpendicular to the acetabular plate. The final positions of the acetabulum and muscle origins, relative to the load application point, were previously determined from cadaveric measurements (Section 14.2 & Figures 51-53).

2. The Knee

Thirty three millimetres of the distal femur was resected so that when potted, the centre of rotation of the ball joint to allow femoral positioning, coincided with the centre of the knee joint. Once the femur was correctly positioned beneath the jig and the straps applied the ball joint was locked off.

3. The Muscle Straps

All straps were made from high tensile (1750N breaking strain) multifilament stainless steel wire, held fast with yachting clamps. The origin, insertion and line of action of the muscle straps were based on cadaveric and skeletal studies of the origin and insertion of the muscle groups and literature review.

a) Iliotibial Band and Abductors:

An abductor strap was attached to the greater trochanter by means of a contoured plate and five screws (Figure 50). This had a similar ‘footprint’ to the original abductors, attached in a similar alignment from the same region

of the greater trochanter. The wire passed from the plate at 20 degrees of varus as previously described, to a pulley on the steel bar adjoining the acetabulum. This wire then passed to a second adjustable pulley and back down the lateral aspect of the femur to insert into a clamp positioned where the lateral tubercle of the femur would have been located. This latter arrangement simulated the position of the line of action of the iliotibial band. The connection with the abductors via the pulleys reduced any preferential loading of the iliotibial band during cycling secondary to lever arm effects (it has a more lateral origin than the abductors) and evenly distributed the load through both muscle groups.

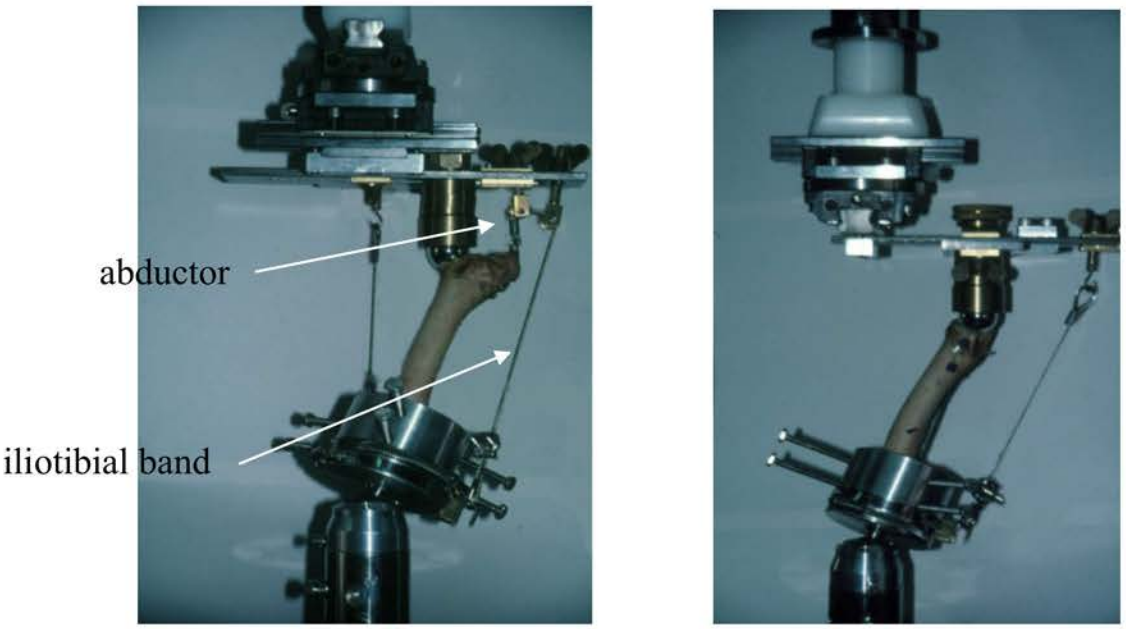

Figure 53. Strap muscles, including abductors and iliotibial band (AP & lateral views)

b) Hamstring/adductor composite:

This single strap was aligned to act in the resultant vector of the adductors and hamstrings. In the antero-posterior direction the strap was in alignment with the load axis in the midline. In the lateral view, the strap passed from a point posterior to the acetabulum, representing the ischial tuberosity, down to the posterior aspect of the distal femur, where it was attached in the midline.

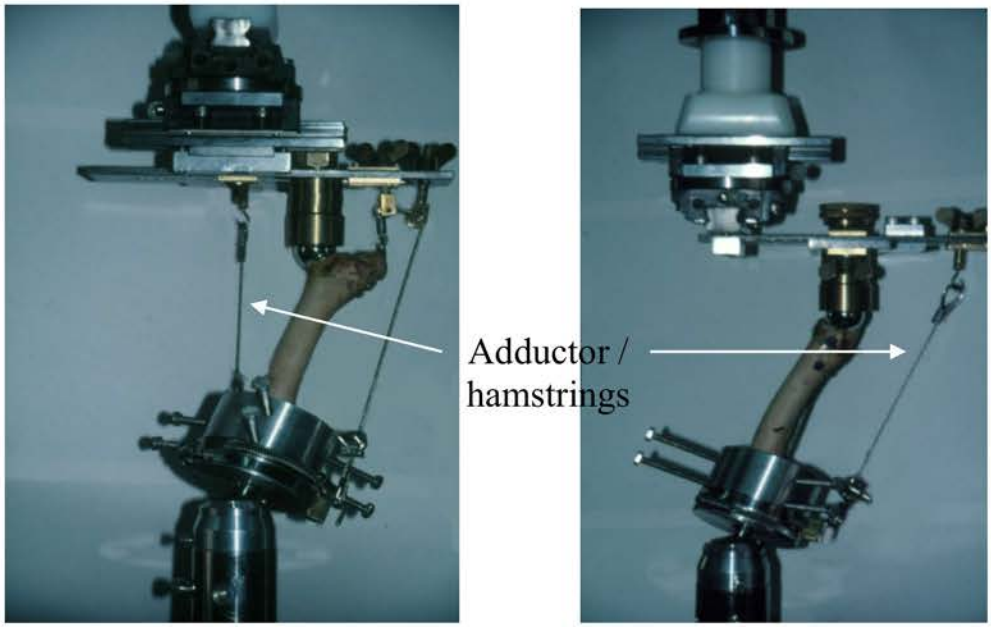

Figure 54. Strap muscles, including adductors and hamstrings

c) Quadriceps:

This strap simulated the quadriceps muscles, originating from just anterior to the acetabulum and reaching a pulley, which was positioned, where the centre of the patella would have been. This pulley was isolated from the load cell (as

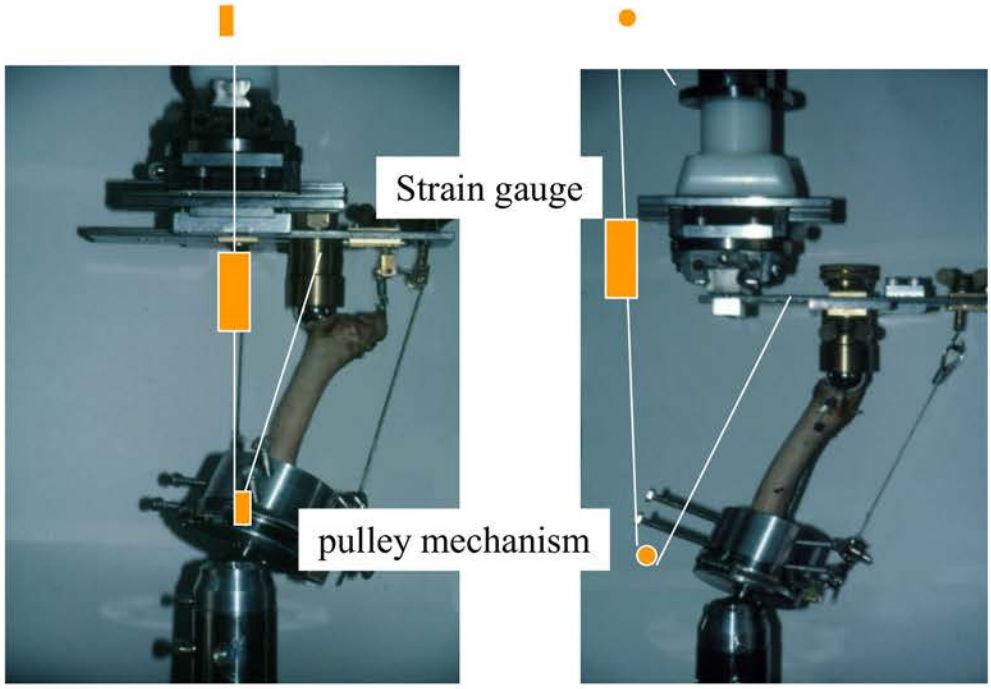

Figure 55. Strap muscles, including quadriceps mechanism

the net load was in a negative direction to the applied load) by fixation to the Instron casing (Figures 55 & 57). From the inferior pulley the wire passed via a series of pulleys until it was attached to the actuator, in the same direction of pull. A load cell and tensioning device were placed in series in the wire to allow correct load transmission.

4. Targets

The implant had a proximal and a distal target directly bonded to the surface, which protruded a distance outward on a wire, on the end of which was a 6mm LASER reflective (blue) cube. The delicacy of this arrangement necessitated a non-contact measuring system to detect motion. Three orthogonal LASER micrometers were arranged to focus on the X, Y & Z aspects of each cube. The cubes were aligned in the long axis, antero-posterior and medio-lateral aspects of the implant. The femoral reference targets were fastened to a collar, which was screwed firmly to the overlying bone, through which the implant target passed. This target could be rotated around the collar, around its mounting rod and also extended outwards from the femur.

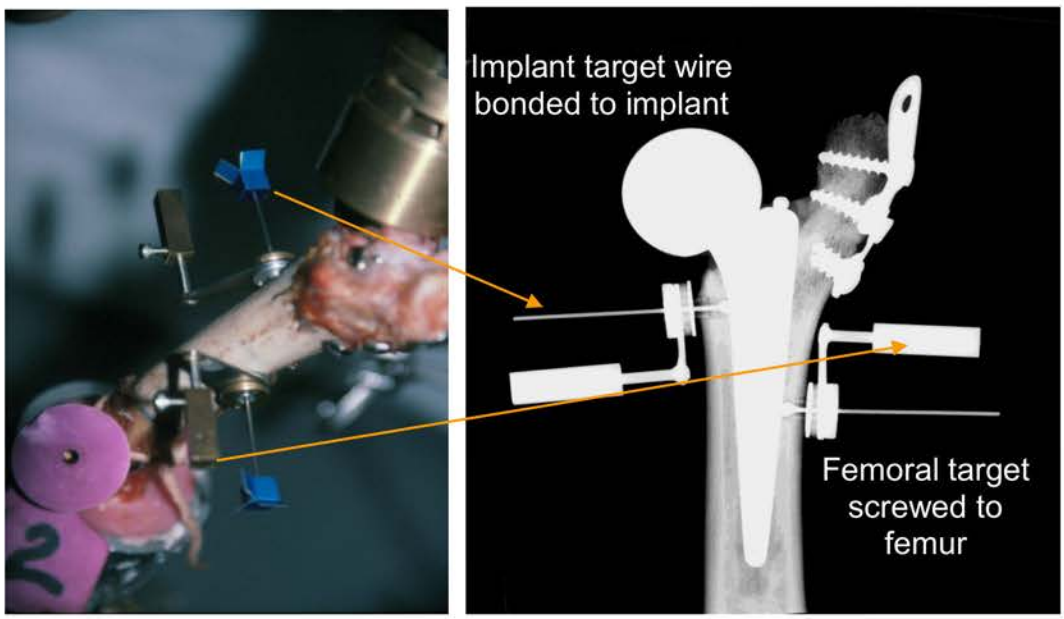

Figure 56. Target set-up a) antero-superior laboratory view b) AP X-ray view

The final position was made after the LASERS were aligned on the blue cube. The femoral target was brought into the working range of the linear variable differential transformers (LVDT's). These were fixed parallel to the LASERS on the orthogonal jig. This ensured correct alignment of the paired femoral/LVDT and implant/LASER systems with respect to each other.

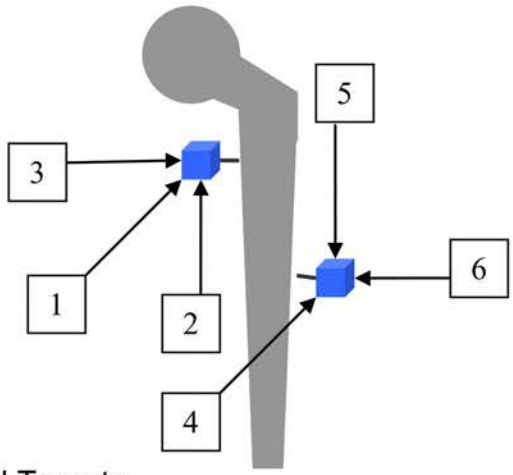

Key:

Proximal Targets

1. LASER1 & LVDT1 Antero-posterior (A/P)
2. LASER2 & LVDT2 Axial
3. LASER3 & LVDT3 Medio-lateral (M/L)

Distal Targets

4. LASER4 & LVDT4 Antero-posterior (A/P)
5. LASER5 & LVDT5 Axial
6. LASER6 & LVDT6 Medio-lateral (M/L)

Figure 57. Schematic diagram showing the relationship between direction of movement and LASER / LVDT number and position (LASER referenced to implant, LVDT referenced to adjacent femur)

5. Signal / Data processing

Six laser transducers (model LB12-72(W), Keyence Corporation, Osaka, Japan) were used.

- Measuring range ~10 mm over ~4V
- Wavelength 780 nm

- Maximum power 3 mW
- Class 3B laser
- Resolution 2 μm (however the best our system could measure was 17 μm)

Six LVDTs (linear variable differential transformers) were used, 3 each of two brands:

Three LVDTs (model GTX 2500, Daytronic Corporation, Ohio, USA) with signal conditioners (model 3130, Daytronic Corporation, Ohio, USA) were used.

- Measuring range ~2.5 mm over ~5V
- Resolution – better than 20μm

Three LVDTs (Lucas Schaevitz model LBB-375-TA-100) with signal conditioners (model AMA-2074B, Lucas, Virginia, USA) were used.

- Measuring range ~2 mm over ~10 Volts
- Resolution – better than 20μm

All were calibrated prior to testing with the best accuracy stated as ~20μm.

Biomechanical tests were performed on a servohydraulic materials testing system (Instron Model 8511, Instron Pty Ltd, High Wycombe, UK).

Figure 58. a) Instron set-up b) close-up of distal target orthogonal jig

The data acquisition system used was a DT2801-A analog/digital board (Data Translation, Marlborough, MA USA). Fourteen channels of data (load, displacement, 6 lasers and 6 LVDTs) were collected and stored using Global Lab software (Data Translations) on an IBM compatible personal computer for further analysis after testing.

Software was written (in Visual Basic) to analyse the data from each test. The minimum and maximum values for each transducer at each cycle were determined. The peak to peak amplitude or difference between the minimum and maximum values was then calculated. This difference was calculated for the "blank" and "test" files with the (test difference – blank difference) finally being calculated and averaged over the last 5 cycles (final cycle discarded) in each file.

14.3.2. Femoral Microstrain Measurement:

The quadriceps and hamstring/adductor composite allowed the pelvis to move via the X/Y table and ball & socket coupling. Prior to the quadriceps strap being added to the system, it was noted that there was marked femoral flexion with tension in the anterior cortex of the mid-shaft of the femur. Two Foil Strain Guages (rosette, guage factor 2.10 +/- 2% – Showa Measuring Instruments Co., Ltd.) were bonded (cyanoacrylate glue) directly to the bone, aligned with the anatomical axis of the femur, in the mid-lateral and mid-medial aspects, as described by Lanyon et al. An additional pair of guages was similarily attached in the midline anteriorly and the mid-line posteriorly at a similar level. During a load cycle, the microstrains were recorded simultaneously in all four guages. The length of the iliotibial band strap and the tension in the quadriceps strap were adjusted until normal physiological loads were seen in the quadriceps mechanism. The microstrains in the anterior and posterior cortex were compressive with medial and lateral microstrains similar to Lanyon et al's in-vivo ovine model. Flexion of the femur on loading was seen to have markedly reduced, with compressive microstrains recorded both anteriorly and posteriorly. This loading regime was used throughout the test period.

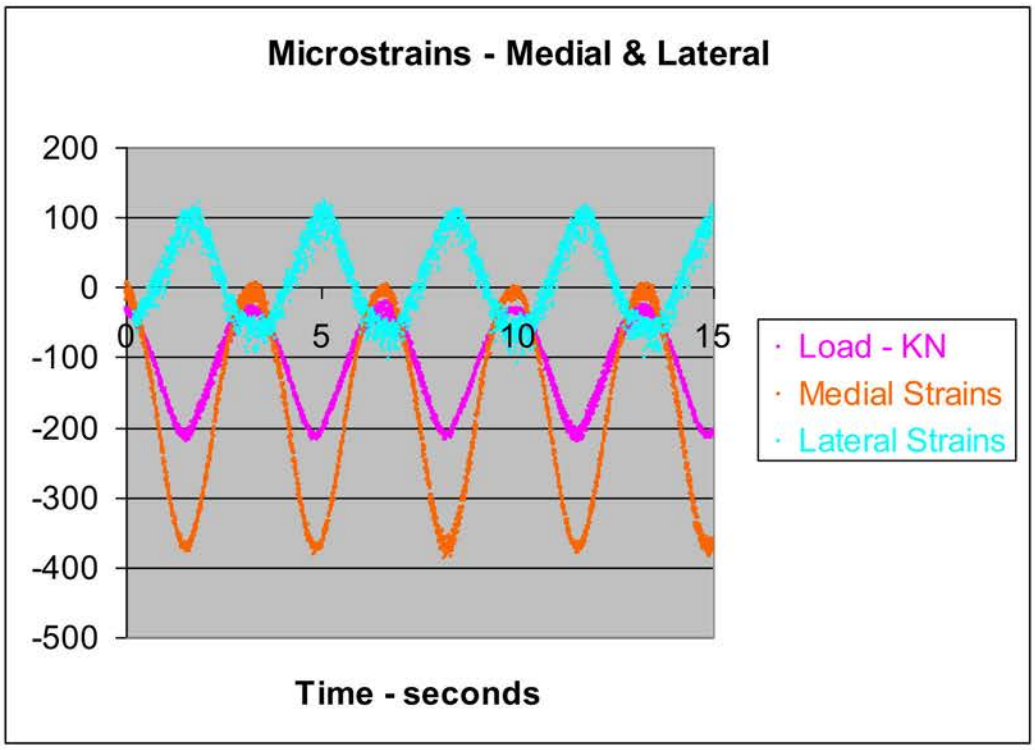

Graph 35. Femoral microstrains

14.3.3. Set-up Protocol:

The following protocol was followed to prepare, jig, align and test the micromotion of the femoral implant relative to the femur:

1. The femur was defrosted by overnight placement in a refrigerator, sealed in its plastic bag to retain moisture.
2. The total length of the femur was measured, from the femoral condyles to the tip of the greater trochanter.
3. A marker pen was used to ring mark the femur (in the antero-posterior plane) at 20, 30, 40, 50, and 60% of the total length, from the proximal end (see Figure 59).
4. The mid-point between the 20 and 30% lines was marked on the medial aspect – line A (see point 8.).
5. The mid-point between the 30 and 40% lines was marked on the lateral aspect – line B (see point 8.)

6. A ring mark was made 33mm proximally from the femoral condyles and resected with a saw. This was equivalent to the distance between the base of the pot, to the centre of the ball joint and thus ensures that the ball joint is in an equivalent position to the previous centre of the knee.
7. The femur is then held in the pot with six retaining screws (modelling clay over screw threads) and cement added (75ml powder polymer + 25ml liquid monomer polymethylmethacrylate). On curing all retaining screws are then removed except for one de-rotation fixation bolt.
8. The pot is then gripped in the vice and the femur aligned to allow the target drill holes to be made. This requires lying the vice on one side with the implant aligned such that the true lateral position, judged from the distal protruding wire, is aligned with the vertical axis. Line A is identified on the medial aspect and its intersection with the mid-point of the implant, as templated from the lateral x-ray, is marked. The vice is then rotated through 180 degrees and similarly marked with regard line B. The vice is then held with a 'G-clamp' on the drill base and the holes drilled. The vice arrangement ensures that holes A and B are exactly parallel to each other in all planes.

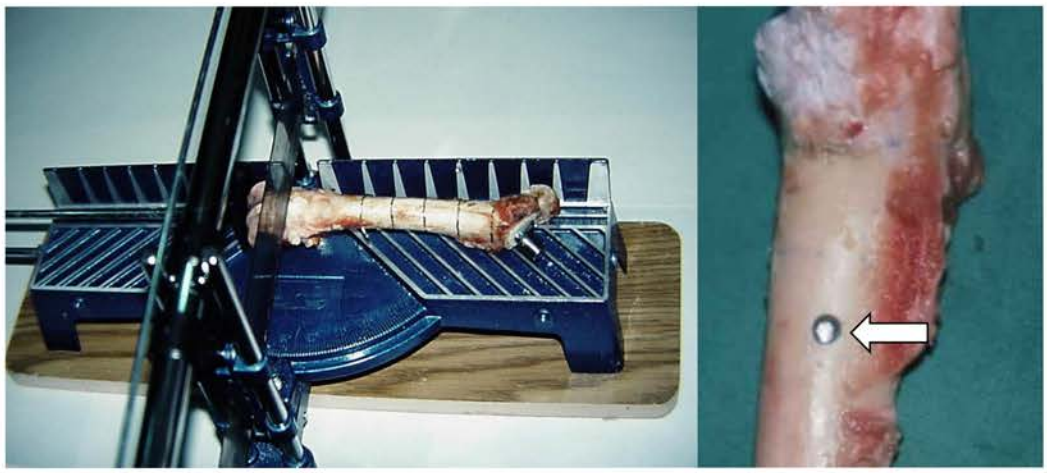

Figure 59. Femoral osteotomy, potting and drilling

9. Drilling technique: A small (1mm) pilot hole is drilled first to ensure correct location of the implant. The 4.2mm drill is then placed in the chuck, without moving the drill stand. This is then drilled until the implant is just located (slight

resistance to progress and reduction in bony swarf) – care is taken not to press on the implant. The 4mm end cutting reamer is then replaced in the chuck, again without moving the drill stand. This is used to gently remove the cement in contact with the implant. Any residual cement is removed with a fine tipped rotary burr under direct vision and dust blown clear. The 4.5mm tap is then used, again in alignment on the drill stand. The process is repeated for the other hole as number 8 above. Femur kept moist with saline soaks. A cotton bud was kept in each hole to keep the implant surface dry for bonding.

10. The abductor strap is now attached. A contoured, specially made plate is held with five 'small fragment' AO screws which have been drilled (3.2mm), a depth gauge used and tapped (3.5mm) appropriately to simulate the abductor insertion (See Figure 50).
11. Mount in the Instron at the 'knee' with the ball joint free and align in the AP and lateral planes with the 'pelvis' above.
12. Attach jig and strap muscles. The femoral head is located in the acetabulum. Abductor inclined 20 degrees in varus. Iliotibial band aligned to brush past the greater trochanter and attach at the level of the lateral femoral condyle on the pot. The hamstrings to pass from a position corresponding to the ischial tuberosity posteriorly, to the level of the back of the knee on the pot, in the midline. The tension in the strap muscles is adjusted until the jig plate is in a neutral horizontal position at cycle mid-phase (110 Newtons). Femur kept moist with saline soaks.
13. The target collar and washer are then screwed into position after the cotton bud is removed. The femoral targets are then attached, aligning the anterior face parallel to the implant axis and tightened. The inferior target is aligned at 10:30 when viewed from the side and the superior target at 04:30 hrs.
14. Implant target bonded directly to the exposed area of the prosthesis by applying a small amount of cyanoacrylate glue to the wire base, with the 4 degree angle correctly aligned with the stem taper and passing it through the collar. With the implant target wire in position, attach the blue cube LASER targets and align anterior face parallel to the long axis of the implant. The femoral target is re-adjusted if necessary so that it protrudes 6mm (width of blue cube) less than the blue cube and is locked fast.

15. The LASER/LVDT assemblies are then swung in with the LVDT's withdrawn slightly. The LASERS are aligned to the cubes in all planes. The LVDT's are then brought up to their working range on the femoral targets. Care was taken to ensure that each device was responding well within its working range without interference from other devices.
16. A final check was made of all fastenings and a check made to ensure clearance of all devices and supporting apparatus from the moving parts of the jig.
17. Data was then recorded for all devices simultaneously with the construct subjected to a Sine wave cycle at 0.3Hz. Start load –110N, amplitude 90N (range –10N to –200N) under amplitude control. Once steady state had been achieved (usually within 10 cycles) a further 20 cycles of data were recorded.
18. The data was then processed and examined for 'noise' (which occasionally happened if one of the devices passed out of range). The test was repeated if any of the devices required range adjustment.
19. The control targets were then positioned. The elbow joint of the detector support assembly was loosened, swinging the devices out of the way. The targets and collar were removed and replaced with the control collar and targets. These were arranged to take up the same position as the previous targets. The devices were swung back in on the support assembly and found to re-align themselves on the new targets.
20. Data was then recorded with the construct subjected to the same loading regime as before.
21. Once data acquisition was complete, correct and backed up, the femur was removed of metalwork and eased from the pot and carefully re-frozen with vermiculite protection to –30°C. Transfer was then arranged for storage at –80°C awaiting histological sectioning and fixation.

14.4. Results

The final implant micromotion is calculated by subtracting the LVDT measurement (femoral motion) from the LASER measurement (implant and femoral motion) for each test. The same calculation is performed on the control tests. The result of the

control test is then subtracted from the actual test (to reduce out of plane errors – Section 14.2) and this represents the true implant micromotion relative to the femur.

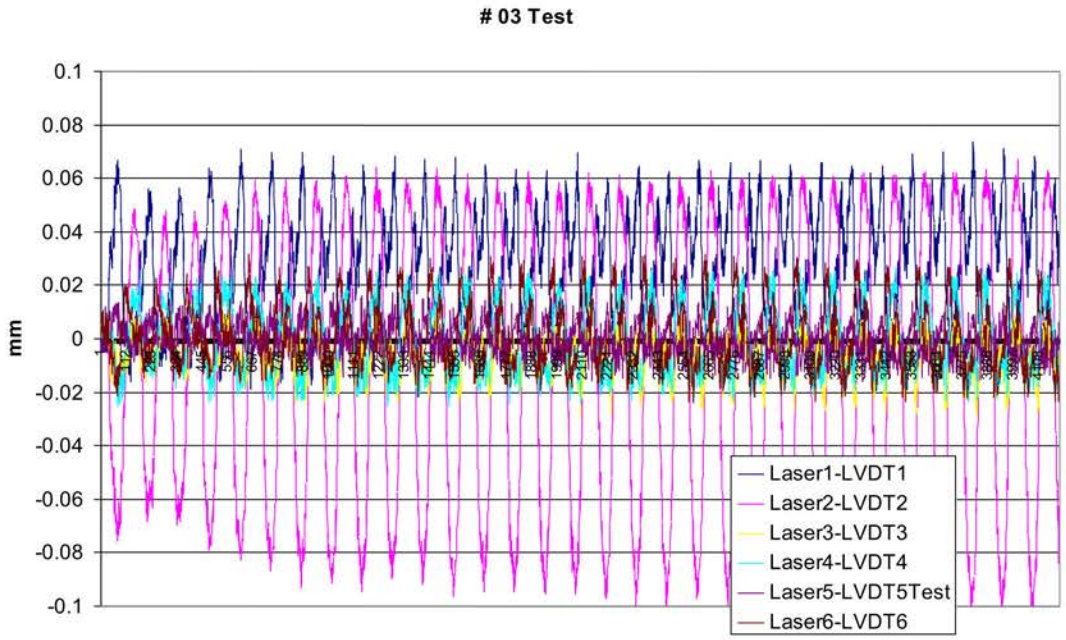

Graph 36. Typical Test, grouped LASER and LVDT sine wave outputs

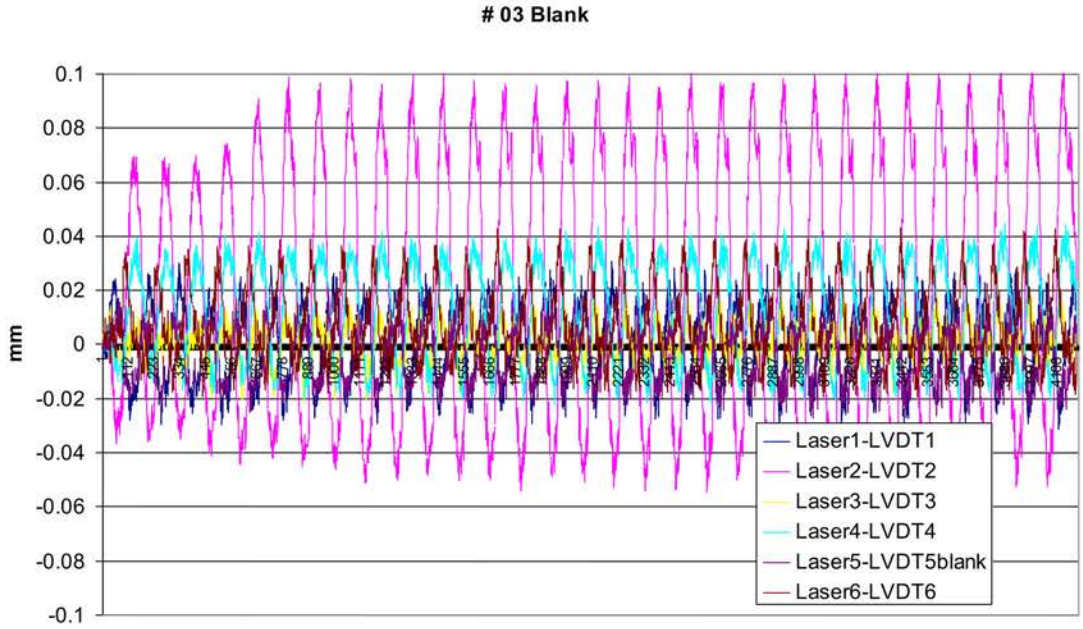

Graph 37. Typical blank (control), grouped LASER and LVDT sine wave outputs

In summary:

The LASER targets measure instantaneous three dimensional movement of the implant AND the femur, relative to the reference jig. The LVDT targets measure the instantaneous three dimensional movements of the femur ONLY.

To deduce implant movement relative to the femur, the LVDT movement is subtracted from the LASER movement:

Implant motion (TEST) = implant/femur motion (LASER) – femur motion (LVDT)

The result is then 'cleaned' of system error, interfacial movement and orthogonal malalignment error by repeating each test with a 'blank' – where the LASER and LVDT targets are fixed together – and subtracting this from the original tests.

True motions = True implant motions (TEST) – controlled motions (BLANK)

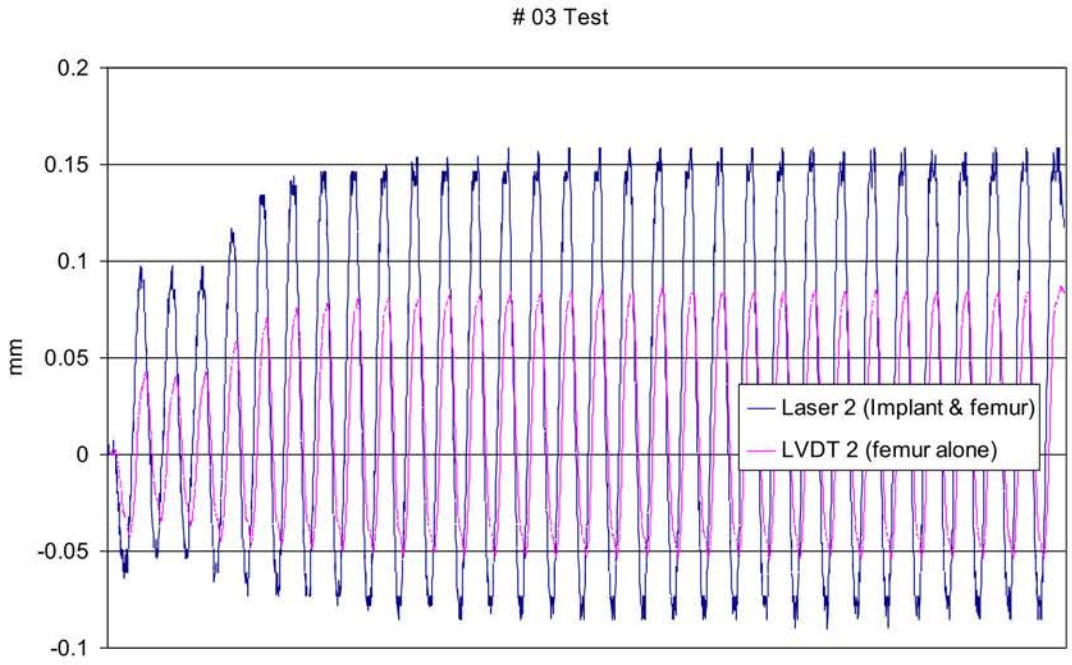

Graph 38. Typical Test, Single pairing of LASER and LVDT sine wave outputs

	Laser1-LVDT1	Laser2-LVDT2	Laser3-LVDT3	Laser4-LVDT4	Laser5-LVDT5	Laser6-LVDT6
Blank	0.050	0.104	0.004	0.041	0.028	0.015
Test	0.067	0.129	0.002	0.022	0.008	0.010
Animal 3	**0.017**	**0.025**	**-0.002**	**-0.019**	**-0.020**	**-0.005**
Blank	0.119	0.086	0.025	0.012	0.157	0.026
Test	0.075	0.089	0.021	0.021	0.016	-0.010
4	**-0.044**	**0.003**	**-0.004**	**0.009**	**-0.141**	**-0.036**
Blank	0.070	0.016	0.043	0.035	0.070	0.035
Test	0.065	0.012	0.020	0.089	-0.019	0.038
5	**-0.005**	**-0.004**	**-0.023**	**0.053**	**-0.090**	**0.003**
Blank	0.110	-0.039	0.050	0.029	0.028	-0.013
Test	0.060	0.042	0.135	0.071	0.026	0.040
6	**-0.050**	**0.081**	**0.085**	**0.042**	**-0.002**	**0.053**
Blank	0.125	0.128	0.027	0.025	0.038	0.075
Test	0.139	0.240	-0.001	0.107	0.089	0.001
7	**0.014**	**0.112**	**-0.027**	**0.082**	**0.050**	**-0.074**
Blank	0.061	0.025	0.000	0.015	0.053	0.030
Test	0.077	0.055	0.013	-0.075	0.074	0.039
8	**0.016**	**0.030**	**0.013**	**-0.090**	**0.021**	**0.009**
Blank	0.092	0.061	0.040	0.018	0.013	-0.010
Test	0.069	0.048	0.064	-0.004	0.091	-0.004
9	**-0.024**	**-0.013**	**0.024**	**-0.022**	**0.078**	**0.006**
Blank	0.158	0.062	0.052	0.034	0.009	0.043
Test	0.141	0.125	0.069	0.064	0.017	0.057
10	**-0.017**	**0.063**	**0.017**	**0.029**	**0.008**	**0.015**
Blank	0.031	0.110	0.033	0.025	0.004	0.006
Test	0.071	0.084	0.039	0.062	0.056	0.020
12	**0.039**	**-0.026**	**0.005**	**0.037**	**0.051**	**0.014**
Blank	0.048	0.057	0.013	0.042	0.005	0.041
Test	0.043	0.078	0.054	0.046	0.022	0.013
14	**-0.005**	**0.021**	**0.041**	**0.004**	**0.016**	**-0.029**
Blank	0.050	0.073	0.145	0.029	0.047	0.081
Test	0.068	0.098	0.018	0.041	0.005	0.066
16	**0.018**	**0.025**	**-0.127**	**0.012**	**-0.042**	**-0.016**
Blank	0.096	0.025	0.041	-0.004	0.005	0.015
Test	0.119	0.059	0.075	-0.098	0.095	0.030
17	**0.023**	**0.034**	**0.034**	**-0.094**	**0.090**	**0.015**
Blank	0.024	0.104	0.017	0.011	0.063	0.121
Test	0.066	0.094	0.017	0.057	0.020	0.034
19	**0.042**	**-0.010**	**0.000**	**0.046**	**-0.043**	**-0.088**
Blank	0.124	0.002	0.109	-0.034	0.087	0.046
Test	0.070	0.032	0.059	-0.029	0.088	0.027
22	**-0.054**	**0.031**	**-0.049**	**0.006**	**0.002**	**-0.018**

Blank	0.025	0.048	0.018	0.030	0.033	0.037
Test	0.200	0.320	0.080	0.280	0.060	0.100
Animal 24	**0.175**	**0.272**	**0.062**	**0.250**	**0.027**	**0.063**
Blank	0.068	0.037	0.046	0.184	0.034	0.029
Test	0.086	0.096	0.004	0.096	0.053	0.061
25	**0.018**	**0.059**	**-0.042**	**-0.088**	**0.018**	**0.033**

Table 9. Numerical micromotion results (motion amplitude in mm, resultant motion in bold).

The raw results in Table 9 can be summarised through simple arithmetic to reveal micromotions in three dimensions for each of the paired targets (six degrees of freedom of motion assuming rigid body stem motion)[207] as shown in Table 10.

Sheep No.	Proximal Axial	Proximal A/P	Proximal M/L	Distal A/P	Distal Axial	Distal M/L
Allograft / Corglaes®						
3	**0.017**	**0.025**	**-0.002**	**-0.019**	**-0.020**	**-0.005**
6	**-0.050**	**0.081**	**0.085**	**0.042**	**-0.002**	**0.053**
8	**0.016**	**0.030**	**0.013**	**-0.090**	**0.021**	**0.009**
12	**0.039**	**-0.026**	**0.005**	**0.037**	**0.051**	**0.014**
14	**-0.005**	**0.021**	**0.041**	**0.004**	**0.016**	**-0.029**
16	**0.018**	**0.025**	**-0.127**	**0.012**	**-0.042**	**-0.016**
22	**-0.054**	**0.031**	**-0.049**	**0.006**	**0.002**	**-0.018**
25	**0.018**	**0.059**	**-0.042**	**-0.088**	**0.018**	**0.033**
Allograft						
4	**-0.044**	**0.003**	**-0.004**	**0.009**	**-0.141**	**-0.036**
5	**-0.005**	**-0.004**	**-0.023**	**0.053**	**-0.090**	**0.003**
7	**0.014**	**0.112**	**-0.027**	**0.082**	**0.050**	**-0.074**
9	**-0.024**	**-0.013**	**0.024**	**-0.022**	**0.078**	**0.006**
10	**-0.017**	**0.063**	**0.017**	**0.029**	**0.008**	**0.015**
17	**0.023**	**0.034**	**0.034**	**-0.094**	**0.090**	**0.015**
19	**0.042**	**-0.010**	**0.000**	**0.046**	**-0.043**	**-0.088**
24	**0.175**	**0.272**	**0.062**	**0.250**	**0.027**	**0.063**

Table 10. Summary micromotion results (blue 50 – 150 microns, red > 150 microns)

The black results represent motion below 50 microns, reported as representing the amount of expected motion in clinically solid, cemented THA's. The red results represent micromotion of more than 150 microns, which is reported to signify

looseness to such a degree that fibrous interposition is the only means of stabilisation. The blue results represent motion between 50 and 150 microns and most likely represent the upper limit of normal motion in impaction grafted hip arthroplasties. It can be seen that specimen No.24 showed significantly more micromotion, in more planes, than the other animals (Graph 39). This animal was euthanised seven days before it was due to complete the study due to lameness secondary to a deep infection, but was included in the micromotion testing as it was considered to represent a probably loose stem. This has been confirmed by the results obtained.

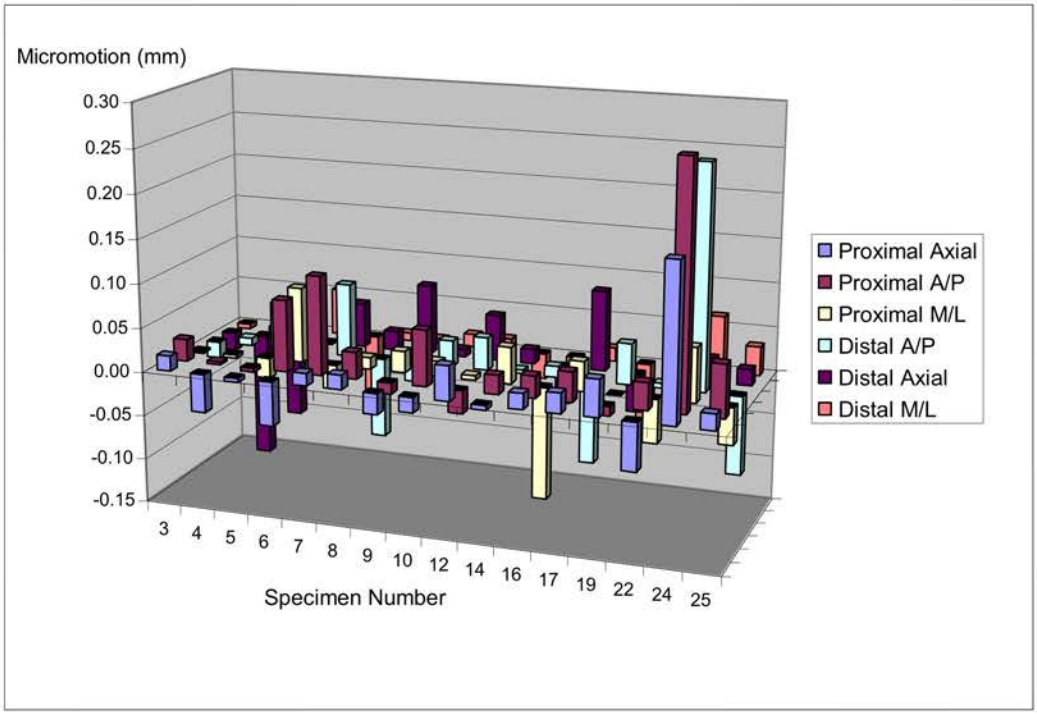

Graph 39. The relative micromotions in each plane for the proximal and distal targets (simplified in Graph 32.).

Graph 39. is complex, but does indicate the range of displacements, with animal specimen number 24 clearly showing signs of greater movement. Using an unpaired t-test to compare the two groups, including specimen No.24, the comparison failed to reach a statistically significant difference ($t = 1.38$, 14 DF, $p = 0.19$). Clearly, by excluding specimen No.24., a difference will be even less likely to be detectable. Using these values, a sample size of 17 animals per group would be required to detect a difference with any significant power.

A simpler graphical representation of motion is shown in Graph 40., where the absolute values have been averaged and represented by the mean +/- 2 standard errors.

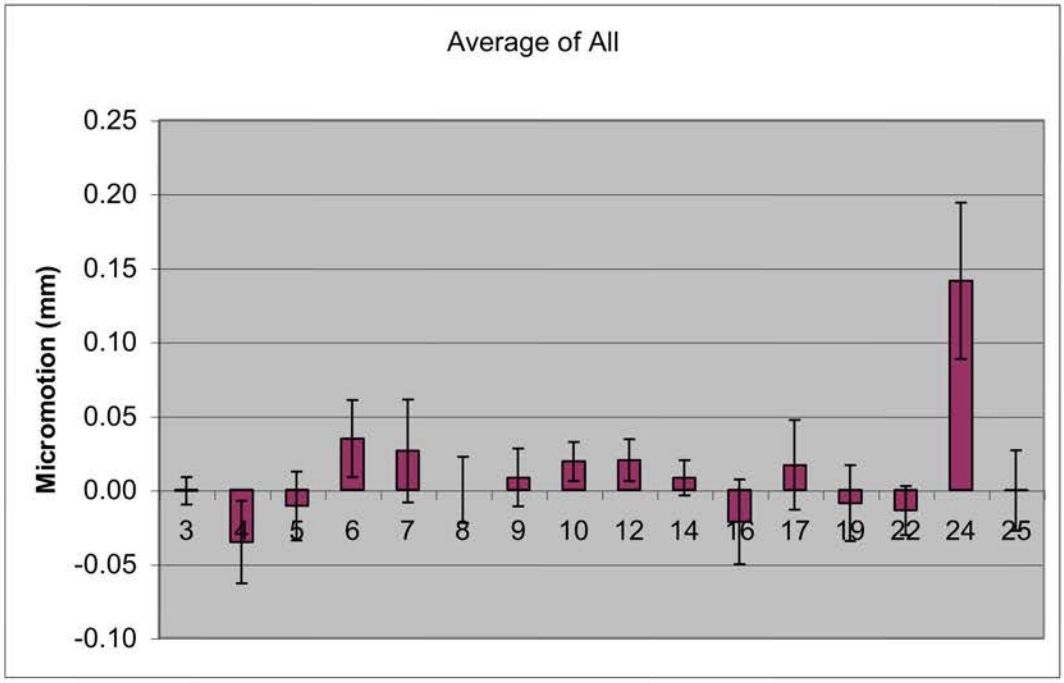

Graph 40. Average micromotion.

Chapter 15 Phase III Summary

15.1. Discussion

Decisions on outcome measures and appropriate study endpoints are multifactorial. The correct parameters to assess the suitability of a graft or graft substitute for clinical uses are still open to debate.

15.1.1. Hemiarthroplasty model

This model was thought to simulate a human revision scenario well, both at the macroscopic level, where the surgical impaction technique was used, but also at the microscopic level.

Biopsies of sclerotic acetabular bone at primary and revision surgery in humans have shown that at the time of revision, the acetabular bone was viable with sufficient vascularity and remodelling activity to provide an acceptable recipient host bone bed for bone graft[205]. Concerns that the over reaming to produce a cortical rim of bone and an enlarged canal would not simulate the typical microscopic environment found at revision surgery in humans, have been shown to be insignificant.

Three cases of femoral fracture with cerclage wiring did not prevent progression of the hairline fracture down the shaft, to induce a mid-diaphyseal fracture later on. It was decided that in future, intra-operative fracture should necessitate withdrawal of the animal from the trial. Ideally the operative procedures, post-op rehabilitation and the field hospital should be located in the same area, as this would reduce the traumatic fracture rate. The other causes of withdrawal were largely unavoidable in the circumstances, despite scrupulous aseptic technique and peri-operative care.

Prophylactic femoral wiring was considered, as advocated by the Exeter group. In cadaveric trials, cerclage wiring doubled the length of the operative procedure and required considerable proximal muscle stripping despite using wire passers as per the human technique. In the three animals where hairline cracks were identified intra-operatively, cerclage wiring failed to prevent progression to femoral fracture in all cases, unlike the human situation. This may be due to the increased brittleness of ovine bone compared to human bone. It was therefore decided not to prophylactically wire the femurs and any future operative fractures should result in immediate withdrawal of the animal from the trial.

15.1.2. Radiological subsidence

We detected relatively large subsidence levels with an accurate and reproducible model. Overall precision was limited by the quality of the X-ray images and not by the measuring technique. We looked at other techniques prior to the study and suggest that only high quality RSA films will overcome this problem.

Dual Emission X-ray Absorptiometry (DEXA) around the prosthesis has previously been reported as a potential indicator of graft incorporation[134]. Our feeling is that this method is not refined enough yet to be of clinical use, as the DEXA system is unable to differentiate cement from graft. Future studies using DEXA may consider using radio-lucent cement.

A commercial computer assisted system (DiagnostiX-32 imaging system, GeMed, Freiburg, Germany) under evaluation in Aberdeen, was considered at the start of the project, based on the method of Muller on standard radiographs. However, subsequent results using this system[157] show an inferior level of intra and inter-observer error, compared to this thesis.
Caution should be used when using digitisers. An X-ray digitiser was tested at the start of the project, but the maximum pixel to pixel resolution was 0.69mm, despite appearing to be more precise than this, due to the readout appearing in millimetres to two decimal places.

15.1.3. Micromotion

We have developed a model with acceptable precision, given the broad banding of categories to be detected: <50 microns, 50-150 microns and > 150 microns. We were able to detect one clinically loose implant from the group. We were not able to detect a statistically significant difference between the groups.

Force plate analysis in the post-operative period has been reported to be used[206] as an indication of implant stability. We chose not to undertake this test as the relationship to actual 'looseness' was considered tenuous. It is also extremely time consuming, with the variability between repeated results and different sheep almost as high as any potential difference. Some veterinarians believe this to be in part due to avoidance behaviour by the sheep to stand on an area of different ground. In the ovine model, the animal almost immediately weight-bears in the post-operative period, unlike the canine model, which may represent an animal more readily assessed by force plate analysis. Our walking score (and maybe force plate analysis) was useful as an indication of gross implant function, but not as a discriminator between well functioning implants.

The load and application position were seen to reproduce femoral microstrains within the in-vivo range previously reported by Lanyon et al in the medial and lateral proximal femur. The anterior and posterior femoral cortical microstrains were found to be compressive. This is in keeping with current ideology regarding bone formation in areas of compressive loading and previous reports of minimal bending of long bones in-vivo on loading.

To measure micromotion of an implant it is necessary to precisely define the micromotion of what against what. Ideally it would be necessary to measure the 3 dimensional motion of three reference points on the implant with reference to the overlying bone. We have assumed rigid body motion of the implant and this requires only two implant reference points. The use of one point is inadequate, as the reference point may itself be at or near the centroid of the implant. The assumption of rigid body motion is appropriate, as the errors based on Finite Element modelling

are at least an order of magnitude smaller than the system error[207]. The femoral reference point should be as close as possible to the implant reference point, as more distant points may be subjected to localising factors altering motion (such as around the trochanter).

Comparison to other systems:

To our knowledge there are no reported systems that are capable of recording implant interface micromotions in three dimensions at two points simultaneously. Of those that have measured three-dimensional micromotion at single points, these can be divided into three groups:

The first group includes that of Buhler et al[204] who mount their measuring device through a single drill hole and reference the femur via this overlying drill hole. Our methodology is similar to this first group, but our system is less compact (and hence cheaper and easier to modify) and simultaneously records data at two points.

The second group comprises authors[160; 208; 209] who have mounted their measuring devices onto the implant proximally and referenced variable places on the femur. This group may be considered rather unsatisfactory due to difficulty in obtaining rigid fixation to the stem (also found with Brumby's work[141]) and also errors in the choice of the femoral reference point, which was often at a distance. Deformation in the femur during loading becomes a significant factor with these regimes.

The third group comprises those authors who have used non-contact measuring devices. These authors do not clearly address the fixation problem[210] and describe problems with performing experiments in total darkness[211] when using Photo Sensitive Devices (PSD's).

Since this project was performed, there has been a move in human revision surgery to produce a thicker cement mantle than the 1mm produced by the original Exeter X-change system. This has been due to an increased awareness of cement mantle fracture in areas of thin cement[59]. In our model, the phantom was designed to produce a cement mantle of only 1mm and this would now be considered too thin.

Additionally;

- We have considered the third dimension in a physiological set-up, validated by reproduction of in vivo femoral strains.

- We have developed a targeting system with a precision approaching +/- 20 microns.

- This is the first model to recreate physiological 3D strains through the femur and to detect movement in all planes simultaneously with 6 degrees of freedom of measurable movement of the implant.

- Typical micromotions:

  Clinically stable implants < 50μm

  Clinically loose implants > 150μm

- This system is applicable to human models and for different implants.

15.1.4. Histology / Histomorphometry

A qualitative and quantitative ovine model of femoral impaction grafting is described (Appendix) which may be used for comparative studies of different impaction grafting techniques and materials. This may allow determination of which conditions maximise bone graft incorporation and long-term implant stability.

Bone graft incorporation was common, though not complete by harvest at 12 weeks post surgery. Angioneogenesis of the graft had occurred distally, but was more rapid from the proximal end. Corglaes® was present primarily in the distal portion of the graft mantle, suggesting a more biologically isolated environment than the Phase II model. Centripetal vascularisation occurred more slowly. There was no fibrous tissue at the cement-graft interface, suggesting stable component fixation (Appendix – Hemiarthroplasty histology).

15.2. Conclusion

The results in the context of the null hypothesis (Section 11.2) were examined;

> "At 12 weeks after implantation, there is no difference in **radiographic subsidence** of the femoral prosthesis when cemented into in a 50/50 mix of sheep allograft / idealised Corglaes®, compared to sheep allograft alone."

This is **unproven**. If there is a difference it is small and would require sample sizes of 32 to show a difference, or to have the power to show there is no difference.

> "At 12 weeks after implantation, there is no difference in **micromotion** of the femoral prosthesis when cemented into in a 50/50 mix of sheep allograft / idealised Corglaes®, compared to sheep allograft alone."

This is **unproven**. If there is a difference it is small and would require sample sizes of 20 to show a difference, or to have the power to show there is no difference.

> "At 12 weeks after implantation, there is no difference in **biological re-incorporation** of the femoral prosthesis when cemented into in a 50/50 mix of sheep allograft / idealised Corglaes®, compared to sheep allograft alone."

This cannot be concluded from this thesis. Further work by other authors may shed light on this in due course.

Chapter 16 Future Direction

These experiments highlight potential mechanisms with which to improve impacted bone graft strength and support further analysis of synthetic materials, including Corglaes® as a bulking agent or bone graft enhancer.

Future projects have come about as a direct result of this project, including further histological analysis of these animals, new projects analysing newer materials +/- enhancers and a grant application to analyse differences between washed and irradiated bone.

The potential reduction in risk of disease transmission by washing graft, combined with seeding of graft and/or synthetic materials with harvested or cultured autogenous stem cells or buffy coat will be a future avenue.

We are currently investigating the role of the taper angle in vitro, in collaboration with the Department of Bioengineering in Adelaide and the Department of Engineering in Exeter.

The degree of compaction and impaction energy applied to the graft could be further investigated to define when graft compaction is complete. This would allow more uniformity and comparison between centres (unreported work, Richardson – Oswestry, UK).

The role of graft particle shape is of further interest, as some mills produce rod-like shapes, which theoretically may have a function rather like the metal rods in reinforced concrete. The transition from spongy cancellous particles to individual solid particles is bound to also play a major role in the further analysis of graft material.

Chapter 17 References

1. Slooff, T. J. The miracle of the black leg : Revision total hip arthroplasty with bone grafts: Valedictory address. 1997. Katholieke Universiteit Nijmegen. (GENERIC)
Ref Type: Thesis/Dissertation

2. Wenger DR, Rang M. *The art and practice of childrens orthopaedics*. New York: Raven press Ltd, 1980;47

3. Garellick G, Malchau H, Herberts P. Survival of hip replacements. A comparison of a randomized trial and a registry. *Clin.Orthop.2000.Jun.;(375.):157.-67.* 157-167.

4. Herberts P, Malchau H. Long-term registration has improved the quality of hip replacement: a review of the Swedish THR Register comparing 160,000 cases. *Acta Orthop.Scand.2000.Apr.;71.(2.):111.-21.* **71**:111-121.

5. Hultmark P, Karrholm J, Stromberg C, Herberts P, Mose CH, Malchau H. Cemented first-time revisions of the femoral component: prospective 7 to 13 years' follow-up using second-generation and third-generation technique [In Process Citation]. *J.Arthroplasty 2000.Aug.;15.(5.):551.-61.[MEDLINE.record.in process.]* **15**:551-561.

6. Malchau, H., Herberts, P., Soderman, P., and Oden , A. Prognosis of total hip replacement; update and validation of results from the Swedish National Hip Arthroplasty Registry 1979-1998. 2000. American Academy of Orthopaedic Surgeons, Scientific Exhibition, Orlando, USA. (GENERIC)
Ref Type: Report

7. Soderman P, Malchau H, Herberts P. Outcome after total hip arthroplasty: Part I. General health evaluation in relation to definition of failure in the Swedish National Total Hip Arthoplasty register [In Process Citation]. *Acta Orthop.Scand.2000.Aug.;71.(4.):354.-9.[MEDLINE.record.in process.]* **71**:354-359.

8. Soderman P, Malchau H, Herberts P, Johnell O. Are the findings in the Swedish National Total Hip Arthroplasty Register valid? [In Process Citation]. *J.Arthroplasty 2000.Oct.;15.(7.):884.-9.[MEDLINE.record.in process.]* **15**:884-889.

9. Callaghan JJ, Salvati EA, Pellicci PM, Wilson PDJ, Ranawat CS. Results of revision for mechanical failure after cemented total hip replacement, 1979 to 1982. A two to five-year follow-up. *J.Bone Joint Surg.[Am.]* 1985;**67**:1074-1085.

10. Surace A, Mineo G, Micale C, Privitera AM, Pietrogrande L. Multiple revision of total hip arthroplasties. *Hip International* 1992;53-62.

11. Behairy Y, Jasty M. Bone grafts and bone substitutes in hip and knee surgery. *Orthop Clin.North Am.* 1999;**30**:661-671.

12. Stockley I, Holt G. Provision of allograft bone for orthopaedic surgery: a census of orthopaedic surgeons. *British Orthopaedic News* 1998;**18**:24-25.

13. Galea G, Kopman D, Graham BJ. Supply and demand of bone allograft for revision hip surgery in Scotland [published erratum appears in J Bone Joint Surg Br 1998 Nov;80(6):1087]. *J Bone Joint Surg.Br.* 1998;**80**:595-599.

14. Khan MT, Stockley I, Ibbotson C. Allograft bone transplantation: a Sheffield experience. *Ann.R.Coll.Surg.Engl.* 1998;**80**:150-153.

15. Anonymous Emerging technologies in orthopaedics: bone graft substitutes, bone growth stimulators and growth factors. The European bone graft market. *Orthop.Prod.News* 1999;**Oct/Nov**:

16. Smith , P. and Gie, G. Impaction bone allografting of the femur. Orthop.Prod.News Jul/Aug/Sep, 32-33. 1998. (GENERIC)
Ref Type: Magazine Article

17. Gie G, Linder L, Ling RS, Simon JP, Slooff TJ, Timperley AJ. Femoral reconstruction cement with graft. In: Galante A, Rosenberg J, Callaghan JJ, eds. *Total hip revision surgery*. New York: Raven press Ltd, 1995;

18. Gie GA, Linder L, Ling RS, Simon JP, Slooff TJ, Timperley AJ. Contained morselized allograft in revision total hip arthroplasty. Surgical technique. *Orthop.Clin.North Am.* 1993;**24**:717-725.

19. Gie GA, Linder L, Ling RS, Simon JP, Slooff TJ, Timperley AJ. Impacted cancellous allografts and cement for revision total hip arthroplasty. *J.Bone Joint Surg.Br.* 1993;**75**:14-21.

20. Slooff TJ, Huiskes R, van Horn J, Lemmens AJ. Bone grafting in total hip replacement for acetabular protrusion. *Acta Orthop.Scand.* 1984;**55**:593-596.

21. Slooff TJ, Buma P, Schreurs BW, Schimmel JW, Huiskes R, Gardeniers J. Acetabular and femoral reconstruction with impacted graft and cement. *Clin.Orthop.* 1996;108-115.

22. Slooff TJ, Schimmel JW, Buma P. Cemented fixation with bone grafts. *Orthop.Clin.North Am.* 1993;**24**:667-677.

23. Ling RS. Femoral component revision using impacted morsellised cancellous graft [letter; comment]. *J.Bone Joint Surg.Br.* 1997;**79**:874-875.

24. Shen G. Femoral stem fixation. An engineering interpretation of the long-term outcome of Charnley and Exeter stems [see comments]. *J Bone Joint Surg.Br.* 1998;**80**:754-756.

25. Alfaro-Adrian J, Gill HS, Murray DW. Cement migration after THR. A comparison of Charnley Elite and Exeter femoral stems using RSA. *J Bone Joint Surg.Br.* 1999;**81**:130-134.

26. Britton AR, Murray DW, Bulstrode CJ, McPherson K, Denham RA. Long-term comparison of Charnley and Stanmore design total hip replacements. *J Bone Joint Surg.Br.* 1996;**78**:802-808.

27. Kiss J, Murray DW, Turner-Smith AR, Bithell J, Bulstrode CJ. Migration of cemented femoral components after THR. Roentgen stereophotogrammetric analysis. *J Bone Joint Surg.Br.* 1996;**78**:796-801.

28. Eldridge JD, Smith EJ, Hubble MJ, Whitehouse SL, Learmonth ID. Massive early subsidence following femoral impaction grafting. *J.Arthroplasty* 1997;**12**:535-540.

29. Sharpe , P., Keene , G. S., Howie , D. W., Graves , S. E., and Mintz , A. D. Impaction grafting or cement alone for femoral revision hip replacement. 1998. ANZORS; Sydney, Australia. (GENERIC)
Ref Type: Conference Proceeding

30. Havelin , L. I., Espehaug , B., Lie , S. A., Engesaeter , L. B., Furnes , O., and Vollset , S. E. Prospective studies of hip prostheses and cements: a presentation of the Norwegian arthroplasty register 1987-1999. 2000. American Academy of Orthopaedic Surgeons,

Scientific Exhibition, Orlando, USA. (GENERIC)
Ref Type: Report

31. Huiskes R. Failed innovation in total hip replacement. Diagnosis and proposals for a cure. *Acta Orthop.Scand.* 1993;**64**:699-716.

32. Huiskes R. Mechanical failure in total hip arthroplasty with cement. *Current Orthopaedics* 1993;239-247.

33. Huiskes R, Hollister SJ. From structure to process, from organ to cell: recent developments of FE-analysis in orthopaedic biomechanics. *J.Biomech.Eng.* 1993;**115**:520-527.

34. Collier JP, Bauer TW, Bloebaum RD, et al. Results of implant retrieval from postmortem specimens in patients with well-functioning, long-term total hip replacement. *Clin.Orthop.* 1992;97-112.

35. Jasty MJ, Floyd WE, Schiller AL, Goldring SR, Harris WH. Localized osteolysis in stable, non-septic total hip replacement. *J.Bone Joint Surg.[Am.]* 1986;**68**:912-919.

36. Anthony PP, Gie GA, Howie CR, Ling RS. Localised endosteal bone lysis in relation to the femoral components of cemented total hip arthroplasties. *J.Bone Joint Surg.[Br.]* 1990;**72**:971-979.

37. Lennox DW, Schofield BH, McDonald DF, Riley LHJ. A histologic comparison of aseptic loosening of cemented, press-fit, and biologic ingrowth prostheses. *Clin.Orthop.* 1987;171-191.

38. Pazzaglia UE. Pathology of the bone-cement interface in loosening of total hip replacement. *Arch.Orthop.Trauma.Surg.* 1990;**109**:83-88.

39. Buly RL, Huo MH, Salvati E, Brien W, Bansal M. Titanium wear debris in failed cemented total hip arthroplasty. An analysis of 71 cases. *J.Arthroplasty* 1992;**7**:315-323.

40. Horowitz SM, Doty SB, Lane JM, Burstein AH. Studies of the mechanism by which the mechanical failure of polymethylmethacrylate leads to bone resorption. *J.Bone Joint Surg.Am.* 1993;**75**:802-813.

41. Goodman SB. The effects of micromotion and particulate materials on tissue differentiation. Bone chamber studies in rabbits. *Acta Orthop.Scand.Suppl.* 1994;**258**:1-43.

42. Buma P, Lamerigts N, Schreurs BW, Gardeniers J, Versleyen D, Slooff TJ. Impacted graft incorporation after cemented acetabular revision. Histological evaluation in 8 patients. *Acta Orthop.Scand.* 1996;**67**:536-540.

43. Ling RS, Timperley AJ, Linder L. Histology of cancellous impaction grafting in the femur. A case report. *J Bone Joint Surg.Br.* 1993;**75**:693-696.

44. Whiteside LA. Cementless fixation issues in revision total knee arthroplasty. *Instr Course Lect* 1999;**48**:177-182.

45. Bonfiglio M, Jeter WS. Immunological responses to bone. *Clin.Orthop.* 1972;**87**:19-27.

46. Burchardt H, Enneking WF. Transplantation of bone. *Surg.Clin.North Am.* 1978;**58**:403-427.

47. Ray RD. Vascularization of bone grafts and implants. *Clin.Orthop.* 1972;**87**:43-48.

48. Goldberg VM, Powell A, Shaffer JW, Zika J, Bos GD, Heiple KG. Bone grafting: role of histocompatibility in transplantation. *J.Orthop.Res.* 1985;**3**:389-404.

49. Tagil M. The morselized and impacted bone graft. Animal experiments on proteins, impaction and load. *Acta Orthop.Scand.Suppl.2000.Feb.;290.:1.-40.* **290**:1-40.

50. Dunlop DG, Griffon D, Howie CR, Madabhushi SP, Usmani AS, Gillespie WJ. An ovine model to evaluate impacted pellets of new synthetic bone graft substitutes. *J.Bone Joint Surg.[Br.]* 2000;**82;Supp I**:65-66.

51. Aspenberg P, Tagil M, Kristensson C, Lidin S. Bone graft proteins influence osteoconduction. A titanium chamber study in rats. *Acta Orthop.Scand.* 1996;**67**:377-382.

52. Horowitz MC, Friedlaender GE. Immunologic aspects of bone transplantation. A rationale for future studies. *Orthop.Clin.North Am.* 1987;**18**:227-233.

53. Davy DT. Biomechanical issues in bone transplantation. *Orthop Clin.North Am.* 1999;**30**:553-563.

54. Heyligers , I. C. Vital cells in bone bank allografts: implications. 2000. Vu Academisch Ziekenhuis - Advanced Exeter Hip Symposium. 17-11-2000. (GENERIC)
Ref Type: Conference Proceedings

55. Hamer AJ, Stockley I, Elson RA. Changes in allograft bone irradiated at different temperatures. *J.Bone Joint Surg.Br.* 1999;**81**:342-344.

56. Boyce T, Edwards J, Scarborough N. Allograft bone. The influence of processing on safety and performance. *Orthop Clin.North Am.* 1999;**30**:571-581.

57. Campbell , D. G. Sterilisation of HIV infected bone allografts. 1990. University of Adelaide, South Australia. (GENERIC)
Ref Type: Thesis/Dissertation

58. Brewster NT, Gillespie WJ, Howie CR, Madabhushi SP, Usmani AS, Fairbairn DR. Mechanical considerations in impaction bone grafting. *J.Bone Joint Surg.Br.* 1999;**81**:118-124.

59. Kawate K, Maloney WJ, Bragdon CR, Biggs SA, Jasty M, Harris WH. Importance of a thin cement mantle. Autopsy studies of eight hips. *Clin.Orthop.* 1998;70-76.

60. Crawford RW, Psychoyios V, Gie G, Ling R, Murray D. Incomplete cement mantles in the sagittal femoral plane: an anatomical explanation. *Acta Orthop.Scand.* 1999;**70**:596-598.

61. Kuiper JH, Merry JC, Cheah K, Robinson DD, van Kampen M, Richardson JB. Early mechanical stability of impaction-grafted prostheses: effects of surgical technique, implant design and graft composition. *J.Bone Joint Surg.[Br.]* 1996;**78;Supp II & III**:136

62. Lee AJ. The time dependent properties of polymethylmethacrylate bone cement: the interaction of shape of femoral stems, surface finish and bone cement. In: Learmonth ID, ed. *Interfaces in total hip arthroplasty*. Springer, 2000;11-19.

63. Ling RS, Lee AJ. Porosity reduction in acrylic cement is clinically irrelevant. *Clin.Orthop.* 1998;249-253.

64. Brumby SA, Howie DW, Pearcy MJ, Wang AW, Nawana NS. Radiographic and histologic analysis of cemented double tapered femoral stems. *Clin.Orthop* 1998;229-237.

65. Crowninshield RD, Brand RA, Johnston RC, Milroy JC. An analysis of femoral component stem design in total hip arthroplasty. *J.Bone Joint Surg.[Am.]* 1980;**62**:68-78.

66. Huiskes R. The various stress patterns of press-fit, ingrown, and cemented femoral stems. *Clin.Orthop.* 1990;27-38.

67. Huiskes R, Weinans H, Dalstra M. Adaptive bone remodeling and biomechanical design considerations for noncemented total hip arthroplasty. *Orthopedics.* 1989;**12**:1255-1267.

68. Oh I, Harris WH. Proximal strain distribution in the loaded femur. An in vitro comparison of the distributions in the intact femur and after insertion of different hip-replacement femoral components. *J.Bone Joint Surg.[Am.]* 1978;**60**:75-85.

69. Whiteside LA, Easley JC. The effect of collar and distal stem fixation on micromotion of the femoral stem in uncemented total hip arthroplasty. *Clin.Orthop.* 1989;145-153.

70. Markolf KL, Amstutz HC, Hirschowitz DL. The effect of calcar contact on femoral component micromovement. A mechanical study. *J.Bone Joint Surg.[Am.]* 1980;**62**:1315-1323.

71. Cheal EJ, Spector M, Hayes WC. Role of loads and prosthesis material properties on the mechanics of the proximal femur after total hip arthroplasty. *J.Orthop.Res.* 1992;**10**:405-422.

72. Crawford RW, Evans M, Ling RS, Murray DW. Fluid flow around model femoral components of differing surface finishes: in vitro investigations. *Acta Orthop Scand.* 1999;**70**:589-595.

73. Friedlaender GE. Bone grafts. The basic science rationale for clinical applications. *J.Bone Joint Surg.[Am.]* 1987;**69**:786-790.

74. Gerber SD, Harris WH. Femoral head autografting to augment acetabular deficiency in patients requiring total hip replacement. A minimum five-year and an average seven-year follow-up study. *J.Bone Joint Surg.[Am.]* 1986;**68**:1241-1248.

75. Harris WH. Allografting in total hip arthroplasty: in adults with severe acetabular deficiency including a surgical technique for bolting the graft to the ilium. *Clin.Orthop.* 1982;150-164.

76. Mankin HJ, Doppelt S, Tomford W. Clinical experience with allograft implantation. The first ten years. *Clin.Orthop.* 1983;69-86.

77. Pollock FH, Whiteside LA. The fate of massive allografts in total hip acetabular revision surgery. *J.Arthroplasty* 1992;**7**:271-276.

78. Springfield DS. Massive autogenous bone grafts. *Orthop.Clin.North Am.* 1987;**18**:249-256.

79. Trancik TM, Stulberg BN, Wilde AH, Feiglin DH. Allograft reconstruction of the acetabulum during revision total hip arthroplasty. Clinical, radiographic, and scintigraphic assessment of the results. *J.Bone Joint Surg.[Am.]* 1986;**68**:527-533.

80. Wilson MG, Nikpoor N, Aliabadi P, Poss R, Weissman BN. The fate of acetabular allografts after bipolar revision arthroplasty of the hip. A radiographic review. *J.Bone Joint Surg.[Am.]* 1989;**71**:1469-1479.

81. Tay BK, Patel VV, Bradford DS. Calcium sulfate- and calcium phosphate-based bone substitutes. Mimicry of the mineral phase of bone. *Orthop Clin.North Am.* 1999;**30**:615-623.

82. Cornell CN. Osteoconductive materials and their role as substitutes for autogenous bone grafts. *Orthop Clin.North Am.* 1999;**30**:591-598.

83. Ludwig SC, Boden SD. Osteoinductive bone graft substitutes for spinal fusion: a basic science summary. *Orthop Clin.North Am.* 1999;**30**:635-645.

84. Scaduto AA, Lieberman JR. Gene therapy for osteoinduction. *Orthop Clin.North Am.* 1999;**30** :625-633.

85. Ikeda N, Kawanabe K, Nakamura T. Quantitative comparison of osteoconduction of porous, dense A-W glass-ceramic and hydroxyapatite granules (effects of granule and pore sizes). *Biomaterials* 1999;**20**:1087-1095.

86. Kawanabe K, Iida H, Matsusue Y, Nishimatsu H, Kasai R, Nakamura T. A-W glass ceramic as a bone substitute in cemented hip arthroplasty: 15 hips followed 2-10 years. *Acta Orthop.Scand.* 1998;**69**:237-242.

87. Kawanabe K, Tamura J, Yamamuro T, Nakamura T, Kokubo T, Yoshihara S. A new bioactive bone cement consisting of BIS-GMA resin and bioactive glass powder. *J.Appl.Biomater.* 1993;**4**:135-141.

88. Kobayashi M, Shinzato S, Kawanabe K, et al. Alumina powder/Bis-GMA composite: effect of filler content on mechanical properties and osteoconductivity. *J.Biomed.Mater.Res.2000.Mar.5.;49.(3.):319.-27.* **49**:319-327.

89. Okada Y, Kawanabe K, Fujita H, Nishio K, Nakamura T. Repair of segmental bone defects using bioactive bone cement: comparison with PMMA bone cement. *J.Biomed.Mater.Res.* 1999;**47**:353-359.

90. Yamamuro T, Nakamura T, Iida H, et al. Development of bioactive bone cement and its clinical applications. *Biomaterials* 1998;**19**:1479-1482.

91. Holmes RE, Bucholz RW, Mooney V. Porous hydroxyapatite as a bone-graft substitute in metaphyseal defects. A histometric study. *J.Bone Joint Surg.[Am.]* 1986;**68**:904-911.

92. Cook SD. Preclinical and clinical evaluation of osteogenic protein-1 (BMP-7) in bony sites [see comments]. *Orthopedics.* 1999;**22**:669-671.

93. Cook SD, Rueger DC. Osteogenic protein-1: biology and applications. *Clin.Orthop.* 1996;29-38.

94. Lamerigts NM, Buma P, Aspenberg P, Schreurs BW, Slooff TJ. Role of growth factors in the incorporation of unloaded bone allografts in the goat. *Clin.Orthop.* 1999;260-270.

95. Tagil M, Jeppsson C, Aspenberg P. Bone graft incorporation. Effects of osteogenic protein-1 and impaction. *Clin.Orthop.2000.Feb.;(371.):240.-5.* 240-245.

96. Burnie J, Gilchrist T, Duff SR, Drake CF, Harding NG, Malcolm AJ. Controlled release glasses (C.R.G.) for biomedical uses. *Biomaterials* 1981;**2**:244-246.

97. Gilchrist T, Glasby MA, Healy DM, et al. In vitro nerve repair--in vivo. The reconstruction of peripheral nerves by entubulation with biodegradeable glass tubes--a preliminary report. *Br.J Plast.Surg.* 1998;**51**:231-237.

98. Gilchrist T, Healy DM, Drake C. Controlled silver-releasing polymers and their potential for urinary tract infection control. *Biomaterials* 1991;**12**:76-78.

99. Lenihan DV, Carter AJ, Gilchrist T, et al. Biodegradable controlled release glass in the repair of peripheral nerve injuries. *J Hand Surg.[Br.]* 1998;**23**:588-593.

100. Craig RF. *Soil mechanics*. London: Chapman and Hall, 1993;

101. Smith GN. *Elements of soil mechanics*. Oxford: Blackwell Science Ltd, 1990;

102. Dunlop , D. G., Howie, C. R., Pankaj , P., Madabhushi, S. P., and Usmani, A. S. The biomechanics of impaction grafting during revision hip surgery. 602:97. 1999. Europ Fed Nat Assoc Orthop Traum (EFORT). (GENERIC)
Ref Type: Conference Proceedings

103. Dunlop DG, Howie CR, Madabhushi SP, Usmani AS. Factors influencing impacted bone graft strength - to wash or not to wash? *J.Bone Joint Surg.[Br.]* 2000;**82;Supp I**:78

104. St. Mathew. *The Holy Bible*. 2000;Mathew 7-24-27

105. Brodt MD, Swan CC, Brown TD. Mechanical behavior of human morselized cancellous bone in triaxial compression testing. *J.Orthop.Res.* 1998;**16**:43-49.

106. Sedlin ED, Hirsch C. Factors affecting the determination of the physical properties of femoral cortical bone. *Acta Orthop.Scand.* 1966;**37**:29-48.

107. Methods of test for soils for civil engineering purposes, parts 1-9. BS1377. 1990. British Standards Institution. (GENERIC)
Ref Type: Report

108. Currey JD. The effects of drying and re-wetting on some mechanical properties of cortical bone. *J.Biomech.* 1988;**21**:439-441.

109. Linde F. Elastic and viscoelastic properties of trabecular bone by a compression testing approach. *Dan.Med.Bull.* 1994;**41**:119-138.

110. Linde F, Sorensen HC. The effect of different storage methods on the mechanical properties of trabecular bone. *J.Biomech.* 1993;**26**:1249-1252.

111. Nafei A, Danielsen CC, Linde F, Hvid I. Properties of growing trabecular ovine bone. Part I: mechanical and physical properties. *J.Bone Joint Surg.Br.2000.Aug.;82.(6.):910.-20.* **82**:910-920.

112. Nafei A, Kabel J, Odgaard A, Linde F, Hvid I. Properties of growing trabecular ovine bone. Part II: architectural and mechanical properties. *J.Bone Joint Surg.Br.2000.Aug.;82.(6.):921.-7.* **82**:921-927.

113. Rohl L, Larsen E, Linde F, Odgaard A, Jorgensen J. Tensile and compressive properties of cancellous bone. *J.Biomech.* 1991;**24**:1143-1149.

114. Lambe TW, Whitman RV. *Soil mechanics - SI version*. London: John Wiley & Sons, 1979;

115. Eldridge, J. D., Hubble , M. J., Nelson , K., Smith , E. J., and Learmonth, I. D. The effect of bone chip size on the initial stability following femoral impaction grafting. 8, 127. 1997. trans Europ Orthop Res Soc, Barcelona, Spain. (GENERIC)
Ref Type: Report

116. Sommers JFA, Timperley AJ, Wendover N, Gie G, Ling RS. Impaction grafting in cemented revision surgery of the acetabulum. *J.Bone Joint Surg.[Br.]* 1999;**81**:217

117. Goldberg VM, Stevenson S. Natural history of autografts and allografts. *Clin.Orthop.* 1987;7-16.

118. Urist MR. Bone: formation by autoinduction. *Science* 1965;**12**:698:893-9

119. Burwell RG. Studies in the transplantation of bone: V. The capacity of fresh and treated homografts of bone to evoke transplantation immunity. *J.Bone Joint Surg.[Am.]* 1963;**65**:239-246.

120. Burwell RG. Studies in the transplantion of bone: VII. The fresh composite homograft-autograft of cancellous bone. An analysis of factors leading to osteogenesis in marrow transplants and in marrow-containing bone grafts. *J.Bone Joint Surg.[Br.]* 1964;**46**:110-140.

121. Horisaka Y, Okamoto Y, Matsumoto N, et al. Subperiosteal implantation of bone morphogenetic protein adsorbed to hydroxyapatite. *Clin.Orthop.* 1991;303-312.

122. Boden SD, Martin GJJ, Morone MA, Ugbo JL, Moskovitz PA. Posterolateral lumbar intertransverse process spine arthrodesis with recombinant human bone morphogenetic protein 2/hydroxyapatite-tricalcium phosphate after laminectomy in the nonhuman primate. *Spine.* 1999;**24**:1179-1185.

123. Johnson EE, Urist MR. One-stage lengthening of femoral nonunion augmented with human bone morphogenetic protein. *Clin.Orthop.* 1998;105-116.

124. Schwartz Z, Somers A, Mellonig JT, et al. Addition of human recombinant bone morphogenetic protein-2 to inactive commercial human demineralized freeze-dried bone allograft makes an effective composite bone inductive implant material. *J.Periodontol.* 1998;**69**:1337-1345.

125. Griffon , D., Dunlop , D. G., Howie, C. R., Pratt , J., and Gillespie, W. J. An ovine model to evaluate pellets of new synthetic bone graft substitutes. 2000. European College of Veterinary Surgeons (ECVS) Annual Scientific Meeting, Bern, Switzerland. 7-9-2000 (GENERIC)
Ref Type: Conference Proceedings

126. Pratt , J., Griffon , D., Dunlop , D. G., Howie, C. R., and Tomlinson , L. Incorporation of idealised, impacted, morselised, allograft and hydroxyapatite-tricalcium phosphate in metaphyseal bone defects. 2000. European College of Veterinary Surgeons (ECVS) Annual Scientific Meeting, Bern, Switzerland. 7-9-2000. (GENERIC)
Ref Type: Conference Proceedings

127. Soballe K. Bone graft incorporation around titanium-alloy- and hydroxyapatite-coated implants in dogs. *Clin.Orthop.* 1992;282-293.

128. Soballe K. Hydroxyapatite coating modifies implant membrane formation. Controlled micromotion studied in dogs. *Acta Orthop.Scand.* 1992;**63**:128-140.

129. Soballe K. Tissue ingrowth into titanium and hydroxyapatite-coated implants during stable and unstable mechanical conditions. *J.Orthop.Res.* 1992;**10**:285-299.

130. Tagil M, Aspenberg P. Impaction of cancellous bone grafts impairs osteoconduction in titanium chambers. *Clin.Orthop.* 1998;231-238.

131. Wang JS, Tagil M, Aspenberg P. Load-bearing increases new bone formation in impacted and morselized allografts. *Clin.Orthop.2000.Sep.;(378.):274.-81.* 274-281.

132. Lamerigts NM, Buma P, Huiskes R, Schreurs W, Gardeniers J, Slooff TJ. Incorporation of morsellized bone graft under controlled loading conditions. A new animal model in the goat. *Biomaterials 2000.Apr.;21.(7.):741.-7.* **21**:741-747.

133. Lamerigts N, Aspenberg P, Buma P, Versleyen D, Slooff TJ. The repeated sampling bone chamber: a new permanent titanium implant to study bone grafts in the goat. *Lab Anim Sci* 1997;**47**:401-406.

134. Eldridge JD, Samuels A, Eveleigh R, Goodship AE, Learmonth ID. DEXA analysis of femoral impaction grafting: a pilot study. *J.Bone Joint Surg.[Br.]* 2000;**82;Supp III**:255.

135. Jain AK, Luthera J, Kumar S. Estimation of rate of neogenesis in humans by tetracycline double labelling. *J.Bone Joint Surg.[Br.]* 1999;**82;Supp I**:

136. Dunlop , D. G., Costi , J. J., Hearn , T., Barker , D., Field , J. R., and Howie, C. R. Design and evaluation of a device to measure the instantaneous three dimensional micromotion of a femoral stem prosthesis. 1999. Virginia, USA. Orthopaedic animal models - CHI. (GENERIC)
Ref Type: Conference Proceedings

137. Dunlop DG, Field JR. Ovine hip hemiarthroplasty: reducing dislocation. *Vet Comp Orthop Traumatol* 2000;**13**:115-118.

138. Dunlop DG, Costi JJ, Barker D, Howie CR, Field JR, Hearn T. Design and evaluation of a device for measuring 3D micromotions of impaction grafted cemented femoral stem prostheses. *J.Bone Joint Surg.[Br.]* 2000;**82;Supp III**:261-262.

139. Field JR, Carbone A, Aberman H, et al. An ovine model for total hip replacement: operative measures and complications. *Vet Comp Orthop Traumatol* 2001;(in press)

140. Phillips TW, Johnston G, Wood P. Selection of an animal model for resurfacing hip arthroplasty. *J Arthroplasty* 1987;**2**:111-117.

141. Brumby, S. A. The effect of surface roughness and a collar on fixation of cemented femoral stems in vivo. 1996. University of Adelaide, South Australia. (GENERIC)
Ref Type: Thesis/Dissertation

142. Field , J. R. Dislocation rate in predated Adelaide ovine hip replacement model. 1998. (GENERIC)
Ref Type: Personal Communication

143. Chapman PG, Villar RN. The bacteriology of bone allografts. *J.Bone Joint Surg.[Br.]* 1992;**74**:398-399.

144. Villar RN, Gross AE, McMinn D. *Revision hip arthroplasty: a practical approach to bone stock loss.* Oxford: Butterworth-Heinmann, 1997;

145. Garrel , T., Knaepler , H., and Seipp , H-M. Experimental and clinical experiences with autoclaved allogenic bone grafts. 36. 1991. (GENERIC)
Ref Type: Conference Proceedings

146. Heiple KG, Chase SW, Hendon CH. A comparative study of the healing process following different types of bone transplantation. *J.Bone Joint Surg.[Am.]* 1963;**45**:1593-1616.

147. Heiple KG, Goldberg VM, Powell AE, Bos GD, Zika JM. Biology of cancellous bone grafts. *Orthop.Clin.North Am.* 1987;**18**:179-185.

148. Gross AE, Hutchison CR, Alexeeff M, Mahomed N, Leitch K, Morsi E. Proximal femoral allografts for reconstruction of bone stock in revision arthroplasty of the hip. *Clin.Orthop.* 1995;151-158.

149. Morgan DAF, Ferguson KL, Benfield JEC, Jonstone PO. Bone banking in the 1990's - a safe efficient system. *Current Orthopaedics* 1993;**7**:36-43.

150. Bruns DP, Olmstead ML, Litsky AS. Technique and results for total hip replacement in sheep: An experimental model. *Vet Comp Orthop Traumatol* 1996;**9**:158-164.

151. Cave EF, Rowe CR. Capsular repair for recurrent dislocation of shoulder: pathologic findings and operative technic. *Surg.Clin.North Am.* 1947;**27**:1289

152. Zarins B, McMahon MS, Rowe CR. Diagnosis and treatment of traumatic anterior instability of the shoulder. *Clin.Orthop.* 1993;75-84.

153. Phillips BB. Recurrent dislocations. In: Canale ST, ed. *Campbell's operative orthopaedics*. Missouri: Mosby, 1998;1334-1404.

154. Mjoberg B, Hansson LI, Selvik G. Instability, migration and laxity of total hip prostheses. A roentgen stereophotogrammetric study. *Acta Orthop.Scand.* 1984;**55**:141-145.

155. Nistor L, Blaha JD, Kjellstrom U, Selvik G. In vivo measurements of relative motion between an uncemented femoral total hip component and the femur by roentgen stereophotogrammetric analysis. *Clin.Orthop.* 1991;220-227.

156. Downing MR, Gibson PH, Sutcliffe A, Smith F, Hukins DW, Ashcroft GP. Incidence of bead loosening in RSA acetabular cups - a 6 month review. *J.Bone Joint Surg.[Br.]* 2000;**82;Supp III**:254

157. Downing MR, Ashcroft GP, Gibson PH. Feasibility of retrospective assessment of femoral stem subsidence. *J.Bone Joint Surg.[Br.]* 2000;**82;Supp III**:253

158. Paterson M, Fulford P, Denham R. Loosening of the femoral component after total hip replacement. The thin black line and the sinking hip. *J.Bone Joint Surg.[Br.]* 1986;**68**:392-397.

159. Haddad RJJ, Cook SD, Thomas KA. Biological fixation of porous-coated implants. *J.Bone Joint Surg.[Am.]* 1987;**69**:1459-1466.

160. Hua J, Walker PS. Relative motion of hip stems under load. An in vitro study of symmetrical, asymmetrical, and custom asymmetrical designs. *J.Bone Joint Surg.Am.* 1994;**76**:95-103.

161. Harris WH, Mulroy RDJ, Maloney WJ, Burke DW, Chandler HP, Zalenski EB. Intraoperative measurement of rotational stability of femoral components of total hip arthroplasty. *Clin.Orthop.* 1991;119-126.

162. Mjoberg B, Hansson LI, Selvik G. Instability of total hip prostheses at rotational stress. A roentgen stereophotogrammetric study. *Acta Orthop.Scand.* 1984;**55**:504-506.

163. Sugiyama H, Whiteside LA, Kaiser AD. Examination of rotational fixation of the femoral component in total hip arthroplasty. A mechanical study of micromovement and acoustic emission. *Clin.Orthop.* 1989;122-128.

164. Nunn D, Freeman MA, Tanner KE, Bonfield W. Torsional stability of the femoral component of hip arthroplasty. Response to an anteriorly applied load. *J.Bone Joint Surg.[Br.]* 1989; **71**:452-455.

165. Duda GN, Brand D, Freitag S, Lierse W, Schneider E. Variability of femoral muscle attachments. *J.Biomech.* 1996;**29**:1185-1190.

166. Duda GN, Heller M, Albinger J, Schulz O, Schneider E, Claes L. Influence of muscle forces on femoral strain distribution. *J.Biomech.* 1998;**31**:841-846.

167. Duda GN, Schneider E, Chao EY. Internal forces and moments in the femur during walking. *J.Biomech.* 1997;**30**:933-941.

168. Finlay JB, Chess DG, Hardie WR, Rorabeck CH, Bourne RB. An evaluation of three loading configurations for the in vitro testing of femoral strains in total hip arthroplasty. *J.Orthop.Res.* 1991;**9**:749-759.

169. Evans FG. Preservation effects. In: Burdi AR, ed. *Mechanical properties of bone*. Springfield: Thomas, 1973;

170. McElhaney J, Fogle J, Byars E, Weaver G. Effect of embalming on the mechanical properties of beef bone. *J Appl Physiol* 1964;**19**:1234

171. Finlay B. Embalming effects upon the mechanical properties of bone: preliminary experiments. In: Little EG, ed. *Experimental mechanics: Technology transfer between High Tech engineering and biomechanics.* Amsterdam: Elsevier Science Publishers, 1992;185-200.

172. Jasty M, Maloney WJ, Bragdon CR, O'Connor DO, Haire T, Harris WH. The initiation of failure in cemented femoral components of hip arthroplasties. *J.Bone Joint Surg.[Br.]* 1991;**73**:551-558.

173. Harman , M. Bone cement in alcohol. 1996. Toronto. (GENERIC)
Ref Type: Conference Proceedings

174. Koch J. The lateral bone architecture. *American Journal of Anatomy* 1917;**21**:177-218.

175. Frankel B. Biomechanics of the hip. In: Tronzo RG, ed. *Surgery of the hip*. New York: Springer-Verlag, 1984;

176. Rydell N. Biomechanics of the hip-joint. *Clin.Orthop.* 1973;**92**:6-15.

177. Radin EL. Biomechanics of the human hip. *Clin.Orthop.* 1980;28-34.

178. Keaveny TM, Hayes WC. A 20-year perspective on the mechanical properties of trabecular bone. *J.Biomech.Eng.* 1993;**115**:534-542.

179. Taylor ME, Tanner KE, Freeman MA, Yettram AL. Stress and strain distribution within the intact femur: compression or bending? *Med.Eng.Phys.* 1996;**18**:122-131.

180. Bergmann G, Graichen F, Rohlmann A. Hip joint loading during walking and running, measured in two patients. *J.Biomech.* 1993;**26**:969-990.

181. Crowninshield RD, Johnston RC, Andrews JG, Brand RA. A biomechanical investigation of the human hip. *J.Biomech.* 1978;**11**:75-85.

182. Cochran GV. Implantation of strain gages on bone in vivo. *J.Biomech.* 1972;**5**:119-123.

183. Cowin SC, Hart RT, Balser JR, Kohn DH. Functional adaptation in long bones: establishing in vivo values for surface remodeling rate coefficients. *J.Biomech.* 1985;**18**:665-684.

184. Schatzker J, Manley PA, Sumner-Smith G. In vivo strain guage study of bone response to loading with and without internal fixation. In: Uhthoff KH, ed. *Current concepts of internal fixation of fractures*. Berlin: Springer-Verlag, 1980;306-314.

185. Schatzker J, Sumner-Smith G, Hoare J, McBroom R. A telemetric system for the strain gauge determination of strain in bone in vivo. *Arch.Orthop.Trauma.Surg.* 1980;**96**:309-311.

186. Lu TW, O'Connor JJ, Taylor SJ, Walker PS. Validation of a lower limb model with in vivo femoral forces telemetered from two subjects. *J.Biomech.* 1998;**31**:63-69.

187. Fetto JF, Austin KS. A missing link in the evolution of THR: "discovery" of the lateral femur [published erratum appears in Orthopedics 1994 Jun;17(6):566]. *Orthopedics.* 1994;**17**:347-351.

188. Finlay JB, Rorabeck CH, Bourne RB, Tew WM. In vitro analysis of proximal femoral strains using PCA femoral implants and a hip-abductor muscle simulator. *J Arthroplasty* 1989;**4**:335-345.

189. Rohlmann A, Mossner U, Bergmann G, Kolbel R. Finite-element-analysis and experimental investigation of stresses in a femur. *J.Biomed.Eng.* 1982;**4**:241-246.

190. Rohlmann, A., Bergmann, G., and Kolbel, R. The relevance of stress computation in the femur with and without endoprosthesis. Simon , B. R. 2, 549-567. 1980. The University of Arizona, Tuscon, Arizona. Finite elements in biomechanics. (GENERIC)
Ref Type: Conference Proceedings

191. Van Rietbergen , B., Muller , R, Ulrich , D., Ruegsegger , P., and Huiskes, R. Quantitative assessment of tissue loading in a proximal femur, using a full scale microstructural FE-model. 62. 1997. San Franscisco. Transactions of the ORS. (GENERIC)
Ref Type: Conference Proceedings

192. Frost HM. Charles C, ed. *The laws of bone structure*. Springfield, IL: Thomas, 1980;

193. Frost HM. Wolff's law and bone's structural adaptions to mechanical usage: an overview for clinicians. *Angle Orthodontist* 1900;**64**:175-188.

194. Wolff J. *Das Gesetz der Transformation der Knochen.* Berlin: Hirschwald, 1892;

195. Rubin CT, McLeod KJ, Bain SD. Functional strains and cortical bone adaptation: epigenetic assurance of skeletal integrity. *J.Biomech.* 1990;**23 Suppl 1**:43-54.

196. McLeish RD, Charnley J. Abduction forces in the one-legged stance. *J.Biomech.* 1970;**3**:191-209.

197. Blount WP. Don't throw away the cane. *J.Bone Joint Surg.[Am.]* 1956;**38**:695-700.

198. Pauwels F. *Biomechanics of the normal and diseased hip.* New York: Springer-Verlag, 1976;

199. Lanyon LE. The measurements of bone strain 'in-vivo'. *Acta Orthop.Belgica* 1976;**Supp 1**:98-108.

200. Lanyon LE, Hampson WG, Goodship AE, Shah JS. Bone deformation recorded in vivo from strain gauges attached to the human tibial shaft. *Acta Orthop.Scand.* 1975;**46**:256-268.

201. Lanyon LE, Paul IL, Rubin CT, et al. In vivo strain measurements from bone and prosthesis following total hip replacement. An experimental study in sheep. *J.Bone Joint Surg.[Am.]* 1981;**63**:989-1001.

202. Lanyon LE, Smith RN. Measurements of bone strain in the walking animal. *Res.Vet.Sci.* 1969;**10**:93-94.

203. Weinans, H., van Loon , P., Roszek , B., and Huiskes, R. Measurement of the load components of the tibia of the goat using in vivo strain guage techniques. 538. 1992. Washington. Transactions of the ORS. (GENERIC)
Ref Type: Conference Proceedings

204. Buhler DW, Oxland TR, Nolte LP. Design and evaluation of a device for measuring three-dimensional micromotions of press-fit femoral stem prostheses. *Med.Eng.Phys.* 1997;**19**:187-199.

205. Lamerigts NM, Buma P, Sardar R, Gardeniers JW, Versleyen DH, Slooff TJ. Viability of the acetabular bone bed at revision surgery following cemented primary arthroplasty. *J.Arthroplasty* 1998;**13**:524-529.

206. Goodship, A. E., Blom , A., and Lawes , T. Evaluation of HA-TCP granules in a revision hip arthroplasty model. 1999. Impaction Grafting Group meeting, Glasgow. 14-9-1999. (GENERIC)
Ref Type: Report

207. Barker , D. Error of rigid body assumption of stem compared to micromotion. 1998. (GENERIC)
Ref Type: Personal Communication

208. Gilbert JL, Bloomfeld RS, Lautenschlager EP, Wixson RL. A computer-based biomechanical analysis of the three-dimensional motion of cementless hip prostheses. *J.Biomech.* 1992;**25**:329-340.

209. Berzins A, Sumner DR, Andriacchi TP, Galante JO. Stem curvature and load angle influence the initial relative bone-implant motion of cementless femoral stems [published erratum appears in J Orthop Res 1995 Jan;13(1):151]. *J.Orthop.Res.* 1993;**11**:758-769.

210. Blomer W. Biomechanische untersuchung zur primarstabilitat der bio-contact-revisionsprothese. In: Weller S, Volkmann R, eds. *Das Bicontact Huftendoprosthesen system*. Stuttgart: Georg Thieme, 1994;147-160.

211. Durselen L, Claes L, Wilke HJ. [Non-contact measuring of small translations and rotations in all degrees of displacement]
Beruhrungsloses Mesen kleiner Translationen und Rotationen in allen Freiheitsgraden. *Biomed.Tech.(Berl.)* 1991;**36**:248-252.

Chapter 18 Appendices

MANUFACTURING PROCESS OF BIOACTIVE GLASSES

Composition

The base elements for bioactive glass are different to silicated glasses, whose crystal structure is based on silica and oxygen. Bioactive glasses have calcium and phosphorus together with oxygen, arranged in a crystal structure. The addition of sodium disrupts the crystal structure and the amount of sodium is directly related to the dissolution rate. The precise concentration of each of these base elements remains a trade secret.

The correct proportions of each compound required to produce the bioactive glass of a given dissolution rate are placed in the mixing drum. The drum is mounted eccentrically and rotated around its axis to thoroughly mix the powders.

Fusion / Reaction Stage

The mixed powder is poured into a refractory bowl, which is plugged at the outlet and thoroughly insulated.

The bowl is mounted inside the gas furnace and heated up to the fusion temperature. The entire furnace is constantly being weighed by means of force transducers on each of the four feet.

The powder during fusion looses water vapour and so reduces in weight. This is detected as a drop in overall weight of the furnace. When the furnace reaches a stable weight - or 'holding weight' - the reaction is complete. This process takes around 2-3 hours.

Pouring
The temperature of the furnace is now reduced to allow safe pouring. The glass is still molten at this stage. A steel trolley is placed under the furnace and the stopper removed from the base of the refractory bowl.

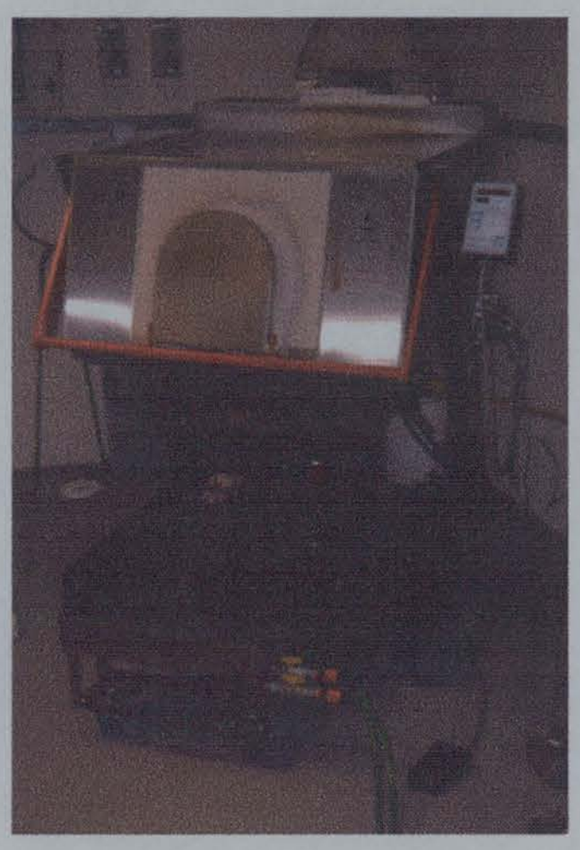

The glass rapidly cools as it sits in the metal trolley causing it to vitrify. On cooling the glass breaks up due to internal stresses. Larger pieces are broken manually into ice-cube sized pieces for collection.

Annealing
When the glass is cool enough to handle safely the pieces are placed in trays which are stacked in the annealing oven (Fig 7.). The glass is then heated at a fixed ramp rate to a temperature between the

transition point and the softening point and allowed to 'soak' for a period. Cooling the glass very slowly, at a fixed rate allows the stresses caused by vitrification to be eased.

Milling

The annealed glass is passed through the jaws of a crushing machine. The setting width of the jaws can be varied precisely to produce particles of a given range of sizes.

Collected crushed glass is then fractionated through a series of vibrating sieves. The largest at the top allowing particles less that 6mm through. Each successive sieve pore size is about 1mm smaller than the one above, with the bottom sieve allowing particles smaller than 0.5mm only to pass.

The final fractions are collected and stored individually in airtight containers.

Axisymmetric wedge model

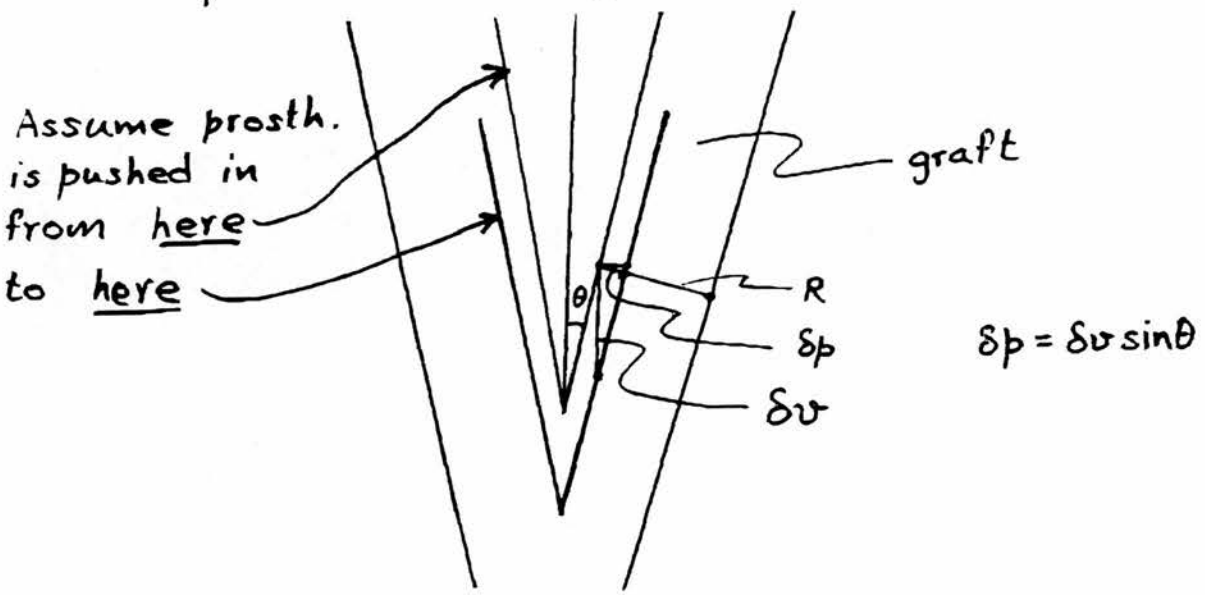

Strain normal to the plane of prosth. ε

$$\varepsilon = \frac{\delta p}{R} = \frac{\delta v \sin\theta}{R}$$

Corresponding stress σ

$$\sigma = E \frac{\delta v}{R} \sin\theta$$

Corresponding force F

$$F = \text{Area} \frac{E \delta v}{R} \sin\theta$$

Max. frictional force $= \mu F$

Max. vertical force carrying capability F_c

$$F_c = \mu F \sin\theta = \mu \frac{E}{R} \times \text{Area} \times \sin^2\theta \times \delta v$$

Comparison of Load carrying capacity for same δv and $2\theta = 15° \& 16°$

$$F_c\,(2\theta = 15°) = 0{\cdot}0170 \left[\mu \frac{E}{R} \times \text{Area}\right] \delta v$$

$$F_c\,(2\theta = 16°) = 0{\cdot}0194 \left[\mu \frac{E}{R} \times \text{Area}\right] \delta v$$

Difference 14%

Comparison of δv if max. load being carried and is the same in 2 cases

$$\delta v = \frac{1}{\sin^2\theta}\left[\frac{R}{\mu E \times \text{Area}}\right] F_c$$

$$\delta v\,(2\theta = 15°) = 58{\cdot}69 \left[\frac{R}{\mu E \times \text{Area}}\right] F_c$$

$$\delta v\,(2\theta = 16°) = 51{\cdot}63 \left[\frac{R}{\mu E \times \text{Area}}\right] F_c$$

Difference 12%

If 2θ increases from 5° to 6° then

$F_c(2\theta = 5°) = 1{\cdot}902651 \times 10^{-3}\,[\cdots]$
$F_c(2\theta = 6°) = 2{\cdot}7390523 \times 10^{-3}\,[\cdots]$
} 1·44 times increase

$\delta v\,(2\theta = 5°) = 525{\cdot}58\,[\cdots]$
$\delta v\,(2\theta = 6°) = 365{\cdot}09\,[\cdots]$ [displ. decreases to 0·7 times]

IMPLANT ANALYSIS LABORATORY
DEPARTMENT OF ORTHOPAEDICS AND TRAUMA
ROYAL ADELAIDE HOSPITAL AND
UNIVERSITY OF ADELAIDE

IMPLANT-BONE HISTOLOGY REPORT

SHEEP FEMORAL IMPACTION GRAFTING – BIOGLASS STUDY

PREPARED BY:
M. MCGEE, K. COSTI, C. WILDENAUER AND A. CARBONE

APPENDIX – HEMIARTHROPLASTY HISTOLOGY

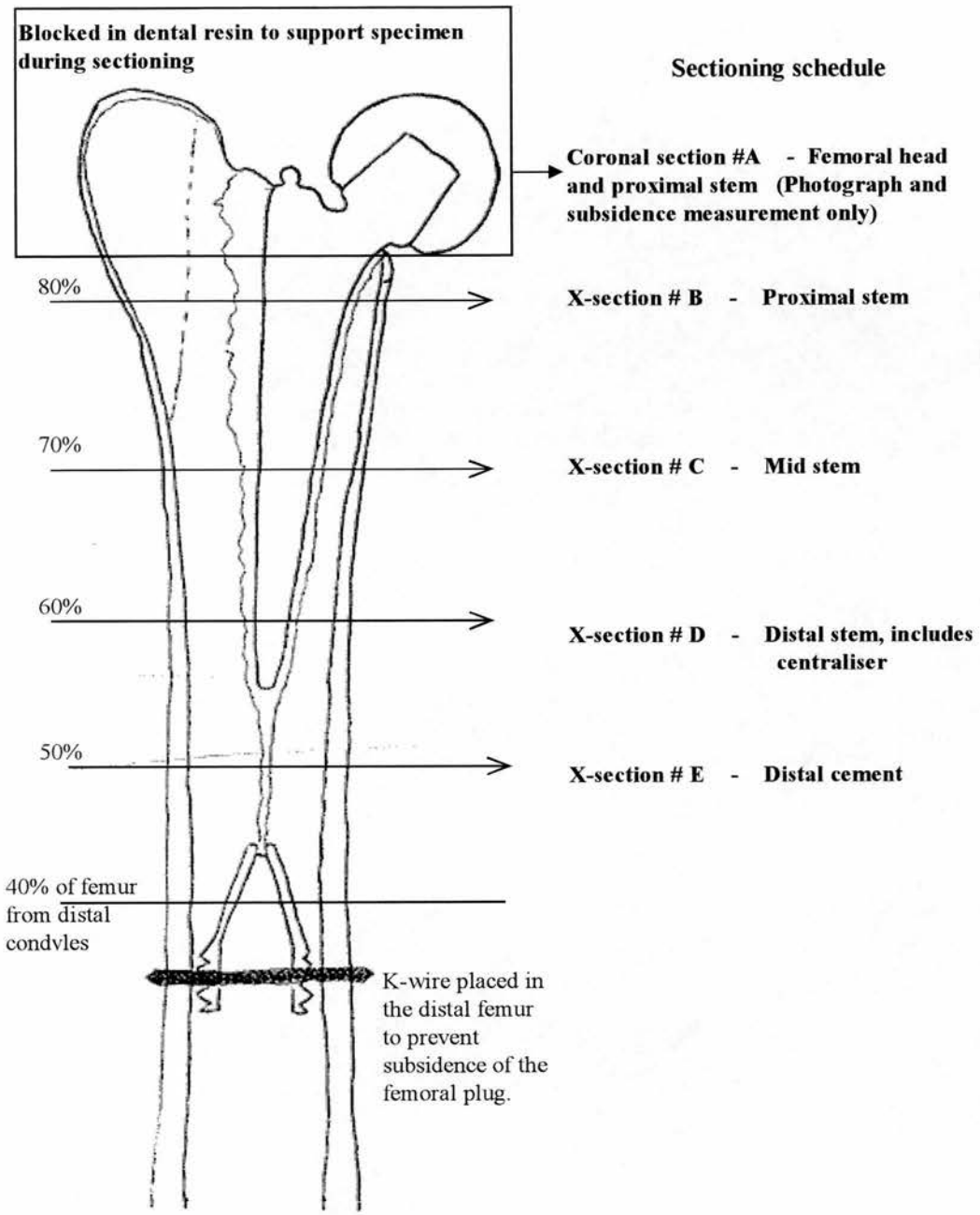

Figure 1 **Sectioning schedule for the sheep femurs with impaction graft, cement mantle and femoral stem component (and contralateral femurs)**

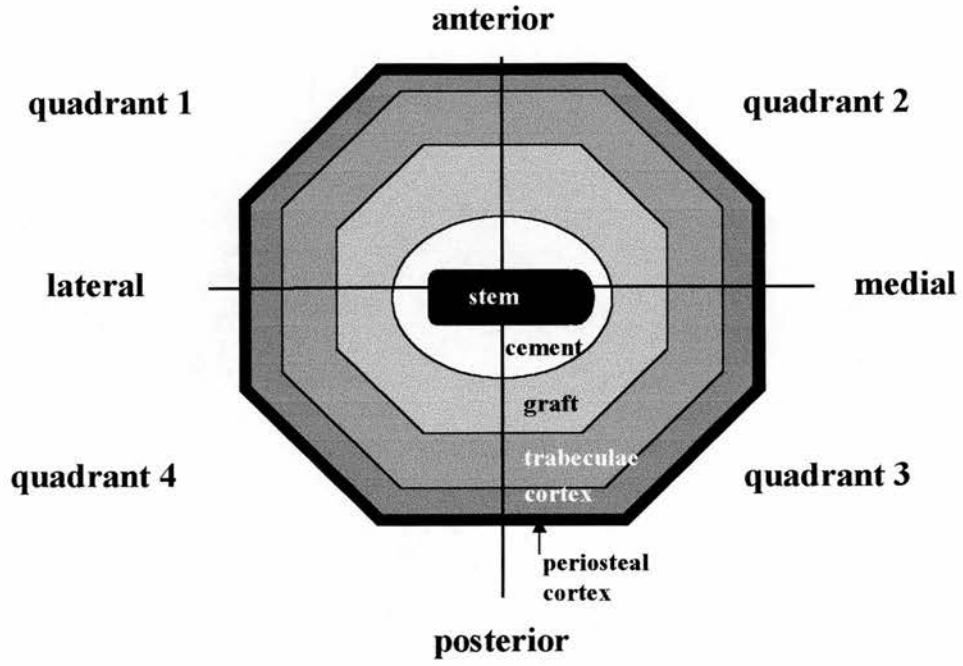

Figure 2 Regions of interest and quadrants used in microradiographic and histological analyses

FLUOROCHROME	TIME GIVEN POST-OP	COLOUR IN SITU	EXCITATION WAVELENGTH (nm)	EMISSION WAVELENGTH (nm)
xylenol orange	4 weeks	orange/red	580	610-615
calcein	8 weeks	green	436	520
oxytetracycline	10 weeks	yellow	353	570

A semi-quantitative grading system was used to describe the amount of fluorescent label in each region of interest within each quadrant.

0 no label
1+ localised label seen but infrequent (on approximately<10% of bone surfaces)
2+ label present on approximately 10-25% of bone surfaces
3+ label present on approximately 25-50 of bone surfaces
4+ label present on approximately 50-75% of bone surfaces
5+ label present on approximately > 75% of bone surfaces

The number of labels that could be visualised was also recorded.

References

Bachus KN, Bloebaum RD. Projection effect errors in biomaterials and bone research. Cells and Materials 1992;2:347-355.

Dickson GR (Ed.). Methods of Calcified Tissue Preparation. Elselvier Science 1984, Amsterdam, NY, p39.

Fornasier Dr Victor L. Personal Communication. Laboratory of Bone and Joint Pathology, Wellesley Hospital, Toronto, Ontario

Goodman SB, Magee FP, Fornasier VL. Radiological and histological study of aseptic loosening using a cemented tibial hemiarthroplasty in the rabbit knee. Biomaterials 1993;14:522-528.

Krizan ME, Schneider RL, Ettinger RL, Buckley MJ, Lavelle WE, Keller JC. Preparation and methods for sequential evaluation of titanium implant interfaces in plastic embedded calcified bone. J Histotechnology 1994;17:333-341.

Sanderson C, McGee MA, Bloebaum RD. Polypropylene containers for the safe and predictable embedding of specimens in PMMA. J Histotechnology 1990;13:131-133.

Enclosed:

Implant-Bone Histology Reports

File Sheep FIG 8103.FIG
Disk:S:\research\Implant Analysis Lab\Figreportprotocol.doc &

MAM/C:/MYDOC/MARG/WEAR/IALAB\MAM\31.5.00

IMPLANT ANALYSIS LABORATORY

Dept. Orthopaedics & Trauma
Royal Adelaide Hospital &
Uni of Adelaide, Adelaide SA
5000
Ph. (61) 08 8222 5078
Fax. (61) 08-8232 3065

IMPLANT-BONE HISTOLOGY REPORT

1. SPECIMEN DETAILS

Study: Sheep femoral impaction grafting - allograft Vs bioglass
Specimen id: FIG 22
Specimen type: 50:50 bioglass:allograft – implanted femur and contralateral femur
Surgeon: D Dunlop
Report to: D Dunlop
Princess Margaret Rose Hospital
Edinburgh

2. RADIOGRAPH OF EXCISED IMPLANTED FEMUR

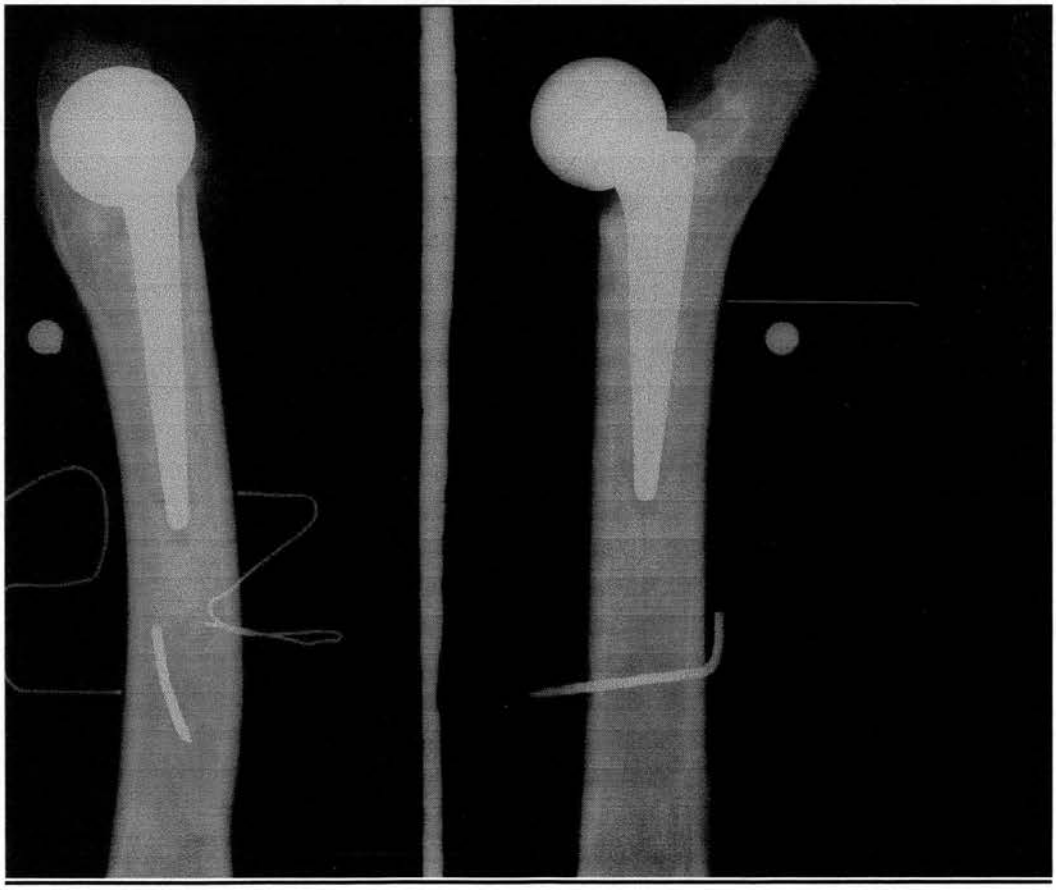

3. PHOTOGRAPH OF EXCISED IMPLANTED FEMUR

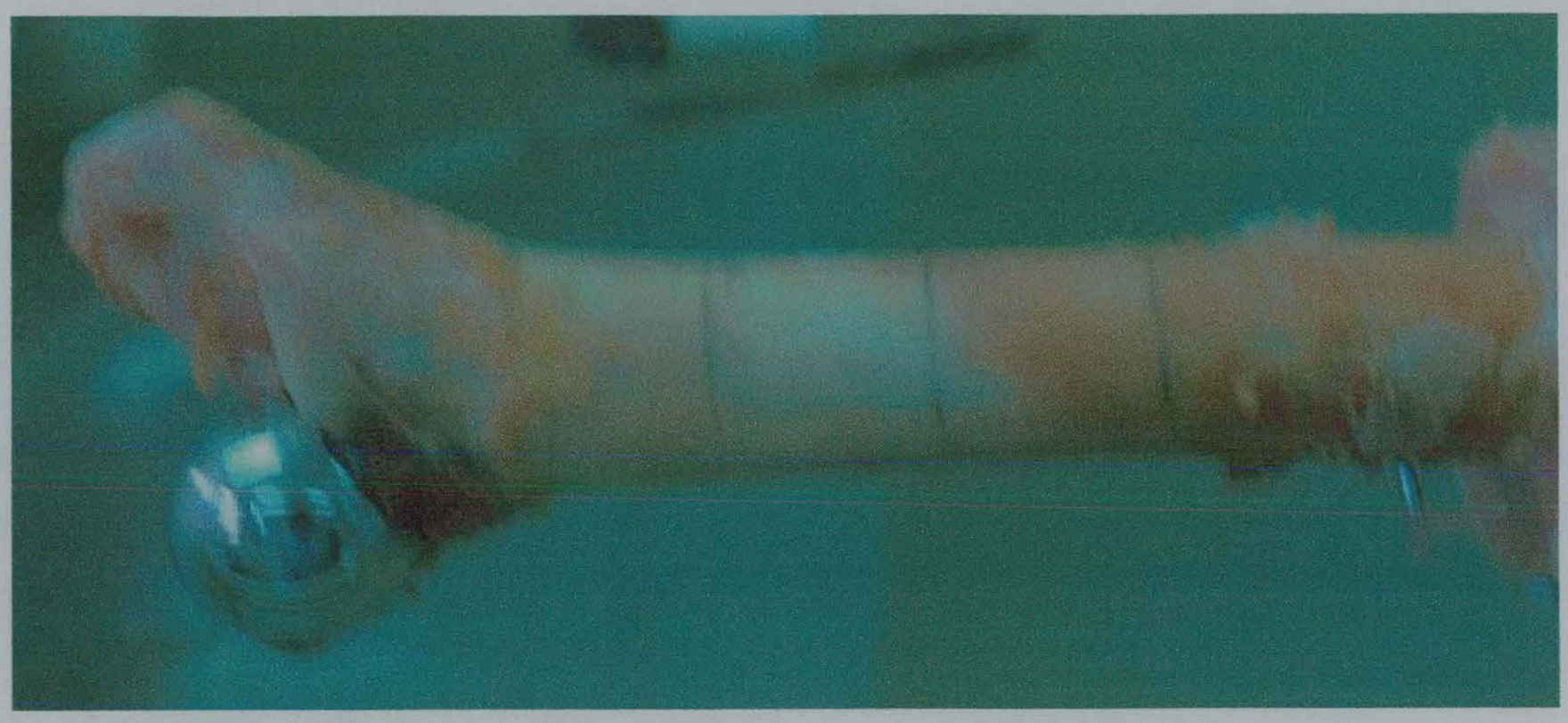

4. PHOTOGRAPH OF BISECTED FEMORAL HEAD AND PROXIMAL FEMUR AND STEM WITHIN CEMENT SUBSIDENCE MEASUREMENT

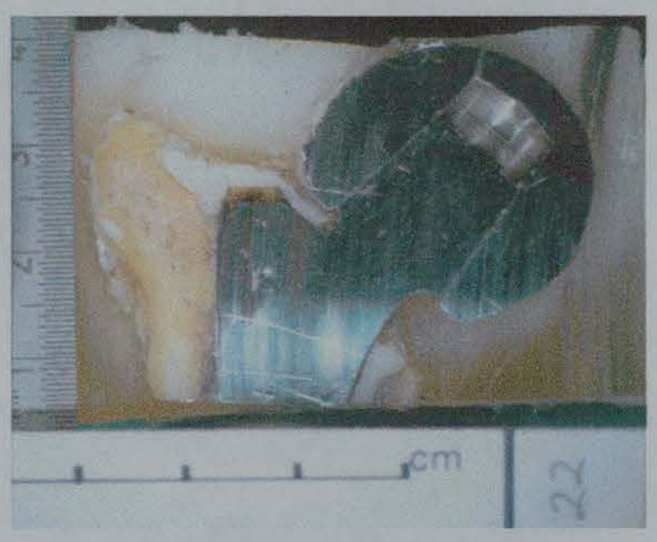

UNSTAINED

STAINED

UNSTAINED

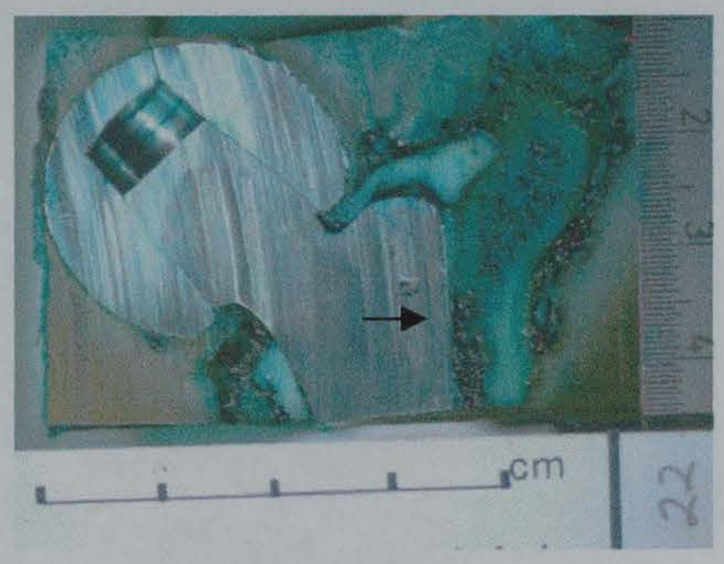

STAINED

Note: absence of lateral cement mantle at site indicated by arrow

Stem within cement subsidence

Stem subsidence = 1.78mm

5. PHOTOGRAPHS OF THICK SECTIONS OF EXCISED FEMURS

Note: Stem loose within cement mantle at the time of sectioning and fell out of thick sections. Because the loose stem was moving during sectioning and creating metal debris,it was removed after the level B sections.

IMPLANTED FEMUR

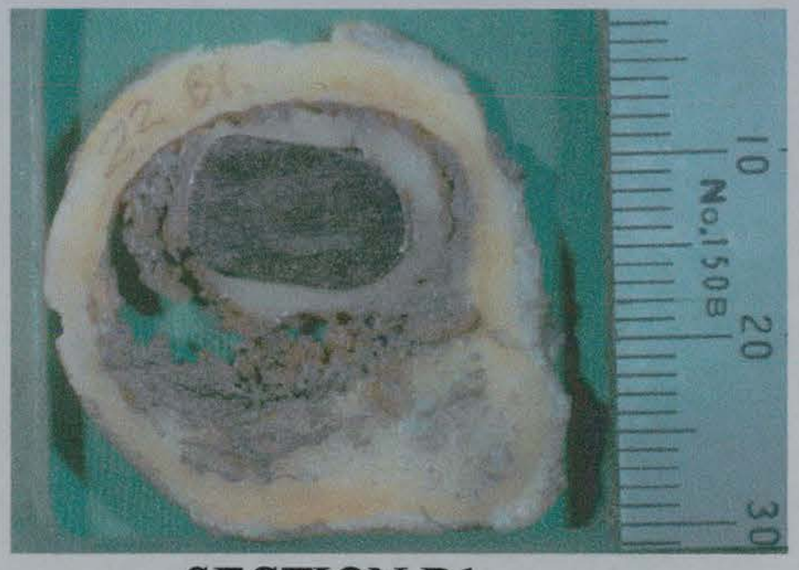

SECTION B1

Note: At level B, the cement mantle interface tissue was very fragmented and friable and much of the tissue fell out either during sectioning or during processing.

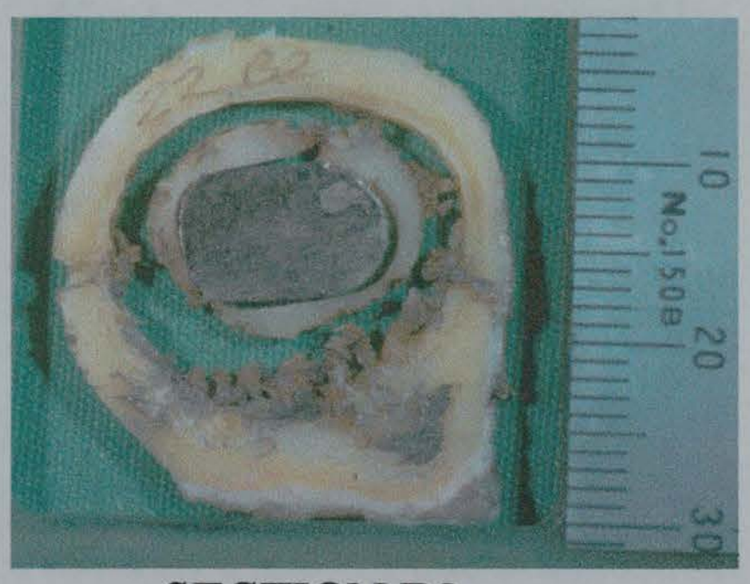

SECTION B2

Not done as graft fragile to touch

SECTION B2 STAINED

SECTION B3

SECTION B3 STAINED

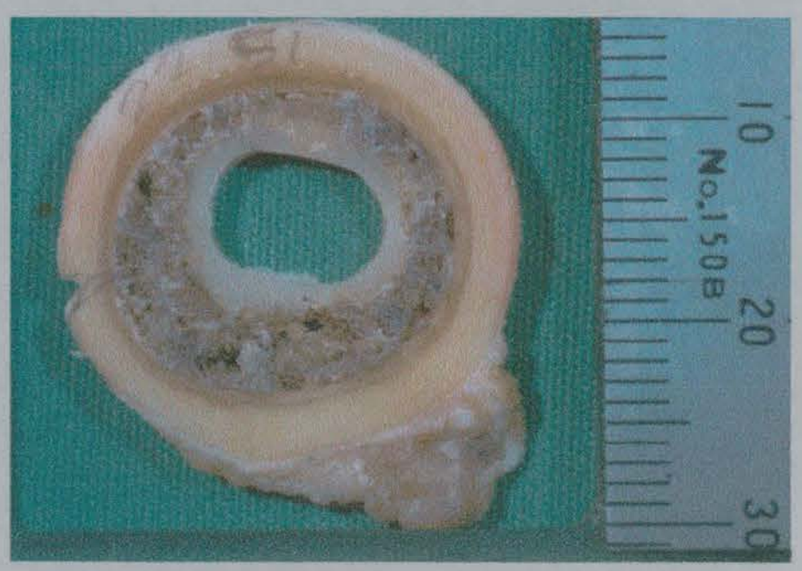

SECTION C1

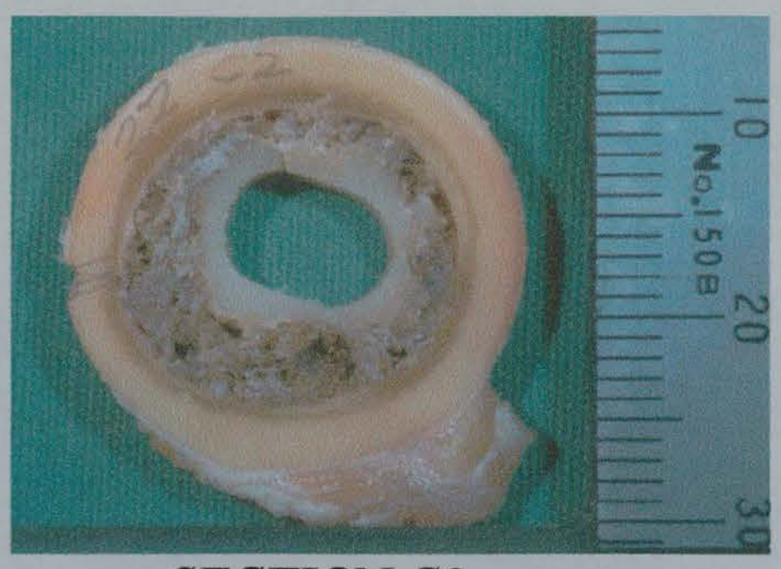

SECTION C2

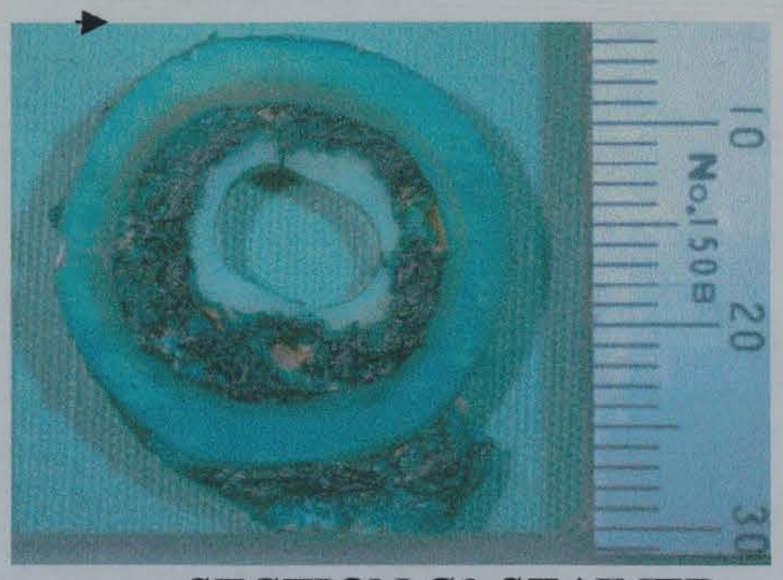

SECTION C2 STAINED

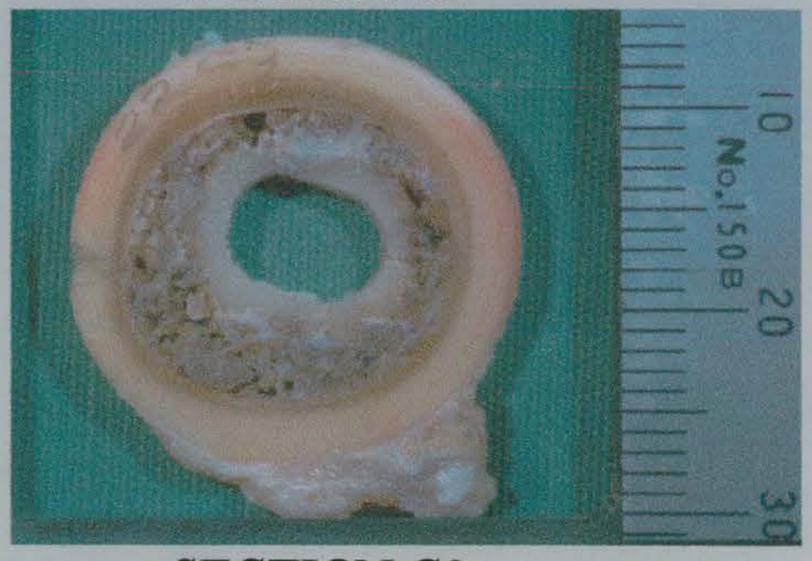

SECTION C3

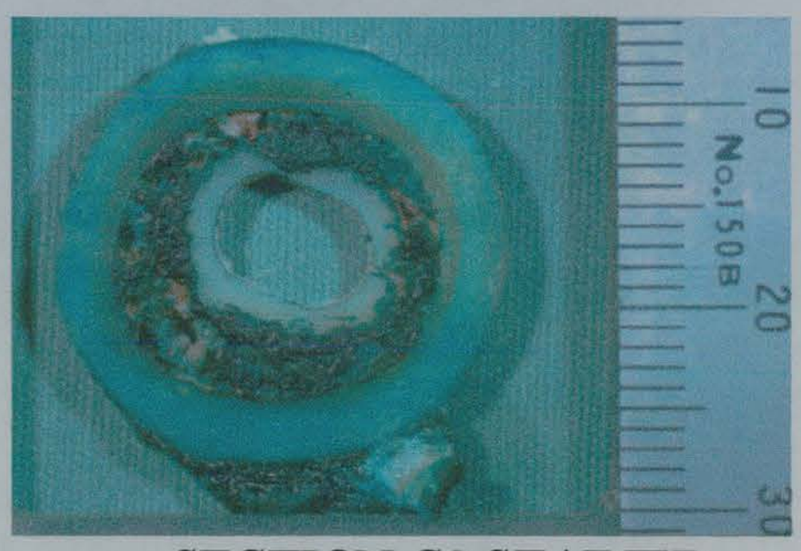

SECTION C3 STAINED

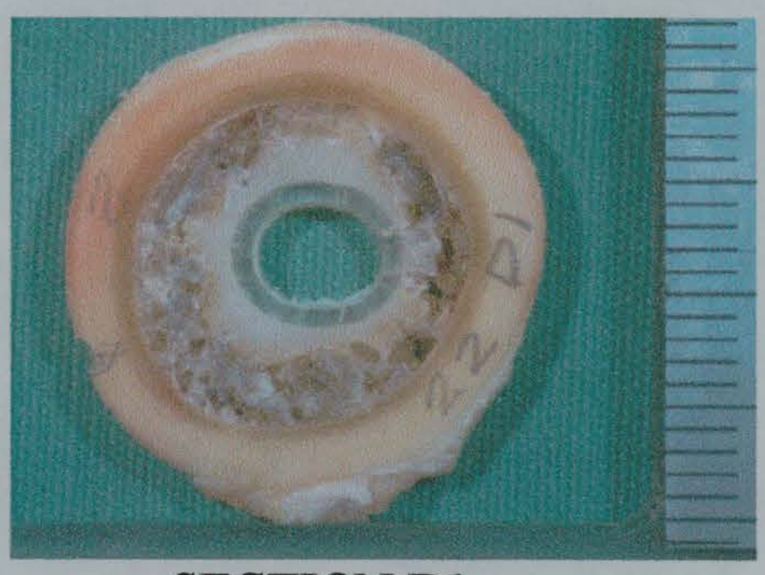

SECTION D1

SECTION D2

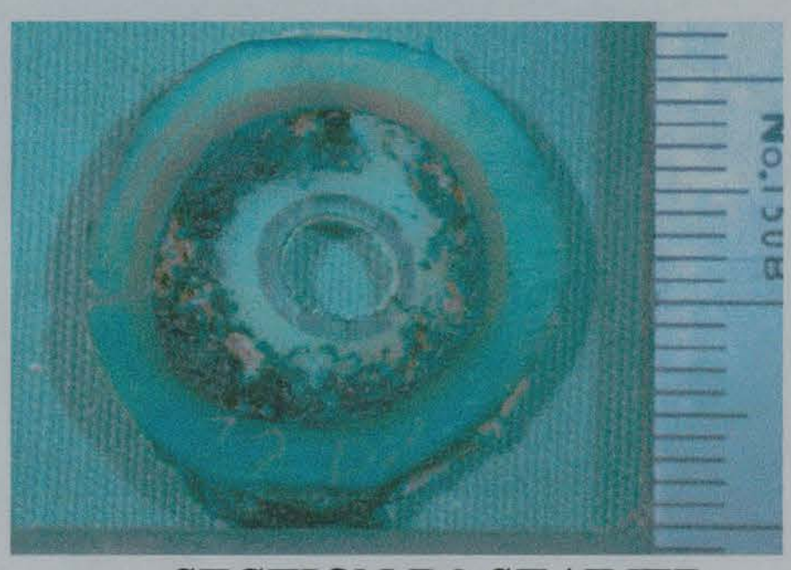

SECTION D2 STAINED

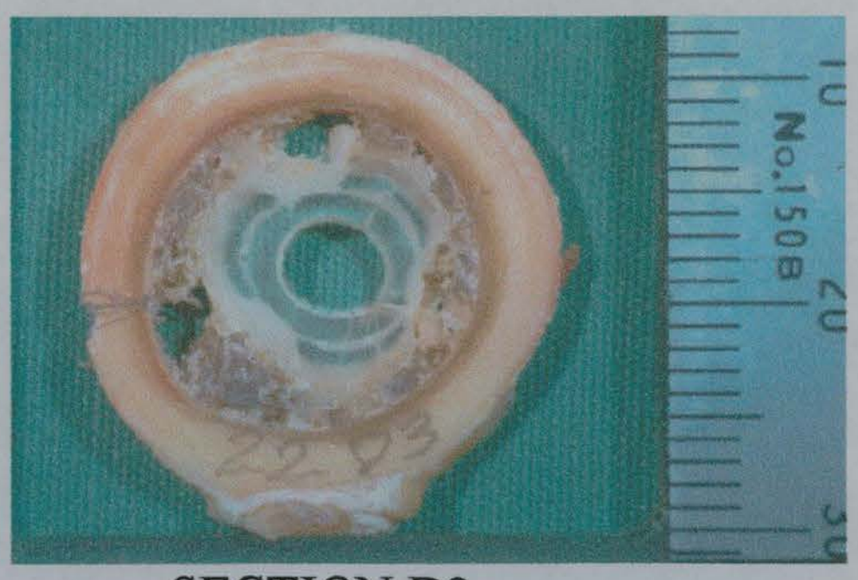

SECTION D3

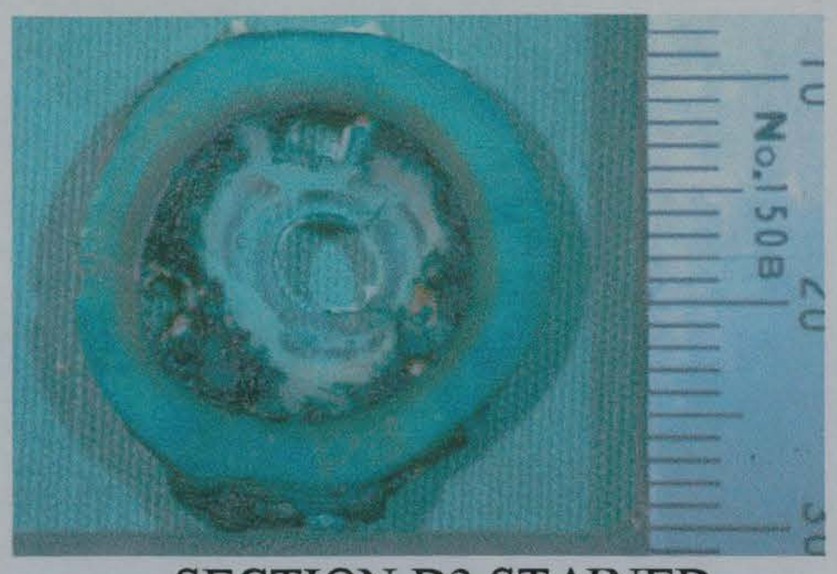

SECTION D3 STAINED

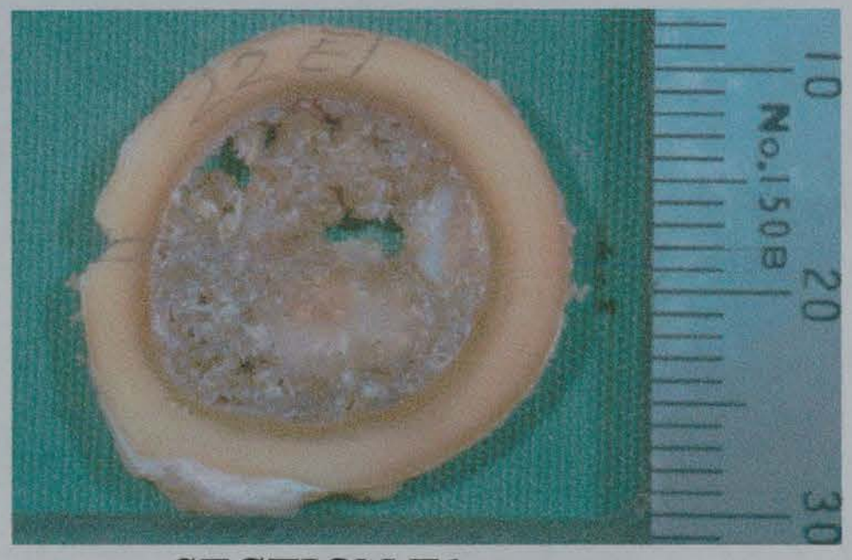

SECTION E1

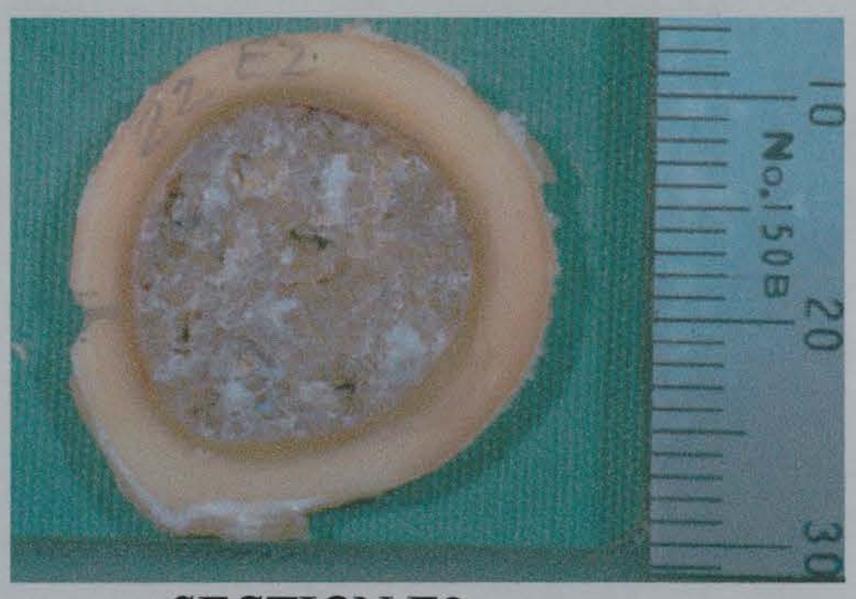

SECTION E2

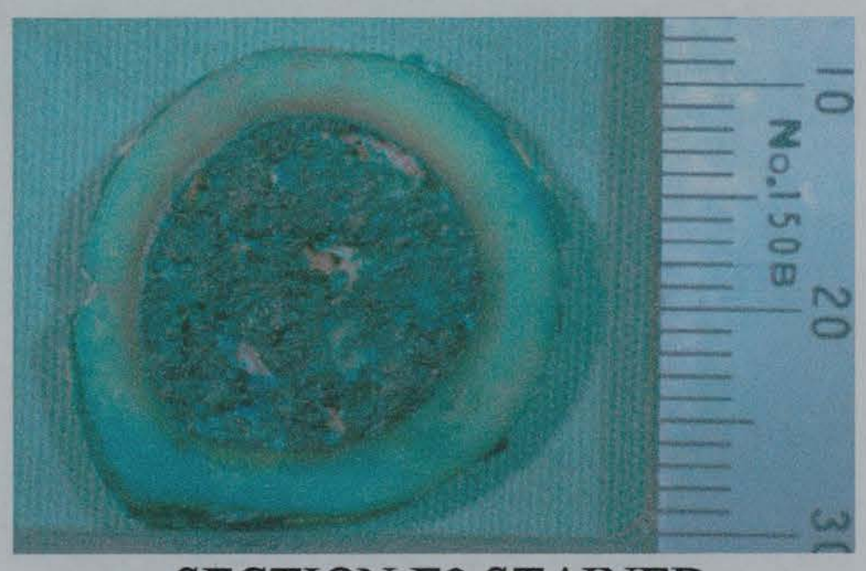

SECTION E2 STAINED

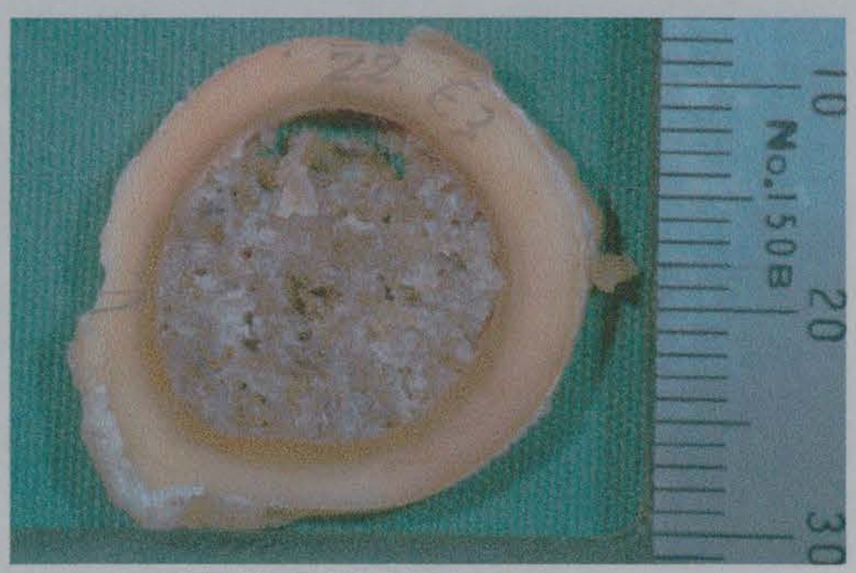

SECTION E3

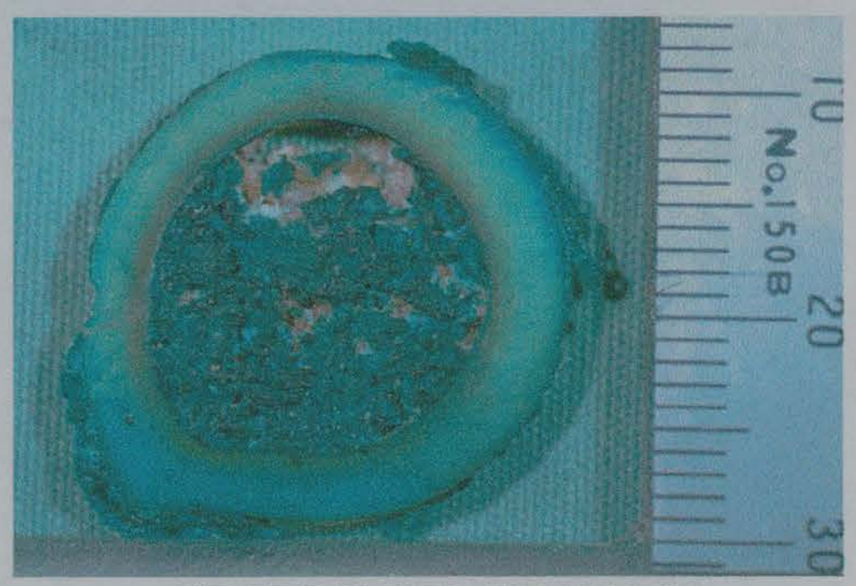

SECTION E3 STAINED

6. MICRORADIOGRAPH OF EXCISED FEMUR THICK SECTIONS

IMPLANTED FEMUR

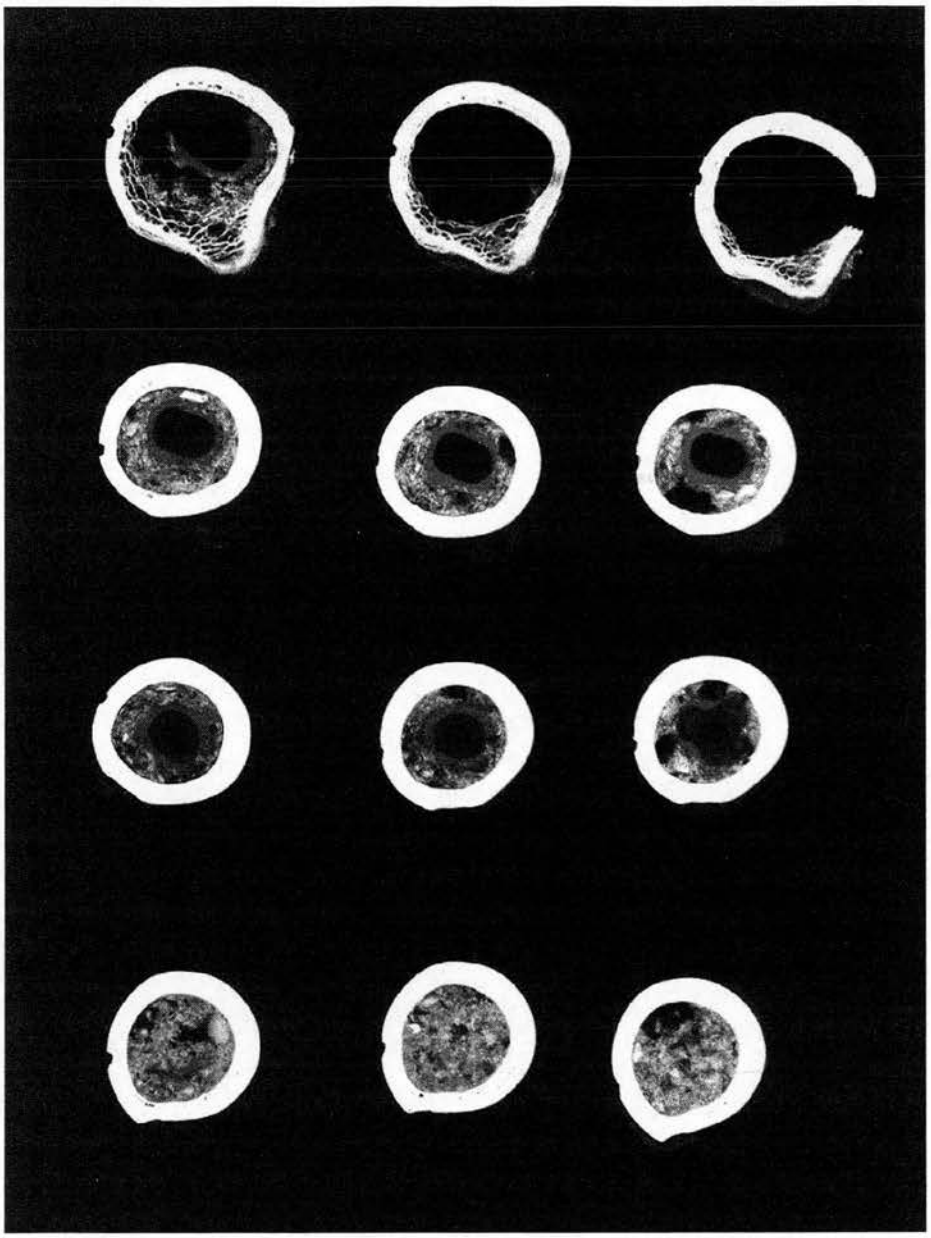

B1	B2	B3
C1	C2	C3
D1	D2	D3
E1	E2	E3

There is increased porosis of the cortical bone in the level B sections when compared to the equivalent sections of the contralateral femur. The porosis is most prominent in quadrant 1 (postero-lateral).

8. ANALYSIS OF FLUOROCHROME LABELS

Results

Level #	Quad-rant	Periosteal-cortex		Cortex		Trabeculae		Graft	
		Grade*	µm**	Grade	µm	Grade	µm	Grade	µm
B	**1**	++		+		n/a		+	Nb. Min graft retained after sectioning
	2	++		++		n/a		-	
	3	-		++		+++	0,21	+	
	4	++		+		++		+	
C	**1**	-		-		n/a		-	
	2	-		+		n/a		-	
	3	-		-		n/a		-	
	4	-		-		n/a		-	
D	**1**	-		-		n/a		-	
	2	-		+		n/a		-	
	3	+		+		n/a		-	
	4	-		+		n/a		-	
E	**1**	-		-		n/a		-	
	2	+		-		n/a		-	
	3	++		+		n/a		-	
	4	+		++		n/a		-	

\# Level B - proximal femoral stem, Level C – mid femoral stem,
Level D – distal femoral stem or centraliser, Level E – distal to tip of stem

* Grade = semi-quantitative grading system of amount of fluorochrome label present

** = µm bone apposition between 1st (4 week) and 2nd (8 week)label, and 2nd (8 week) and 3rd (10 week) label

There is some remodelling activity in the cortex at each level and this is localised to the mid to endosteal region of the cortex.

Only minimal bone formation activity was found in the graft material retained in the level B section. No labels were identified in the graft in sections taken at levels C,D and E.

The only significant bone apposition activity, occurring between 8 and 10 weeks, was in the trabecular bone in the proximal femur (level B).

8. SELECTED FLUOROCHROME IMAGES

Colours assigned to the fluorochrome labels by the Confocal Assistant program

xylenol orange: red
calcein: yellow
oxytetracyline: blue

Note:
At most sites there is almost co-localisation of the first two labels (red and yellow).
The results indicate that oxytetracyline has bound to the first fluorochrome in-situ as the oxytetracycline label consistently mimics the xylenol orange label.

Trabeculae, level B, quadrant 3

Trabeculae, level B, quadrant 3

File Sheep FIG 8103.FIG
Disk:S:\research\Implant Analysis Lab\Fig22rep2.doc &
mam/C:/mydoc/marg/wear/ialab\mam\17.5.00

9. LIGHT MICROSCOPY REPORT

Level B – proximal stem

At the time of section preparation, the stem-cement composite was only loosely fixed within the area which was originally bone graft. The stem and a large proportion of the bone graft fell out of the bone during sectioning on the band saw. The bone graft close to the cement mantle had been replaced by a whitish coloured soft tissue.

There has been minimal activity of the endocortex including the endocortical surface abutting the bone graft (slide 22b1-1-40x). In quadrant 2 there is increased porosity of the cortex (slide 22b2-2-40x) through remodelling. Osteoclastic resorption of the periosteal surface in quadrant 2 (slide 22b2-3-100x) and the endosteal surface in quadrant 1 (slide 22b1-4-100x) is noted.

There is osteoid present on some of the trabecular bone surfaces suggesting remodelling activity but this is most often seen in the greater trochanter region in quadrant 3 (slide 22b3-5-40x).

Some graft has remained in the section, peripherally near the cortex in quadrant 2 and in the trabecular region of quadrants 3 and 4. The graft is embedded in a connective tissue which stains brown on these Spurrs embedded ground sections (slides 22b2-6-100x, 22b3-7-40x, 22b4-8-100x, 22b4-9-200x). Some black discolouration of this connective tissue has occurred during sectioning of the femur and metal stem.

There has been no osteoclastic resorption of the dead bone graft but some edges are diffuse where they have taken up stain.

Some bioglass particles are also noted within the graft composite (slide 22b3-10-200x).

Level C - mid femoral stem

The stem is absent from this section as it was removed prior to sectioning. The cement mantle and graft are however retained (slide 22c-11-40x). Fractured bioglass particles are identified within the graft (slide 22c-12-100x). New bone forming on the endosteal cortex is seen in quadrant 1 (slide 22c1-13-100x).

Level D – distal femoral stem or centraliser

The centraliser is present in this section. The cement mantle is intact and extends to the endosteal surface of the cortex in quadrants 2 and 3 (slide 22d3-14-40x).

There is no activity on either the endosteal or periosteal cortical bone surfaces. Furthermore there is little remodelling in the haversion systems of the cortical bone (slide 22d-15-40x).

There are gaps in the graft, which are lined by connective tissue and probably represent bioglass or bone particles that has fallen out during section preparation (slide 22d-16-100x).

In other regions, the bioglass particles are present within the graft (slides 22d-17-200x, 22d-18-200x). The bioglass demonstrates refractile properties under polarised light when it has fractured (slides 22d-19-100x, 22d-20-100x polarised light). There is no evidence of graft incorporation.

Level E – distal to femoral stem

The canal of the femur contains cement and graft. There is some limited cortical remodelling in quadrants 2, 3 and 4 with associated increased porosity.

Histological features of graft as described for level D. There is no evidence of graft incorporation with bone and bioglass resident within a loose tissue matrix (slides 22e-21-40x, 22e-22-100x, 22e-23-100x,22e-24-100x).

Summary of light microscopy findings

⇒ Unstable bone graft, cement and stem proximally.
⇒ Replacement of original bone graft closest to cement mantle in proximal femur by soft tissue.
⇒ No evidence of bone graft incorporation at each level of the femur. (No resorption or bone formation activity).
⇒ Bioglass particles still present in graft at each level of femur.
⇒ Bioglass particles commonly have fractures and these particles are refractile under polarised light.
⇒ No evidence of graft collapse

10. LIGHT PHOTOMICROGRAPHS
Undecalcified ground sections, toluidine blue stain

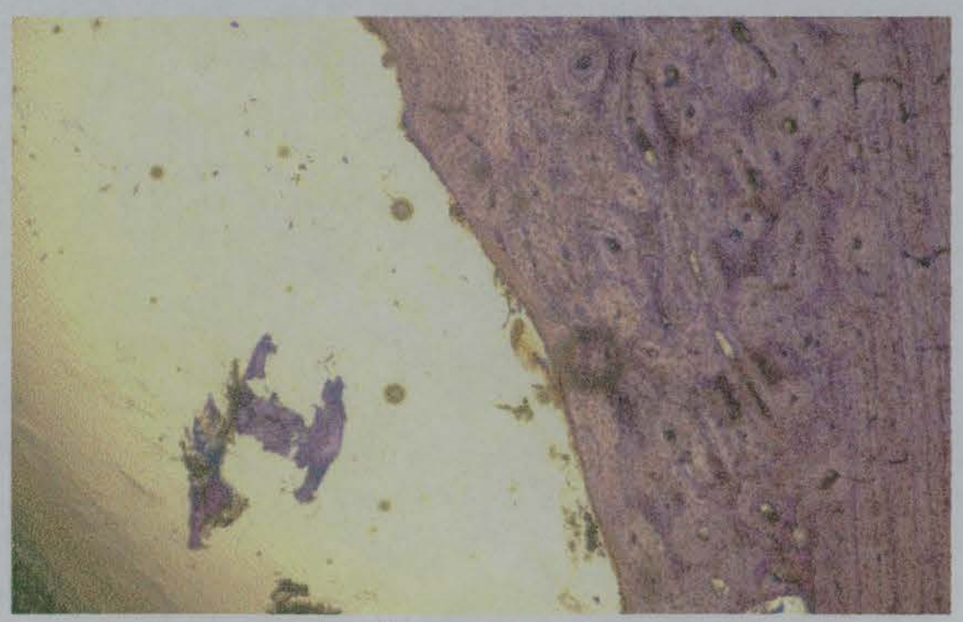

22b1-1-40x

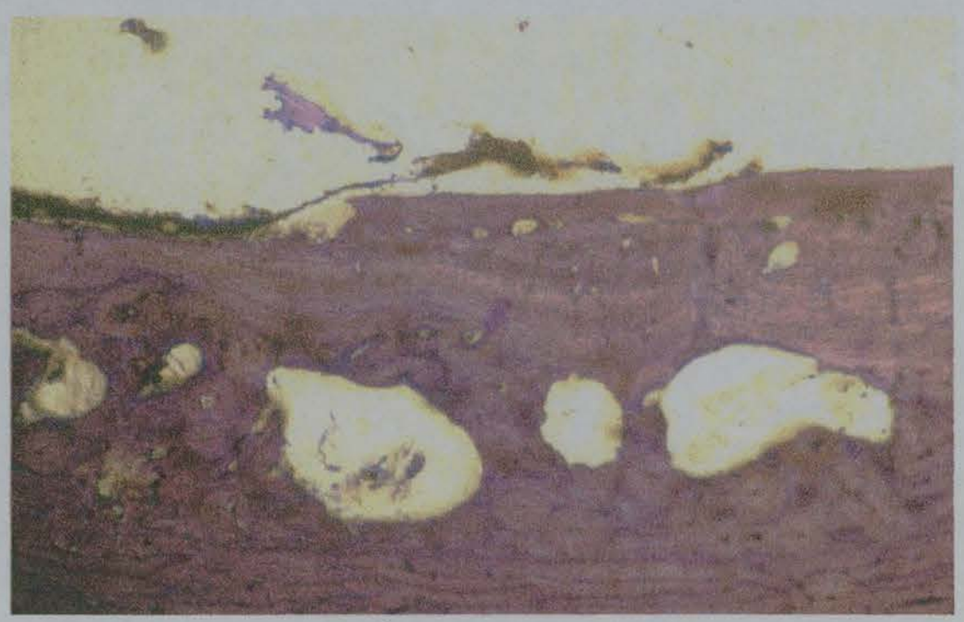

22b2-2-40x

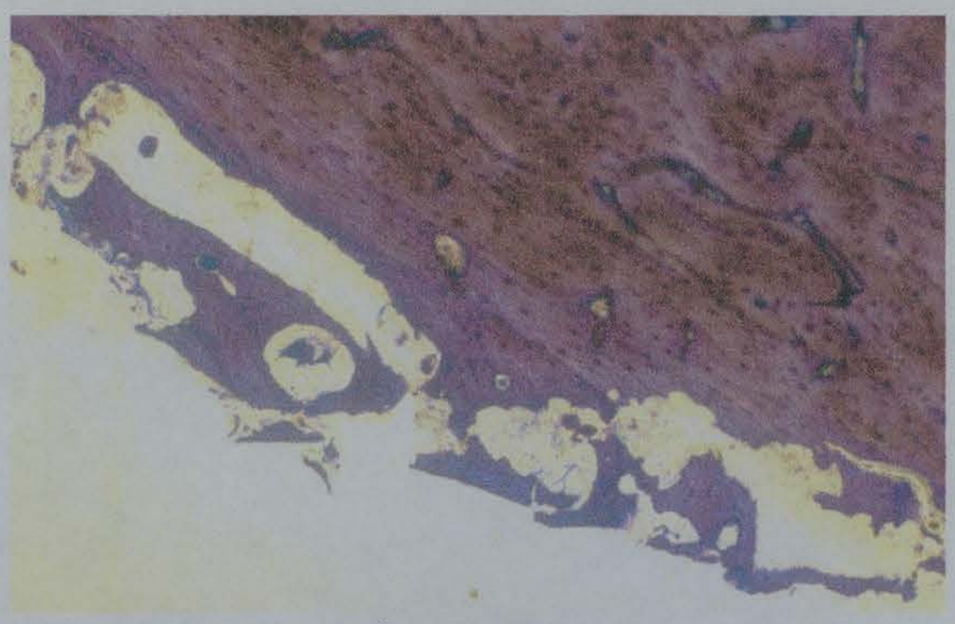

22b2-3-100x

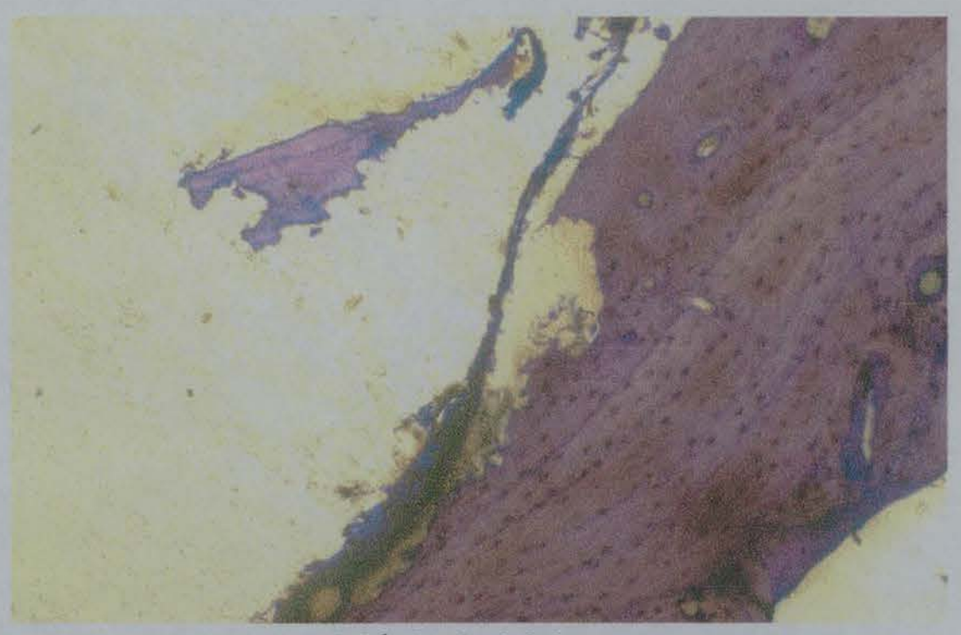

22b1-4-100x

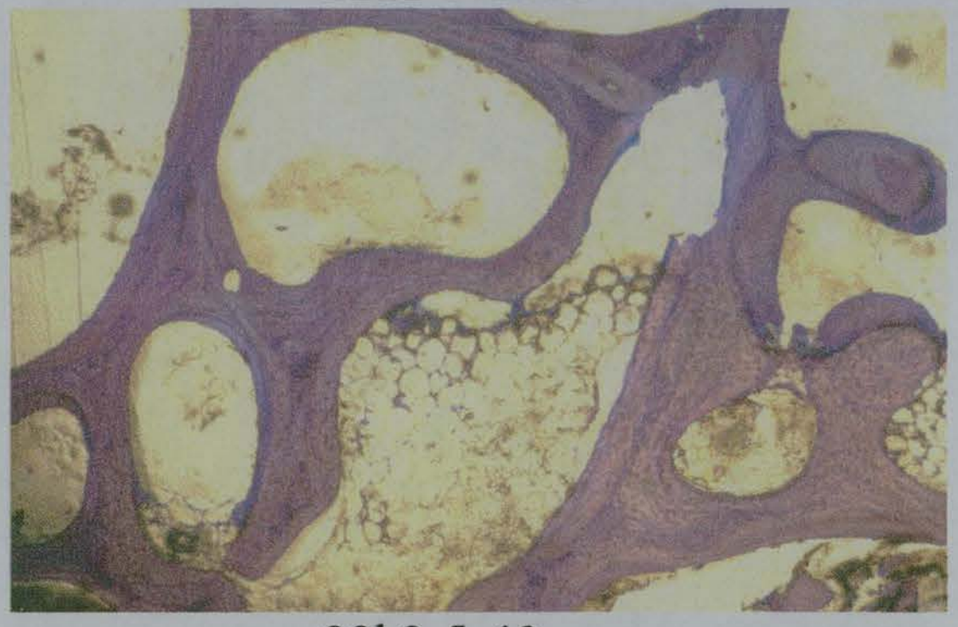

22b3-5-40x

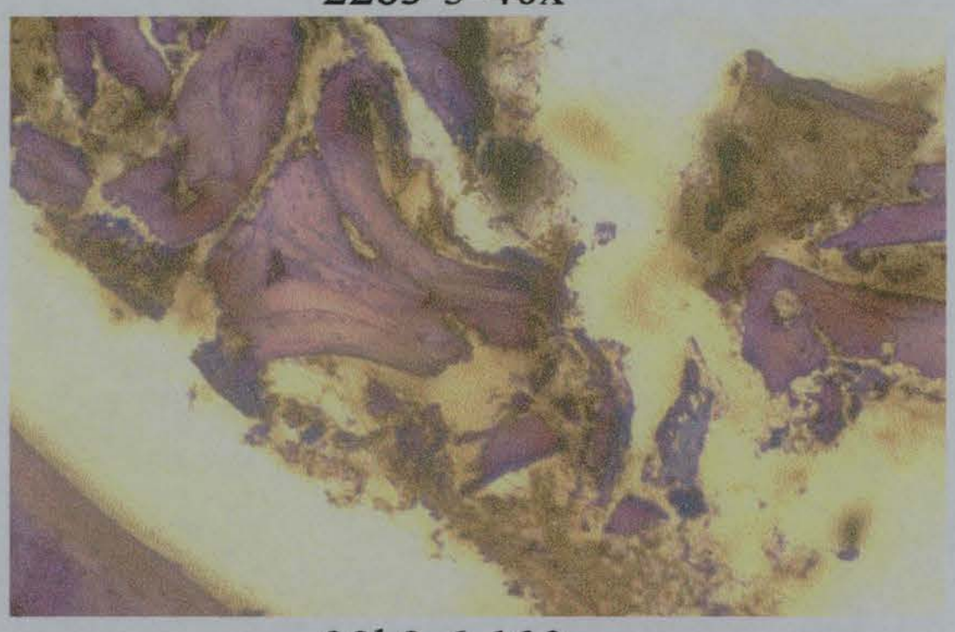

22b2-6-100x

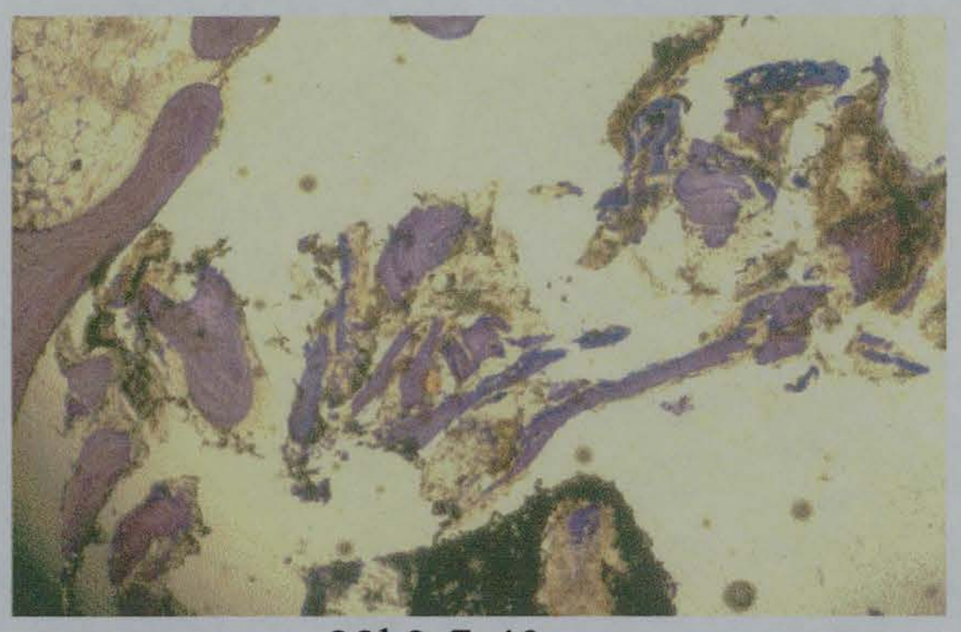

22b3-7-40x

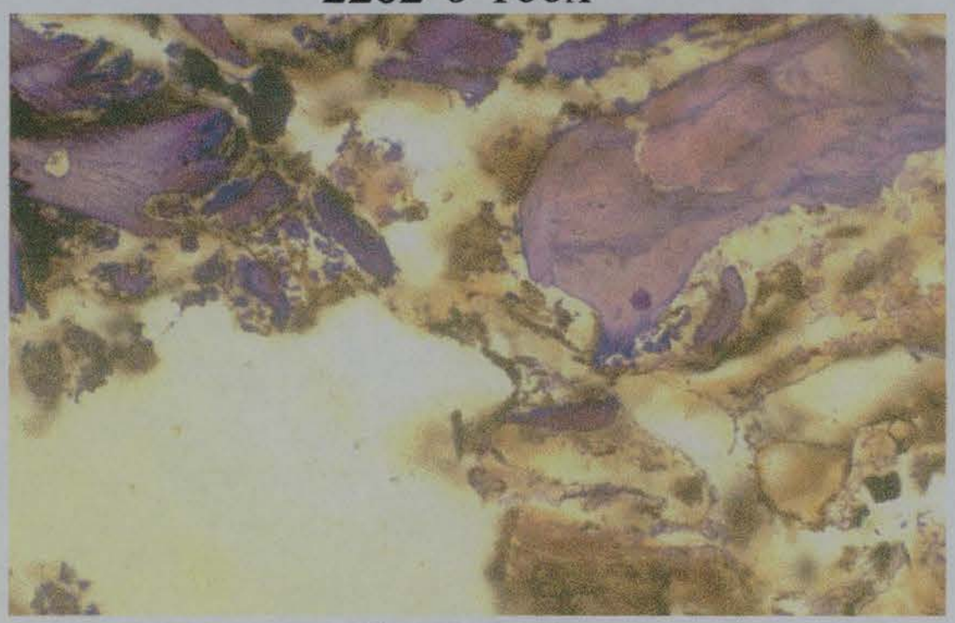

22b4-8-100x

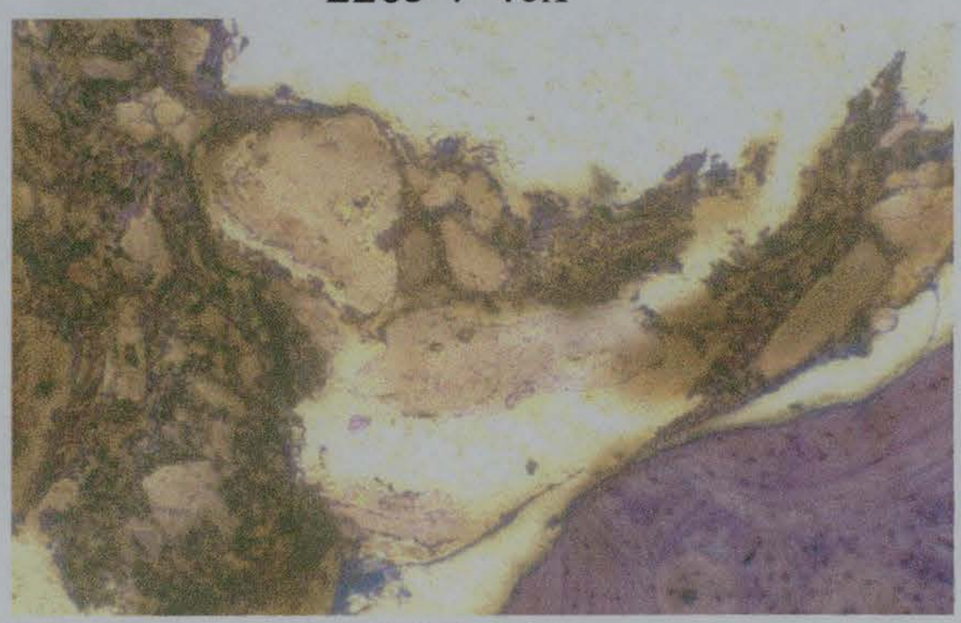

22b4-9-200x

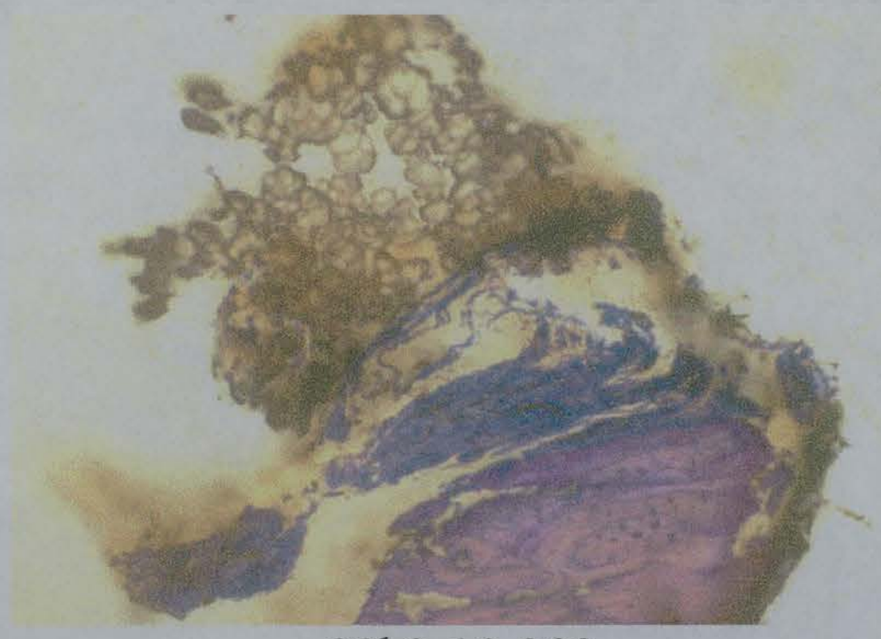

22b3-10-200x

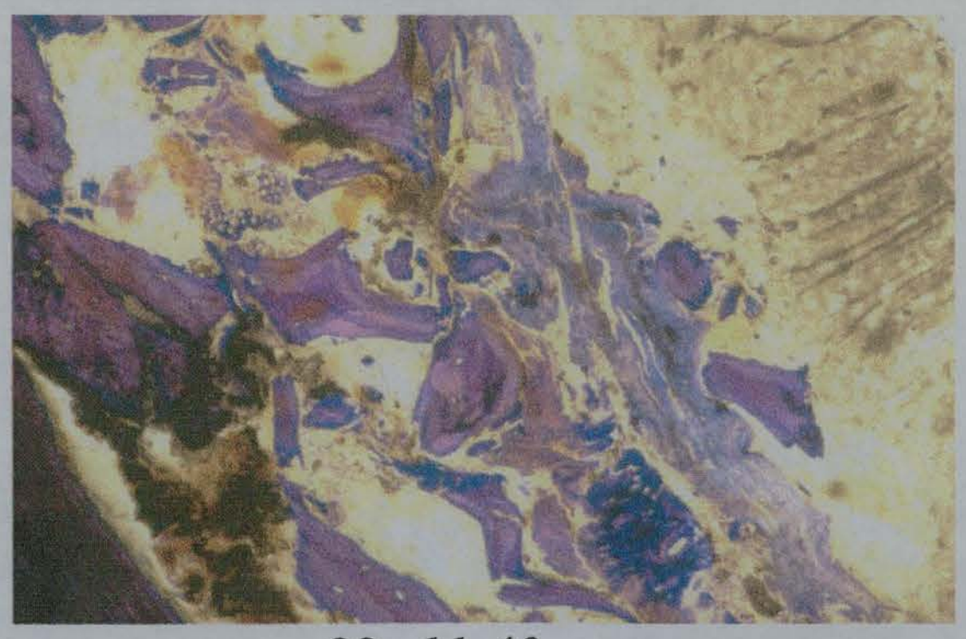

22c-11-40x

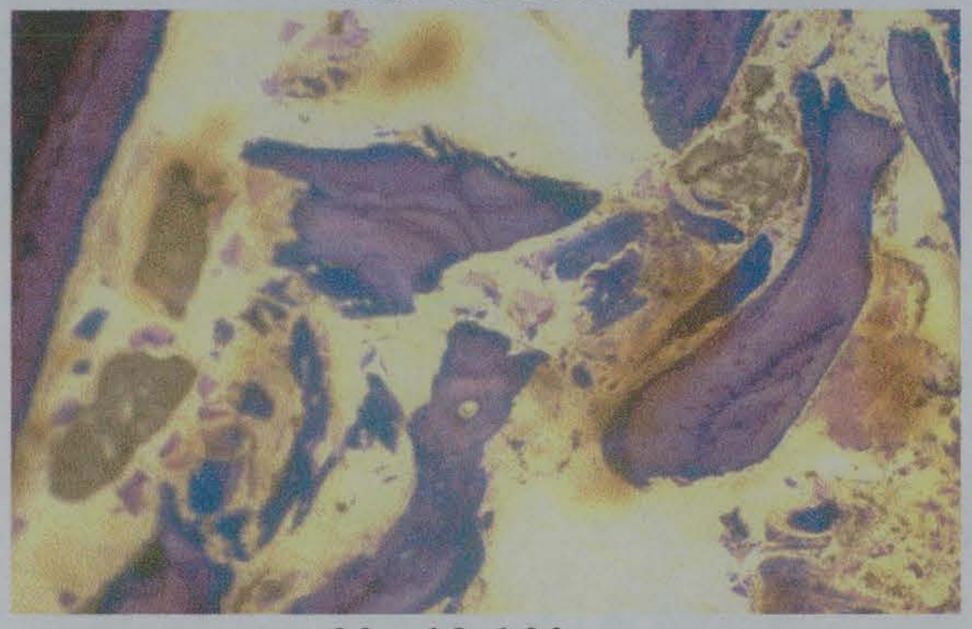

22c-12-100x

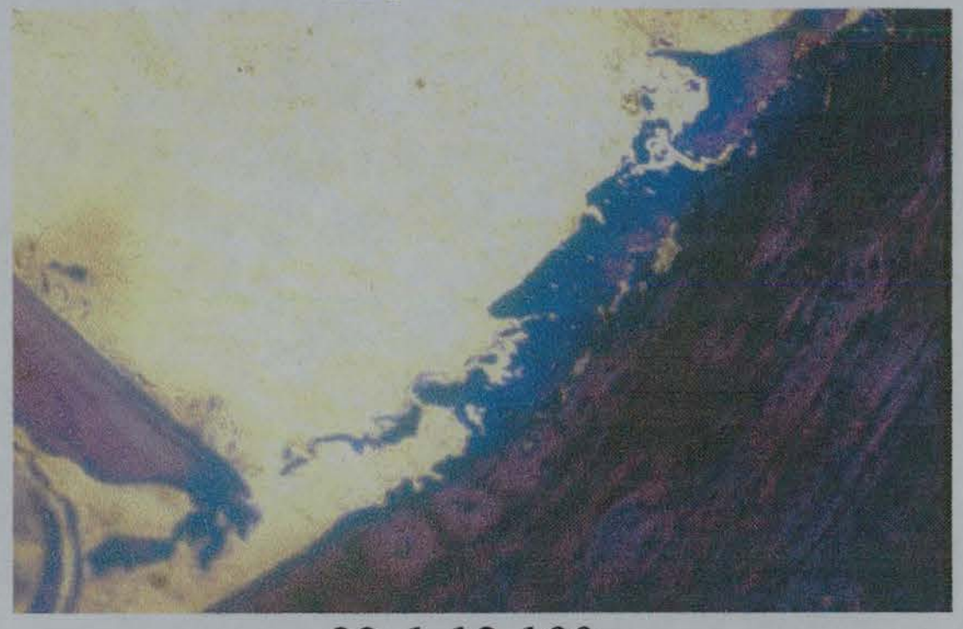

22c1-13-100x

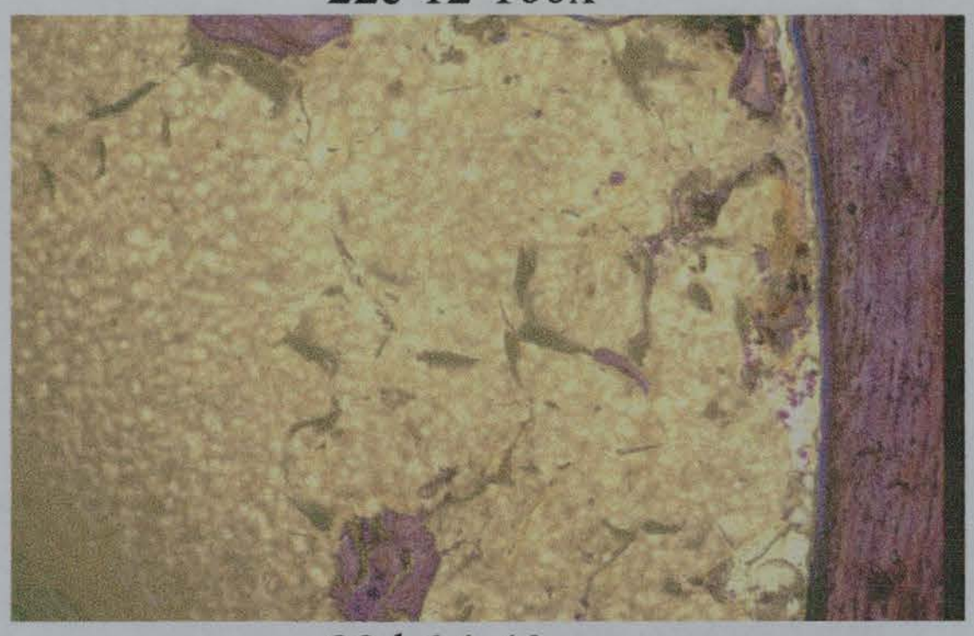

22d-14-40x

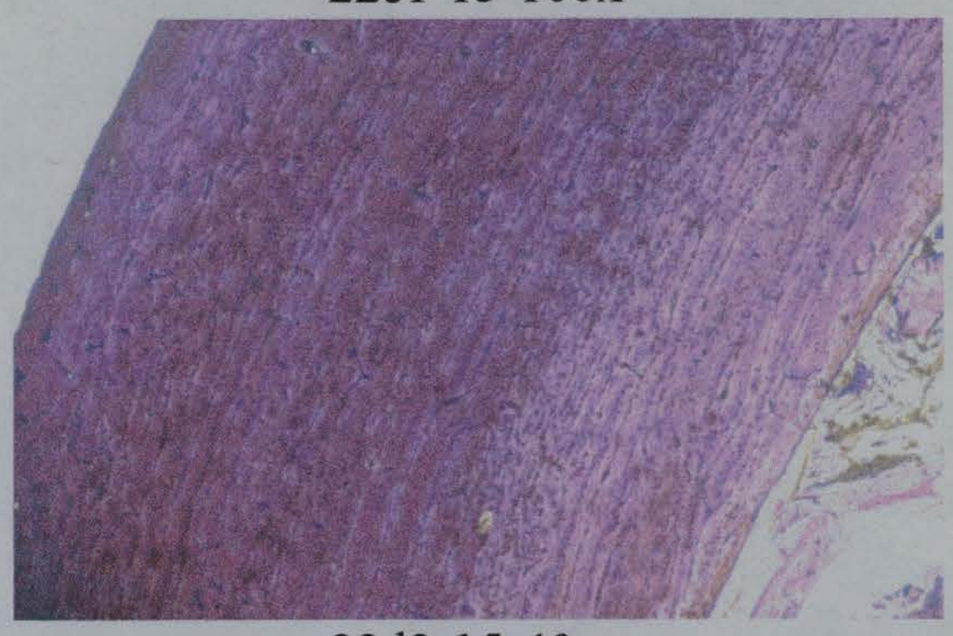

22d3-15-40x

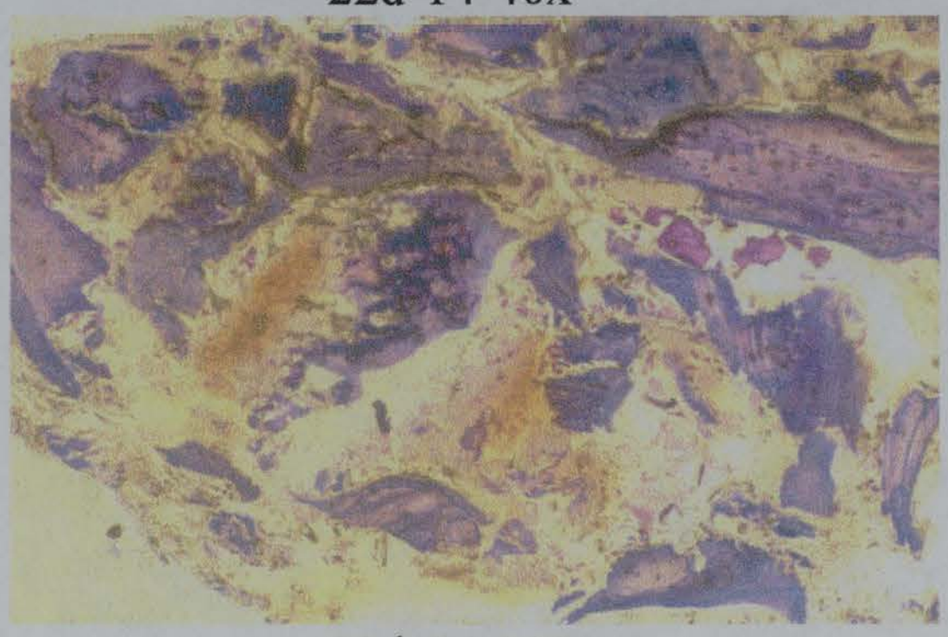

22d-16-100x

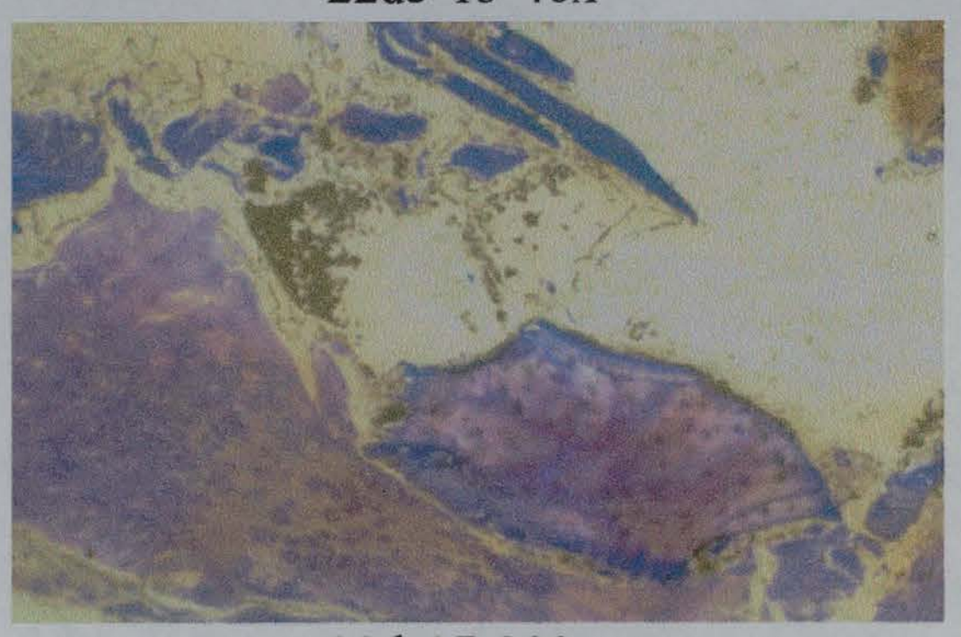

22d-17-200x

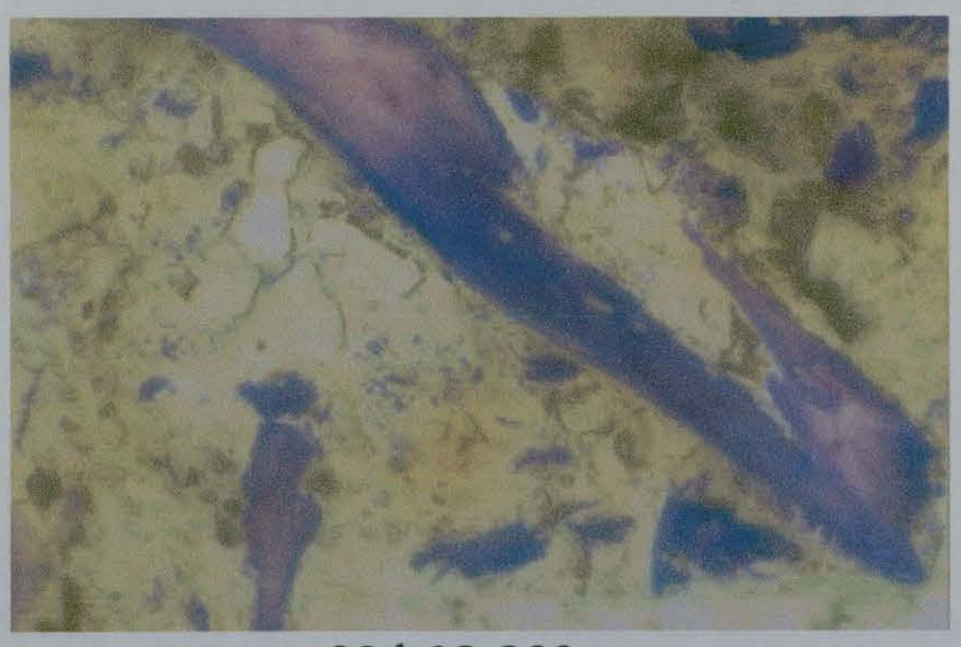

22d-18-200x

22d-19-100x polarised

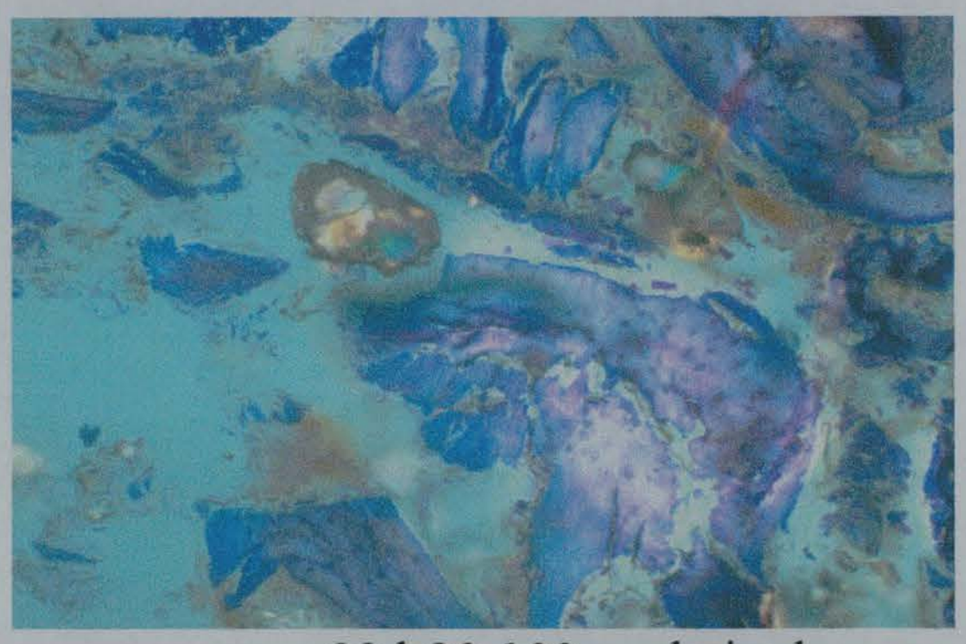

22d-20-100x polarised

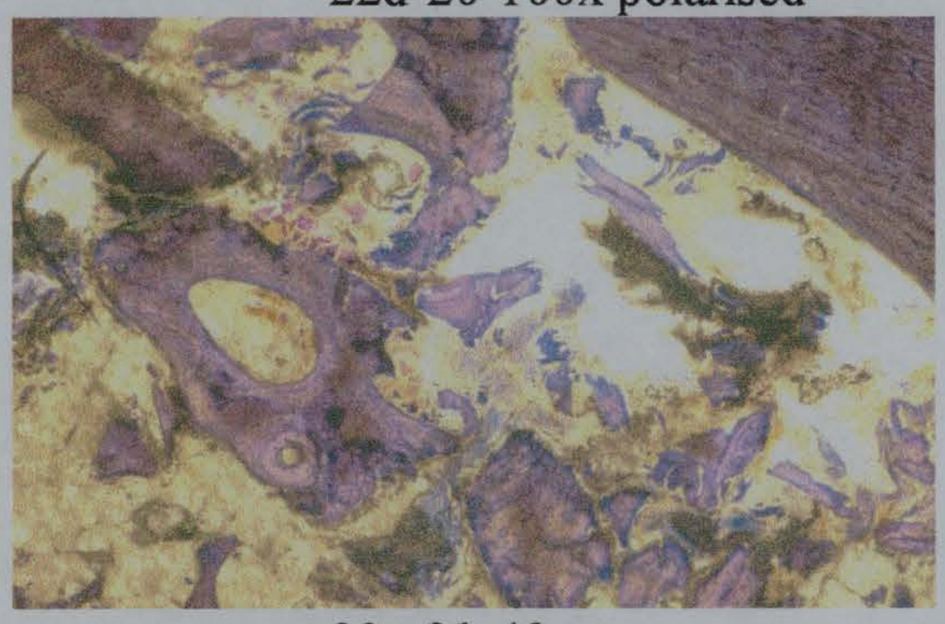

22e-21-40x

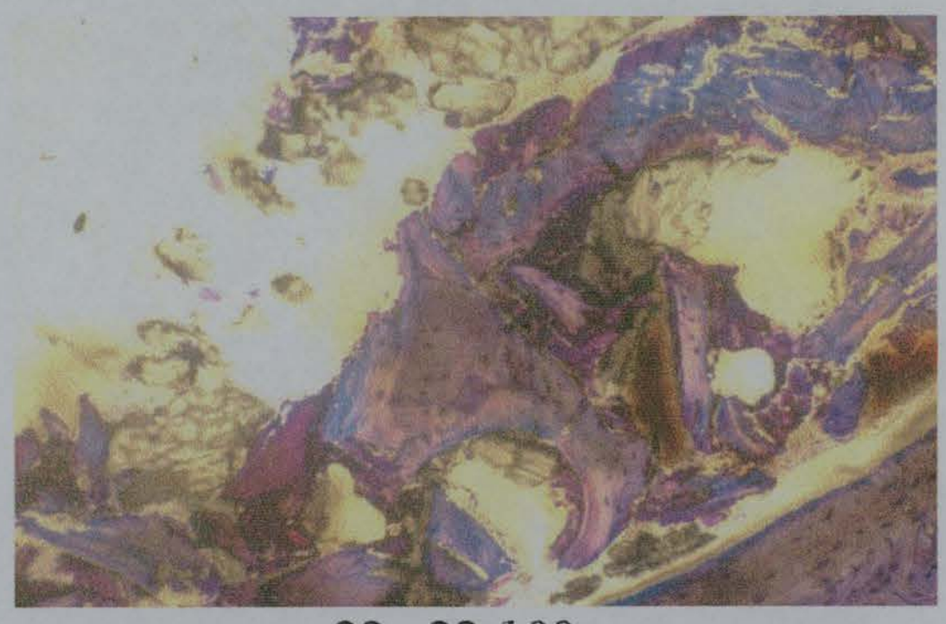

22e-22-100x

22e-23-100x

22e-24-100x

MECHANICAL ASPECTS OF IMPACTION GRAFTING IN THR – THE EFFECT OF PARTICLE SIZE DISTRIBUTION, ADDITIVES AND WASHING

DG Dunlop, CR Howie, Pankaj, SPG Madabhushi, AS Usmani
From the University of Edinburgh and Princess Maragret Rose Orthopaedic Hospital, Edinburgh, Scotland.

ıtroduction

ear strength (τ_f) of an aggregate such as milled bone graft, is a measure of the ability to ;tain stresses without failure. It is a function of internal friction (ϕ) and cohesion (c) of the ·ticles, under a given normal stress (σ). The angle of internal friction is determined by the ·ding (particle size distribution) of the sample and to a lesser extent on the particle shape. well-graded sample has greater internal friction. The addition of a fluid, especially a lubricant d such as fat, will reduce the frictional resistance of an aggregate by lubricating the contacting rfaces between particles. The relationship between all of these is given by the)hr Coulomb[1,2] equation:

$$\tau_f = c + \sigma \tan\phi$$

▸aterials and Methods

rty fresh frozen Human femoral heads were thawed and milled in the standard fashion ·ough two different bone mills (Fig 1.).

▸eving

e particle size distribution curve for each mill was determined[3].

▸echanical Shear Testing

pacted samples in a modified Shear tester (Fig 2.) were used as previously described[4], to ıerate shear stress versus shear strain graphs (Fig 3.). The axial normal loads were between l 10Kg to produce a family of curves within normal human physiological loading. The shear ess is determined at 9.5% shear strain and used to generate the shear strength versus rmal stress graphs (Figs 4-6.). The best fit straight line variation between normal stress, σ, d shear strength τ_f represent the Mohr Coulomb failure envelope, from which the friction gle and cohesion can be determined.

▸ashing Technique

ing a Pulse Lavage Gun, warmed 0.9% saline was washed over the graft in a 300-micron ve, until the graft appeared clear of macroscopically obvious fat and marrow tissue (Fig 7.).

▸dditives

bioactive glass (BG) and a tricalcium phosphate / hydroxyapatite mixture (TCPHA) were ·estigated. These compounds were either used as a well graded 50/50 mixture with the ıft or to improve the grading of the graft (idealise) by replacing the missing particle sizes.

▸esults

Mill A produced a particle size distribution that was nearer to the ideal than Mill B (Fig 8.).

Mill A produced graft that was significantly more resistant to shear than Mill B (Fig 4.).

Washing significantly increases the shear resistance of bone graft from both mills (Fig 5.).

The additives improved the shear resistance of graft from either mill (Fig 6.).

▸onclusions

The particle size distribution and state of hydration of an aggregate such as bone graft determine its mechanical behaviour (e.g. sandcastles).

Washing bone graft enhances graft strength. This is thought to be due to the removal of fat, which appears to lubricate the individual particles.

The addition of synthetic particles of the correct size improves the shear strength. This is because the mechanical properties of any collection of particles is more dependent upon the particle size distribution, than on the individual properties of the particle.

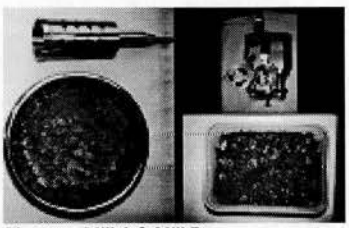

Fig 1. Mill A & Mill B

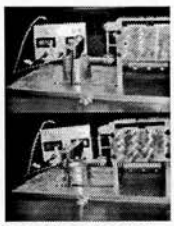

Fig 2. Cam shear tester

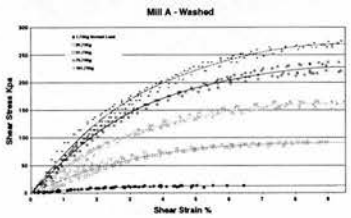

Fig 3. Shear stress V's shear strain graph

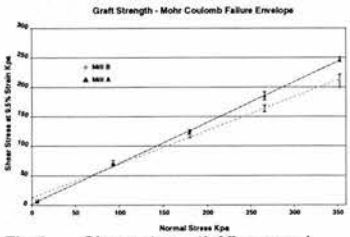

Fig 4. Shear strength V's normal stress graph

Table of Graphical Results

	Cohesion	Angle of Internal Friction
Test Mills		
Mill A	2	35
Mill B	12.5	30
Additives		
Mill A + BG 50/50	6	36
Mill A + TCP/HA 50/50	12	37
Mill B Idealised with BG	12	37.5
Washing		
Mill A washed	17	38
Mill B washed	10.5	34

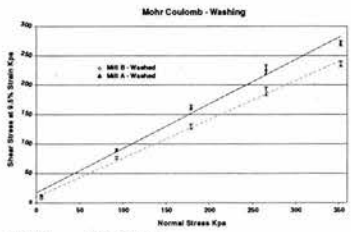

Fig 5. Washing

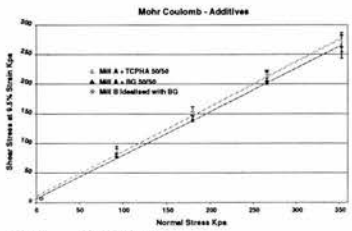

Fig 6. Additives

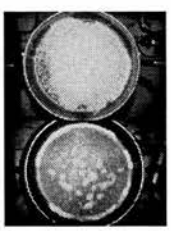

Fig 7. Washed graft in sieve

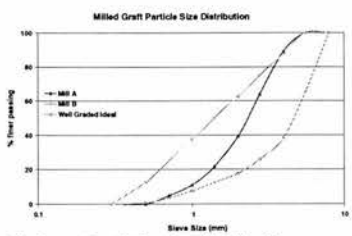

Fig 8. Particle size distribution

ddendum

hether washing fat and marrow tissue from allograft, which is foreign to the host, is an added advantage, ·et to be proven. Certainly the bioburden of immunogenic material will be reduced. There will potentially more inter-particle spaces empty of dead foreign tissue available for faster invasion by host angioneogenesis. rrently the practice of pre-washing the graft before impaction is being undertaken at our centre and will reported in due course.

References

1. GN Smith. *Elements of Soil Mechanics*. 6th Edition. Blackwell Science. ISBN 0-632-02616-2.
2. Craig RF. *Soil Mechanics*. 5th Edition. London: Chapman and Hall, 1993.
3. British Standard 1377 guidelines.
4. NT Brewster, WJ Gillespie, CR Howie et al. *Mechanical considerations in impaction bone grafting*. J Bone Joint Surg [Br] 1999;81-B:118-24.

.C.O.T.
F.K. Schattauer Publishers, Stuttgart – New York (2000)

Clinical Communication

. G. Dunlop[1], J. R. Field[2]

Ovine hip hemiarthroplasty: reducing dislocation

From the [1]Princess Margaret Rose Orthopedic Hospital, Edinburgh, Scotland and [2]Repatriation General Hospital, Orthopedic Unit, Daw Park, South Australia, Australia

Keywords
Hip hemiarthroplasty, tenorrhaphy, dislocation

Ve present a surgical modifica-
on which can be performed
uring hip hemiarthroplasty, in
ıe ovine model, that may sig-
ificantly reduce the periopera-
ve dislocation rate. A modi-
ed tenorrhaphy technique was
erformed on the tendinous in-
ertion of the accessory gluteal
ıuscle during wound closure
ollowing hemiarthroplasty.
ubsequently only one of six-
een animals (6%) dislocated.
his compares favourably with
ther studies in which signifi-
antly higher rates of disloca-
on have been reported. The
ıacroscopic appearance of the
epair was assessed at the time
f necropsy and found to be
atisfactory.

eceived 99.12.02, Accepted 00.05.04

Introduction

The sheep is becoming an increasingly popular model for studying the biological response to orthopedic interventions and for delineating the cellular response to biomaterials (1-8). Total hip arthroplasty (1, 2) and hemiarthroplasty studies (7, 8) have utilized an ovine model with varying degrees of success. The major complications for animals undergoing these procedures have been postoperative fracturing (1, 2) and dislocation (7, 8).

Of the published approaches to the animal hip there are many described for the canine (9-13) but fewer for the sheep or goat (1, 2, 7, 14). The surgical approaches to the coxofemoral joint of the sheep that have been described include a cranio-lateral or dorso-ventral curvilinear incision centred over, or caudal to, the greater trochanter. Often (1, 7), the incision and reflection of various muscles is performed as a means of gaining adequate exposure of the joint. In some instances, unacceptably high rates of dislocation occur particularly in the hemiarthroplasty model (7, 8). Dislocation is usually the result of either inappropriate selection of the femoral head size (15), femoral prostheses with large neck diameters (16), or a failure to adequately close the soft-tissue space surrounding the prosthetic joint. We propose a surgical modification to a sucessfully utilized surgical approach to the sheep hip (2) as a means of reducing the rate of dislocation (23%) previously encountered at this centre (7). A definitive repair involving 'double-breasting' of the tenotomy and capsular repair, with follow-up in 16 cases, is outlined.

Materials and Methods

Sixteen mature Merino wethers (3 yr. old) underwent hip hemiarthroplasty as part of a randomized trial to evaluate a bone-substitute utilizied in impaction grafting of femoral stems. The surgical approach to the sheep hip and peri-operatice care, described previously for total hip arthroplasty, were utilized (2). The protocol for animal utilization had been approved by the Animal Ethics Committee, University of Adelaide.

The tenotomy of the accessory gluteal tendinous insertion and subsequent capsular repair, were modified as this step was thought to be a contributory factor in the dislocation rate previously reported (7, 8). The modification was conceived with a background knowledge of shoulder stabilization techniques utilized in humans. In the human situation a 'double-breasting' technique is employed to reinforce the anterior capsule of the shoulder joint to reduce anterior subluxation (17).

Surgical procedure

With the animal positioned in lateral recumbency, a curvi-linear incision was made centred over the greater trochanter and which entended cranially toward the tuber coxae (6 cm) and distally along the cranial femur (10 cm). The tissue plane defining the fascia lata and the cranial aspect of the biceps femoris and superficial gluteal muscle was incised. This adequately exposed the vastus lateralis and middle gluteal muscles between which another plane of dissection was created. Gelpi self-retaining retractors enabled retraction of these muscles to expose the tendinous portion of the accessory gluteal muscle as it inserts onto the greater trochanter (Fig. 1). A consistent large vessel supplying the undersurface of the middle gluteal muscle was cauterized.

The transverse tenotomy of the accessory gluteal tendinous insertion was made at a level 3 cm from its insertion on the greater trochanter (Fig. 2). The incision was extended to half the depth of tendon. The superficial fibres on the femoral side were elevated by intratendinous sharp dissection and teased towards the femur, almost to the insertion, thus creating a tendinous flap (Fig. 3). The deeper half of the tendon was divided across its width at the insertion with the greater trochanter thus allowing a double breasted closure. These deeper muscles were divided transversely, 1 cm from their femoral insertion to expose the capsule lying beneath (Fig. 4) revealing the accessory gluteal minor m. (Fig. 5).

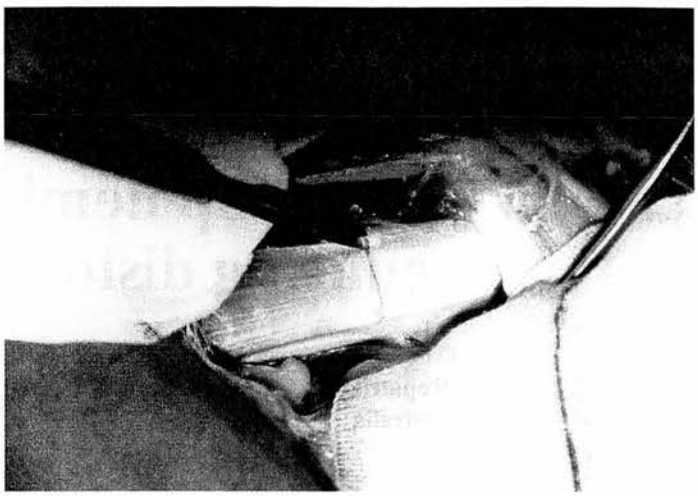

Fig. 2 Incision through the superficial half of the accessory gluteal major tendon, 3 cm from its trochanteric insertion.

A 'T'-shaped capsulotomy was performed, with the horizontal bar of the 'T' parallel to the attachment along the femoral neck. The free corners were marked with stay sutures, which also helped retract the soft-tissues. Hemostasis was ensured at this time. Traction on the leg allowed the joint to be visualized and a pair of curved Mayo scissors were used to section the ligamentum teres. Care was taken not to damage the acetabular cartilage. The femur was then dislocated and the neck exposed by subperiosteal reflection of the vastus lateralis.

The femoral canal was then broached to provide sufficient space to allow for impaction grafting of morsellized bone and bone substitute. A single size, modular Exeter V40 stem[a] was used for all individuals. This allowed placement of different head sizes to match the acetabulum snuggly and also, if required, had allowances for head offset of ±3 mm. A first generation cementing technique was employed.

On completion of the femoral head excision and surgical implantation of the hemiarthroplasty the joint capsule was repaired. The stay sutures, which enabled retraction and alignment of the capsular edges, were removed and the t-shaped capsulotomy repaired using 0-PDS in a simple continuous pattern.

The deeper gluteal muscles were reattached to their tendinous femoral origin with 0-PDS in a simple continuous pattern. The accessory gluteal major was repaired to its original state with continuous 0-PDS around the four sides of the double-breasted tenotomy, commencing with the deep transverse layer (Fig. 6). Joint stability was reassessed at this juncture prior to completion of the wound closure.

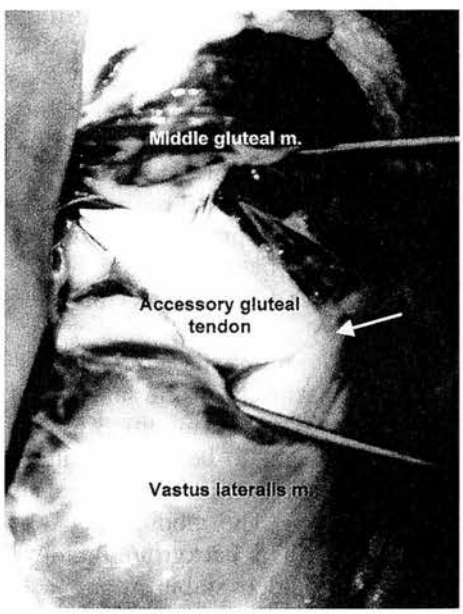

Fig. 1 Cranio-lateral approach with division between Middle gluteal m. and Vastus lateralis m., exposing tendinous insertion of Accessory gluteal m. Arrow indicates location of Greater trochanter.

Fig. 3 The superficial half is teased back (arrow) to within 1 cm of the insertion.

[a] Howmedica Inc. Staines, Middlesex, UK

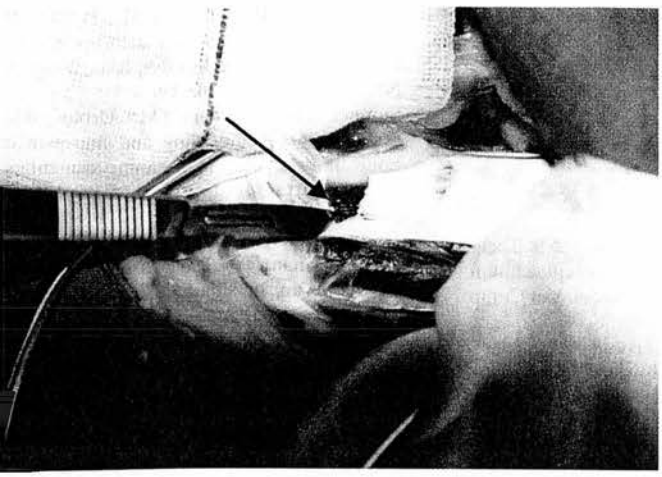

Fig. 4 The tenotomy is continued through the remaining deep half.

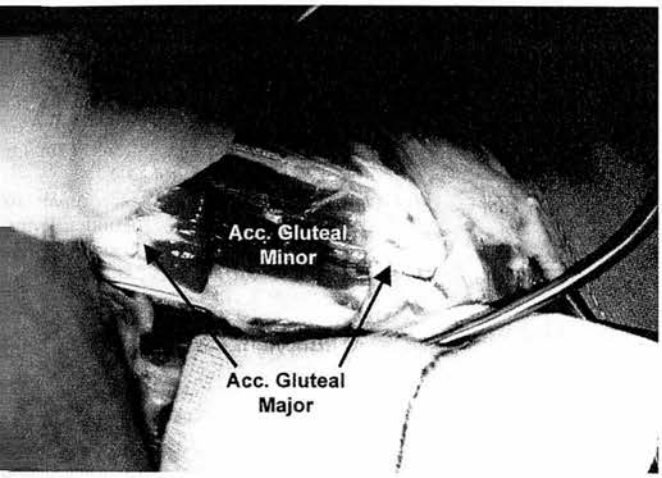

Fig. 5 The Deeper Accessory gluteal minor m. is revealed.

Fig. 6 Four sides of the tenotomy square are repaired in 'double-breasted' manner (·····).

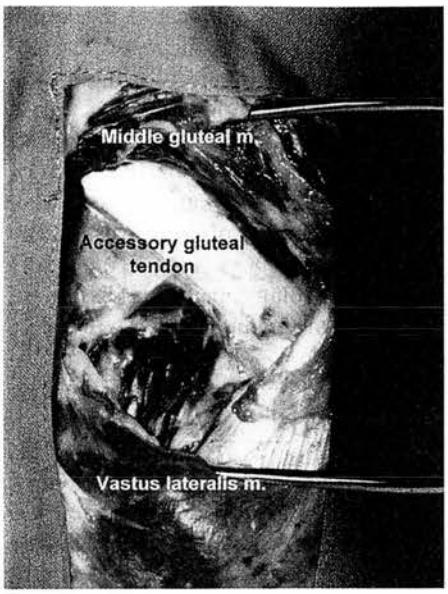

Fig. 7 Typical appearance of healing tendon at 12 weeks post-operatively.

Animals were recovered in a sling
ı which they remained for one day
ost-anesthesia. The sling allowed toe-
ɔuching weight bearing and provided
ɔme control over the animals during
ıeir recovery from anesthesia. A constant-infusion system for drug administration (2) provided for post-operative intravenous analgesia. Following removal from the sling, sheep were maintained in pens (3 metres sq.) for three weeks after which time they were moved to a small paddock (20 metres sq.) for the duration of the project. Activity was unrestricted but not forced.

Animals were expected to be fully weight bearing after removal from the sling. Daily assessments of their ability to ambulate were made. If any individuals remained only partially weight bearing for more than a day the analgesia protocol (2) was reinstituted following a physical exam. Failure to respond over two days resulted in euthanasia of the animal.

Results

At post mortem examination, 15 of the 16 repairs (94%) showed very good tendon and capsular reconstitution as shown in Fig. 7. This was the typical appearance of the healing tendon at 12 weeks post-surgery. These animals, prior to euthanasia, demonstrated a gait similar to that of normal, un-operated sheep. A mild gait deficit during running was an occasional finding in the early stages of recovery. The mobility was felt to be much improved when compared to previous animal rehabilitation seen prior to the technique modification. A direct comparison could not be made as the early study did not utilize a walking score.

One individual dislocated the hemiarthroplasty on the first post-operative day and was euthanised without any attempt at reduction. It was noted at the time of surgery that the implanted femoral head was oversized and of borderline stability, but the reduction acceptable. In light of this it was felt the dislocation was inevitable. At post mortem the capsular repair was disrupted, but the tenotomy intact.

Discussion

We have described a modification of the surgical approach to the sheep hip with a view to reducing the previously high rate of dislocation (23%) encountered, at this centre, in the early post-operative period following hemiarthroplasty (7). The technique of 'double-breasting' (17) involved a staggered incision of the full thickness of the musculo-tendinous insertion, does not bring about a shortening of structures and hence places minimal tension on the closure.

There was good tendon and capsular reconstitution at 12 weeks following hip hemiarthroplasty (Fig. 7). The technique described was felt to improve the function and importanly, the stability of the arthroplasty thereby reducing the dislocation rate in this ovine model of hemiarthroplasty. With only historical controls it is difficult to prove the reduced rate of dislocation is due to the new procedure; this feature warrants further investigation.

Acknowledgments

The authors are indebted to Mr. A. Carbone and Professor D. W. Howie for their assistance with this project.

REFERENCES

1. Bruns DP, Olmstead ML, Litsky AS. Technique and results for total hip replacement in sheep: An experimental model. Vet Comp Orthop Traumatol 1996; 9: 158-64.
2. Field JR, Aberman H, Carbone A, Sharpe P, Smith N, Dunlop DG, Howie DW. An ovine model for total hip replacement: Operative procedure and complications. Vet Comp Orthop Traumatol, in press.
3. Dunlop DG, Griffon D, Howie CR et al. An ovine model to evaluate impacted pellets of new synthetic bone graft substitutes. J Bone Jt Surg 2000; 81-B: Supp I.
4. Dunlop DG, Field JR, Costi J et al. Design and evaluation of a device for measuring 3-D micromotions of impaction grafted cemented femoral stem prosthesis. J Royal Coll Surg, Edinburgh 1999.
5. Newman E, Turner AS, Wark JD. The potential of sheep for the study of osteopenia: Current status and comparison with other animal models. Bone 1995; 16: 277S-84S.
6. Turner AS, Eckhoff DG, Dewell RD. Periapatite coated implants improve fixation in osteoporotic bone. 44th Ann Meeting Orthop Res Soc New Orleans, Louisiana, 1998.
7. Wang AW. Femoral bone remodelling following cemented hip arthroplasty in a sheep model. PhD Thesis, University of Adelaide 1998; 52-62.
8. Brumby SA, Howie DW, Pearcy MJ, Wang AW, Nawana NS. Radiographic and histologic analysis of cemented double-tapered femoral stems. Clin Orthop Rel Res 1998; 355: 229-37.
9. Olmstead ML, Hohn RB, Turner TM. A five year study of 221 total hip replacements in the dog. J Am Vet Med Assoc 1983; 183: 191-4.
10. Montgomery RD, Milton JL, Pernell R, Aberman HM. Total hip arthroplasty for treatment of canine hip dysplasia. Vet Clin Nth Amer 1992; 22: 703-19.
11. Sumner DR, Turner TM, Urban RM, Galante JO. Remodeling and ingrowth of bone at two years in a canine cementless total hip-arthroplasty model. J Bone Joint Surg (Am) 1989; 74: 239-50.
12. Rashmir-Raven AM, DeYoung DJ, Abrams CF, Aberman HA, Richardson DC. Subsidence of an uncemented canine femoral stem. Vet Surg 1992; 21: 327-31.
13. DeYoung DJ, DeYoung BA, Abrams CF, Kenna RV, Hungerford DS. Implantation of an uncemented total hip prosthesis. Technique and initial results of 100 arthroplasties. Vet Surg 1992; 21: 168-77.
14. Radin EL, Rubin CT, Thrasher EL et al. Changes in the cement-bone interface after total hip replacement. J Bone Jt Surg (Am) 1982; 64-A: 1188-200.
15. Kelley SS, Lachiewicz PE, Hickman JM et al. Relationship of femoral head and acetabular size to the prevalence of dislocation. Clin Orthop Rel Res 1998; 355: 163-70.
16. Turner RS. Postoperative total hip prosthetic femoral head dislocations. Clin Orthop Rel Res 1994; 301: 196-204.
17. Cave EP, Rowe CR. Capsular repair for recurrent dislocation of the shoulder: Pathologic findings and operative technique. Surgical Clin Nth Amer 1947; 27: 1289-93.

Dr. John R. Field
Orthopedic Unit
Repatriation General Hospital
Daws Rd., Daw Park
South Australia, 5041
Australia
Phone: +61 8 8275 1042
Fax: +61 8 8374 0712
E-mail: Lantbruks@bigpond.com

V.C.O.T.

J. R. Field[1], H. Aberman[2], A. Carbone[1], P. Sharpe[1], N. Smith[3], D. Dunlop[4], D. W. Howie[1]

An ovine model for total hip replacement: operative procedure and complications

[1]Department of Orthopedics and Trauma, Royal Adelaide Hospital, North Terrace, and Institute of Medical and Veterinary Science, Adelaide, South Australia, Australia; [2]Howmedica Inc., Rutherford, New Jersey, USA; [3]Howmedica Inc., Staines, Middlesex, UK; [4]Princess Margaret Rose Hospital, Edinburgh, Scotland

Keywords
Total hip replacement, sheep model

Thirty-seven mature Merino wethers were utilized for an evaluation of a new acetabular cup design using a modular cemented total hip replacement system. The ovine model for total hip replacement provided a reliable and manageable method for the evaluation of component design and tissue response.

Received 99.11.01, Accepted 00.04.20

Summary

A cranio-lateral curvilinear incision in the skin was centered over the greater trochanter. The subsequent approach to the acetabulum involved blunt dissection and avoided the need for significant muscular incision. The major post-operative complications encountered were fracturing of the proximal (2/37) and distal femur (4/37), caudal neuropathy (2/37) and septic femoral stem loosening (1/37). At two years post-operatively, the morbidity rate was 24% and the mortality rate 19%.

A regime of analgesia, involving constant infusion of xylazine, was developed and appeared very effective.

Introduction

The mechanical and biological performance of total hip replacement systems has become increasingly important in light of problems encountered where aseptic loosening of components occurs in response to wear debris generated at the articulating surfaces (1-7).

As a means of evaluating "wear particle disease" and new implants designed to overcome these problems, passage through an appropriate animal model is normally required prior to clinical trials in human subjects (8-13). To this end the sheep is becoming increasingly popular as a model for orthopedic related conditions (11, 14 to 16).

Various surgical approaches to the coxofemoral joint have been utilized including the cranio-lateral and dorsoventral curvilinear incisions centered over, or caudal to, the greater trochanter (11, 14). Either approach requires the incision and reflection of various muscles as a means of gaining adequate exposure of the joint.

The major complication, for animals undergoing hip arthroplasty, is perioperative fracturing of the femur. This occurs in response to the inappropriate use of the broach when preparing the femoral canal, or as a traumatic postoperative event usually associated with sudden movement (11). Other problems that are also commonly encountered in the human and canine patient include septic and aseptic loosening of the prostheses (1, 3, 5-7), dislocation

(11, 14) or neurological deficits in the hind limbs (17, 18).

In any animal model peri-operative care is a major concern particularly the issue of species-specific analgesia. It is increasingly apparent that analgesic agents routinely and efficaciously used in one species can be inadequate in another species. Currently used analgesic regimes for sheep include epidural morphine, intramuscular buprenorphine over several days and fentanyl patches (19). Recent evidence casts doubt on the efficacy of buprenorphine which appeared ineffective in the management of acute pain in the sheep (20).

The purpose of this report is to detail a simple surgical approach to the sheep hip, for total hip arthroplasty, which avoids the need for major soft-tissue dissection, the peri-operative animal care and the complications encountered.

Materials and Methods

Thirty-seven mature Merino wethers (3 years old) with a mean weight of 55 kg (47-70 kg) were used. The protocol for animal utilization had been approved by the Animal Ethics Committee, University of Adelaide.

All sheep had a standard perioperative antibiotic, anti-inflammatory and analgesia protocol.

Pre-operative preparation

The day prior to surgery the left and right hindlegs were shorn, including the perineum, dorsally and cranially to provide a substantial surgical field. Food was withheld overnight prior to surgery (12 hours). Access to water was unrestricted.

Perioperative drugs

Antibiotics: 2 grams of a first generation cephalosporin[a] in 500 ml normal saline was administered at the time of anesthetic induction with another 2 grams in 1000 ml intravenous saline solution administered throughout the procedure. Following recovery from anesthesia a further 2 gram of Keflin in 500 ml of normal saline was administered intravenously and then at four hourly intervals for a further two doses. These levels (approx. 40 mg/kg) are significantly higher than that recommended for the dog (22 mg/kg); predetermined doses were administered as we did not have a means of accurately determining body weight nor was there any information on therapeutic levels of this antimicrobial for the sheep.

Anti-inflammatory drugs: 50 mg of flunixin meglumine[b] was administered intravenously (approx. 1 mg/kg) at the time of anaesthetic induction and at the time of recovery from the procedure and thereafter twice daily for a further two days post-operatively. This provided a sound level of non-steroidal anti-inflammatory drug cover for the peri-operative period.

Analgesia: A significant improvement in our ability to control post-operative pain has been the institution of a syringe driver[c] providing a continuous infusion of analgesic agent over the 48-72 hour post-operative period. One mg of xylazine[d] per hour was infused continuously for a minimum of 48 hours post-operatively. This could be continued (through i/v access) if required. This procedure was well tolerated by the sheep and in current studies appears to be providing excellent levels of analgesia (Fig. 5) and comfort without sedation. The method of algesimetry has been reported and validated. It relies on documentation of a leg withdrawal response to subcutaneous electrical stimulus (20).

Anesthesia

Five mg of xylazine (0.2 mg/kg) was administered intramuscularly (i/m) 30 minutes prior to induction providing good sedation and levels of analgesia throughout the procedure. At induction a 5-inch indwelling jugular catheter was placed and remained in place for three days post-operatively. The catheter and extension tubing were glued using cyanoacrylate[e] and sutured to the skin to reduce the possibility of pullout. A stomach tube was not placed for any individual; no problems were encountered with regurgitation.

Anesthesia was induced with a bolus of one gram of Pentothal intravenously. Thereafter the animal was intubated with a cuffed endotracheal tube and halothane administered in oxygen at 2-3%.

Induction suite

The animal was positioned in lateral recumbency. All preliminary preparation was performed in the induction suite and not in the surgical suite as a means of better controlling infection. Fine clippers were used to remove remaining wool follicles; shaving was not performed. An incise drape could not be used because of its poor adherence.

The operative leg was suspended to isolate the surgical site. Povidone-iodine scrub was used for the initial preparation of the entire operative field. This was removed with clean towels and repeated. Gauze swabs, containing 90% ethanol were utilized to defat the operative site and allowed to volatilize. Povidone-iodine solution (10%) was then applied. The animal was then moved to the surgical suite.

Operative procedure

With the operative leg suspended a "scrubbed-in" member of the surgical team performed a final preparation of the operative site with 10% povidone-iodine solution. Draping of the limb ensued providing a number of layers finishing with the application of a water-repellant "hip drape"[f].

Incision

A craniolateral curvilinear incision was made (Fig. 1) extending caudally from the mid-point between the tuber coxae and the greater trochanter of the proximal femur. At the level of the greater trochanter the incision was angled ventrally along the cranial aspect of the femur approximately 10 cm. The total incision length was approximately 15-20 cm. Electrocautery was used for haemostasis. With the animal in lateral recumbency, the rear limb was held

[a] Keflin, Eli Lilly Co. Melbourne, Australia
[b] Finadyne, Ilium Co. Melbourne, Australia
[c] Graseby Medical, Watford, Hertfordshire, UK
[d] Rompun, Ilium Co. Melbourne, Australia
[e] Supaglue, Selleys Inc. Adelaide, Australia
[f] Johnson and Johnson Inc. Adelaide, Australia

slightly abducted to remove tension on the incision site. The tensor fascia lata was incised in a similar manner to the skin exposing the biceps femoris muscle ventral to the greater trochanter and the superficial gluteal m., dorsal to the greater trochanter. A dorso-ventral plane of dissection was defined between these muscles and extended using manual, blunt dissection. Large Gelpi self-retaining retractors were placed to expose the underlying muscle groups (middle gluteal m. and vastus lateralis m.). Manual dissection at the interface (Fig. 2) between these muscles was performed and a second pair of Gelpi retractors placed. This exposed the accessory gluteal m. and its tendinous insertion to the greater trochanter. This was elevated using curved Kelly forceps and the tendinous insertion transected with a scalpel leaving a stump of approximately 1 cm attached to the greater trochanter (Fig. 3). Gentle soft-tissue manipulation with sterile swabs allowed any remaining tissue to be reflected exposing the joint capsule.

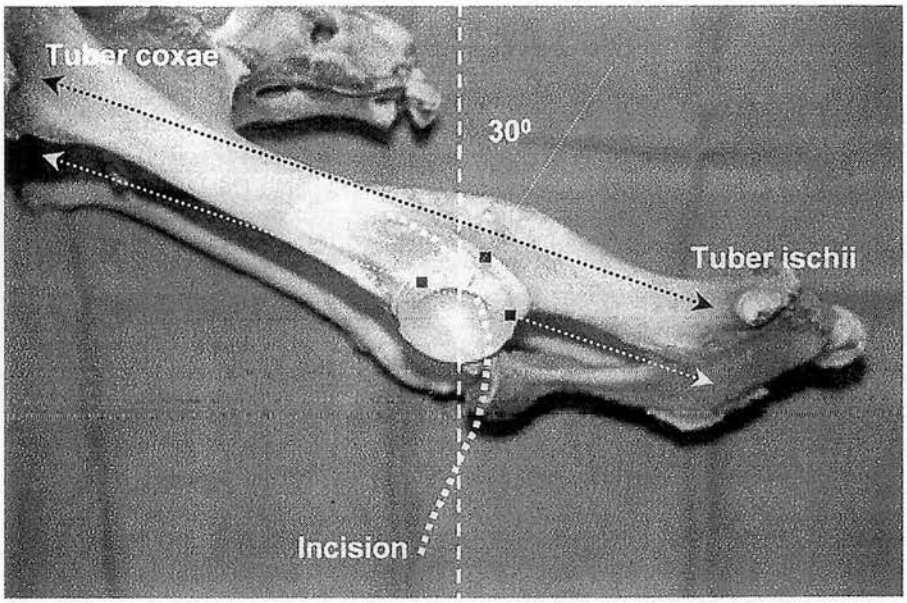

Fig. 1 Cadaveric specimen of a sheep hip depicting approximate location of incision, notable landmarks and orientation of prosthesis. The two parallel lines (....) are defined to enable correct alignment of the acetabular cup in this plane.

Joint capsule

With the limb in anatomical full extension a dorso-ventral incision was made through the joint capsule. The incision extended 2-3 cm dorsal and ventral to the edge of the joint. A straight spade-head periosteal elevator was used to access the joint prior to insertion of a Hatt spoon[g] that was used to transect the ligamentum teres (acetabular lig.). A periosteal elevator was used to remove soft-tissue remnants on the femoral neck, ventral to the head, to the level of the greater (lateral) trochanter.

Femoral neck osteotomy

With the leg held in external rotation an adjustable neck-cutting guide was utilized to approximate the orientation of the femoral neck osteotomy. With subsequent experience the guide was not required. The osteotomy was performed using a 2.5 cm saw blade with a battery charged saw[h]. A Lewin bone clamp enabled removal of the femoral head following its excision.

Acetabular preparation

A small Hohmann retractor was positioned under the ventral rim of the acetabulum and used to lever the femur providing good exposure of the acetabulum. So as not to interfere with acetabular reaming a #15 scalpel blade was used to remove any capsular attachment or soft tissues interposed.

Utilizing a tissue protector, to prevent the reamer from injuring surrounding soft tissues and commencing with a 26 mm reamer[i], the acetabulum was prepared with successive increases in the size of reamer through 28 and

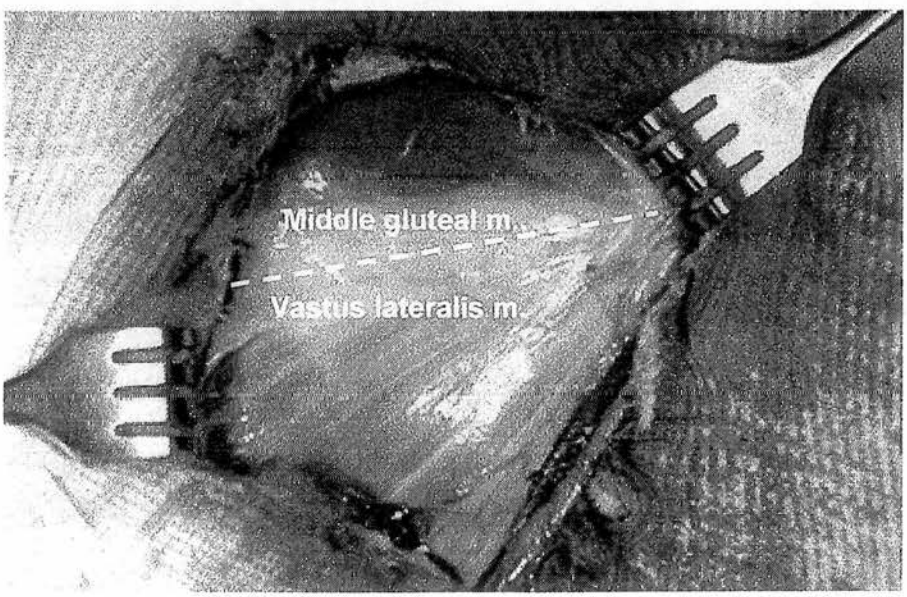

Fig. 2 Plane of blunt dissection (- - - -) between middle gluteal m., and vastus lateralis m.

[g] Richards Surgical, Adelaide, Australia
[h] Stryker Pty Ltd, Kalamazoo, Michigan, USA
[i] Howmedica Inc., Rutherford, New Jersey, USA

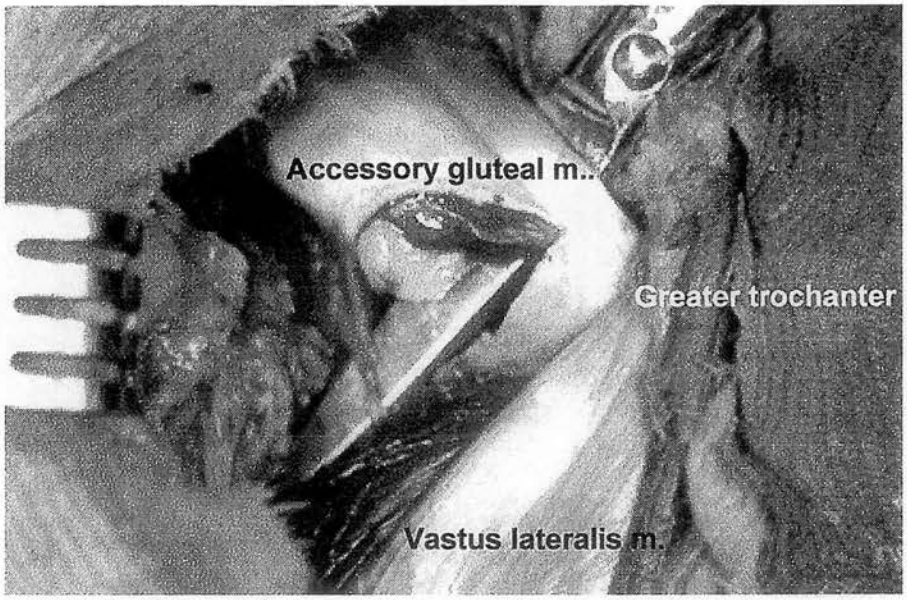

Fig. 3 Sectioning of the accessory gluteal m., leaving the tendinous stump attached to the greater trochanter for subsequent re-attachment.

30 mm. The bone surface was reamed to expose cancellous surface petechial bleeding. In doing so the version angle of the reamer was maintained as close to anatomical as was possible; this was performed by visual assessment. A trial cup was used repeatedly in order to determine the extent of the reaming and the possible thickness of the cement mantle.

The final step in preparation of the acetabulum was the drilling of 4 × 4.5 mm holes in a "clockface" manner. The depth and width of the holes were approximately the same. Acetabular lavage, with sterile saline, was followed by the placement of a gauze swab soaked in pre-filtered (0.2 microns) 1.5% hydrogen peroxide (H_2O_2). This solution was utilized with a view to reducing the incidence of infection (21, 22) and dislodging blood clots from the endosteal interstices hence allowing better cement penetration (23). It was allowed to remain in the acetabulum while the cement was prepared.

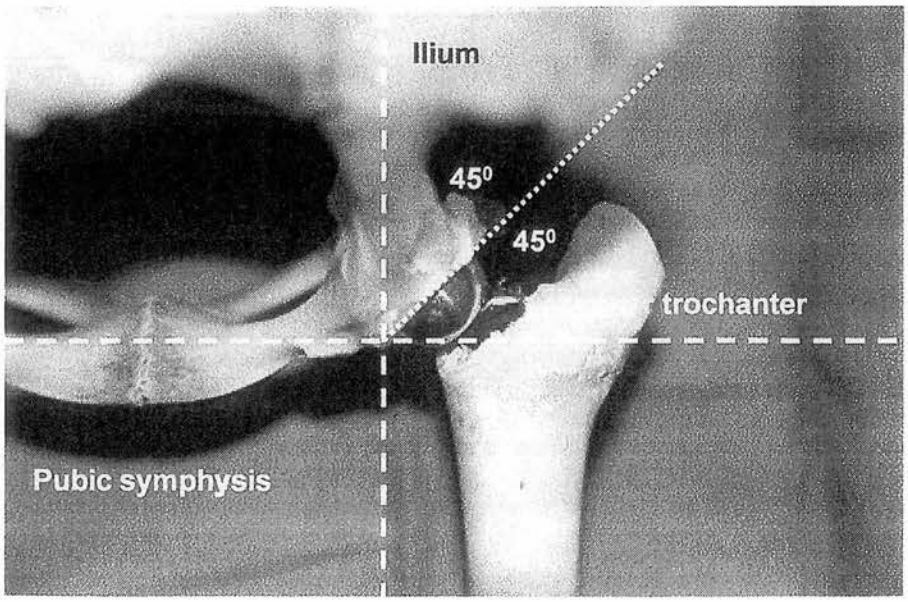

Fig. 4 Cadaveric specimen depicting approximate angle of cup closure in the sagittal plane.

Acetabular cup positioning/cementing

One size of polyurethane acetabular cup was used for all of the individuals (30 mm ext. diam.). Using a sterile surgical marker pen[j], the most ventral aspect of the tuber coxae and the tuber ischii were located and marked. The acetabular cup was also marked on the exposed surface at the 3, 12 and 9 o'clock locations. The 3 and 9 o'clock marks allow these locations to be aligned parallel to an imaginary line running between the tuber coxae and the tuber ischiae (Fig. 1). This allowed for accurate positioning of the cup without the need for elaborate positioning devices. One 20-gram packet of cement[i] was used for fixation of the acetabular cup.

The cement was mixed, using a first-generation cementing technique, until of "doughy" consistency (approximately 5 minutes). At this point a small wad (approximately 15 ml) was packed into the acetabulum and, in order to evenly distribute the cement, particularly into the drill holes, thumb pressure was applied. Using the cup-positioning rod with a trial head attached, at six minutes after commencement of cement mixing, the cup was introduced. The cup hood was positioned at approximately 45° to the saggital plane (Fig. 4). This provided adequate closure of the cup. During cement curing (approx. 12 minutes) a small dental curette was used to remove any excess cement from around the cup. After completion of initial cement curing the strength of the bond to the cup was checked by digital palpation followed by lavage of the site.

Femoral preparation

As a means of protecting the acetabulum a saline-soaked gauze was placed in the cup whilst a sheet of water repel-

j Codman Surgical, Johnson and Johnson Inc, Adelaide, Australia

lant paper was placed over the cup. This technique prevented excess cement oozing down the medial aspect of the femur and interfering with the cup. At six minutes after commencement of cement mixing. Following placement of the femoral components, both the paper and the swab were removed.

With the femur externally rotated, a Cobra-headed elevator was placed under the caudal aspect of the exposed femur effectively covering, but not interfering with, the acetabular cup while providing good access to the femoral canal.

A T-handled reamer was used to create a core in the medullary canal to a depth of 10 cm. The proximal femur was prepared manually using sequentially a number 1 and number 2 broach to enlarge the canal. The smaller broach (#1) was used first to remove cancellous bone particularly lateral and medial. Using a mallet, the large #2 broach was then tapped gently down the canal until the broach hub rested at the level of the femoral cut. Broach orientation was parallel to the cranial femoral plane. This provided an appropriate size of canal for a cement mantle of 1-2 mm at its most proximal aspect. The canal was then lavaged with normal saline (room temperature) followed by suction. A 1 cm intramedullary brush was introduced to a level of 10 cm. This very effectively removed any debris (medullary canal content). Fifteen mls of sterile 1.5% hydrogen peroxide was introduced into the canal, allowed to activate and then suctioned off (23).

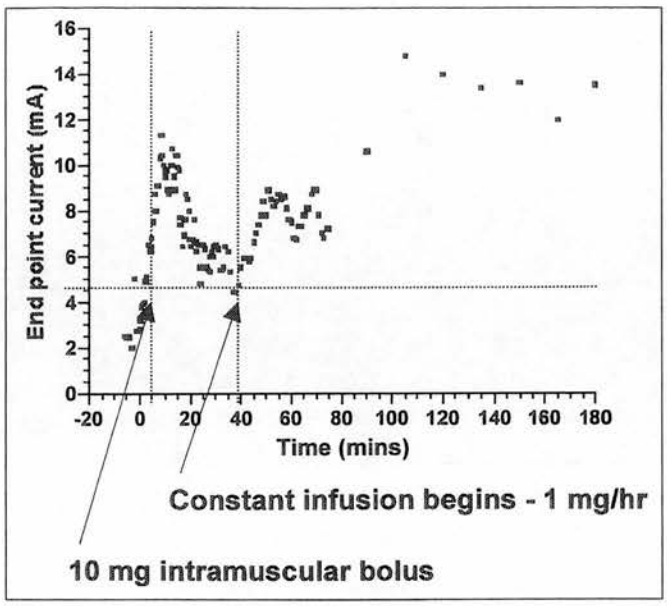

Fig. 5 Graphic representation of an individual animal's response to noxious stimuli following intramuscular injection of xylazine compared to its response following continuous infusion of xylazine (i/v) at 1 mg per hour.

Femoral component cementing

The femoral stem was a scaled-down version of the Exeter stem[j]. This is a highly polished, double taper stem incorporating a Morse taper lock for placement of the femoral head. For placement of these components the leg was maintained in external rotation. Two packets (40 grams) of polymethylmethacrylate cement were mixed for this procedure. The tip of the plastic cement gun was cut to a length of 10 cm, to match that of canal preparation.

While the cement was being mixed, a foam gasket was made that mimicked the outer diameter shape of the proximal femur. This was fitted to the base of the cement gun and allowed pressurization of the cement during its application. At 4.5 minutes following commencement of cement mixing the cement was introduced into the canal to the full depth of the nozzle (10 cm). While repeatedly pressing the trigger, the cement gun was gradually extracted with retrograde cement insertion. The pressurizing gasket was held in place after removal of the gun whilst the stem was prepared for insertion.

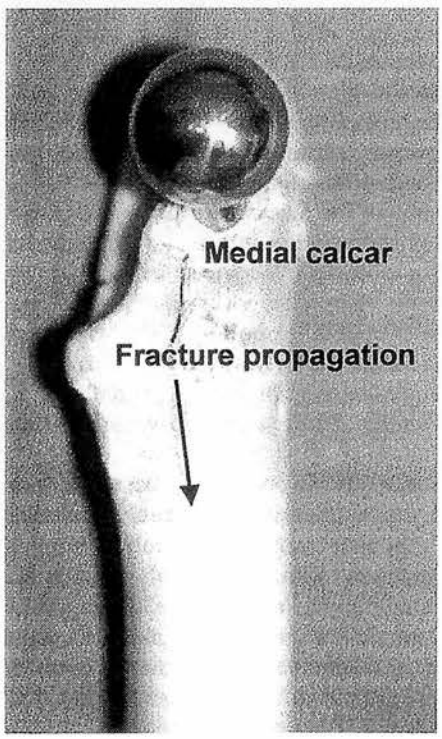

Fig. 6 Fracture propagation along the medial aspect of the proximal femur following aggressive use of the broach.

The femoral stem, with centralizer attached, was introduced to the level of the stem neck in one continuous motion and then held in place while the cement firmed and excess was removed. The packing material protecting the acetabulum was then removed and any excess cement remaining was removed with curette or rongeur.

Femoral head

A trial head was used to determine which head would ultimately be used. Options were offsets of –3.0 and +3. Gentle tapping of the head applicator by mallet ensured the head was secured via the Morse taper lock. The cup was aggressively lavaged and checked for cement debris before joint reduction was performed. Copious saline lavage was again applied.

Wound closure

The accessory gluteal muscle was reapposed, with the remnant left on the greater trochanter, using 1-Polydiaxonone[k] in a simple interrupted cruciate

[k] Ethicon, Johnson and Johnson Inc, Adelaide, Australia

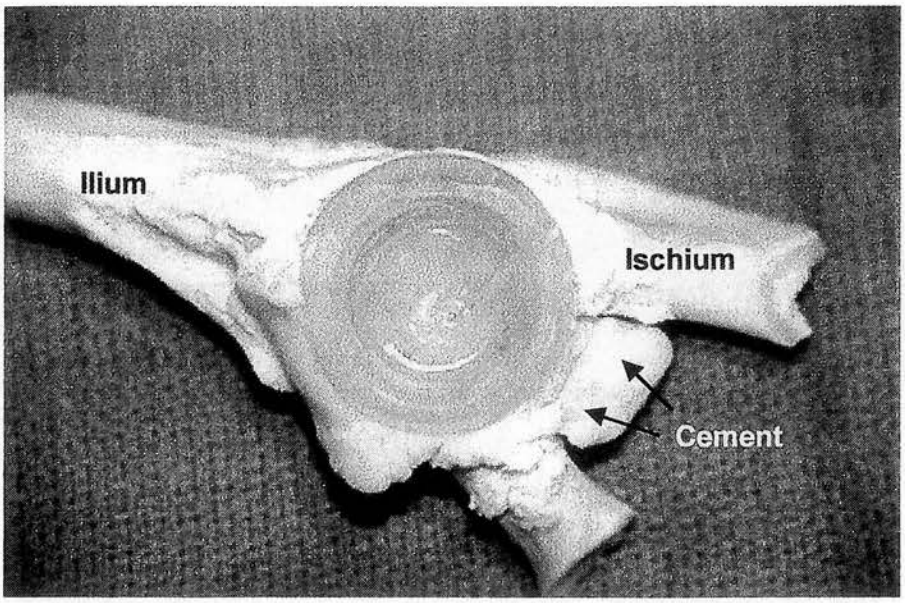

Fig. 7 Location of excess cement, causing possible impairment of obturator nerve function and caudal paresis.

pattern. This layer was closed completely, thus providing the initial closure over the joint. Because of tissue resection closure of the joint capsule itself was not undertaken. The middle gluteal m. and the vastus lateralis m. was reapposed using Vicryl[k] (4 metric) in a simple interrupted cruciate pattern also. The final layer of deep tissue closure, the fascia of the tensor fascia lata m. was also closed with 1-Vicryl in a simple continuous pattern. 2-0 Vicryl (3 metric) was used to close down the subcutaneous tissues in a simple continuous pattern with periodic reduction of dead space. Vicryl (3.5 metric) on a cutting needle was used to close the subcuticular tissue in a simple continuous pattern. The skin was apposed using skin staples which were left in place for the experimental duration.

Recovery and post-operative care

The sheep were placed in a cotton/canvas sling prior to transfer from the operating room to the recovery stall (1M × 2M). They remained in this sling for one day; the sling allowed toe-touching weight bearing only. The sheep were then transferred to a larger pen (3M × 3M), holding two individuals, to allow free ambulation for 21 days prior to their transfer to a small paddock (50 M × 50 M).

When required, euthanasia was performed by the administration of 20 ml of barbiturate[l] intravenously.

Results

Thirty-seven animals underwent total hip arthroplasty as a means of evaluating the biological response to a new design of acetabular component. Complications occurred in nine of 37 (morbidity rate 24%) necessitating the destruction of seven of these (mortality rate 19%). Survival to two years post-operatively was 30 of 37 (81%). Most complications occurred either at the time of surgery or in the immediate post-operative period (30 days) and included the following:

1. Fracturing of the proximal femur related to the aggressive use of the broach (Fig. 6). In both instances (2/37) this occurrence was observed intra-operatively and circumferential wire cerclage performed in an attempt to limit the distal propagation of the fracture. One of the two animals survived through one post-operative year. The other attempted repair was not successful and the animal was euthanatized.
2. Fracturing of the distal femur (Fig. 8) occurred during required movement of animals (4/37). These occurred randomly at times ranging from 7 to 30 days post-operatively. The animals were immediately destroyed.
3. A caudal paresis was evident in two animals the day of their removal from the sling. Treatment involved continued analgesia and non-steroidal anti-inflammatory medication over several days. There was not any response and so the animals were destroyed. In both cases, necropsy revealed large amounts of cement lying directly over the obturator nerve (Fig. 7), as it passed through obturator foramen. This was the only significant finding.
4. Septic femoral stem loosening was observed in one individual (1/37) at the scheduled retrieval of the implant (at six months following the operation). This was diagnosed radiographically with lucency evident around both the cup and stem (Fig. 9). At necropsy the cup was securely fixed, however, the stem "pistoned" mildly in the proximal femur. The surface of the femur displayed considerable proliferative new bone formation.

At the time of necropsy, radiographs were routinely taken for each individual as a means of assessing any changes in the fixation of either the femoral stem or acetabular cup. Of those sheep remaining in the study at "two years" obvious gait deficits were not apparent; each animal possessed unrestricted range of motion.

Algesimetry was performed on one individual that had not undergone surgical intervention. The results are depicted in Fig. 5 showing the individual's response to a "one-off" intramuscular injection of xylazine when compared to the effect of continuous infusion of the agent over a prolonged period of time. As is the threshold of responsiveness, the duration of efficacy of the i/m injection was quite limited. The constant infusion provided ongoing analgesia with a substantially higher pain threshold achieved. None of the operated animals, treated in this manner, displayed any paresis that might be attributed to the compound nor did they appear sedated in any way.

[l] Lethobarb, Verbac Co. Sydney, Australia

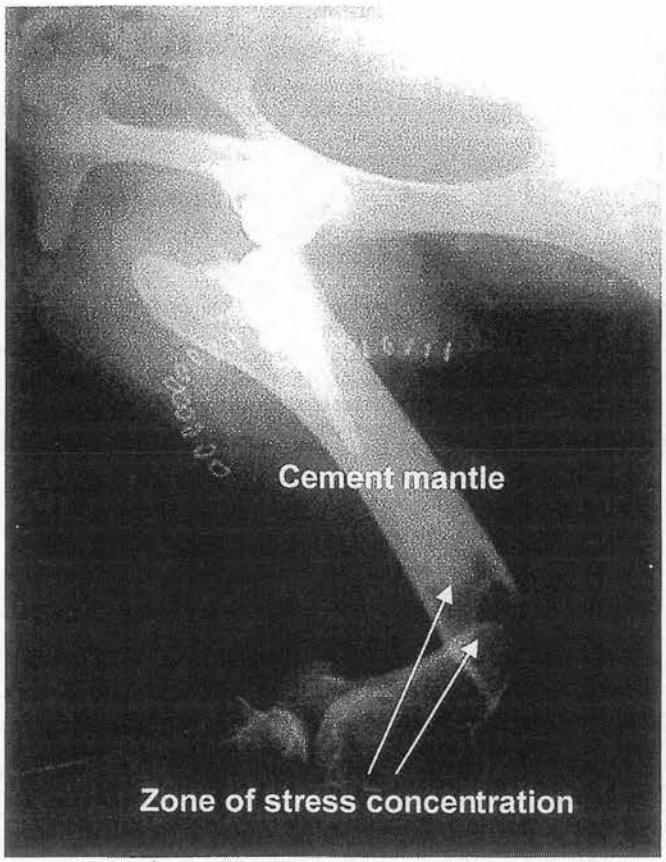

Fig. 8 Traumatic fracturing of the distal femur emanating at the zone of stress concentration is depicted.

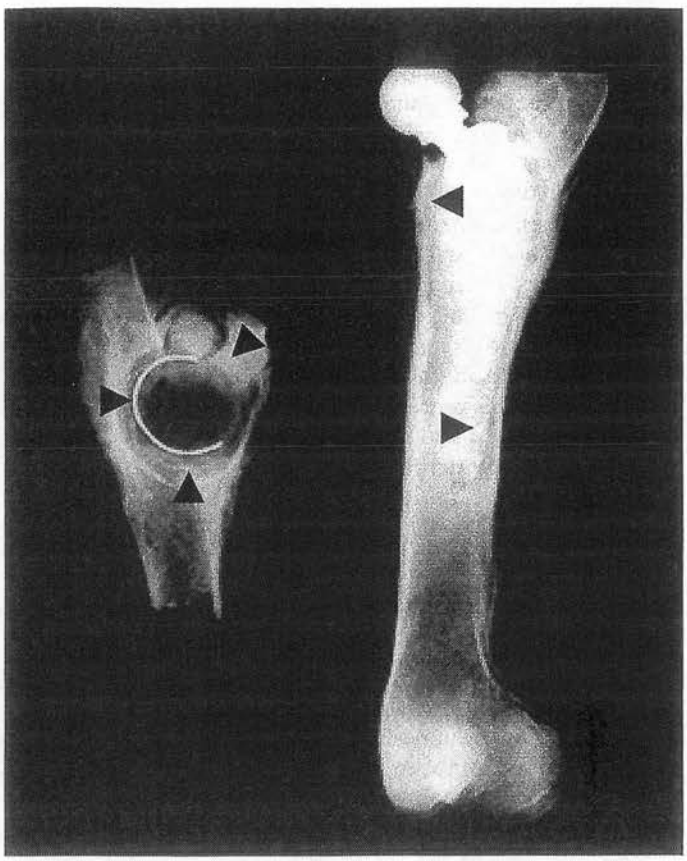

Fig. 9 Osteomyelitis involving the femoral and acetabular prostheses. Associated lucency is readily apparent (▶).

Discussion

We have developed a surgical approach to the sheep coxofemoral joint utilizing a curvilinear cranio-lateral incision centered over the greater trochanter (Fig. 1). The superficial gluteal and biceps femoris muscles form a continuous band that appears in the middle of the skin incision. By utilizing blunt dissection this band of muscle can be elevated and stripped clear of the deeper tissues and retracted using Gelpi retractors. Unlike other reports (11), we did not transect the vastus lateralis muscle. The tendinous insertion of the accessory gluteal m. was transected close to the greater trochanter (Fig. 3). In all cases incisional infections were not experienced. At necropsy, tissue apposition was quite anatomical with fibres of the accessory gluteal m., remarkably well aligned. We attribute the absence of incision problems to the overall reduction in soft-tissue trauma.

Previous reports cite morbidity, for sheep hip arthroplasty, to range from 20-40% (11, 14, 23, 24). With experience in peri-operative care of the species and attention to surgical protocol we have reduced the morbidity, at this centre, to 24%. Appropriate husbandry is deemed the most critical feature in reducing post-operative morbidity and mortality.

Following fracture of the proximal femur (Fig. 6), due to aggressive broaching, the use of circumferential cerclage prior to cementing of the femoral stem allowed one animal to remain in the study. Fracturing of the distal femur (Fig. 8) occurred randomly and seemed related to the need to move animals within our facility. The sheep is an unpredictable animal, and when startled is prone to rapid movement. Through education of our animal house personnel and a reduction of the number of moves required, we have effectively eliminated this problem that has been reported elsewhere (11).

The development of hindlimb paresis in two individuals was initially quite perplexing. The usage of a sling does, in some individuals, precipitate a transitory posterior paresis immediately after the animals are removed from it; this resolves within four to six hours. The animals involved remained paretic for some time post-operatively and did not respond to anti-inflammatory medication. The necropsy findings of large amounts of cement over the obturator n. (Fig. 7) provided circumstantial evidence that the neuropathy was the result of cement extrusion (17, 18). Careful attention to cup positioning and judicious removal of excess cement appears to have overcome this problem.

Septic loosening of one femoral stem was observed (Fig. 9). Streptococcus fecalis was cultured from the site. This was the first arthroplasty performed in the series and we attribute the infection to prolonged operative time (150 minutes) and our lack of surgical experience in the procedure.

Except for component cementing, two individuals comfortably performed the majority of the procedure. A third person scrubbed for cement preparation and assistance in cup positioning. Our operative time (skin-to-skin) was consistently 90-100 minutes which, we believe, has helped in reducing the morbidity rate. Total anaesthesia time was approximately 140 minutes.

The institution of a constant intravenous infusion of analgesia has been seen as a significant advance in the performance of this procedure in sheep. Some doubt exists as to the efficacy of agents, such as buprenorphine and flunixin meglumine, in the provision of adequate analgesia in the sheep (20, 25, 26). Intravenously administered xylazine has demonstrated a clear anti-nociceptive effect in sheep, when they are subjected to both thermal and mechanical systems (27).

We have observed a dramatic improvement in the disposition of our animals following conversion from intramuscular to continuous infusion of analgesic agent. We further suggest that the periodic administration of xylazine intramuscularly may not provide adequate levels of analgesia. These findings require substantially more investigation, before we can categorically claim a better means of controlling post-operative pain in the sheep.

By utilizing a less traumatic surgical approach, with appropriate levels of effective post-operative analgesia, strict attention to sterile technique and post-operative husbandry, the ovine model has enabled a significant amount of relevant data to be obtained prior to clinical trials in humans. Moreover, the sheep has provided an economical alternative, whose physiological and psychological needs appear better able to be met, when compared to the canine model.

Acknowledgments

The authors are indebted to Ms. G. Summersides and Dr. T. Kuschel, I. M. V. S., Adelaide, South Australia, for performance of the Algesimetry. The assistance of Bristol-Meyers-Squibb Co. is acknowledged.

REFERENCES

1. Howie DW, Middleton RG, Costi K. Loosening of matt and polished cemented femoral stems. J Bone Joint Surg (Br) 1998; 80-B: 573-6.
2. Anthony PP, Gie GA, Howie CR, Ling RS. Localised endosteal bone lysis in relation to the femoral components of cemented total hip arthroplasties. J Bone Joint Surg (Br) 1990; 72: 971-9.
3. Pritchett JW. Femoral bone loss following hip replacement. A comparative study. Clin Orthop 1995; 314: 156-61.
4. Maloney WJ, Jasty M, Burke DW, O'Connor DO, Zalenski EB, Bragdon C, Harris WH. Biomechanical and histologic investigation of cemented total hip arthroplasties. Clin Orthop 1989; 249: 129-40.
5. Howie DW, Vernon-Roberts B. Synovial macrophage response to aluminum oxide and cobalt-chrome alloy wear particles in rats. Biomaterials 1988; 9: 442-8.
6. Howie DW, Vernon-Roberts B. Long-term effects of intra-articular cobalt-chrome allow wear particles in rats. J Arthroplasty 1988; 3: 327-36.
7. Jasty M, Maloney WJ, Bragdon CR, O'Connor DO, Haire T, Harris WH. The initiation of failure in cemented femoral components of hip arthroplasties. J Bone Joint Surg (Br) 1991; 73: 551-8.
8. Olmstead ML, Hohn RB, Turner TM. A five year study of 221 total hip replacements in the dog. J Am Vet Med Assoc 1983; 183: 191-4.
9. Montgomery RD, Milton JL, Pernell R, Aberman HM. Total hip arthroplasty for treatment of canine hip dysplasia. Vet Clin Nth Amer 1992; 22: 703-19.
10. Sumner DR, Turner TM, Urban RM, Galante JO. Remodeling and ingrowth of bone at two years in a canine cementless total hip-arthroplasty model. J Bone Joint Surg (Am) 1989; 74: 239-50.
11. Bruns DP, Olmstead ML, Litsky AS. Technique and results for total hip replacement in sheep: An experimental model. Vet Comp Orthop Traumatol 1996; 9: 158-64.
12. Rasmir-Raven AM, DeYoung DJ, Abrams CF, Aberman HA, Richardson DC. Subsidence of an uncemented canine femoral stem. Vet Surg 1992; 21: 327-31.
13. DeYoung DJ, DeYoung BA, Aberman HA, Kenna RV, Hungerford DS. Implantation of an uncemented total hip prosthesis. Technique and initial results of 100 arthroplasties. Vet Surg 1992; 21: 168-77.
14. Brumby SA, Howie DW, Pearcy MJ, Wang AW, Nawana NS. Radiographic and histologic analysis of cemented double-tapered femoral stems. Clin Orthop 1998: 355: 229-37.
15. Newman E, Turner AS, Wark JD. The potential of sheep for the study of osteopenia: current status and comparison with other animal models. Bone, 1995; 16: 277S-84S.
16. Turner AS, Eckhoff DG, Dewell RD. Peri-apatite coated implants improve fixation in osteopenic bone. New Orleans, Louisianna: 44th Ann Meeting Orthop Res Soc. 1998.
17. Middleton RG, Reilly DT, Jessop J. Occlusion of the external iliac vein by cement. J Arthroplasty 1996; 11: 346-7.
18. Ratcliff AHC. Vascular and neurological complications. In: Complications of total hip replacement. Ling RSM (ed). New York: Churchill Livingston 1984; 18.
19. Wagner AE. Analgesic management of animals used in orthopedic research. Proc. Orthopedic Animal Models. Virginia: Arlington 1999.
20. Grant C, Upton RN, Kuchel TR. Efficacy of intra-articular analgesis for acute pain in sheep. Aust Vet 1996; J 73: 129-32.
21. Scherr DD, Dodd TA, Buckingham WW. Prophylactic use of topical antibiotic irrigation in uninfected surgical wounds. J Bone Joint Surg (Am) 1972; 54: 634-40.
22. Lineweaver W, Howard R, Soucy D et al. Topical antimicrobial toxicity. Arch Surg 1985; 120: 267-70.
23. Wang AW. Femoral bone remodelling following cemented hip arthroplasty in a sheep model. PhD Thesis, University of Adelaide 1998; 52-62.
24. Radin EL, Rubin CT, Thrasher EL et al. Changes in the bone-cement interface after total hip replacement. J Bone Jt Surg (Am) 1982; 64-A: 1188-200.
25. Waterman AE, Livingston A, Amin A. Further studies on the antinocioceptive activity and respiratory effects of buprenorphine in sheep. J Vet Pharmacol Ther 1991; 14: 230-4.
26. Chambers JP, Waterman AE, Livingston A. The effects of opiod and alpha 2 adrenergic blockade on non-steroidal anti-inflammatory drug analgesia in sheep. J Vet Pharmacol Ther 1995; 18: 161-6.
27. Nolan A, Livingston A, Waterman AE. Antinociopceptive actions of intravenous alpha 2-adrenoceptor agonists in sheep. J Vet Pharmacol Ther 1987; 10: 202-9.

Dr. John R. Field
Dept Orthopedic Surgery
Repatriation General Hospital
Daws Rd., Daw Park
5041 South Australia, Australia
Phone: +61 8 8275 1042
Fax: +61 8 8374 0712
E-mail: Lantbruks@bigpond.com